

**Packaging from Nature: Understanding the Mechanical and
Molecular Properties of Cellulosic Films**



Alex Louise Larsen Gresty
School of Physics and Astronomy
University of Leeds

Submitted in accordance with the requirements for the degree of

Doctor of Philosophy

September 2023

The candidate confirms that the work submitted is her own and that appropriate credit has been given where reference has been made to the work of others.

This copy has been supplied on the understanding that it is copyright material and that no quotation from the thesis may be published without proper acknowledgement

The right of Alex Louise Larsen Gresty to be identified as Author of this work has been asserted by Alex Louise Larsen Gresty in accordance with the Copyright, Designs and Patents Act 1988

Conferences

- Poster presentation at Leeds Doctoral College Showcase 2021, Online
- Oral presentation at SOFI Showcase 2022, Leeds, UK
- Poster presentation at ACS 'Sustainability in a changing world' 2022, Chicago, USA
- Poster presentation at EPNOE Junior Meeting 2022, Aveiro, PT
- Poster presentation at STEM for Britain 2023, London, UK
- Poster presentation at SWE Local 2023, Barcelona, ES
- Poster presentation at SCI Scholar's Showcase 2023, London UK
- Oral presentation at Parliamentary and Scientific Committee Meeting 2023, London, UK
- Oral presentation at CDTBrum 2023, Birmingham, UK
- Poster presentation at ISMC 2023, Osaka, JP

Prizes

- **Henry Cavendish Gold Medal** issued by Institute of Physics and Parliamentary and Scientific Committee at STEM for Britain 2023
- **Dyson Sustainability Award** second prize in the Dyson Sustainability Awards at STEM for Britain 2023
- **First Place Poster Prize** issued by Society of Chemical Industry at SCI Scholars Showcase

Publications

- Gresty, A.L.L. Food packaging from Nature: Cellulosic films for the 21st Century. *Science in Parliament*, 79(2):20-22, 2023

I dedicate this thesis to my Grandmas; Betty and Di

*They are not long, the days of wine and roses:
Out of a misty dream
Our path emerges for a while, then closes
Within a dream*

Ernest Dowson

Acknowledgements

The list of those who should be acknowledged must begin with my supervisors; Professor Mike Ries and Dr Peter Hine. Having been at the University of Leeds since I was 18, I have become an adult in your presences and learnt to negotiate not only the trials of academia, but the trivias of life. Over the last 4 years we have overcome many challenges together and no amount of thank-yous for your endless support and unwavering belief can ever come close to my gratitude. Collectively you have taught me infinitely more than 'just' biopolymer physics and my total gratefulness goes out to you both. It will be a very sad day when we have our last flat white together.

As I write these acknowledgements I am on a 21 hour journey from Japan to Manchester after having attended The International Soft Matter Conference 2023. So, it's fitting that next I thank those at my industry sponsor, The Futamura Group, whose birth place is Japan. Over the last 4 years we have battled lockdown regulations, tackled teams meetings (often as a result of myself accidentally muted) and coordinated numerous visits. All of this has driven my pursuit of this work; meeting and collaborating both in labs and online as well as being able to see the applications of my work has been a privilege. Everyone at Futamura, in particular: Martin, Liz and Hannah; I cannot thank-you enough for your commitment, support and faith throughout this time.

A special thank you must also go to Dr Dan Baker, who tirelessly holds the Soft Matter Physics labs together; I think you've probably seen me through some of my lowest and highest points over the last four years. Thank-you, not only for your literally unlimited knowledge

of every lab technique ever, but also for all your extremely wise and down-to-earth advice and chats. In addition I would like to thank Dr Emma Cochrane for being a role-model and friend over the years, Dr Yoselin Benitez-Alfonso and Emily Newcombe for the excellent discussions and flowing ideas in meetings, Dr Mannan Ali for some extremely thorough liquid nitrogen dewer-filling training and everyone in The Mechanical Workshop for aiding the conception of some novel techniques (along with the seemingly endless repairs to the impact tester).

I would also like to thank everyone in the Soft Matter Physics Group at Leeds. In particular, all members past and present of Mike and Peter's 'Biopolymer Dream Team'. Watching this group grow over the last 4 years has created an incredible base of support and guidance for us all. I've been able to meet people from all corners of the world and made valuable friendships for life. A special mention must also go to my 1.35 office mates (and friends of 1.35): Adele, Aileen, Emily, Afaf, Viola and Meg. A PhD can be a very lonely experience at times and our frequent laughs and silliness have not made it so. Never have I been part of such a supportive group of women who want nothing but for each other to succeed, I have never felt an ounce of competitiveness between us navigating this world that is new to us all.

Of course, my highs and lows throughout this project have always been enhanced or alleviated by the love and support of my family, partner and friends. In particular I would like to thank my sister Bel. You are my idol in life and if I can achieve half of what you have in the last few years in the next few of mine I'll be extremely proud of myself: Mum and Dad, you did well.

Last and certainly least there is a special thank-you to my A-level maths teacher who laughed in my face in front of my Mum and Dad at a parents evening when I voiced that I'd like to do Physics at University. Who's laughing now?

Abstract

Society is living through a time-critical shift towards a more sustainable and circular economy. The daunting question plagues the passions of this generation of scientists: How can we sustain and enable a developed lifestyle worldwide to our growing population with finite resources? Over the last century; synthetic plastics, derived from fossil-based resources, have dominated the field of material sciences, providing innovative and functional solutions for a wide range of applications and advancing our lifestyles immeasurably. However, due to the limited nature of this resource, coupled with the fact that many synthetic polymers are non-biodegradable, there is an imperative drive for a more sustainable alternative. In fact, we are rapidly approaching the absolute threshold of plastic consumption that our planet can sustain, with the packaging industry alone contributing over one third of global plastic production, with a staggering 141 million tons of plastic packaging destined for landfill produced annually [1]. Clearly, it is vital that this industry's contribution to global warming and plastic pollution is addressed. As such, the food-packaging industry is seeing a resurgence in the popularity of biopolymer-based products. In particular, cellulose-based films, manufactured using the Viscose Method from sustainable forests are becoming a vital competitor to their synthetic counterparts.

First commercialised in the 1930s, the Viscose Method is used to extract cellulose from wood or plant pulp and convert it to functional films that are both biodegradable and renewable. Over the years, this technology has been optimised to provide high-quality food packaging with competitive mechanical and barrier properties. One of these

developments, was the addition of plasticisers in order to improve ductility, an essential property in application. The Futamura Group are the World's largest producers of these cellulose films, and currently employ a range of softeners and additives to improve performance. Their most effective plasticiser being a 3 component softener package containing Glycerine, MPG and Urea. With mounting pressures to reach global sustainability goals, it is important to investigate the efficacy of this softener package and ascertain how it could be altered and substituted for cheaper, greener alternatives.

As such, this thesis presents findings regarding the function of a range of established and potential softeners in both commercial and lab-softened films. We investigate the fluctuations of mechanical and molecular properties of films with varying concentrations of both individual and combination softeners packages, as well as an inclusion of a hemicellulose blend. To assess mechanical performance, a combination of tensile and strain-dependent impact testing, was employed. Molecular behaviour has been hypothesised through the application of Dynamic Mechanical Thermal Analysis across a range of frequencies and temperatures to identify key molecular relaxations of cellulose molecules under the influence of various softeners.

With this work, we have embarked on the beginning steps of a large scale commercial sustainability project that will see the revolution of plant-based films. This work will alleviate the limitations of relying on costly plasticisers that limit these films biodegradability, making cellulosic films *the* sustainable packaging of the future.



Figure 1: *Visual abstract of project*

Abbreviations

DMTA Dynamic Mechanical Thermal Analysis

XRD X-Ray Diffraction

MD Machine Direction

TD Transverse Direction

DP Degree of Polymerisation

MFA Microfibril angle

PVC Polyvinyl chloride

THF Tetrahydrofuran

wt % Weight percentage

MPG Monopropylene glycol

PEG Polyethylene glycol

LVDT Linear vertical displacement transducer

GCA Gas cooling accessory

GTA Glycerol triacetate

TTS Time-temperature superposition

f Frequency

T Temperature

W_i Initial weight

W_f Final weight

σ Stress

F Force

A Cross Sectional Area

ε Strain

Δl extension

l/L_0 original length of tensile, impact and slow puncture tests

v Poisson's Ratio

r Radius of impact testing area
 e Related to radius of impact testing area
 Y Young's Modulus
 e Sinusoidal strain
 e_0 Maximum sinusoidal strain
 σ_0 Maximum sinusoidal stress
 ω Angular frequency
 t Time, Thickness
 $\dot{\epsilon}$ sinusoidal strain rate
 η viscosity
 δ Phase lag
 E^* Complex modulus
 E' Storage modulus
 E'' Loss modulus
 T_γ Temperature at which the γ transition occurs
 T_β Temperature at which the β transition occurs
 T_α/T_g Temperature at which the α transition occurs (The glass transition temperature)
 T_m Melting temperature
 T_B Boiling temperature
 E_a Activation energy
 R Molar gas constant
 x Extension of impact and slow puncture testing
 ϵ Strain rate
 $\Delta\epsilon$ Strain
 v velocity
 w mass fraction

Contents

Dedication	i
Acknowledgement	ii
Abstract	iv
Abbreviations	vii
Contents	ix
List of Figures	xiii
List of Tables	xxiv
1 Introduction	1
1.1 Overview	1
1.2 Aims and objectives	3
1.3 Structure of Thesis	5
2 Literature Review	7
2.1 Cellulose	7
2.1.1 Earth's most abundant biopolymer	7
2.1.2 The plant cell wall	9
2.1.3 Extraction and regeneration	12
2.1.4 A brief history of cellulose advancements: From papyrus to polymer science	16
2.2 Cellulose Films	20

2.2.1	History of Cellophane	20
2.2.2	Futamura’s production process	23
2.3	Plasticisers	29
2.3.1	Function and performance	30
2.3.2	Plasticisers of cellulose	33
2.4	Project motivations	37
3	Experimental Methods	40
3.1	Materials	41
3.1.1	Commercial Films	42
3.1.2	Lab-made Films	43
3.2	Macroscopic Testing	49
3.2.1	Tensile Testing	50
3.2.2	Impact Testing	53
3.3	Molecular Property Testing	56
3.3.1	Dynamical Mechanical Thermal Analysis	57
3.4	Strain rate conversions	67
3.4.1	Conversion of speed to strain rate (Impact, puncture and tensile testing)	67
3.4.2	Conversion frequency to strain rate (DMTA)	71
3.4.3	Summary of speeds and strain rates	73
4	Commercial Films, Results and Discussions	74
4.1	Softener Content	74
4.2	Tensile Properties	75
4.2.1	Material property relationships	78
4.2.2	Machine and transverse uniaxiality	78
4.2.3	Variation of softener and additives	80
4.3	Falling weight and slow puncture impact properties	81
4.3.1	Crack Formation	85
4.3.2	Strain rate dependency	85
4.3.3	Variation of softener and additives	86
4.4	Dynamic Mechanical Thermal Analysis	88
4.5	Commercial films summary	95

4.6	Next Steps	96
5	Plasticiser variation of lab-based films, Results and Discussion	98
5.1	Softener Content	98
5.2	Tensile Properties	107
5.2.1	Material property relationships	110
5.2.2	Machine and transverse uniaxiality	110
5.2.3	Variation of softener	111
5.2.4	Comparison to commercial Films	120
5.3	Falling weight and slow puncture impact properties	121
5.3.1	Variation of strain rate and softener	122
5.3.2	Comparison to commercial films	128
5.4	Dynamic Mechanical Thermal Analysis	131
5.4.1	Variation of softeners on γ transition	133
5.4.2	Comparison to tensile properties	134
5.4.3	Water removal procedure	137
5.4.4	Multifrequency temperature ramps	142
5.5	Lab-based plasticiser variation summary	148
5.6	Next Steps	150
6	Hemicellulose variation of lab-based films, Results and Discussion	151
6.1	Softener Content	152
6.2	Tensile Properties	156
6.2.1	Material property relationships	159
6.2.2	Machine and transverse uniaxiality	159
6.2.3	Variation of hemicelluloses	159
6.2.4	Comparison to commercial and lab-plasticised films	163
6.3	Falling weight and slow puncture impact properties	166
6.3.1	Variation of hemicelluloses	167
6.3.2	Comparison to commercial and lab-plasticised films	170
6.4	Dynamic Mechanical Thermal Analysis	172
6.4.1	Variation of hemicelluloses on γ transition	173
6.4.2	Comparison to tensile properties	175

CONTENTS

6.4.3	Comparison to lab-plasticised films	178
6.4.4	Water removal procedure	181
6.5	Lab-based hemicellulose variation summary	185
7	Conclusions	189
7.1	Summary of outcomes	189
7.2	Future Work	197
A	Additional Figures	200
A.1	Room temperature peak analysis	200
A.2	Dynamic relaxations fittings	206
	References	220

List of Figures

1	<i>Visual abstract of project</i>	vi
2.1	<i>Repeating cellulose monomer unit, where $n = \text{Degree of Polymerisation}$</i>	8
2.2	<i>Schematic diagram representing the elementary model of the plant cell wall, including the architecture of the primary and secondary cell walls with cellulose microfibrils of crystalline and amorphous regions arranged helically with respect to a microfibril angle</i>	11
2.3	<i>Timeline indicating some key points in the understanding and development of cellulosic materials</i>	19
2.4	<i>DuPont advertising posters 1947-1950</i>	22
2.5	<i>The Viscose Process of extracting cellulose from wood pulp and converting it to films</i>	24
2.6	<i>Xanthation reaction of alkali cellulose to sodium cellulose xanthate by addition of carbon disulphide</i>	26
2.7	<i>Theories of the mechanisms of plasticisation: Lubricity, gel and free volume</i>	32
2.8	<i>Futamura plasticisers: Glycerine, Mono Propylene Glycol, Urea and Polyethylene Glycol</i>	35
3.1	<i>Depiction of the softening process employed to produce lab made films</i>	44
3.2	<i>Photograph of cellulose wet gel placed in A4 frame to be dried</i>	45
3.3	<i>Photograph of Frames drying in Oven rack</i>	46

LIST OF FIGURES

3.4	<i>Dumbbell cutting layout for tensile testing with dimensions of dumbbells annotated. This cutting stencil allowed for 5 repeats in both Machine (MD) and Transverse (TD) Directions</i>	50
3.5	<i>Instron Tensile Tester used to perform tensile measurements on samples, with clamping of dumbbell highlighted schematically . . .</i>	51
3.6	<i>Typical stress/strain curve indicating regions of tensile response typical for a polymeric material: Elastic region, Plastic Region and Breaking Point</i>	52
3.7	<i>Rosand Impact Tester with dart and sample plates highlighted schematically</i>	54
3.8	<i>Typical Force/extension graph with maximum force, extension and energy indicated on the graph</i>	55
3.9	<i>Slow puncture impact test set-up using Instron tester in compression mode, with dart and specialised clamp highlighted</i>	56
3.10	<i>Graphical depiction of oscillatory force and resultant material deformation (strain) observed in DMTA measurements.</i>	59
3.11	<i>Depiction of phase lag, δ, of material strain in response to oscillatory stress for (a) Elastic (b) Viscous and (c) Viscoelastic materials.</i>	61
3.12	<i>Discovery DMA 850 from TA instruments, with tensile clamp highlighted.</i>	62
3.13	<i>Crankshaft depiction of polymer chain, used to demonstrate movement of side chains which has been shown by Atomic Force Microscopy to be an appropriate approximation of the molecular chain</i>	63
3.14	<i>Viscoelastic response of an idealised polymer from low to high temperature, representing a number of transitions depending on side chain and backbone motion.</i>	64
3.15	<i>Depiction of deformation used to calculate strain rates for (a) Impact and slow puncture testing (modelled as a centrally loaded circular plate with edges supported) and (b) Tensile Testing</i>	68
3.16	<i>Depiction of Time Period of oscillation</i>	72
4.1	<i>Typical stress/strain curves for the unsoftened and 3 component softener commercial films</i>	75

LIST OF FIGURES

4.2	<i>Ashby Plots depicting the variation of tensile properties for the commercial film set in their machine (square markers) and transverse (diamond markers) directions (a) Young's Modulus against strain at failure, (b) Strength against strain at failure and (c) Strength against Young's Modulus</i>	77
4.3	<i>Depiction of two processes that impart uniaxiality: extrusion and tension and resultant film with machine (MD) and transverse (TD) directions</i>	79
4.4	<i>Typical force/extension curves for the unsoftened and 3 component softener commercial films</i>	82
4.5	<i>Falling weight and slow puncture impact properties across a range of strain rates for the commercial film set where the black dotted line indicates the strain rate at which tensile testing was performed (a) Strain against strain rate, (b) Normalised Maximum Force against strain rate, (c) Normalised energy against strain rate</i>	84
4.6	<i>Annotated image of crack formation of films from impact</i>	85
4.7	<i>Dynamic Mechanical Thermal Analysis of commercial film set from -100 °C to 260 °C at oscillating frequency of 1 Hz (a) $\tan \delta$ against Temperature, (b) Storage Modulus against Temperature and (c) Loss Modulus against Temperature</i>	89
4.8	<i>Storage modulus (G' in this example) and $\tan \delta$ profile of cellulose acetate plasticised by increasing concentrations (85/15 wt % - 60/40 wt %) GTA and the varying effect on primary (α) and secondary (β, γ) transitions</i>	93
4.9	<i>$\tan \delta$ transitions of commercial film set, with varying peak positions, zoomed in on (a) presumed α transition between 160 °C to 260 °C and (b) another secondary sub-zero relaxation between -100 °C to 0 °C</i>	94
5.1	<i>Lab-softened films visual appearances. Migration effects clearly visible for Urea films</i>	99

LIST OF FIGURES

5.2	<i>Softener in film and softener in bath wt % comparison for individual and blend softeners of lab-plasticised films with enrichment factors indicated as data labels. Where the 3 component softener contains (This text has been removed by the author of this thesis for confidentiality reasons) [REDACTED]</i>	103
5.3	<i>Interactions of plasticisers (Glycerine, MPG and Urea) and water with cellulose polymer chains</i>	106
5.4	<i>Ashby Plots depicting the variation of tensile properties for the lab-plasticised film set in their machine (square markers) and transverse (diamond markers) directions (a) Young's Modulus against strain at failure, (b) Strength against strain at failure and (c) Strength against Young's Modulus</i>	109
5.5	<i>Variation of tensile properties with increasing Glycerine content (a) Young's Modulus (b) Strength and (c) Strain at failure</i>	112
5.6	<i>Variation of tensile properties with increasing MPG content (a) Young's Modulus (b) Strength and (c) Strain at failure</i>	113
5.7	<i>Variation of tensile properties with increasing Urea content, with blue dashed line indicating the plateau in properties experienced due to maximum uptake (a) Young's Modulus (b) Strength and (c) Strain at failure</i>	115
5.8	<i>Variation of tensile properties with increasing 3 Component Softener content (a) Young's Modulus (b) Strength and (c) Strain at failure</i>	117
5.9	<i>Variation of tensile properties with increasing Glycerine, MPG, Urea and 3 Component Softener content (a) Young's Modulus (b) Strength and (c) Strain at failure</i>	119

5.10 *Ashby Plots depicting the variation of tensile properties for the commercial and lab-plasticised unsoftened and 3 component softener (This text has been removed by the author of this thesis for confidentiality reasons) ██████ films in their machine (square markers) and transverse (diamond markers) directions with dashed lines indicating the two different trendlines that result from production process causing a difference in orientation of polymeric chains (a) Young’s Modulus against strain at failure, (b) Strength against strain at failure and (c) Strength against Young’s Modulus 120*

5.11 *Falling weight and slow puncture impact properties across a range of strain rates for glycerine lab-based film set where the black dotted line indicates the strain rate at which tensile testing was performed (a) Strain against strain rate, (b) Normalised Maximum Force against strain rate, (c) Normalised energy against strain rate 122*

5.12 *Falling weight and slow puncture impact properties across a range of strain rates for MPG lab-based film set where the black dotted line indicates the strain rate at which tensile testing was performed (a) Strain against strain rate, (b) Normalised Maximum Force against strain rate, (c) Normalised energy against strain rate 123*

5.13 *Falling weight and slow puncture impact properties across a range of strain rates for urea lab-based film set where the black dotted line indicates the strain rate at which tensile testing was performed (a) Strain against strain rate, (b) Normalised Maximum Force against strain rate, (c) Normalised energy against strain rate 125*

5.14 *Falling weight and slow puncture impact properties across a range of strain rates for 3 component softener lab-based film set where the black dotted line indicates the strain rate at which tensile testing was performed (a) Strain against strain rate, (b) Normalised Maximum Force against strain rate, (c) Normalised energy against strain rate 127*

LIST OF FIGURES

5.15 *Falling weight and slow puncture impact properties across a range of strain rates for the commercial and lab-plasticised unsoftened and 3 component softener (This text has been removed by the author of this thesis for confidentiality reasons) ██████ films where the black dotted line indicates the strain rate at which tensile testing was performed (a) Maximum strain against strain rate, (b) Normalised Maximum Force against strain rate, (c) Normalised energy against strain rate 130*

5.16 *Dynamic Mechanical Thermal Analysis, $\tan \delta$ profiles, of lab-plasticised film set from -100°C to 120°C at oscillating frequency of 1 Hz (a) Glycerine (b) MPG (c) Urea and (d) 3 Component Softener, each compared to the lab-based unsoftened film 132*

5.17 *Variation of γ peak with plasticiser content of lab-plasticised films (a) temperature of γ transition (b) amplitude of γ transition . . . 134*

5.18 *Variation of γ transition $\tan \delta$ peak amplitude with tensile properties for lab-plasticised film set (a) Young's Modulus (b) Strength and (c) Strain at Failure 135*

5.19 *Variation of γ transition $\tan \delta$ peak temperature with tensile properties for lab-plasticised film set (a) Young's Modulus (b) Strength and (c) Strain at Failure 136*

5.20 *Dynamic Mechanical Thermal Analysis (water removal procedure from -100°C to $+120^{\circ}\text{C}$) $\tan \delta$ profiles of glycerine lab-plasticised films (a) 10 % Glycerine film (b) 20 % Glycerine film (c) 30 % Glycerine film. Where run (1) represents the first run to remove free water from films and (2) represents the second run on the dried film. 138*

5.21 *Dynamic Mechanical Thermal Analysis (water removal procedure from -100°C to $+120^{\circ}\text{C}$) $\tan \delta$ profiles of MPG lab-plasticised films (a) 10 % MPG film (b) 20 % MPG film (c) 30 % MPG film. Where run (1) represents the first run to remove free water from films and (2) represents the second run on the dried film. 139*

LIST OF FIGURES

5.22	<i>Dynamic Mechanical Thermal Analysis (water removal procedure from -100 °C to + 120 °C) tan δ profiles of urea lab-plasticised films (a) 10 % Urea film (b) 20 % Urea film (c) 30 % Urea film. Where run (1) represents the first run to remove free water from films and (2) represents the second run on the dried film.</i>	140
5.23	<i>Dynamic Mechanical Thermal Analysis (water removal procedure from -100 °C to + 120 °C) tan δ profiles of 3 component softener lab-plasticised films (a) 10 % 3 Component Softener film (b) 20 % 3 Component Softener film (c) 30 % 3 Component Softener film. Where run (1) represents the first run to remove free water from films and (2) represents the second run on the dried film.</i>	141
5.24	<i>Dynamic Mechanical Thermal Analysis (multifrequency scans at 0.1, 1, 10 and 100 Hz from -100 °C to + 120 °C) tanδ profile for 20 % glycerine films</i>	143
5.25	<i>Arrhenius Plot of ln(f) against 1/T for glycerine 18 % films from tanδ analysed across four frequencies 0.1, 1, 10, 100 Hz. Gradient = 13000 ± 2000</i>	146
5.26	<i>Variation in temperature of γ peak with increasing frequency of temperature ramps</i>	147
6.1	<i>Constituents of hemicellulose hydrolysate, depicted to indicate their hydrophilic nature due to number of hydrogen bond forming sites .</i>	153
6.2	<i>Hemicellulose-incorporated films visual appearances. Migration effects visible as brown hue on films</i>	153
6.3	<i>Softener in film and softener in bath wt % comparison for hemicellulose-based films with enrichment factors indicated as data labels</i>	155
6.4	<i>Softener in film and softener in bath wt % comparison for hemicellulose-based films and lab softened glycerine film with enrichment factors indicated as data labels</i>	156

LIST OF FIGURES

6.5	<i>Ashby Plots depicting the variation of tensile properties for the hemicellulose-based film set in their machine (square markers) and transverse (diamond markers) directions (a) Young's Modulus against strain at failure, (b) Strength against strain at failure and (c) Strength against Young's Modulus</i>	158
6.6	<i>Variation of tensile properties with increasing hemicellulose content (a) Young's Modulus (b) Strength and (c) Strain at failure . .</i>	160
6.7	<i>Variation of tensile properties with increasing 2 component softener content (a) Young's Modulus (b) Strength and (c) Strain at failure</i>	162
6.8	<i>Ashby Plots depicting the variation of tensile properties for the commercial, lab-plasticised and hemicellulose based films that contain (This text has been removed by the author of this thesis for confidentiality reasons) ██████████ in their machine (square markers) and transverse (diamond markers) directions (a) Young's Modulus against strain at failure, (b) Strength against strain at failure and (c) Strength against Young's Modulus</i>	165
6.9	<i>Falling weight and slow puncture impact properties across a range of strain rates for hemicellulose lab-based film set where the black dotted line indicates the strain rate at which tensile testing was performed (a) Strain against strain rate, (b) Normalised Maximum Force against strain rate, (c) Normalised energy against strain rate</i>	167
6.10	<i>Falling weight and slow puncture impact properties across a range of strain rates for 2 component softener lab film set where the black dotted line indicates the strain rate at which tensile testing was performed (a) Strain against strain rate, (b) Normalised Maximum Force against strain rate, (c) Normalised energy against strain rate</i>	169

LIST OF FIGURES

6.11	<i>Falling weight and slow puncture impact properties across a range of strain rates for the commercial, lab-plasticised and hemicellulose films that contain (This text has been removed by the author of this thesis for confidentiality reasons) ██████████, where the black dotted line indicates the strain rate at which tensile testing was performed (a) Strain against strain rate, (b) Normalised Maximum Force against strain rate, (c) Normalised energy against strain rate</i>	171
6.12	<i>Dynamic Mechanical Thermal Analysis, $\tan \delta$ profiles, of hemicellulose-based film set from $-100\text{ }^{\circ}\text{C}$ to $120\text{ }^{\circ}\text{C}$ at oscillating frequency of 1 Hz (a) Hemicellulose films (b) 2 Component Softener films, each compared to the lab-based unsoftened film. Position of expected γ transition annotated on graphs.</i>	172
6.13	<i>Variation of γ peak with 2 component softener content (a) temperature of γ transition (b) amplitude of γ transition</i>	174
6.14	<i>Variation of γ transition $\tan \delta$ peak amplitude with tensile properties for 2 component softener films (a) Young's Modulus (b) Strength and (c) Strain at Failure</i>	176
6.15	<i>Variation of γ transition $\tan \delta$ peak temperature with tensile properties for 2 component softener films (a) Young's Modulus (b) Strength and (c) Strain at Failure</i>	177
6.16	<i>Comparison of variation of γ transition $\tan \delta$ peak amplitude with tensile properties for 3 component and 2 component softener films (a) Young's Modulus (b) Strength and (c) Strain at Failure</i>	179
6.17	<i>Comparison of variation of γ transition $\tan \delta$ peak temperature with tensile properties for 3 component and 2 component softener films (a) Young's Modulus (b) Strength and (c) Strain at Failure</i>	180
6.18	<i>Dynamic Mechanical Thermal Analysis (water removal procedure from $-100\text{ }^{\circ}\text{C}$ to $+120\text{ }^{\circ}\text{C}$) $\tan \delta$ profiles of hemicellulose-based films (a) 11 % hemicellulose film (b) 18 % hemicellulose film (c) 28 % hemicellulose film. Where run (1) represents the first run to remove free water from films and (2) represents the second run on the dried film.</i>	182

LIST OF FIGURES

6.19	<i>Dynamic Mechanical Thermal Analysis (water removal procedure from -100 °C to + 120 °C) tan δ profiles of 2 component softener lab-based films (a) 8 % 2 Component Softener film (b) 14 % 2 Component Softener film (c) 32 % 2 Component Softener film. Where run (1) represents the first run to remove free water from films and (2) represents the second run on the dried film.</i>	183
7.1	<i>Master Ashby Plots providing comparisons between tensile properties for commercial and lab-made films where the axis of (a) and (b) have been presented on a logarithmic scale to display the relationship between Young’s modulus and strength with strain at failure</i>	191
7.2	<i>Master DMTA temperature ramp tanδ profiles providing comparisons between dynamic transitions for for commercial and lab-made films</i>	193
7.3	<i>Master plot of the variation of γ transition tanδ peak amplitude with tensile properties</i>	193
7.4	<i>Master falling weight and slow puncture impact graphs providing comparisons of impact properties across a range of strain rates for commercial and lab-made films</i>	194
A.1	<i>Room Temperature presumed β peak variation with plasticiser content (a) Shift in temperature (b) Increase in peak intensity</i>	200
A.2	<i>Variation of mechanical performance of plasticised films with tanδ presumed β peak height</i>	201
A.3	<i>Variation of mechanical performance of plasticised films with tanδ presumed β peak temperature</i>	202
A.4	<i>Room Temperature presumed β peak variation with hemicellulose and 2 component softener content (a) Shift in temperature (b) Increase in peak intensity</i>	203
A.5	<i>Variation of mechanical performance of hemicellulose films with tanδ presumed β peak height</i>	204
A.6	<i>Variation of mechanical performance of hemicellulose films with tanδ presumed β peak temperature</i>	205

LIST OF FIGURES

A.7 <i>Asymmetric double Sigmoidal function fitting applied by python to determine peak positions of $\tan\delta$ γ transition</i>	206
---	-----

List of Tables

3.1	<i>Table of all commercial and lab-made films investigated in this work</i>	48
3.2	<i>Table of average thickness of commercial and lab-based films.</i>	70
3.3	<i>Table of falling weight and slow puncture impact speeds converted to strain rates.</i>	71
3.4	<i>Summary of conversions of speeds and frequencies to strain rates for all testing methods</i>	73
4.1	<i>Summary of commercial films tested in this Chapter</i>	74
4.2	<i>Tensile Test results of commercial films in machine and transverse directions for Young's Modulus, Strength and Strain at Failure</i>	76
5.1	<i>Table of lab-softened films and their softener in film content. Where 3 component softener: (This text has been removed by the author of this thesis for confidentiality reasons)</i>	100
5.2	<i>Tensile Test results of lab-based plasticised films in machine and transverse directions for Young's Modulus, Strength and Strain at Failure</i>	108
6.1	<i>Table of lab-made films and their hemicellulose or 2 component softener (This text has been removed by the author of this thesis for confidentiality reasons)</i>	154
6.2	<i>Tensile Test results of lab-hemicellulose films in machine and transverse directions for Young's Modulus, Strength and Strain at Failure</i>	157

Chapter 1

Introduction

1.1 Overview

For the duration of my PhD I have been lucky enough to collaborate with Industry Partners, The Futamura Group. This partnership has given me an insight into industry, which has proved to be a powerful driving force behind my research, providing meaningful and impactful focal points. I've had the opportunity to see their production process first hand during tours of the entire Wigton production plant and spent time using their facilities and working alongside their researchers. I would be remiss not to mention the invaluable friendships and mentorships I have developed with their incomparably welcoming staff. From the first visit, it was clear that I was to be integrated immediately into their friendly and approachable environment that was upheld throughout my time there. I think it must be incredibly rare to have such a positive experience with an industry partner in the way that these collaborations are modelled as being and it is something that I have appreciated more and more throughout my project. This forging of industry and academia has been a genuine strive towards experimental understanding, embodying the true essence of scientific pursuit that we all yearn for. Despite the warnings from co-workers about the arduous nature of thesis writing, I have found this work to be a joy to write as I have reminisced over the last 4 years of my life and the lessons and challenges this time has provided; I am able to say I am proud of everything I have achieved with Futamura's help and guidance

Established in Japan in 1947, The Futamura Group are the world's largest producer of cellulose films [2]. Their flagship products, CellophaneTM and NatureFlexTM, offer renewable food packaging solutions manufactured from wood pulps, with a clear drive for sustainability being advocated throughout this company's ethos. These films have exceptional mechanical and barrier properties; making them suitable for a wide range of applications from food packaging of confectionery to pharmaceuticals and personal care.

As with many industrial PhDs, the focus at the beginning of this 4 year endeavor was extremely broad, with many interesting avenues available to explore. Back in March 2020, Futamura provided 5 different commercially-available CellophaneTM products, each with varying amounts of softeners and coatings. This instigated the initial tensile testing of these samples, to assess the mechanical performance of each film and the influence of the softeners and additives. As the project evolved, the vision soon became clear; to link the macroscopic and molecular properties of these films in order to elucidate how the softeners interact with cellulose, resulting in a plasticising effect. Bombardment was our strategy, and a barrage of material analysis techniques were applied to these 5 films, including; tensile and impact testing, Raman spectroscopy, X-Ray Diffraction, Nuclear Magnetic Resonance and Dynamic Mechanical Thermal Analysis. Eventually, we began to understand how each of these techniques might aid our understanding of this softening process. It became clear that some interesting trends were emerging when aligning mechanical performance with the molecular movement seen in DMTA results. This led to the manufacturing of lab-plasticised films, whereby individual and blend softeners were added in specific quantities to the films. Thus, the contribution of individual softeners could be identified and allied with the properties of commercial films.

Linking and aligning these macroscopic and molecular properties has given insights into the performance of plasticisers in Futamura's films. We for-see that the results from this project will inspire a host of future work possibilities with regards to the optimisation for Futamura's production and plasticising process. Through this work we have been able to apply academic level materials research to the properties of an industrial product, with the hope of making a meaningful impact on their company and process.

Despite having lost a year of lab-work to both COVID 19 and a building move for the whole of Physics, accompanied by the difficulty in navigating publishing around an industrial product; I believe I have thrown my self at every opportunity this PhD has offered and am so incredibly grateful for so many life defining and developing experiences. I have travelled to 5 countries within 3 continents for conferences and had the chance to engage with the wider scientific community on countless occasions, always learning about the breadth of research carried out across the globe. At these events, the interest and engagement regarding my project was astounding, seeing sustainability at the forefront of many researchers focus is an honour to be a part of. As well as this, I was able to engage a wider general audience with my work, making an art installation using Futamura's films in collaboration with the Leeds School of Design for Leeds Light Night; allowing the platform for the public to engage with research level science. I have been fortunate enough to be awarded several prize for my contribution in competitions and events including The Henry Cavendish Gold Medal and Dyson Sustainability Silver Award, which led me to presenting my work to members of parliament and heads of esteemed scientific bodies at The Parliamentary and Scientific Committee Meeting July 2023. Being able to share this work with an engaged audience of people who want to make a change was undoubtedly a highlight of the last four years and the opportunities that this PhD have allowed me have been undoubtedly once in a lifetime.

1.2 Aims and objectives

The scope for this project branches across several overall objectives. On a personal level and something that is also integral to Futamura's vision, is the contribution towards a sustainable future. The climate crisis is reaching a critical stage and the advancement of renewable, biodegradable materials is n vital piece of this ever growing puzzle. As we begin to reduce our reliance on fossil-based resources, cellulose and other biopolymers will pave the way in this new wave of material science. Futamura emphasise and evidence their own commitment to sustainability. They concentrate on the renewability of wood pulps from certified forests, Life Cycle Assessments and end of life compostability; all of which have resulted

1.2 Aims and objectives

in a reduction of their carbon foot print of 30 % since 2006 [2]. These films already boast strong sustainability credentials, providing an excellent alternative to synthetic plastics.

This project and the work of Futamura's research group instigate the possibility of improving these credentials even further. For example, in this work, the impact of Futamura's softener packages on mechanical and molecular properties of films is reviewed. Through this understanding, it is hoped that steps can be taken to improve the existing process of plasticisation. Furthermore, this report details the experimental inclusion of a blend of plant-based sugars to investigate whether they induce a similar plasticising affect to traditional softeners, based off literature examples that demonstrate the softening effect of residual hemicelluloses in cellulosic products [3]. Finding an effective, renewable plasticiser that interacts with these films similarly to Futamura's current 3-component and 1-component softener packages would be a giant leap forward with regards to both sustainability and costs, eliminating the reliance for expensive softeners. Understanding how these softeners function in their interactions with cellulose through this project, we are one step closer to enabling the wide scale conception of plant-derived plasticisers.

Additionally, this work also facilitates the possibility of reducing costs on expensive plasticisers that Futamura currently depend on. Presently, Futamura's standard 3 component softener package containing glycerine, MPG and urea has been unchanged since its conception as it is an effective blend that enhances properties of the films in a way that makes them effective in application. However, in the past, it was generally accepted that glycerine was the expensive primary softener that contributed the majority of the softening affect, whilst the MPG and Urea were considered secondary components, included to reduce costs. However, in recent years, Futamura report that the commercial prices of MPG and Urea have been steadily increasing, throwing their role and necessity in the package into question. This work assesses their softening contribution at various concentrations, with the end goal of making recommendations of how Futamura can alter these components as well as incorporating novel softeners to reduce costs.

Lastly, and certainly not least, is the contribution to the advancement of plant sciences and the role and properties of the cellulose molecule. The architecture of the plant cell wall exists as a complex, and varied, blend of cellulose, hemicelluloses, pectin and lignin; whose combination has been optimised by Nature over millions of years. Research on how these components interact is key to understanding a plant's mechanical, structural and biological properties; and by extension, the properties of cellulose bi-products such as Cellophane. However, due to vast divergences in cell wall structure between plant species (as well as within species with regards to environmental growth conditions) a comprehensive understanding of the relationships and physical parameters that drive a plant's characteristics remains elusive. This work will contribute just a small part of this greater understanding of Nature's complexity. However, with the resurgent dawn of plant based materials, this understanding is essential in our advancement of these materials for a greener world.

1.3 Structure of Thesis

To begin this thesis, a literature review has been conducted to introduce the reader to some key research surrounding this topic. First, some information about the biopolymer that makes these films, cellulose, is provided; including some basic properties as well as its origin, extraction and use throughout human advancement. Its importance as an abundant and sustainable material is highlighted during this section, as well as how plasticisers are used to alter its properties to make it suitable for a range of different applications.

Following this literature review, the methods of analysis are included. The films tested in this work consist of three groups: commercial, plasticised lab-based and hemicellulose lab-based. For each set of these films, the same techniques have been applied to characterise performance. Macroscopic testing in the form of tensile and impact testing has been compared to molecular testing in the form of Dynamic Mechanical Thermal Analysis.

Analysis of these techniques takes the form of three results chapters describing each group of films: commercial, plasticised lab-based and hemicellulose lab-based. The commercial chapter details the complexity in understanding the

plasticisation packages that Futamura currently employ. The plasticised lab-based film chapter aims to explain the performance of these commercial films by separating commercial softeners into their individual components to determine their contributions at varying concentrations. Finally, the hemicellulose lab-based chapter aims to incorporate an alternative, plant-based additive as a plasticiser in films, based off hypotheses formed in the lab-plasticised results chapter about the importance of water on the softening of these materials.

Finally, the summary aims to link these results together and provide overarching findings and the hypothesis that have been drawn. Based off these results, recommendations have been proposed to Futamura about how these findings can lead to the selective choosing of alternative softeners and what attributes of plasticisers might result in optimum performance of films. These recommendations to softener packages, along with further experimental and simulation testing have been proposed for candidates of future work.

Chapter 2

Literature Review

2.1 Cellulose

Cellulose is a valuable raw material with a diverse breadth of applications in the materials industry, including: paper, textiles, biocomposites and importantly for this work; food packaging films. Its influence over societal evolution trickles throughout history, with examples of flax-based ropes dating back as far as the 6th Century BC, not to mention enabling and propelling the written word on papyrus in Ancient Egypt. This section aims to discuss this polysaccharide's prevalence as a renewable material, including its extraction methods and packaging advancements. First, some basic facts will be outlined.

2.1.1 Earth's most abundant biopolymer

Cellulose was discovered in 1838 thanks to the efforts of renowned French chemist, Anselme Payen, who identified this extract as the main chemical constituent of plants, with molecular formula $C_6H_{10}O_5$ [4][5]. Since then, applied research into this material has directed the field of plant science. Its extraction and properties have been tirelessly progressed and expertly exploited to provide a range of advanced materials.

Cellulose is a polysaccharide, typically extracted from plants such as cotton or hemp, but also existing in some algae and bacteria, as well as being first synthetically polymerised in 1992 [6]. Despite some diversity in nomenclature, it is ac-

cepted that cellulose is a linear chain polymer of $\beta(1\rightarrow4)$ linked D-glucopyranose units, linked via acetal covalent interactions between carbohydrate units attached to C4 and C1 carbons, as shown in Figure 2.1 [7]. Polymer chain length is defined by the Degree of Polymerisation (DP), or the number of monomer units, of the cellulose chain, which can range anywhere between 800-10000 in plant fibres, reducing to 250-500 when regenerated in extraction processes due to unavoidable chain degradation [8].

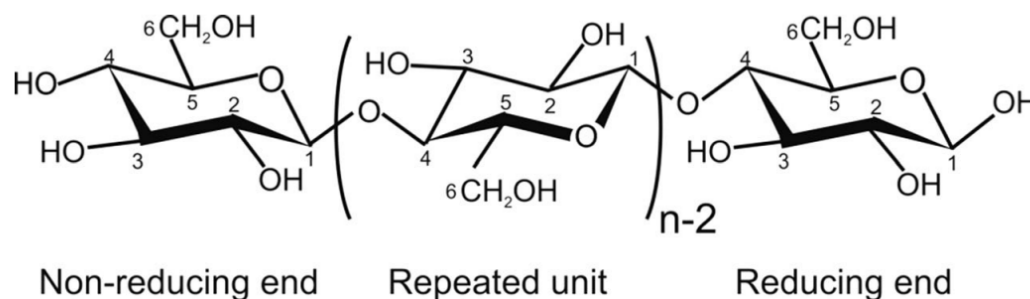


Figure 2.1: *Repeating cellulose monomer unit, where $n = \text{Degree of Polymerisation}$ [7]*

In plants, cellulose polymer chains exist as ‘microfibrils’ within in a complex laminate matrix composing of hemicelluloses, lignin, pectins and waxes. This composite blend has evolved to effectively maintain the structure of plants and withstand the environmental forces of Nature. As such, cellulose is inherently challenging to extract from plants. In fact, a modern assessment of the Lindman Hypothesis tells us that hydrogen bonds and van der Waals interactions act to inhibit cellulose’s solubility in water and most organic solvents [9]. This insolubility, coupled with a high melting (after significant thermal degradation of chains) temperature of 467 °C, means that cellulose processing is not trivial [10]. As such, a number of extraction techniques have been developed and advanced since its first discovery to obtain this resource in the most efficient and environmentally friendly manor.

With the development of characterisation techniques such as X-Ray Diffraction; it was discovered that cellulose can exist in a range of allomorphs. In plant materials; its native crystal structure exists as cellulose I. However, once

regeneration during extraction processing or other chemical processes such as derivatisation have taken place, this origin structure is destroyed and is no longer achievable. As such, the allomorphs: cellulose II, cellulose III and cellulose IV are observed, as well as various ester derivatives. Enhanced donor reactivity of cellulose's numerous hydroxyl groups allows for an extensive network of hydrogen bonds that instigate the differing structures of these multiple allomorphs, resulting in cellulose's distinctive traits such as hydrophilicity, chirality and degradability [8].

Cellulose's structure consists of a long polymeric chain of carbohydrate monomers units, first revealed by Hermann Staudinger's 'Über Polymerisation'; where as it was previously assumed that cellulose formed aggregated clusters of the carbohydrate units [11]. The revelation that these units were in fact linked via covalent interactions between carbohydrate units to form a long chain was ground breaking, awarding Staudinger the Nobel Prize in Chemistry in 1958; marking the origin of polymer science. For cellulose, this discovery embodied the combination of two different fields: organic carbohydrate and polymer sciences. This macromolecule has architecture, reactivities and properties governed by the polymer dynamics of intermolecular interactions, cross-linking, functional groups and the degree of polymerisation [8].

Cellulose is the world's most abundant biopolymer and, despite processing challenges, extraction makes up 1.5 teratonnes of total annual biomass [8]. The volume of this production speaks for cellulose's most treasured properties and consequential suitability for numerous applications.

2.1.2 The plant cell wall

The architecture of the plant cell wall exists as a complex and varied blend of cellulose microfibrils, hemicelluloses, pectin and lignin; whose combination has been optimised by Nature over millions of years of evolution. The symbiotic relationship between each of these components is the key to understanding a plants mechanical performance. However, due to the vast divergences in cell wall structure between plant species, as well as within species with regards to environmental growth conditions; a comprehensive understanding of the relationships

that drive a plant's characteristics remains elusive. This knowledge is vital in the drive for unlimited utilisation of plants for endless applications in the materials and agricultural industries, in order to accelerate the switch to renewable and biodegradable materials. This is particularly prevalent for Futamura who employ a range of wood pulps in their film manufacturing such as eucalyptus and western hemlock; with current research by their team looking into the efficacy of tomato stalk origin pulp. Despite much of the plant's original architecture being destroyed during processing, it is important to understand how nature has developed plant's structure components to work together to impart strength such that we can elucidate how the properties of regenerated products contribute to performance.

Figure 2.2 shows a schematic diagram for the standard model of the plant cell wall; although, it should be noted that there is much diversity in this representation between species. In this model, the plant cell wall is a composite laminate material made of one primary and three secondary cell walls surrounding a central cavity, known as the lumen. In these cell walls, cellulose chains form 'microfibrils'; clusters of up to 36 cellulose chains joined via hydrogen bonding, with both amorphous and crystalline regions. These microfibrils form the main reinforcing network of the cell wall composite. Whilst the matrix component of the composite consists of hemicelluloses (heterogeneous polymers of sugars) and lignins (complex 3D branched polymers of phenylpropane units) which act to reinforce the cellulose microfibril network [12]. Due to the cell walls multiple laminate layers, determining mechanical performance of plant fibres is complex and unpredictable. However, as the second secondary cell wall is normally the thickest layer, it often governs the overall properties of the fibre [13]. In the primary cell wall, microfibrils are randomly orientated, whilst in the secondary cell walls the microfibrils are helically arranged with respect to a microfibril angle (MFA), wrapping around and creating a preferential direction of growth [12]. The MFA of each secondary layer is different, manifesting in high tensile strength in multiple directions of the fibre.

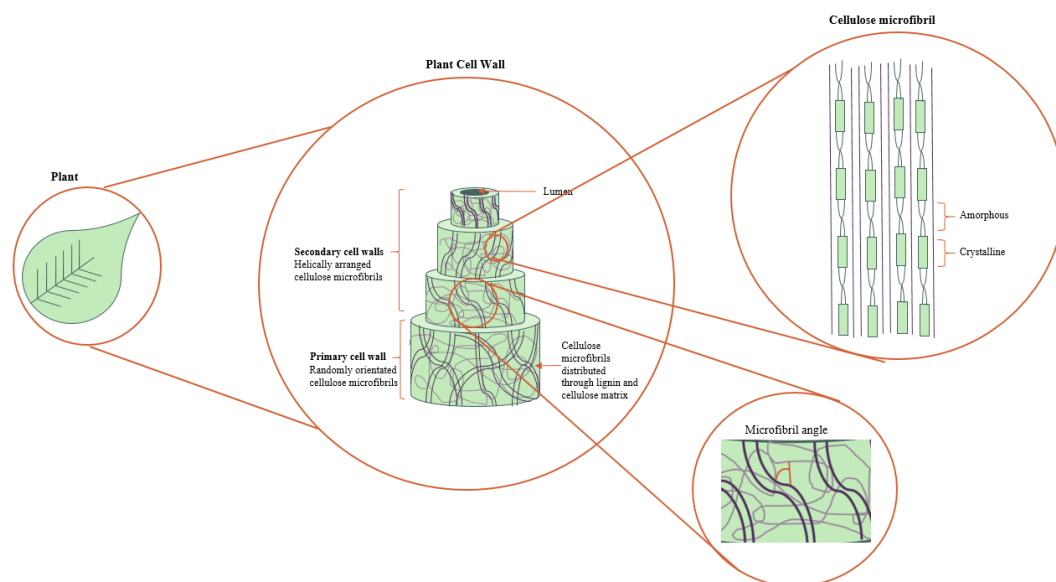


Figure 2.2: Schematic diagram representing the elementary model of the plant cell wall, including the architecture of the primary and secondary cell walls with cellulose microfibrils of crystalline and amorphous regions arranged helically with respect to a microfibril angle. Adapted from [14]

One important step towards comprehending how cellulosic products can be optimised is the elucidation of how cell wall components impact the mechanical properties of a plant fibre. In particular, it is generally accepted that composition, microfibril angle and lumen size are the key indicators of fibre performance [15]. However, other features such as degree of polymerisation and crystallinity also play a role, yet their contributions are not considered a driving force. Understanding how all these features work together to enhance the mechanical performance of a fibre is the end goal of years of important research from many institutions. It is also important for researchers of cellulosic products to have this understanding as the same properties that impact raw plant fibres are likely to impact regenerated fibres or films, despite much of the original structure being destroyed. For many researchers, the first material characterisation techniques employed to analyse cellulosic products are those that would be used to assess the variable plant fibre structures listed above.

2.1.3 Extraction and regeneration

Before cellulose can be utilised as a biopolymer, it must first be isolated from plant material, a process that comes with its own challenges. As already touched upon, the cellulose molecule requires non-traditional solvents for extraction from the complex plant composite due to close packing of cellulose chains of lengths up to 15000 units (cotton) joined by hydrogen bonding [16]. Furthermore, due to the molecule's inherently high melting temperature, it is also impossible to attain through heat treatments without considerable degradation to its properties. As a result of these obstacles, much of cellulose research is focused on developing effective and sustainable routes for extraction, resulting in a host of advancements seen with the resurgence of these biopolymers. Typically, techniques aim to dissolve the cellulose in a chosen solvent, shape the resulting solution for intended application such as fibre or film and regenerate the cellulose in a chosen anti solvent.

The assessments of the environmental repercussions of these techniques are crucial to maintain cellulose's green credentials. In fact, a number of novel techniques have been discovered in recent years and have awarded recognition and several prizes for this sector of materials development due to cellulose's importance as a sustainable material [16]. Not only must these extraction solutions be sustainable and as environmentally benign as possible (i.e non-toxic with little poisonous gas release) in order to maintain cellulose's sustainable status. They should also cause little-to-no degradation to cellulose chains during separation from the lignin matrix. This task is no small feat and extensive research has been carried out to find a processing method that meets these criteria. This section will give a general overview of these techniques and their advancements, whilst Section 2.2.2 will cover Futamura's Cellophane specific process in more detail.

- **The Viscose Process:** First patented in 1894 as a technique to produce artificial silk, The Viscose Process (also referred to as The Xanthate Process) remains the most commonly used method of cellulose regeneration in industry today. Despite being developed over a century ago, between the years 2000 - 2010, global viscose fibre production rose by 6.7 % annually [17]. The films produced by Futamura make up part of this global viscose market,

as well as popular fibres such as Rayon. In this process, sodium hydroxide pre-treated dissolving pulp is used to derivatise plant-based cellulose with carbon disulphide, creating a viscous solution of sodium xanthogenate. This cellulose xanthate is then mixed with aqueous sodium hydroxide, creating a ‘viscose’ solution. Once shaped and subsequently precipitated with acidic solution, high purity cellulose can be regenerated [8] [18]. The resulting product, coined by various names including viscose, rayon and modal, has a wide range applications that have gained popularity, particularly in the textiles and packaging industries.

However, The Viscose Process does not provide a wholly green and sustainable solution to cellulose extraction. Despite research efforts spanning 100 years, this process still requires toxic chemicals, production of harmful carbon disulphide and a large quantity of fresh water, not to mention the associated degradation of the cellulose backbone which has a negative effect on cellulose fibre properties. Futamura are focused on counteracting these drawbacks. Since 2006 they have concentrated on the Life Cycle Analysis of their products, with a goal to negate these challenges. As a result, they have reduced their carbon foot print by 35 % in just 13 years, with a predicted further reduction of 40 % by 2027 via initiatives such as the inclusion of agricultural waste feed stocks for dissolving pulp [2].

As The Viscose Process cannot yet be considered a net zero process, numerous alternative techniques have been developed with the use of solvents, that have the potential to provide a ‘greener’ alternative up until that day. The Viscose Process is discussed more thoroughly and with a concentration on packaging production in Section 2.2.2.

- **N-methylmorpholine-N-oxide (NMMO)**: The NMMO process was first patented in 1936 and later commercialised in brands known as ‘Tencel’ or ‘Lyocell’ to produce cellulosic fibres. In modern times, processing can be used to manufacture a range of products including films, powders, beads, membranes and filaments [19][20]. This process utilises the organic solvent N-methylmorpholine-N-oxide (NMMO) monohydrate and water in solution to dissolve cellulose due to the strong N-O dipole of NMMO that has the

ability to disrupt the intermolecular network of hydrogen bonds that form cellulose and instead form new hydrogen bonds between the cellulose chains and the solvent [21][20]. The cellulose can then be precipitated in a water bath and shaped to provide a variety of products.

In comparison to The Viscose Process, Lyocell produces higher concentrations of cellulose fibres with a higher elastic modulus but lesser elongation at breaking point due to lyocell fibre's higher degree of crystallinity [22]. Furthermore, NMMO is less toxic, re-useable and biodegradable, in contrast to some of the chemicals used in The Viscose Process. This process also consists of far less steps and requires no derivatization of the cellulose backbone [22]. Despite these advantages, NMMO is a thermally unstable solvent that is solid at room temperature, meaning that this reaction requires high temperatures which contribute significantly to the financial and environmental considerations of commercialising Lyocell preferentially to The Viscose Process [20].

- **Ionic Liquid Dissolution:** Liquids composed of ions that are fluid around or below 100 °C, or Ionic Liquids, offer an exciting new solvent route for cellulose processing [23]. In 2002, 1-Butyl-3-methylimidazolium (C4MIM) based ionic liquids were identified as the first to dissolve cellulose. Since then, extensive further research has established numerous alternate ionic liquids suited to dissolving and regenerating cellulose with higher final weight percentages including 1-allyl-3-methylimidazolium chloride ([AMIM][Cl]) and 1-ethyl-3-methylimidazolium methylphosphonate ([EMIM][CH₃PO₃]) [24].

In order to execute this dissolution process, untreated cellulose is added to the ionic liquid of choice and heated to 100 °C - 110 °C in order to maximise the dissolution process. The resultant viscous solution can be used to obtain regenerated cellulose by coagulation from the solution using water [25]. Despite the number of ionic liquids that have been identified to dissolve cellulose, the mechanisms behind the physical process of dissolution are still hotly debated. It is generally accepted that an ionic liquid containing anions that are considered good hydrogen bond acceptors are the most effective as cellulose solvents due to their ability to disrupt the

hydrogen bonds between neighbouring units. On the other hand, the role of the cations remains unclear as to whether they influence dissolution by hydrogen bonding or not [24]. Understanding the exact cellulose dissolution process of individual ionic liquids is imperative in determining the most effective method of obtaining pure cellulose from this method. The surge in ionic liquid solvent research has produced an overwhelming number of different studies from various institutions and industries that vary in any number of factors including type of ionic liquid, origin of cellulosic material and operating conditions, meaning that a conclusive description of the dissolution mechanism is yet to be verified.

Extensive research has been conducted in cataloguing a range of ionic liquids and their ability to dissolve cellulose due to their attractive properties. Ionic liquids are non volatile and exhibit high thermal stabilities and low vapour pressures, along with the potential to be tailored for specific purposes by altering the anion and cation conformation, resulting in approximately one trillion different ionic liquid configurations to be utilised as solvents [26][27]. Perhaps the most attractive facet of ionic liquid dissolution of cellulose is the fact that ionic liquids can be recycled through this process via reverse osmosis and used again [28]. This is of massive industrial advantage in comparison to alternative methods of isolating cellulose fibres. Ionic liquid dissolution offers a process that can dissolve cellulose from not only plant materials with no pre-treatment, but also from end of use cellulose based materials such as paper or various textiles; opening up a new recycling route for these products. One advantage of this process is that the regenerated cellulose can be extracted in a range of forms such as powders, tubes or films with no degradation to the cellulose microfibrils [29].

These methods have been highlighted to present some prominent contemporary methods of regenerating cellulose from plants. In fact, there are a number of additional solvents and techniques that have been identified in recent years including: NaOH aqueous solution at 4 °C (1984), Alkali/urea and NaOH/thiourea aqueous solution at -12 °C in 2 minutes regarded a "milestone in the history of cellulose processing technology (2005), tetra butyl ammonium fluoride/dimethyl

sulfoxide system at room temperature in 15 minutes (2000), metal complex of transition metal ions and nitrous ligands aqueous solutions and inorganic salt hydrates [30][31][32][33]. However, these techniques have yet to prove industrial viability.

2.1.4 A brief history of cellulose advancements: From papyrus to polymer science

Although Payen discovered the cellulose molecule as recently as the 1800s and we attribute the conception of isolated cellulose as the commercialisation of The Viscose Process in the 1920s; cellulose's influence has punctured throughout history as early as the paleolithic era. The earliest preserved evidence of the use of cellulosic materials as tools begins in 6th-7th millennium BC, where flax has been discovered in modern day Swiss' lake settlements. From this point we see the influence of cellulose fibres proliferating across modernising groups; allowing for technology that improved everyday life. Examples such as hemp rope in China from 4500 BC and spinning of cotton for clothing first appearing in India and Egypt in 4500 BC. Perhaps the most prominent landmark event being the first example of paper in the form of Ancient Egyptian papyrus appearing in 3000 BC [34]. This discovery marks a profound turning point in human culture. Paper enabled the written word's proclivity and with it, a new way of communicating across culture.

These revelations were a precursor to this biopolymer's success in the modern materials industry, and since these discoveries, many more valuable applications have been explored, allowing for the betterment of human lives across the last 9000 years. The cyclic nature of sustainably through the giving and taking from the resources our planet provides embodies our usage of this biopolymer. The methods for which we continue to consciously cultivate this resource must be an example of this way of life for society to progress. This polysaccharide experienced a booming commercial success, even before its elementary properties were fully understood. Then, with realisation of cellulose's structure and function, came more applications through the insight gained from unlocking molecular formula,

polymer conformation, crystal structure and chain length [34]. Some common applications of regenerated cellulose today are listed:

- **Cellulose films:** The invention of cellulose films was marked by the work of Swiss Chemist Brandenburger in the early 1900s [35]. Commercialised as ‘Cellophane’ by the 1930s, this product soon became a household name. As well as food packaging, these films are also utilised in cosmetics, pharmaceutical casings and tapes, amongst more. However, with the emergence of polyolefine films that provided a cheaper and quicker manufacturing process compared to cellulose films, their popularity ebbed [36]. In modern times, cellulosic films are seeing a major resurgence due to their net zero potential. In this market, Futamura are the world leading producers of cellulose films, with products such as NatureFlex™ and Cellophane™ dominating the market.
- **Cellulose fibres:** Regenerated cellulose fibres have been prevalent throughout the textiles industry since the commercialisation of the viscose process, whereby the viscose solution is extruded through a small hole into a regeneration bath to produce a fibre. Lenzing are now leading producers of cellulose fibres, with popular fibres: Viscose, Modal and Tencel. They promote a cleaner life cycle analysis of these cellulose-based products compared to their PET fibre counterparts [37]. In recent years, these fibres have developed medical potential with examples of scaffolds in in-vitro cartilage tissue engineering [38].
- **Hydrogels and aerogels:** In the early 2000s, cellulose hydrogels gained recognition as they provide biodegradable and low cost solutions to a range of materials challenges in drug delivery, biomedical, agriculture and more sectors due to superior absorbent properties [39]. Cellulose hydrogels consist of a cross linked 3D cellulose chain that are able to absorb water and form a 3D structure due to the hydrophilicity of cellulose’s hydroxyl groups [40]. Cellulose aerogels on the other hand, replace this water with gas to provide extremely low density, high porosity and surface area materials for use in biomedical, thermal insulation, adsorption and separation materials industries [41][42].

- **Microspheres and beads:** Regenerated cellulose spherical particles of μ -mm diameter were discovered in 1951 by dropping of viscose solution into regeneration baths from a height to form a sphere with applications including chromatography, protein immobilisation and delayed drug release [43][44].

Although this thesis concentrates on the optimisation of cellulosic films, it is important to acknowledge the breadth of applications of regenerated cellulose across sectors since this research could impact those materials understanding and be used to hone their properties. This is to convey the potential of this naturally occurring biopolymer in a range of applications that have the scope to transform the materials industry.

Figure 2.3 indicates some vital learning points in the development and employment of this versatile biopolymer.

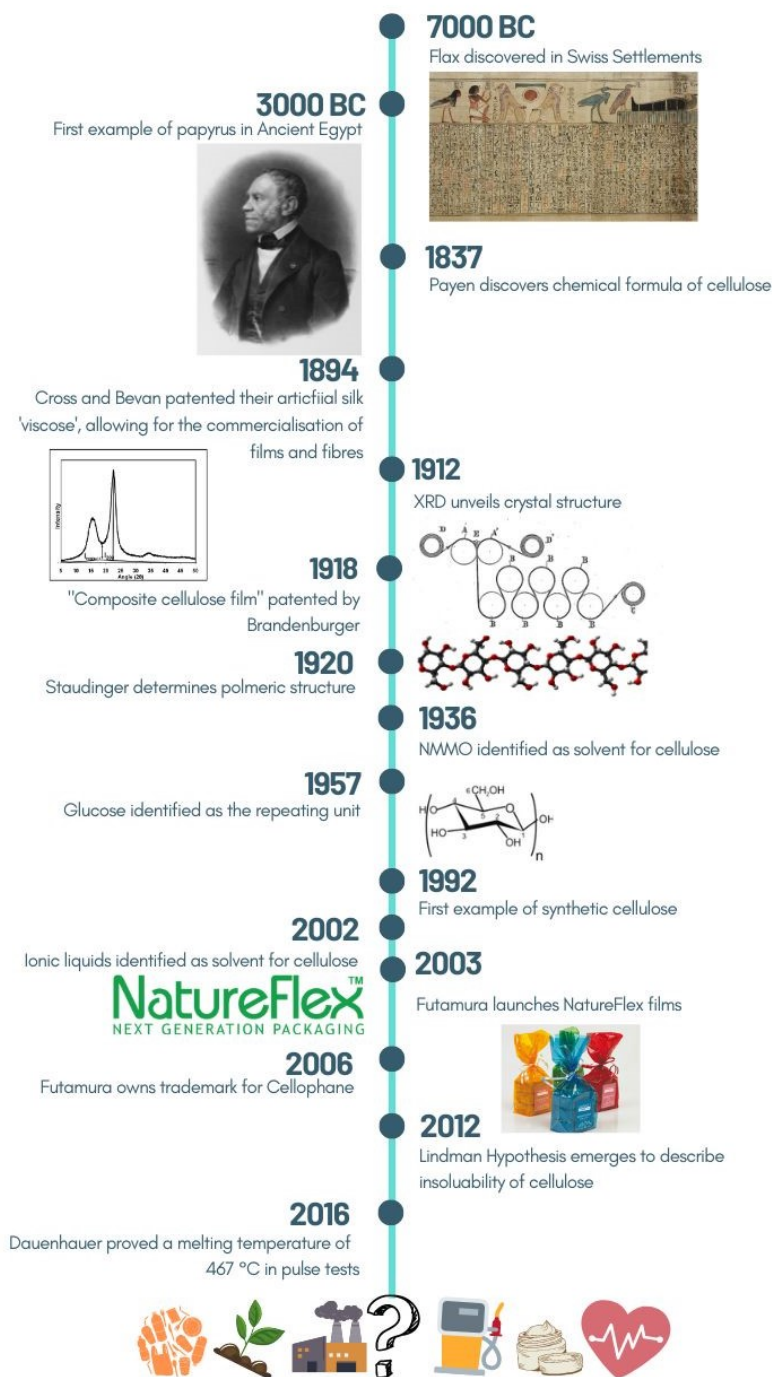


Figure 2.3: Timeline indicating some key points in the understanding and development of cellulosic materials [2][6][7][9][10][11][19][25][34][35][45][46][47][48]

2.2 Cellulose Films

2.2.1 History of Cellophane

The commercialisation of Cellophane undoubtedly instigated the transformation and modernisation of retail in the 1920s as the prolonged shelf life of consumables enabled the phasing in of self-service retailing of perishable items for consumers [36]. Cellophane provided a sturdy packaging solution with effective moisture and oxygen barrier properties, as well as being transparent: a key advertising point, as it meant that shoppers could see what they were buying and assess the quality of the produce themselves. This transparency is what really propelled Cellophane's success and changed the face of retail.

However, this revolutionary product's conception came about somewhat by chance. In 1900, Chemist Jacques Brandenburger, observed wine spill and absorb into on a table cloth at a restaurant, and resolved to create a fabric that could repel such liquids. He decided to start by spraying viscose, patented by Cross and Bevan just 6 years earlier, onto cloth, resulting in this coating creating a fragile film. He then spent the next 18 years developing this product, experimenting with plasticisation to prevent brittle fracture and machinery for processing. In 1918 Brandenburger filed a patent for a manufacturing process for "Cellophane", a "Composite Cellulose Film" [35]. This event prompted the beginning of over 100 years of Cellophane research and development. Primarily utilised as food packing, this universal material has since provided a range of alternative applications from tapes, battery membranes, dialysis tubing and release agents.

By 1922, La Cellophane Société Anonyme had commercialised this revolutionary new product and were thriving, particularly in American retail, with 40 % of their stock being shipped across the Atlantic. This success catalysed the purchasing of the rights to produce Cellophane in America by industrial giants, DuPont, in 1923 [49]. DuPont soon recognised the urgent requirement to adjust the properties of these films such that they became moisture proof as well as water proof if they were to achieve wide scale commercialisation for a diverse range of varying perishability food items. As such, chemists at DuPont developed a nitrocellulose lacquer, or coating, that accomplished this goal and between

1928-1930 Cellophane sales tripled, making up 25 % of DuPont's profits since this packaging material became suitable to a whole new market of consumables including; meats, grocery and bakery items [50][51]. In subsequent years, DuPont optimised the viscose film process as well as experimenting with the inclusion of various softeners and additives to enhance their properties, alongside different competitor's efforts.

DuPont's business strategy throughout this period of development is another factor to Cellophane's success. They dominated the water and moisture-proof packaging market by endorsing research that promoted the significant effect on sales of a consumer's ability to see food and check quality, thus influencing the decisions of traders. For example, one DuPont study showed that 85 % of purchasing was initiated visually. This research was supported by increases in food sales when switching to Cellophane for pound cake of 60 % and for crackers of 55 % in 1932 [52][36]. Clearly, their visual marketing strategy transformed the industry. DuPont tactfully managed to empower the smart shopper of the day by conveying sensory information about food through sight; propelling self-service for bakery, meats and grocery items. Some examples of early advertising are shown in Figure 2.4.

2.2 Cellulose Films



Figure 2.4: DuPont advertising posters 1947-1950[53][54][55]

Despite their success and influence on consumer patterns and preservation of foods, the invention of synthetic plastic using petroleum-based polymers, marked the beginning of the end of Cellophane's dominion over the packaging industry in the 20th Century. By the 1960s, polyvinyl chloride (PVC) films had replaced Cellophane due to its ease of production, cost effectiveness and superior preservation qualities [56].

Despite this, Cellophane has been continuously produced by various companies since the 1930s, with fluctuations in popularity seen throughout that time. In modern times, with the recent rush for biodegradable and sustainable alternatives to petrochemical-based films, a rise in Cellophane sales and research is being observed. The well-established, century-old Cellophane industry has discovered and refined numerous enhancements to the production process over the years. This, coupled with the increased demand for biofilms, has seen the process mature, with constant improvements being made to material properties, cost effectiveness and environmental considerations. With The Futamura Group purchasing the trademark for Cellophane in 2006, their research and development of this product is launching it into the 21st Century.

2.2.2 Futamura's production process

Since Brandenburger's first patent, the process has refined, with continual development endorsed by The Futamura Group to this day. This process starts with dissolving pulp sheets, produced via The Kraft Process carried out off site by another provider. These pulp sheets are subject to a rigorously regulated Viscose Process, with concentration, temperatures and extraction being closely monitored since the early 90s to finesse the process and optimise production. Futamura are constantly innovating; new wood pulps, softeners and processes are trialled to cement Cellophane as the sustainable film of the future.

Dissolving Pulp Production

Rather than raw plant material, The Viscose Process uses a start material called 'Dissolving Pulp', most commonly produced via The Kraft Process which accounts for over 80 % of US pulp manufacture [57]. The Kraft Process is a chemical process that takes plant material and removes hemicelluloses and other lignin to produce a 'dissolving pulp' with > 90 % cellulose content [58]. This 'delignification' process chemically degrades the lignin in raw plant or wood material whilst maintaining no degradation to cellulose microfibrils. Firstly, wood chips of a chosen plant source are saturated in 'white liquor' (a mixture of sodium sulphide and sodium hydroxide) and subsequently digested in heated, pressurised vessels. This acts to degrade the lignin and hemicelluloses, which are then dissolved in the white liquor. The remaining pulp is washed and bleached to produce the dissolving pulp of high cellulose content [58]. This method is essential in the production of regenerated cellulose as once other plant materials are removed, subsequent processes (such as The Viscose Process) can be used to obtain isolated cellulose microfibrils.

The Viscose Method

The Viscose Process is the most commonly used method of cellulose extraction in industry today [8]. The films produced by Futamura, tested later in this report, are fabricated using The Viscose Process from a hardwood eucalyptus dissolving

2.2 Cellulose Films

pulp. Figure 2.5 depicts a schematic of the viscose processing of wood pulp into regenerated cellulose films [59].

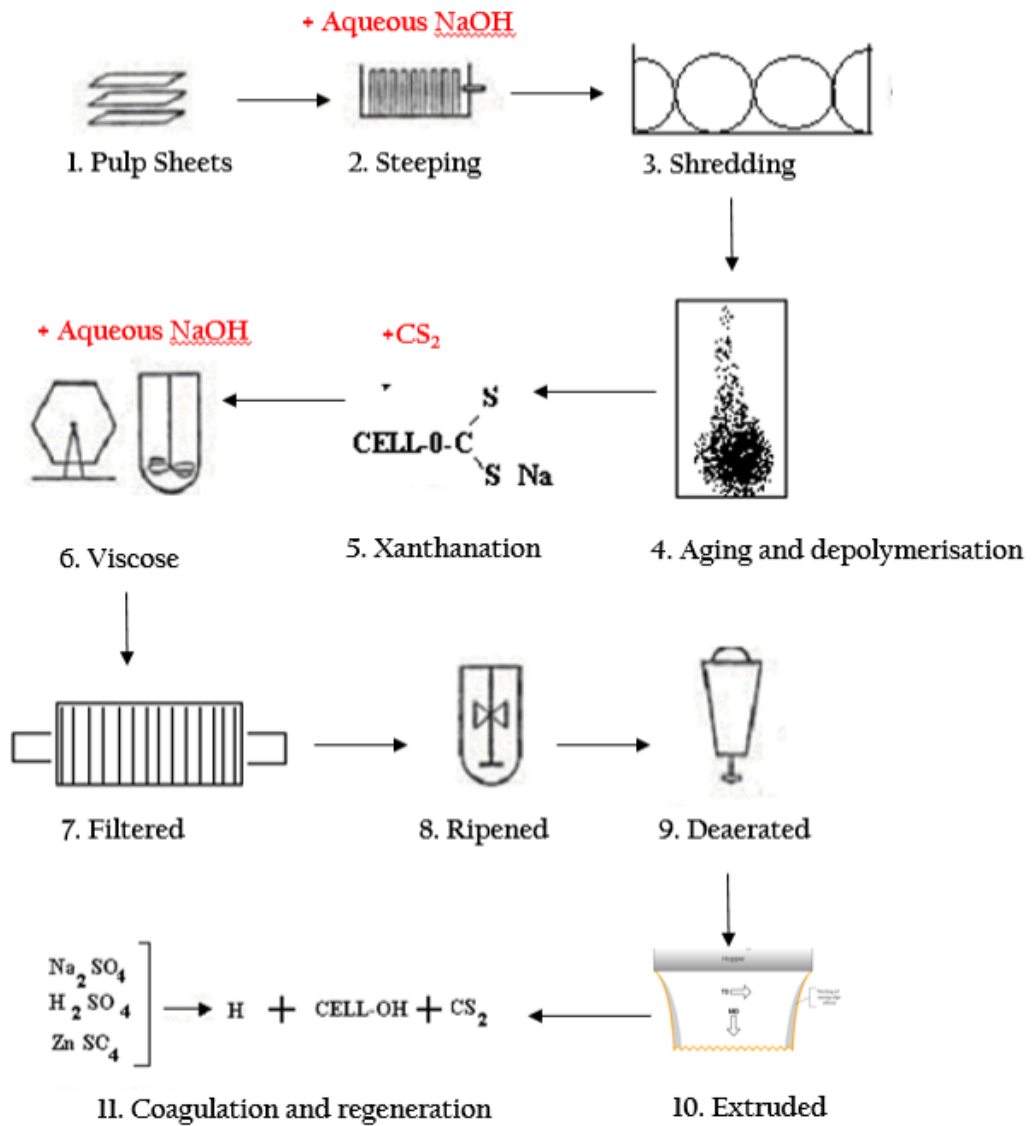


Figure 2.5: *The Viscose Process of extracting cellulose from wood pulp and converting it to films. Adapted from [60][59]*

Following this process schematic:

1. **Pulp Sheets** produced from eucalyptus hardwood wood chips are used as the input material for the viscose films in this project. Futamura have also employed the use of alternate wood pulps such as Western Hemlock. Altering wood pulp often results in a variation of final films properties. This diversity in performance is clearly a limitation to wide-scale industrial commercialisation, hence why wood pulp origin is typically kept constant. However, this ‘limitation’ could be exploited as a method of tailoring film properties providing a greater understanding of how wood pulp impacts final film properties is brought to light in future work.
2. The pulp sheets are **steeped** in aqueous sodium hydroxide (NaOH, Lye, Caustic Soda) to form alkali cellulose. This step is essential as it acts to make the hydroxyls on cellulose chains accessible for future reactions in the process. If controlled at a particular concentration and temperature, the NaOH swells amorphous regions of cellulose and removes residual hemicelluloses. Once the steeping stage has achieved optimum swelling, the mixture is pressed to remove the caustic soda.
3. Next, the pressed alkali cellulose and NaOH mixture is **shredded** into ‘crumbs’ to increase the surface area of the alkali cellulose to aid in homogenous xanthation later in the viscose process.
4. The crumbs are then exposed to atmospheric oxygen in an **aging and depolymerisation** process whereby the cellulose chains are somewhat degraded. The aging process is important to regulate the molecular weight distribution of the cellulose [61].
5. Once the aging process is complete, carbon disulphide (CS₂) is added in order to **xanthate** the activated cellulose hydroxyls to form the ester, sodium cellulose xanthate, as demonstrated by Figure 2.6 [62].

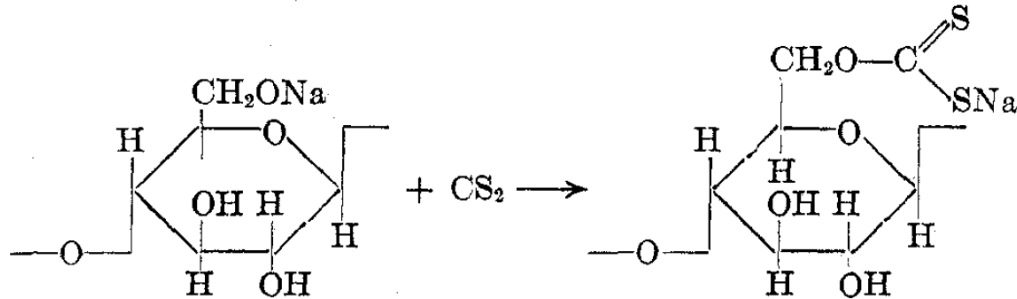
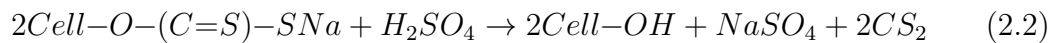
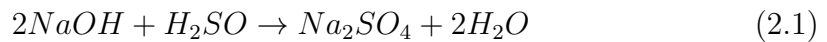


Figure 2.6: Xanthation reaction of alkali cellulose to sodium cellulose xanthate by addition of carbon disulphide, taken from [62]

6. Next, the cellulose xanthate produced through this reaction and dilute NaOH are mixed thoroughly to form a uniform colloidal system, known as **viscose**. This causes the cellulose chains to be pushed apart by the action of the swollen xanthate groups. This has the effect of diminishing the interchain hydrogen bonding, meaning that the water molecules can solvate the chains, allowing for a solution of soluble cellulose to be created.
7. Once this stage is complete, the solution can be **filtered** to remove any constituents that haven't responded to reactions.
8. Next the solution is **ripened** by exposure to atmospheric oxygen to ensure maximum xanthate substitution prior to extraction of pure cellulose.
9. The viscose solution is **de-aerated**
10. Finally, the solution is **extruded** through a narrow slit
11. Extruded solution undergoes **coagulation and regeneration** during the casting process. The colloidal viscose solution will coagulate once extruded into a salt containing regeneration bath of sulphuric acid and sodium sulphate. During this process, cellulose xanthate is precipitated out of the viscose solution whilst the sulphuric acid acts to neutralise the alkali. Regeneration occurs via acid hydrolysis of the coagulated cellulose xanthate to a skin of regenerated cellulose [61].

Casting process

The Casting Process is the procedure of converting the viscose solution of cellulose xanthate and dilute NaOH into regenerated cellulose films. In order to do this, viscose is extruded through a narrow slit into a salt containing regeneration bath containing sulphuric acid (H_2SO_4) and sodium sulphate (Na_2SO_4). This results in coagulation due to ‘salting out’ of the viscose solution by sodium sulphate, neutralisation of alkali viscose by sulphuric acid and regeneration by acid hydrolysis of precipitated cellulose xanthate to cellulose II. The regeneration steps for both caustic soda and cellulose xanthate are represented by Chemical formulae:



These processes all act to form a skin of regenerated cellulose that restricts diffusion from the bath into the center of the film, resulting in a diversity in properties throughout the cross section of the final film. Therefore, the rates of these processes are closely controlled by Futamura to produce the most uniform film possible efficiently. Composition, concentration, extrusion flow rate, temperature and viscosity are each diligently controlled in order to attain the optimum balance between these processes to manage the highest quality film.

Finally, a number of purification steps are performed during which excess acid, salts and other byproducts are removed whilst the regenerated film is kept under tension on rollers. At this stage, the film is called a ‘wet gel’. This wet gel is unsoftened regenerated film that is kept in water before finishing treatments, resulting in swelling of the gel and increasing ductility during finalising steps. This wet gel is kept on rollers throughout subsequent processes to keep films under tension. This, along with the extrusion process result in a machine and transverse direction of films due to cellulose chains being more oriented in the machine direction. The impacts of this uniaxility are discussed in Results chapters.

Plasticisers and additives

Plasticisers and additives can be included to improve the performance and appearance of the films either pre or post-casting stage. Futamura adds these products according to the following procedures.

- **Plasticisers** are added to improve ductility of the films since their performance is inherently brittle. Futamura pull the cellulose ‘wet gel’ under tension on rollers into an aqueous softener bath of chosen percentage softener for a period of ≈ 10 s. The functionality of these softeners are discussed more in the following section since understanding their interaction with cellulose is the focus of this work.
- **Coatings** are added in order to improve barrier properties of the films, by way of dissolving the coating additives in Tetrahydrofuran (THF) and Toluene, and passing the films through the solvent/coating bath to deposit a thin film of the solvent/coating mixture on the films. Films are then passed through a drier to evaporate the solvent, leaving a 1-2 μm continuous layer of coating on the film surface. The coatings used by Futamura are not a focus for this work and will not be disclosed during this thesis.
- **Colourings** are added to change the appearance of the films. For example, Titanium Dioxide (TiO_2) is injected into the viscose solution prior to casting, resulting in roughly 5 % encapsulated TiO_2 in the films to provide opaque white colouring suitable for some food items. Colourings are of great interest for Futamura’s customer base since confectioners often use bright packaging to attract shoppers.

Futamura’s end products

Today, Futamura’s cellulosic films are split into two categories: Cellophane and Natureflex.

- **Cellophane:** In 2006, Futamura invested in the Trademark household name ‘Cellophane’. Futamura are committed to the continual advancement of this food packaging solution and are contributing resources to research to improve the sustainability and cost of these films sourced from

sustainable forests. Cellophane is provided with an assortment of coatings to provide a range of barrier protection, as well as being available in a series of colours. Perhaps most famously popularised in the confectionery market; these breathable films are also used for bakery items and heat-resistant packaging. Further applications including tapes and battery separators and more [2].

- **NatureFlex:** With environmental pressure mounting on industry and government, companies are seeking new ways to improve the life cycle analysis of their products to make conscious steps towards a greener society. One of the ways that Futamura have instigated this is with the launch of Natureflex, a cellulosic film that is certified compostable according to European and American guidelines. NatureFlex offers the same high quality performance as Cellophane films but with superior green credentials [48].

2.3 Plasticisers

The use of plasticisers, or ‘softeners’, is well established in material science due to their development alongside polymeric materials for their ability to alter to the mechanical performance of goods. Their exact function differs from material to material, but in general, their inclusion in polymers is to alter flexibility and/or processibility by way of reducing the Glass Transition Temperature, T_g [63]. Plasticisers act to amplify the internal motion of polymers such that elasticity is altered in a way that makes it easier to respond to applied stresses, in other words: increased ductility. The surge in engineering plastics seen throughout the last century would not have been possible without the advancement of accompanying plasticisers. This optimisation of properties has allowed plastics to infiltrate other materials markets (e.g metals) due to their enhanced and tunable properties [64]. For better or for worse this has resulted in a boom in polymeric materials which have, undeniably, impacted on the betterment of human life, so much so that this plastic revolution is irreversible; making the development of sustainable biopolymers vital.

The criteria for an effective plasticiser changes for each application but generally they are selected based off their compatibility, processibility, cost, toxicity, as well as their thermal, electrical, rheological and mechanical properties of desired product and resistance to outside affects such as water, UV or chemicals [64]. In 2017, the Chemical Economics Handbook reported that since the conception of plasticisers, over 30000 different substance's plasticisation ability had been tested and yet only around 50 have achieved commercial market success [65]. Plasticisers can be classified in a number of ways depending on how they interact with polymers. For example, internal plasticisers act by way of plasticiser molecules forming part of the internal polymer network, imparting a significant temperature dependence on performance; whilst external plasticisers are not part of the network through any primary interactions and thus can be subject to leeching affects [66]. Furthermore, plasticisers can be described as primary or secondary; where primary plasticisers act to impart the majority of the softening effect, being the most effective component. Whereas secondary softeners are blended with primary softeners as a filler constituent to reduce the amount expensive primary softener used [67].

These plasticisers can transform the properties of a material, enabling a diversity of application. For example, in the case of polyvinyl chloride (PVC); unsoftened PVC is used as window frames, yet the the inclusion of softener di(ethylhexyl)phthalate allows for the adoption of a range of entirely different uses such as flexible sheeting or footwear [68]. With rising costs and environmental pressures heavily impacting this market, more and more researchers and industries are looking towards the discovery of alternative plasticisers. Another opportunity for market growth lies in the development of so-called 'anti-plasticisers' that act to increase modulus but decrease failure strain, suitable material properties for some applications.

2.3.1 Function and performance

The International Union of Pure and Applied Chemistry have defined a plasticiser as "a substance or material incorporated in a material (usually a plastic or elastomer) to increase its flexibility, workability or distensibility". Plasticisers

act to achieve these changes to performance by altering the balance of material properties including: tensile properties, hardness, density, viscosity, conductivity, chain mobility, stiffness, dielectric constant, crystallinity, amongst many more [69]. In particular, for these materials, a trade-off between modulus and strength with strain at failure is investigated and analysed through the use of material selection graphs known as ‘Ashby Plots’, discussed in more detail in future Chapters. This tunability is an extreme advantage to industry as it means that polymers can be optimised for a number of varying applications. Typically, plasticisers consist of low molecular weight, non-volatile and high boiling point liquids with linear or cyclic carbon chains consisting of 14-30 carbons [70][71]. In addition, for cellulose-based materials, it is also speculated that water itself acts as a plasticiser; throwing into question whether the role of ‘traditional’ softeners in cellulosic materials is to actually soften themselves or to bring in water due to their hydrophilic nature. The historic interpretation of the function of plasticisers describes that, due to their low molecular weight (300 - 600), plasticiser molecules are small enough to inhabit the intermolecular space between amorphous polymeric chains, forcing those chains apart [64][72]. This results in fewer intermolecular (secondary: hydrogen bonding, Van der Waals) forces between chains thus altering 3-dimensional molecular configuration in a way that reduces energy for increased molecular motion and reduces the glass transition temperature. There are three theories used to depict the function of plasticisers and their effect on performance: Lubricity Theory, Gel Theory and The Free Volume Theory, depicted in Figure 2.7:

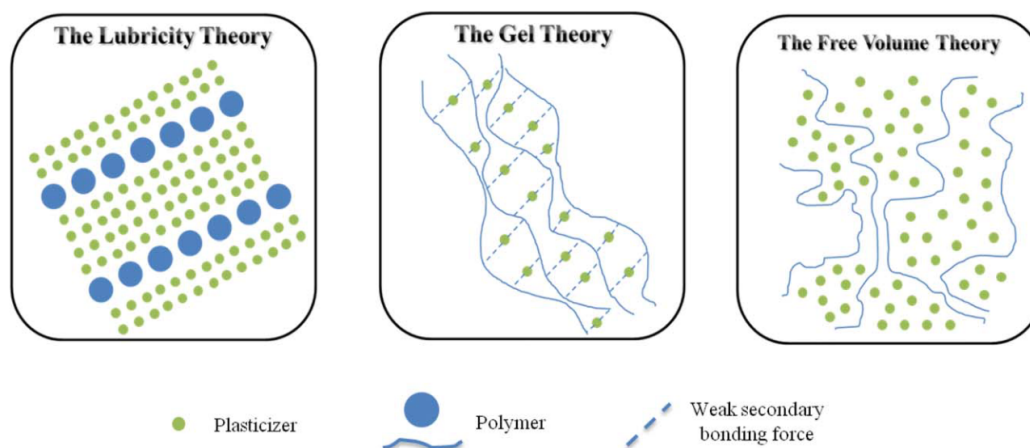


Figure 2.7: *Theories of the mechanisms of plasticisation: Lubricity, gel and free volume. Taken from [73]*

- **The Lubricity Theory** describes that the chosen plasticiser solvates between pairs of polymer chains. This acts to reduce interactions between the chains as well allowing for lubrication if the polymer is deformed, such that parallel alternating layers of plasticiser and polymer are allowed to ‘slide’ over one another [74].
- **The Gel Theory** describes the 3D polymer network as incorporating the plasticiser molecules through bonding via weak secondary forces. Thus, the secondary forces between the polymer chains themselves are disrupted resulting in reduced points of attraction between chains [74].
- **The Free Volume Theory** describes when a plasticiser is added to a polymer, free volume is increased, thus increasing molecular motion and mobility of chain ends, side chains and main chain [75].

This Free Volume Theory is the most recent (1950) and can be used to most accurately predict a polymers response to plasticisation, exemplified by the PVC plasticisation mechanics [76].

2.3.2 Plasticisers of cellulose


As with many biopolymers, the unsoftened performance of regenerated cellulose is unsuitable for many modern applications since it is fundamentally brittle due to the high tensile strength of cellulose polymer chains as a result of their extensive hydrogen bonded network. If cellulose is to be utilised as the biopolymer of the future then it is necessary to expand its property range to discover its conceivably unlimited possibilities.


It transpires that cellulose was one of the first materials that was historically plasticised to provide cultivated properties. In the early 1900s, camphor and castor oil were used as plasticisers for celluloid or celluloid lacquers, suited for use as camera film [69]. With the development of carbohydrate and polymer science, ester plasticisers such as triphenyl phosphate or tributyl phosphate, were employed to much more effectively alter properties. Brandenburger himself identified the challenges that the stiffness of the unsoftened materials posed and identified glycerine as a plasticiser for Cellophane films. Since then a number of other compatible softeners have been identified and are in commercial use across cellulosic materials. In particular, the use of polyols such as sorbitol, propylene glycol, and polyethylene glycol have proved effective at softening hydrophilic polymers due to the number of hydrogen bond acceptors that have the ability to disrupt polymer networks [77]. In addition, this hydrophilicity is also key to understanding how water effects cellulosic polymer systems. Water itself imparts ductility due to its interactions with polymer molecules and resultant reduction of T_g , and thus is considered the most powerful "natural" plasticiser [78]. In later Chapters, we elucidate the actions of plasticisers and how their ability to incorporate water into films is a vital indicator of their plasticising ability. Furthermore, with societal pressures to increase sustainability at every production step mounting, the emergence of more plant-based softeners is being observed including the use of residual hemicelluloses to act as softeners [3].

Futamura's plasticisers

Since the individual operation of plasticisers with cellulose molecules is varied and thus the plasticisation mechanisms distinct, this literature review will only

cover the effect of plasticisers currently employed by Futamura in their Cellophane films; however, there are numerous other cellulose softeners on the market.

For this work, Futamura provided films that contained four different, commonly used, polyol plasticisers that have proved effective at providing ductility to these films since their early commercialisation. A 3 component softener package containing *(This text has been removed by the author of this thesis for confidentiality reasons)* 

is incorporated into films, as well as a single component *(This text has been removed by the author of this thesis for confidentiality reasons)* 

softener. As well as requiring compatibility and effectiveness in their functions as a plasticisers; Futamura's needs also require additional challenges. Namely, that softener packages must be FDA approved due to the films intended application of food packaging. The chemical configuration of each of these softeners is shown in Figure 2.8.

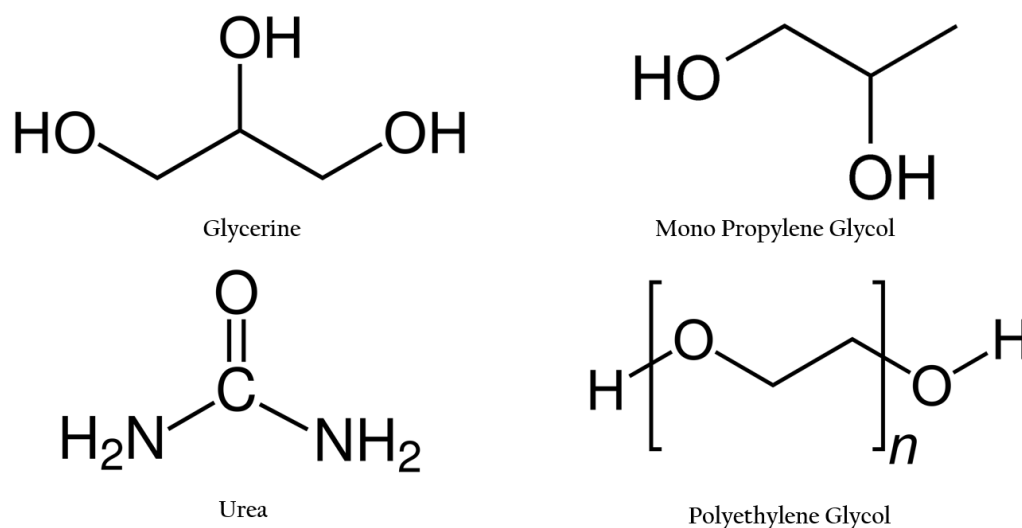


Figure 2.8: *Futamura* plasticisers: *Glycerine*, *Mono Propylene Glycol*, *Urea* and *Polyethylene Glycol*

- **Glycerine** is a triol of chemical formula $C_3H_8O_3$ extracted from plants or animals that is colourless, non-toxic and odorless. Its universal usage spans from medical treatments to food additives and of course plasticisers in cellulosic films for which they are well established [79]. Glycerine acts to disrupt hydrogen bonding between cellulose chains and also to incorporate water into films to induce an additional softening effect due to its hydrophilic nature arising from the presence of 3 hydroxyl groups on the molecule [80].
- **Mono Propylene Glycol (MPG)** is a diol of chemical formula $C_3H_8O_2$ typically produced in industry from propylene oxide that is colorless, non-toxic and odorless for applications ranging from pharmaceutical to cosmetics and is approved by the FDA for indirect food use. It is recognised as a plasticiser in biofilms but its performance is poor compared to that of glycerine, meaning that *Futamura* are likely to include it as a secondary plasticiser to reduce glycerine usage since it is more expensive [81][82]. We aim to elucidate the reduced effectiveness as a plasticiser of this molecule and whether the fewer hydroxyl groups contribute to these observations.
- **Urea** is a diamide of carbamic acid with chemical formula $CO(NH_2)_2$, first

laboratory synthesised in 1828. Like glycerine and MPG is colourless and odorless; however is classed as ‘practically non-toxic’. Urea has well established commercial use for the fertiliser in the agricultural industry as well as having a number of additional uses from medicinal to explosives. Its use as a plasticiser is recognised but its abilities are typically inferior compared to that of glycerine, making it a secondary plasticiser [83][84]. We also aim to investigate whether the 3 hydrogen bond acceptors of urea are effective at increasing water content of films to induce additional plasticity in these films

- **Polyethylene glycol (PEG)** is a polyether extracted from petroleum with many established medicinal and chemical applications. Its application as a plasticiser is well documented. It is considered a ‘traditional plasticiser’ with similar plasticising ability to Glycerine [85][86][82].

Theory and hypotheses of the mechanisms of glycerine, MPG and Urea and how they interact with and plasticise cellulose films and water are discussed in the results section of this work. At this stage we hypothesise that the hydrophilicity of plasticisers is a key indication of their softening ability since the importance of water content in films has been highlighted, this is indicated by their number of hydrogen bond forming sites; suggesting that glycerine and urea are expected to be the most effective softeners in Futamura’s current softener packages. We hypothesise that plasticisers should be hydrophilic such that they are able to bring water between polymer chains. However with the additional caveat that they should not be ‘too’ hydrophilic such that the water is not allowed to detach from plasticisers and embed between polymer chains as both free and bound water. Essentially, plasticisers should be hydrophilic but less so than cellulose so that water preferentially bonds with cellulose hydroxyls once the plasticisers have acted to bring the water into the polymer network.

Alternate plasticisers

With modern commercial pressures to alter Futamura’s production process, one of their concentrations for development is to branch out to using alternate plasticisers to reduce costs and reliance on plasticiser companies as well as boosting

sustainability. One of the ways this can be achieved is the investigation of the efficacy of plant-based softeners in these films. There have been numerous literature examples of alternate softeners in literature that have worked to impart a softening effect on films to achieve this goal.

For example, in 2009, Shaikh et al reported the plasticisation effect of residual hemicelluloses in cellulose acetates. They reported a 5 % hemicellulose (xylan) content as having a distinct softening affect [3]. Thus, rather than being viewed as impurities, ligno-cellulosic agricultural wastes have the potential to be incorporated to the advantage of the end product. Furthermore, in 2020 the plasticisation of cellulose acetate by green solvents: lactates and octanoic acid, was quantified using Dynamic Mechanical Thermal Analysis to assess the variation of reactions and drop in Glass Transition Temperature indicative of a change in softness [87]. Furthermore, triethyl citrate has been reported to be an effective plasticiser to cellulosic products in comparison to glycerine; opening a potential alternative plasticising option [88]. In 2022, Rebelo reported the internal plasticisation effect of soybean oil incorporated prior to dissolution of cellulose from wood pulp. The results showed increased ductility and hydrophilicity of the films, evidencing this novel plasticisation effect [89].

Clearly, there are multiple avenues for investigation with regards to the variation of plasticisers within these films. This thesis includes the results from an attempted inclusion of a potential plasticising substance consisting of a blend of plant extracted hemicelluloses. It was hoped that this blend would induce a plasticising affect if incorporated into films using a method analogous to Futamura's softening process, based off the work of Shaikh et al [3].

2.4 Project motivations

The modern materials industry is facing a dilemma with its approach to production and sustainability. The use of plastics in today's society is arguably unavoidable as it has become a valuable resource that has transformed quality of life across the globe. Human's reliance on plastics has become ingrained into our culture in less than a century in a way that is irreversible if we want to uphold modern standards of living. However, there is a striking problem with

2.4 Project motivations

these revolutionary materials as they are non-biodegradable and non-renewable, thus contribute to land and sea pollution as well as global CO₂ emissions during production. In fact, reckless overuse of plastic is already evident in the fossil record of the current geological era, namely; ‘the plastisphere’ [1]. Moreover, this problem is only escalating; with predictions suggesting that by 2050, 12000 million metric tons of plastic waste are destined for landfill, compared to the 5000 million metric tons sitting there today [90]. Coupled with the fact that less than 10 % of plastic is currently recycled, it is clear that a drastic change is vital [1].

Plant-based materials are rising in popularity as a fierce competitor to synthetic polymers for countless applications. In fact, The 2020 Technology Road Map for Plant/Crop-based Renewable Resources aims to see 50 % of basic chemical building blocks being plant-derived by the year 2050 [91]. With packaging contributing up to 36 % of plastic production, the food packaging industry in particular is seeing a resurgence of biopolymer based products [1][92]. Cellulose based films provide a popular alternative, due to their multi faceted attractive properties. Namely; renewability, abundancy, non-toxicity, low cost, sustainability, biocompatibility, biodegradability, thermal and chemically stability, tensile properties and derivability [16]. With The Futamura Group at the forefront of cellulosic films production, this title comes with an onus to drive these products forwards such that they can constitute responsible materials for the sustainable advancement of society.

Clearly, there are multiple ways that Futamura can, and are, approaching this challenging duty. Since there are numerous steps in the production of these films, each step can be addressed and optimised with sustainability, performance and cost being the three main drivers for improvement. Starting wood pulp, The Viscose Process and additive addition are all key focuses currently undergoing extensive research by Futamura’s Research and Development Group. For this thesis, the focus is to elucidate understanding of the operation of plasticisers within these films so that Futamura can enhance this step of their production process. Despite the importance of plasticisers role in dictating mechanical performance (and also affecting water permeability since they are hydrophilic molecules), the softeners used at Futamura have remained unchanged for many years. With constantly fluctuating costs, it is imperative to understand and justify the effectiveness of

2.4 Project motivations

softeners. It is hoped that the results of this work will impact Futamura and allow for the imagination and recommendation of new softener packages. By assessing the function and performance of each of their softeners individually, their effectiveness has been quantified and contribution to softening effect determined. Further work has included the incorporation of plant-based hemicelluloses with the hope of inducing a softening effect. Furthermore, trialling of additional plant-based softeners seen in literature would constitute an excellent continuation of this work.

Chapter 3

Experimental Methods

To introduce this section, it is important to provide an overarching aim and story that we hope to provide with this work. At the start of this project, Futamura provided five commercial films that employed the use of two different softener packages, as well as an unsoftened film to provide comparisons. The first commercial softener being Futamura's '3 Component Softener' package containing *(This text has been removed by the author of this thesis for confidentiality reasons)* [REDACTED], whilst the second commercial softener blend is their '1 Component Softener' package containing *(This text has been removed by the author of this thesis for confidentiality reasons)* [REDACTED]. These films were analysed using a combination of mechanical and structural testing. From these tests it was clear that softeners needed to be separated to understand their individual and cooperative contributions to the plasticisation of the system. As such, a collection of lab-based films were produced. The 3 Component Softener was separated into its constituents and incorporated into films at varying concentrations. Glycerine, MPG and Urea and a recreation of the 3 Component Softener blend have been included in films in 4 %, 8 % and 15 % softener in bath wt %. Alongside these plasticised films, an unsoftened lab-based film was produced in order to compare to the softening effects. Once these films had been analysed using mechanical and structural testing, the importance of hydrophilicity of the softeners was highlighted and as such a hemicellulose blend was employed as a potential plasticiser in the final set of films due to their hydrophilic nature. The hemicellulose blend and a 2 Component Softener blend containing

(This text has been removed by the author of this thesis for confidentiality reasons) ██████████ blend were incorporated into films in 4 %, 8 % and 15 % softener in bath wt % and their effect on mechanical and structural properties were been analysed.

The techniques and testing methods used to create and analyse these samples are described throughout this section.

3.1 Materials

The films characterised in this work can be separated into two categories: Commercial and Lab-made, which are summarised in Table . The **Commercial films** provided by Futamura at the beginning of this project, consist of five market films each with different softener packages and additives; supplied to a range of customers for a varied selection of products. Following initial characterisation tests of these films, the variation of plasticisers became a clear interest and the project direction steered towards understanding the molecular interactions of these individual plasticisers with the cellulose chain and the resulting impact on mechanical performance. In order to investigate this further and understand the effect of individual and combination plasticisers as they increase in concentration, Futamura's lab facilities were used to manufacture **Lab-based films** with varying plasticiser content, concentrating primarily on Futamura's most popular softener package: A 3 component softener containing Glycerine, MPG and Urea which were separated and included in films individually and as a lab-created blend in a range of concentrations. In addition to this, a final set of lab-based films was produced, with a hemicellulose sugar blend incorporated using the same technique that the plasticisers were added, with the hope of inducing plasticisation effects utilising plant-based alternatives to traditional softeners. These two sets of lab-based films could be compared, with the aim of understanding how Futamura can optimise their plasticising process to increase sustainability and reduce costs.

3.1.1 Commercial Films

The initial set of films provided by Futamura includes 5 samples that are all commercially available cellulosic films produced at the Futamura factory in Wigton, UK. Each of the five films were made using The Viscose Process, described in section 2.2.2, using a Eucalyptus hardwood dissolving pulp, with varying amounts of softeners, coatings and colourings added during the final production stages. Softeners are intended to improve the ductility of the final product, whilst coatings improve barrier properties and colourings change the colour of the films, in this case from transparent to opaque white for aesthetic purposes. This set of 5 films and their characteristics are listed below and shown in Table 3.1:

- Unsoftened (No plasticiser/coatings/colourings added)
- 3 Component softener*
- 3 Component softener (coated)*+
- 3 Component softener (TiO₂) particles*-
- 1 Component softener**

With:

*The 3 component softener blend included in films 2-4 consists of (*This text has been removed by the author of this thesis for confidentiality reasons*)

**The 1 component softener used in the final film is (*This text has been removed by the author of this thesis for confidentiality reasons*)

+ Coatings are added by way of dissolving the coating additives in Tetrahydrofuran (THF) and Toluene, and passing the films through the solvent/coating bath to deposit a thin film of the solvent/coating mixture on the films. Films are then passed through a drier to evaporate the solvent, leaving a 1-2 μm continuous layer of coating on the film surface. The coatings will not be disclosed during this thesis

-TiO₂ is injected into the viscose solution prior to casting, resulting in roughly 5 % encapsulated TiO₂ in the films to provide colouring.

The softener in the bath weight percentage of each of these softeners on plant is estimated to be ~ 8 wt %, this results in a softener in film estimation of ~ 18 wt %.

A range of physical tests were performed on this set of films to elucidate the effects of these softeners and additives. In order to gain an understanding of these film's performance drivers, the independent softeners were investigated separately at various concentrations to gauge their contribution to overall plasticisation.

3.1.2 Lab-made Films

To assess individual softener performance, films were manufactured using a lab based method, developed by Futamura's lab team, that emulates the commercial method of incorporating softener post Viscose Process casting. For the purpose of this project, the 3 component softener package containing *(This text has been removed by the author of this thesis for confidentiality reasons)* was investigated, as well as each of those individual softeners, at varying concentrations. The one component softener as well as the addition of coatings and colourings has not yet been investigated but would constitute valuable candidates for future work.

Lab-based film production

To produce Lab-based films, cellulose 'wet gel' was cut from the production line at the post-casting stage and kept in water to prevent drying before films could be softened in the lab. Wet gels were cut into rectangles of ~ 30 cm x 40 cm, with the longitudinal length in the machine direction. Rectangles were individually submerged and softly stirred by hand in softener-in-water baths for 10 s. Softener-in-water baths were made in 4 %, 8 % , 15 % softener:water wt % for a range of different individual and combination softeners. These percentages were chosen as *(This text has been removed by the author of this thesis for confidentiality reasons)*

Once submerged, films were screwed into A4-size metal frames and dabbed lightly with a tissue to remove excess water:softener bath. Once secured in the frames, films were placed in an oven at 60 °C for 30 minutes to dry. Once removed and

3.1 Materials

cooled to room temperature for a further 30 minutes, films could be cut from the frames. A total of 5 films were made for each softener bath, creating 5 repeats. See Figures 3.1, 3.2, 3.3 for clarification.

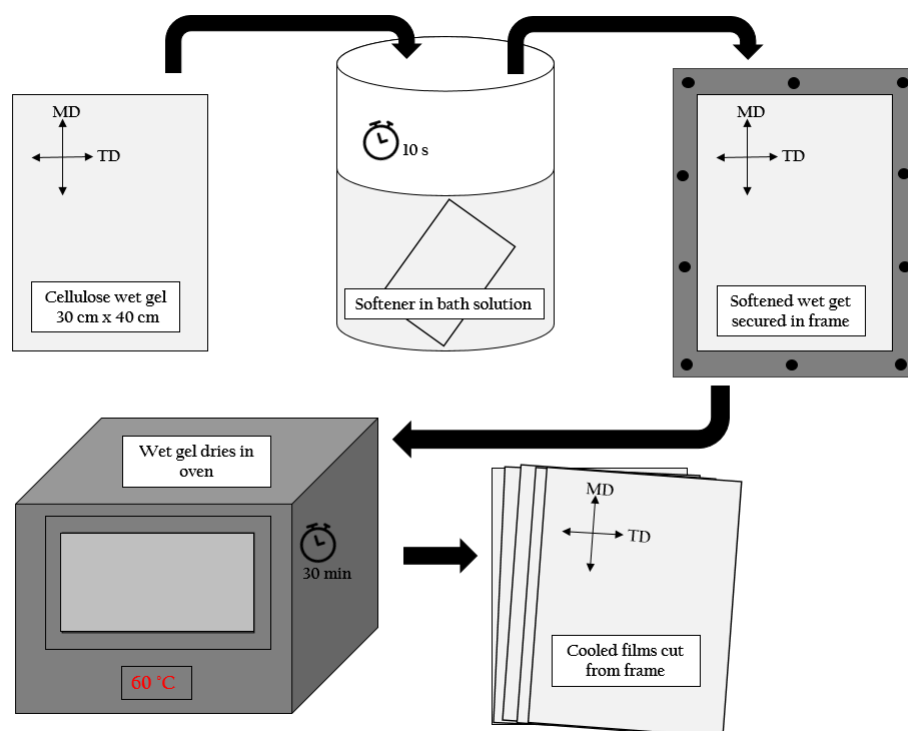


Figure 3.1: *Depiction of the softening process employed to produce lab made films*

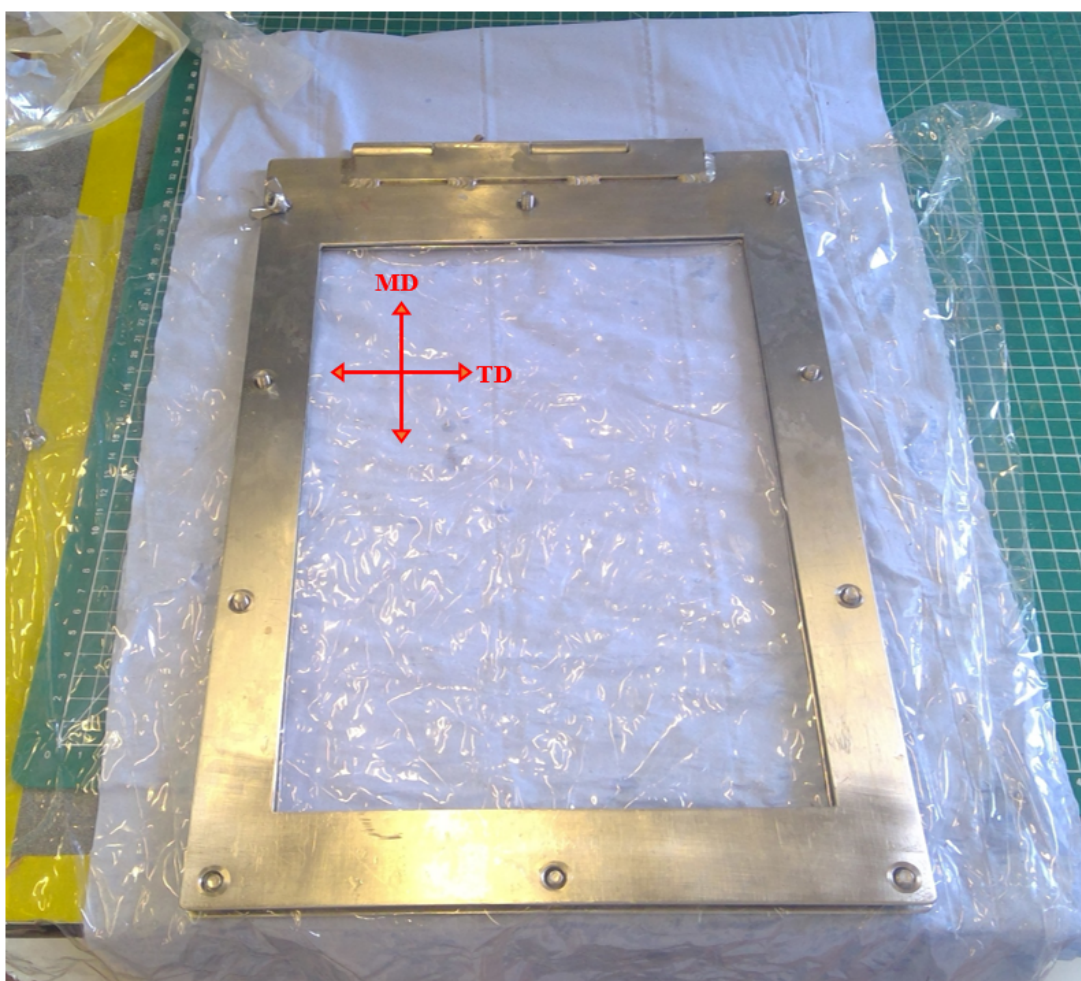


Figure 3.2: *Photograph of cellulose wet gel placed in A4 frame to be dried*



Figure 3.3: *Photograph of Frames drying in Oven rack*

This method was used to produce lab-softened films with the aim of recreating and dividing Futamura's most popular softener blend, the 3 component softener, detailed in Table 3.1. Thus, the following films were produced:

- 4 %, 8 %, 15 % (softener in bath) Glycerine
- 4 %, 8 %, 15 % (softener in bath) MPG
- 4 %, 8 %, 15 % (softener in bath) Urea
- 4 %, 8 %, 15 % (softener in bath) 3 Component Softener (*This text has been removed by the author of this thesis for confidentiality reasons*)

Furthermore, during literature searches, several works on the softening effects of plant-based hemicelluloses were discovered [3]. As such, a second set of lab-based films were manufactured using this lab-based method to incorporate a hemicellulose sugar blend that had been supplied to Futamura by Bio-Sep Limited; a technology company using ultrasonic processing of woody biomass to

extract high-value, renewable biochemicals with a range of applications. Their ‘*Hemicellulose Hydrolysate*’ is a combination of sugars extracted from spruce softwood using an ultrasonic process with mild organic acids. The syrup consists of *(This text has been removed by the author of this thesis for confidentiality reasons)*

These lab-made films were made using the same procedure as the first set of softened films but by incorporating the Hemicellulose Hydrolysate into the water bath rather than softeners. In addition to incorporating the sugar mix alone, a softener:sugar blend was also trialled, known as ‘2 component softener’. This 2 component softener contained *(This text has been removed by the author of this thesis for confidentiality reasons)* mixture in order to emulate and compare to Futamura’s 3 component softener (where the Hemicellulose Hydrolysate makes up the MPG and urea portion). As such the following films were produced (also detailed in Table 3.1):

- 4 %, 8 %, 15 % Hemicellulose Hydrolysate in bath
- 4 %, 8 %, 15 % (softener and Hemicellulose Hydrolysate in bath) 2 component softener *(This text has been removed by the author of this thesis for confidentiality reasons)*

To clarify, Table 3.1 provides a summary of all the films tested in this work and their softener in bath percentage.

Table 3.1: Table of all commercial and lab-made films investigated in this work

Film	Softener blend concentration	Softener in bath wt %
Commercial		
Commercial Unsoftened	No softener	0
3 component Softener	(This text has been removed by the author of this thesis for confidentiality reasons)	~ 8
3 component Softener (coated)	(This text has been removed by the author of this thesis for confidentiality reasons)	~ 8
3 component softener (TiO ₂)	(This text has been removed by the author of this thesis for confidentiality reasons)	~ 8
1 Component Softener	(This text has been removed by the author of this thesis for confidentiality reasons)	~ 8
Lab made		
Lab Unsoftened	No softener	0
Glycerine	100 % Glycerine	4 8 15
MPG	100 % MPG	4 8 15
Urea	100 % Urea	4 8 15
3 Component Softener	(This text has been removed by the author of this thesis for confidentiality reasons)	4 8 15
Hemicellulose blend	(This text has been removed by the author of this thesis for confidentiality reasons)	4 8 15
2 Component Softener	(This text has been removed by the author of this thesis for confidentiality reasons)	4 8 15

It should be noted that the softener content of the films differs to the 4 %, 8 % and 15 % softener-in-bath concentrations created in this lab based method. Thus, softener content of the films was determined using a method that removes all of the softener from the films and compares initial and final weights to find softener weight percentage. In order to do this, 5 cm x 5 cm squares were cut from 3 different films in the same set of repeats. These squares were placed in a conditioning oven at 30 °C for 1 hour to control humidity and ensure the water uptake of the films was uniform. Then, squares were then weighed to determine their initial weight, W_i . Once this was recorded, squares were placed in individual beakers on magnetic stirring hot plates at ~ 90 °C at medium speed for 1 hour in order to remove the softeners from the films into the water. Then squares were rinsed with water to remove excess softener and placed in an oven to dry at 60 °C for 30 minutes. Finally, they were reconditioned in the conditioning oven for 1 hour and weighed to find their final weight, W_f . Then equation 3.1 was used to determine the percentage softener in the films.

$$\text{Softener in film \%} = \frac{W_i - W_f}{W_i} \times 100 \quad (3.1)$$

The values of softener content of films is used in graphs and data for this thesis rather than softener in bath concentrations as it was clear from visual observations that certain softeners have a saturation limit as they show evidence of migration effects.

3.2 Macroscopic Testing

Macroscopic Testing is an extremely important step in the assessment of material properties to evaluate performance. One category of macroscopic testing concentrated on in this work is mechanical performance. In their application as food packaging, these films are subject to a range of impacts and manipulations that can cause them to stretch and fracture. Clearly, breakages in these films are undesirable as they result in exposure to oxygen and moisture, possibly resulting in food spoiling. Thus, mechanical performance is closely monitored and assessed by Futamura. In this thesis, Tensile and Impact testing are used to quantify a

range of mechanical performance properties for each of the films and assess how the addition of plasticisers affect these properties. In future work, it would also be valuable to assess other macroscopic properties of the films. For example, oxygen and moisture permeability would be a key performance drivers to link with food decomposition to prevent waste.

3.2.1 Tensile Testing

In order to determine the tensile properties of the films, samples were laser cut into dumbbells with dimensions shown in Figure 3.4, allowing for 5 repeats in both the machine and transverse directions for each sample.

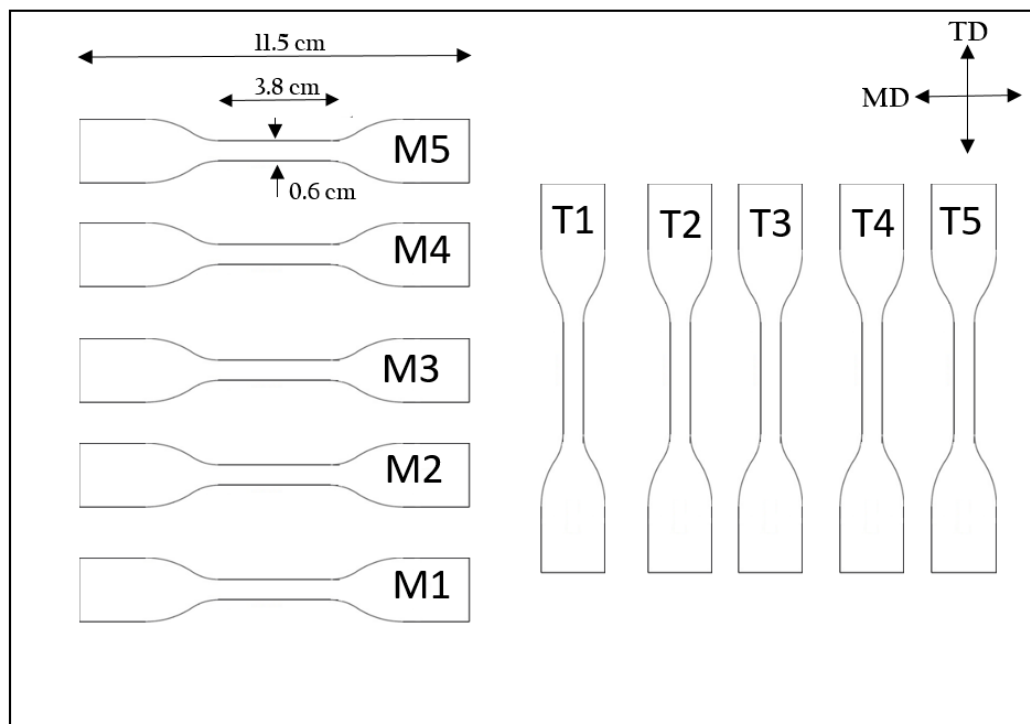


Figure 3.4: *Dumbbell cutting layout for tensile testing with dimensions of dumbbells annotated. This cutting stencil allowed for 5 repeats in both Machine (MD) and Transverse (TD) Directions*

3.2 Macroscopic Testing

Each of these dumbbells were clamped into an Instron 5654 tensile tester, shown in Figure 3.5, using emery board between clamps to prevent slippage during tension. Force and extension were measured as the dumbbells were stretched uniaxially at a constant rate of 10 mm/min up to their fracture point. Using this data, stress/strain curves were constructed by converting force into stress and extension into strain using equations 3.2 and 3.5 respectively.

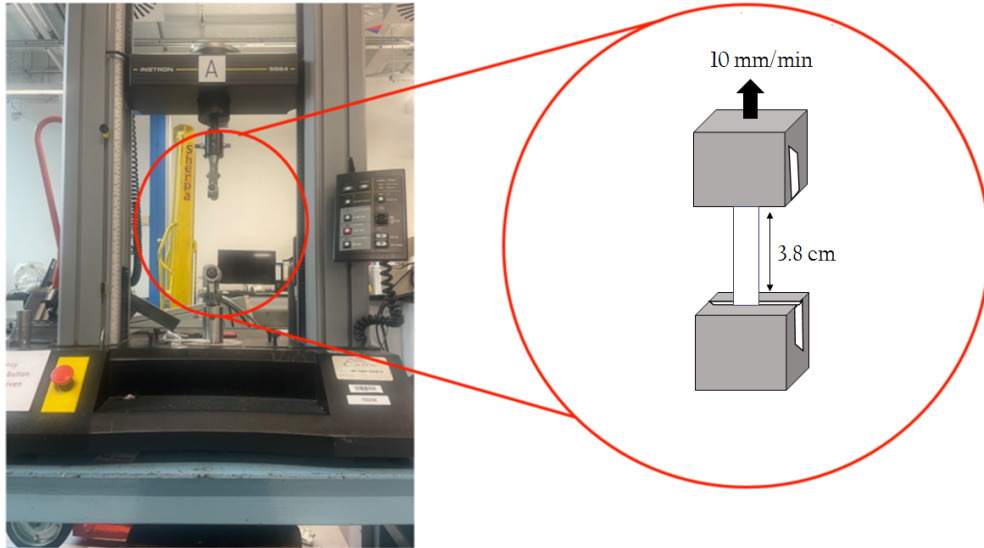


Figure 3.5: Instron Tensile Tester used to perform tensile measurements on samples, with clamping of dumbbell highlighted schematically

$$\sigma = \frac{F}{A} \quad (3.2)$$

Where σ gives stress, F gives Applied Force and A gives cross sectional area; given by cross sectional area = width \times thickness. Width of the dumbbells was measured using a centimetre ruler and thickness was measured using a micrometre and averaged across three measurements

$$\varepsilon = \frac{\Delta l}{l} \quad (3.3)$$

Where ε gives the strain, Δl gives the extension and l gives the original length that was measured using a centimetre ruler.

An annotated example of the stress/strain graphs produced from this data can be seen in Figure 3.6.

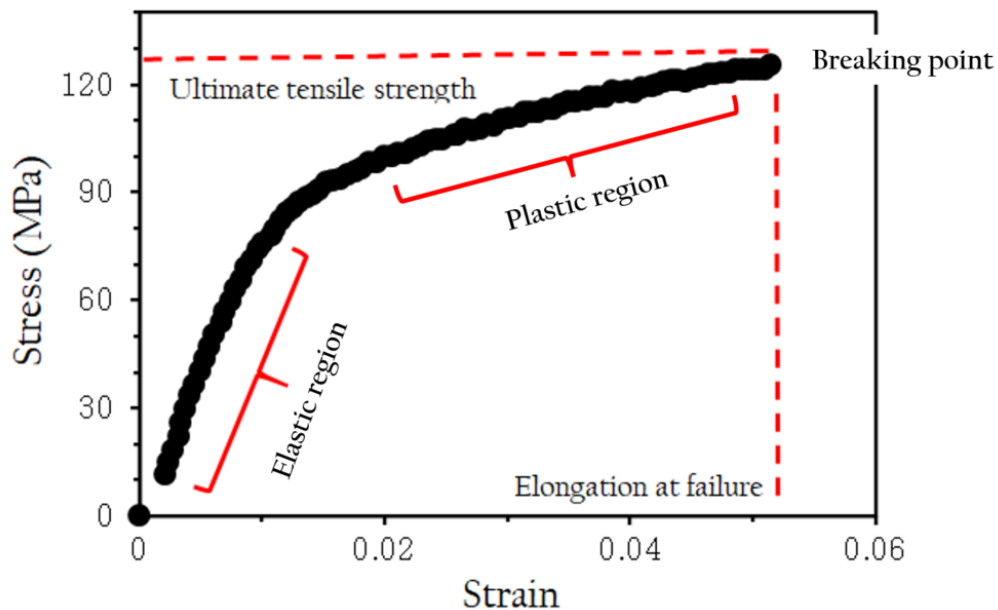


Figure 3.6: *Typical stress/strain curve indicating regions of tensile response typical for a polymeric material: Elastic region, Plastic Region and Breaking Point*

Shown on this example curve are 3 distinct regions, characteristic for polymeric materials such as these films: an elastic region, a plastic (viscous) region and a breaking point; described below. These regions are used to determine the mechanical properties of the films, namely; Young’s Modulus, Tensile Strength and strain to failure for each sample.

- The **elastic region** refers to the initial linear segment of Figure 3.6, where the material obeys Hooke’s law as the intermolecular bonds are stretched. If the sample was removed from the test whilst still in this elastic region, it would return to its original length as it has not gone through permanent deformation. In this region, stress is proportional to strain and the ratio of

these two properties is a constant known as **Young's Modulus**, 3.4.

$$Y = \frac{\sigma}{\varepsilon} \quad (3.4)$$

Where Y gives Young's Modulus, σ gives stress and ε gives strain

Also known as 'stiffness', Young's Modulus is defined as the relationship between the deformation of a material and the force required to deform it. It can be determined from these stress/strain graphs by calculating the gradient of the linear region.

- **The plastic region** occurs after the elastic region, where stress and strain are no longer proportional. This is also known as the strain hardening region as the intermolecular bonds in the sample absorb energy and experience dislocations, changing their microstructure as they undergo plastic deformation to prevent breakage. Unlike the elastic region, if the test was stopped and the sample removed once it had entered this plastic region, it would not return to its original length due to these changes in the intermolecular bonds.
- Finally, the **breaking point** is the point at which the sample fractures and thus the load drops to zero. At this point, **ultimate tensile strength** and **strain to failure** can be determined by reading their maximum values off the graph to give the maximum values that a material can withstand before fracture. Strain at failure is also known as a material's ductility or brittleness. Materials with high ductility are able to absorb more energy as they undergo plastic deformation up to their fracture point.

3.2.2 Impact Testing

Falling dart impact testing

As well as tensile testing, falling dart impact tests were also performed to assess the mechanical properties of the films. This is a useful test in assessing the effectiveness of materials subject to various impacts during application and production. A Rosand impact tester, shown in Figure 3.7, was used to implement

3.2 Macroscopic Testing

these tests, with a 12.7 mm rounded-tip dart to fracture the films. 10 cm x 10 cm cut outs of the films were sandwiched between two metal plates with emery board surfaces to prevent slippage. A circular hole, $d = 76$ mm, in the centre of these plates exposed the films to the dart, allowing the dart to fall through and puncture the films during testing. Samples were loaded into a pressurised lower compartment to press the two metal plates together and keep the sample and plates in place. During testing, the dart was allowed to free-fall onto the films from a height above the films of 200 mm at an impact speed of 2 m/s (120000 mm/min), whilst the software measured the force on the dart at 5.9×10^{-5} s intervals. Force-extension graphs can be plotted using this data, which can be used to determine the **maximum force** and maximum extension which was converted to **strain** using Equation 3.19, that the films can withstand under impact. Furthermore, the **energy absorbed** during impact can be found by integrating the area under the force/displacement graph and normalising by dividing by the thickness of the film. A typical Force vs Extension graph for these films is shown in Figure 3.8

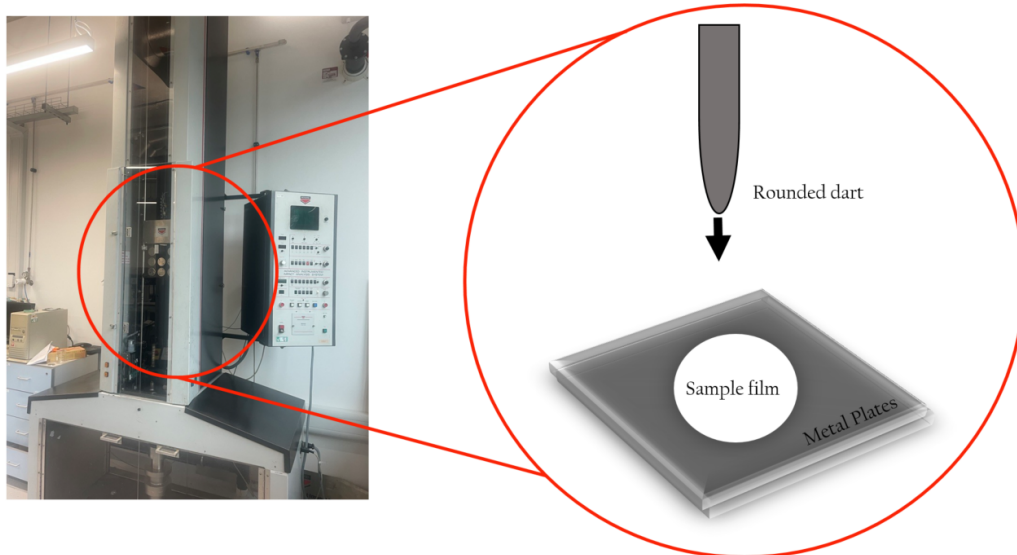


Figure 3.7: *Rosand Impact Tester with dart and sample plates highlighted schematically*

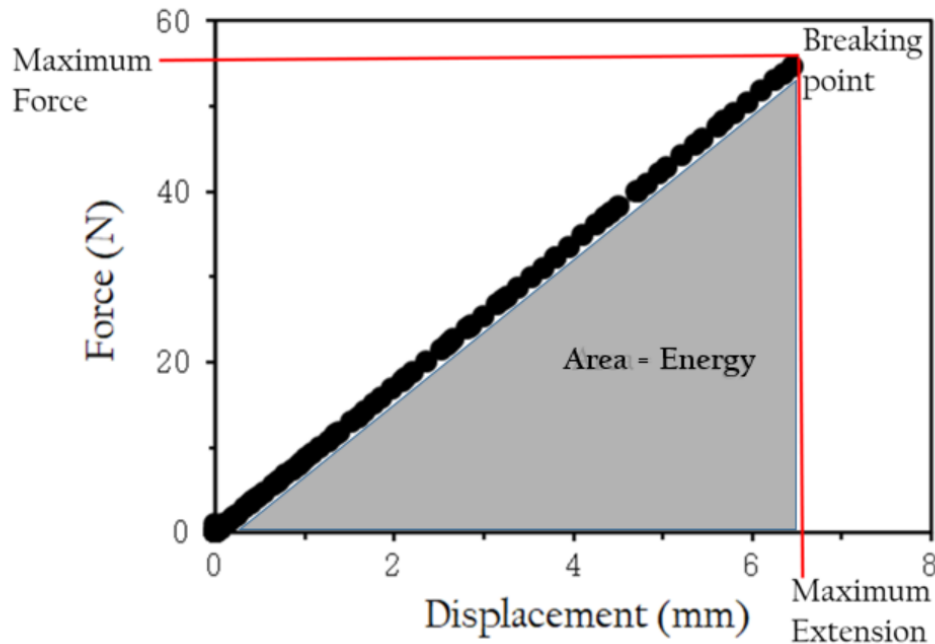


Figure 3.8: *Typical Force/extension graph with maximum force, extension and energy indicated on the graph*

Slow Puncture Impact Testing

As well as free-fall impact tests, another impact method so forth termed “slow puncture impact tests” was developed using the compression mode of the Instron tensile tester along with specialist apparatus commissioned by the Mechanical Workshop here at The School of Physics and Astronomy at Leeds. This novel test was created in order to determine any variation in the film’s impact behaviour at varying speeds with the same geometry. The results of these tests instigated a turning point in the project that helped to determine our overall story. Without these tests we might not have been able to acknowledge a difference in molecular motion that led us to Dynamic Mechanical Thermal Analysis.

For this testing method, demonstrated by Figure 3.9, the 12.7 mm dart used in the traditional falling weight impact test replaced the upper clamp of the tensile tester. The tested film was sandwiched between a custom made clamp with the same central hole diameter as the cut out in the impact tester plates, $d = 76$ mm,

3.3 Molecular Property Testing

in order to try and emulate that test as closely as possible so that results were comparable. This custom clamp was placed onto a hollow base so that the dart could strain the films before fracture without crashing into the base. Once samples were installed, the rounded dart was driven into films at speeds of 1 mm/min, 100 mm/min, 300 mm/min (for commercial films only) and 1000 mm/min for a total of five repeats for each film (Due to the limited quantities of lab-based films, the speeds 1 mm/min, 100 mm/min, 1000 mm/min and 120000 mm/min were prioritised) During analysis, strain, maximum force and normalised energy were calculated using Force vs Extension graphs and compared to the falling dart impact tests performed at a speed of 2 m/s (120000 mm/min).

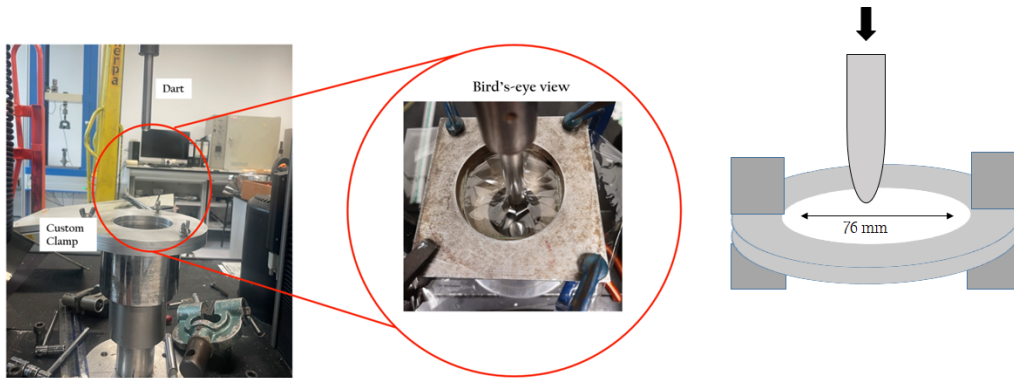


Figure 3.9: *Slow puncture impact test set-up using Instron tester in compression mode, with dart and specialised clamp highlighted*

3.3 Molecular Property Testing

Once mechanical testing was concluded on the commercial films, it was clear that there was some variation of performance at different impact speeds. This was an extremely important finding, not only in terms of the project direction, but also for Futamura's production process as films are subject to a range of possible breakages due to operating speed during manufacturing and processing. With these results, operators can apply or avoid certain speeds and hopefully reduce breakages.

The next step was to determine the origin of the observed fluctuation of properties. For this answer, we looked to one of the fundamental principles of Soft Matter Physics to explain the polymer behaviour of the cellulose chain. Namely, that polymers are extremely sensitive to changes in external stimuli; be that temperature, force, light, charge or something else. One way to understand this behaviour is by investigating the variation of molecular motion of the cellulose molecule in these films whilst varying external factors, using a technique called, Dynamic Mechanical Thermal Analysis (DMTA). These links are the key to understanding the functionality of these films and ultimately how their production can be optimised. Literature tells us that brittle yielding occurs due to crack formation as a result of a lack of molecular response to the stress in a given time. In fact, fracture occurs when the time taken to reach failure is equal to or greater than the speed of the transition process that controls mechanical behaviour that temperature. This reliance of fracture mechanics on microscopic timescales is what prompted the investigations into dynamic behaviour across a range of temperatures.

3.3.1 Dynamical Mechanical Thermal Analysis

Basic Principles

The operation of DMTA can be summed simply in one sentence:

”Applying an oscillating force to a sample and analysing the materials response to that force”

This technique has advanced significantly since the first example of using an oscillatory force to assess elasticity by English Physicist J.H.Poynting in 1909 [93]. First commercialised in the 1950s in the form of the Weissenberg rheogoniometer and the Rheovibron; this technology soon proved to be an essential tool in a polymer scientist’s kit due to the ability to characterise viscoelastic materials by providing a more complex characterisation of modulus [94]. With this technique, analysis of damping (energy loss) and recovery (elasticity), help to describe changes in free volume in order to identify polymer transitions [95][96].

3.3 Molecular Property Testing

DMTA is somewhat similar to the linear tensile deformations discussed in Section 3.2.1, in the sense that a stress is applied and the material response, or strain, is measured. In DMTA, this is an oscillatory stress, meaning that frequency can be changed and the effects on internal structure of the polymer determined. In addition, a temperature controlled chamber surrounds the sample allowing both temperature and frequency to be altered, changing the behaviour of the material. This is especially useful in polymer science since polymeric materials are sensitive to a range of transitions between their solid and liquid phases that can be identified using this technique.

To describe how DMTA does this, we start with a sample held at a constant pre-load force within its linear viscoelastic region. This pre-load is applied to assure the sample remains in its tensile regime. If we apply a sinusoidal force of a certain frequency at this point, the material will respond with a sinusoidal strain, as depicted in Figure 3.10. The resultant stress is measured depending on the type of material being tested whether it is elastic, viscous or viscoelastic.

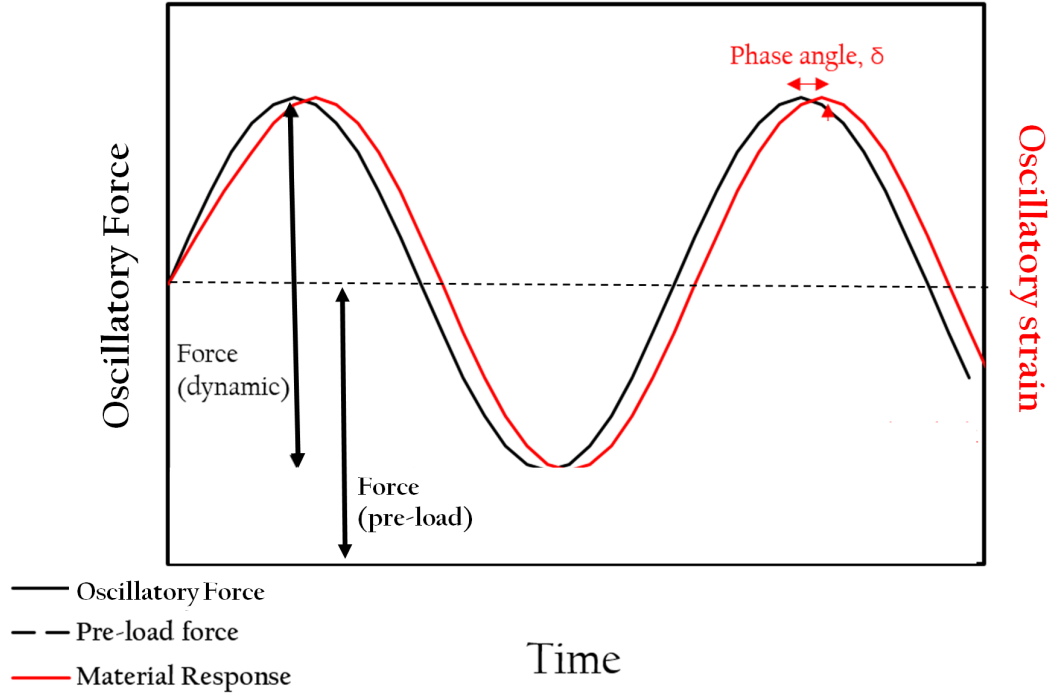


Figure 3.10: Graphical depiction of oscillatory force and resultant material deformation (strain) observed in DMTA measurements. Adapted from [94]

Since this material response strain is oscillatory and not linear like that of the tensile testing strain, we must do some maths to quantify this graph and obtain meaningful moduli for which we can describe the tested material. For this sinusoidal strain:

$$e = e_0 \sin(\omega t) \quad (3.5)$$

where e gives the strain at a given time, ω gives the angular frequency and e_0 gives the maximum strain

The resultant stress, σ will depend on the nature of the material:

- For an *elastic* solid, Hooke's law applies and so stress is proportional to strain with relation to the modulus of the solid, Y . This means that stress and strain are in phase, as shown in 3.11(a)

$$\text{elastic stress; } \sigma = Y e = Y e_0 \sin(\omega t) = \sigma_0 \sin(\omega t) \quad (3.6)$$

3.3 Molecular Property Testing

- For a *viscous* liquid, Newton's law of viscosity applies so stress is proportional to strain rate, \dot{e} , with relation to viscosity, η . This means that stress and strain are out of phase by 90° . as shown in 3.11(b):

$$\text{viscous stress; } \sigma = \eta \dot{e} = \eta e_o \omega \cos(\omega t) = \eta e_o \omega \sin(\omega t + \frac{\pi}{2}) \quad (3.7)$$

While viscous behaviour is not relevant in this study, it is important to understand so that we can explain viscoelastic behaviour.

- For a *viscoelastic* material, the phase lag is somewhere between 0° (ideal solid) and 90° (ideal liquid) as shown in 3.11(c).

$$\text{viscoelastic stress; } \sigma = \sigma_0 \sin(\omega t + \delta) \quad (3.8)$$

This stress consists of a viscous and an elastic component. As such, we must define a complex modulus, E^* , to represent both components as the ratio of sinusoidal stress and strain. Converting to exponential gives:

$$E^* = \frac{\sigma}{e} = \frac{\sigma_0 e^{i(\omega t + \delta)}}{e_0 e^{i\omega t}} = \frac{\sigma_0}{e_0} e^{i\delta} \quad (3.9)$$

using $e^{i\delta} = \cos\delta + i\sin\delta$:

$$E^* = \frac{\sigma_0}{e_0} (\cos\delta + i\sin\delta) \quad (3.10)$$

$$E^* = E' + iE'' \quad (3.11)$$

where E' is the in phase component, known as the **Storage Modulus**:

$$E' = \frac{\sigma_0}{e_0} \cos\delta \quad (3.12)$$

and E'' is the out of phase component, known as the **Loss Modulus**:

$$E'' = \frac{\sigma_0}{e_0} \sin\delta \quad (3.13)$$

Lastly, we can define a third quantity, **$\tan\delta$** by taking the ratio of E' and

$$E'' \quad \frac{E''}{E'} = \frac{\sin\delta}{\cos\delta} = \tan\delta \quad (3.14)$$

$\tan\delta$ is defined as the material loss factor and is not dependent on geometry of measured material. The higher the $\tan\delta$ of a material, the more viscous its behaviour.

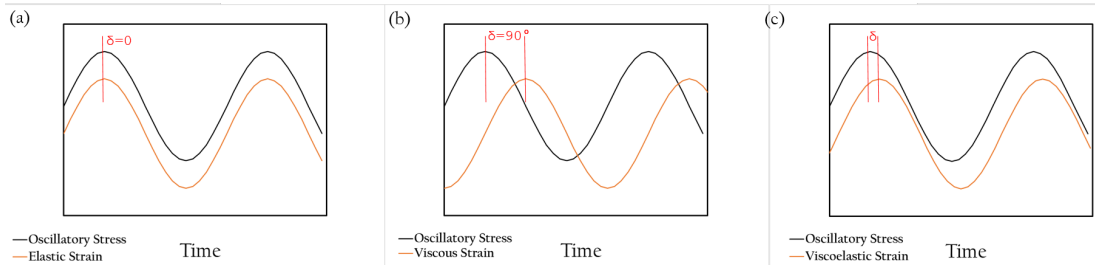


Figure 3.11: *Depiction of phase lag, δ of material strain in response to oscillatory stress for (a) Elastic (b) Viscous and (c) Viscoelastic materials. Adapted from [94]*

In the results section we will assess how these three properties: Storage Modulus, Loss Modulus and $\tan\delta$ differ across a range of temperatures for the suite of films described in Table 3.1. Analysing how these properties change in response to stimuli can help determine molecular structure and to identify primary (α) and secondary (β, γ) transitions of these materials.

Equations and theory have been derived from [94][68]. More in depth derivations found in [97], but for the purpose of this thesis, this level of detail should be sufficient.

Instrumentation

The instrument used in this work is a TA instruments Discovery DMA 850 analysed with TRIOS software. A tensile clamp was used to apply a uniaxial deformation to films in the machine direction with a typical width = 5 mm and gauge length = 20 mm, shown in Figure 3.12.

3.3 Molecular Property Testing

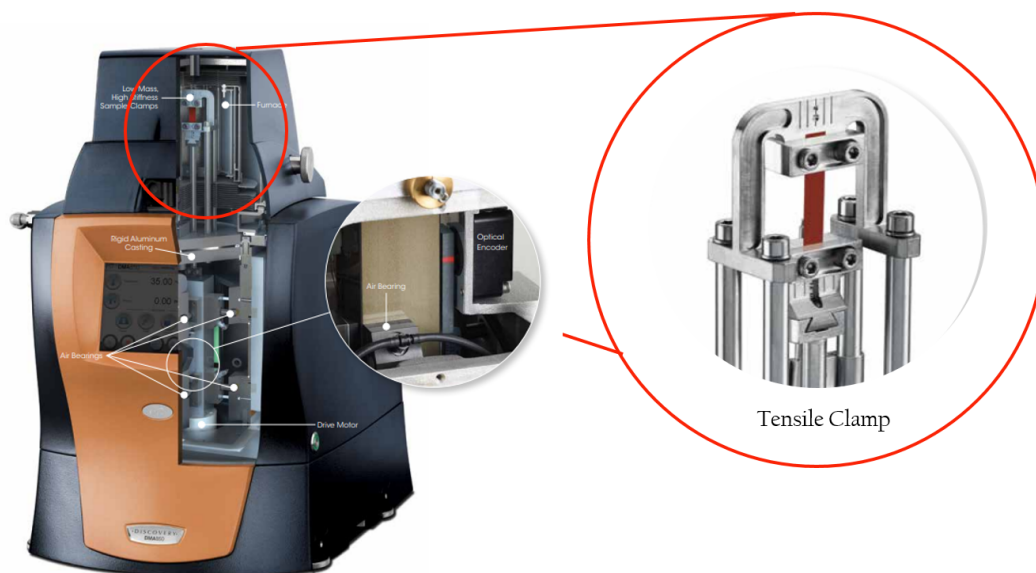


Figure 3.12: *Discovery DMA 850 from TA instruments, with tensile clamp highlighted. Taken from [98]*

This machine is a forced resonance analyser, meaning that the sample is controlled by a non-contact motor to provide static or dynamic deformation for a range of motion up to 25 mm. To control temperature, the furnace choice of a bifilar wire wound furnace provides rapid temperature response over a large range and is a common choice for DMTA temperature control across devices. Unlike most DMTAs that use a linear vertical displacement transducer (LVDT) to determine probe position, this device uses a high resolution optical encoder, that provides position measurements based on diffraction of light through gratings for accurate displacements as small as 5 nm. This equipment is used in conjunction with a Gas Cooling Accessory (GCA) in order to cool samples down to $-100\text{ }^{\circ}\text{C}$ using controlled evaporation of liquid nitrogen stored in the GCA tank [98]. As well as the tensile clamp, there are a number of different clamp accessories available with this instrument including dual/single cantilever, 3-point bend, compression and shear.

Viscoelastic behaviour of polymers

This thesis applies ‘Temperature Ramps’ to sample films; whereby a sample is oscillated at a set frequency from a low temperature to a high temperature whilst E' , E'' and $\tan\delta$ are measured with each oscillation. These results can be used to identify changes in the free volume of molecules and thus polymer transitions identified.

Free Volume, v_f is defined as the space a molecule has for internal movement within a system. A rudimentary visualisation often used to describe this molecular movement is to imagine a crank shaft with the polymer consisting of several different sections, each capable of some degree of independent movement and rotation [99], shown in Figure 3.13.

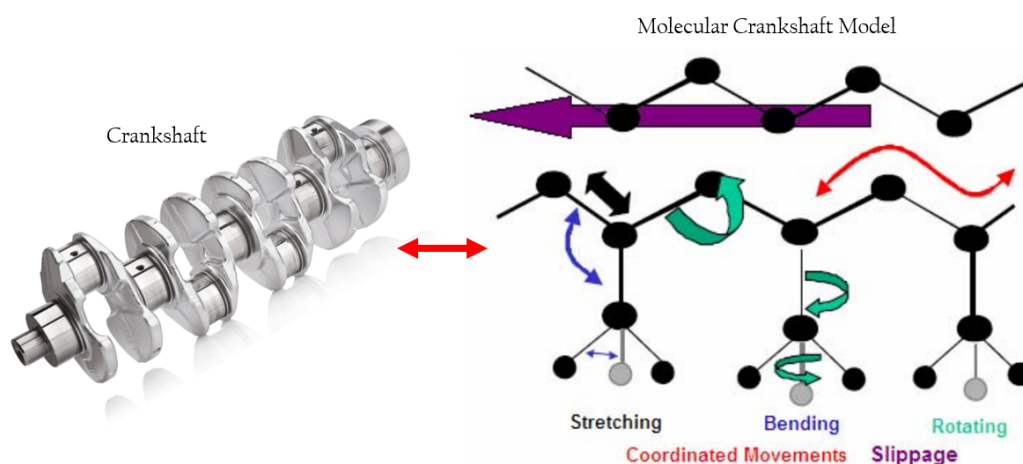


Figure 3.13: Crankshaft depiction of polymer chain, used to demonstrate movement of side chains which has been shown by Atomic Force Microscopy to be an appropriate approximation of the molecular chain. Crankshaft picture taken from [100]; molecular model taken from [101]

3.3 Molecular Property Testing

As the temperature increases during a DMTA test, the free volume increases as a result of a mobility increase of polymer side chains and backbone, resulting in a reduced modulus and peaks in $\tan \delta$ over a range of transitions ($\gamma - \alpha$). These transitions and resultant reduction of modulus for an idealised polymer can be seen in Figure 3.14

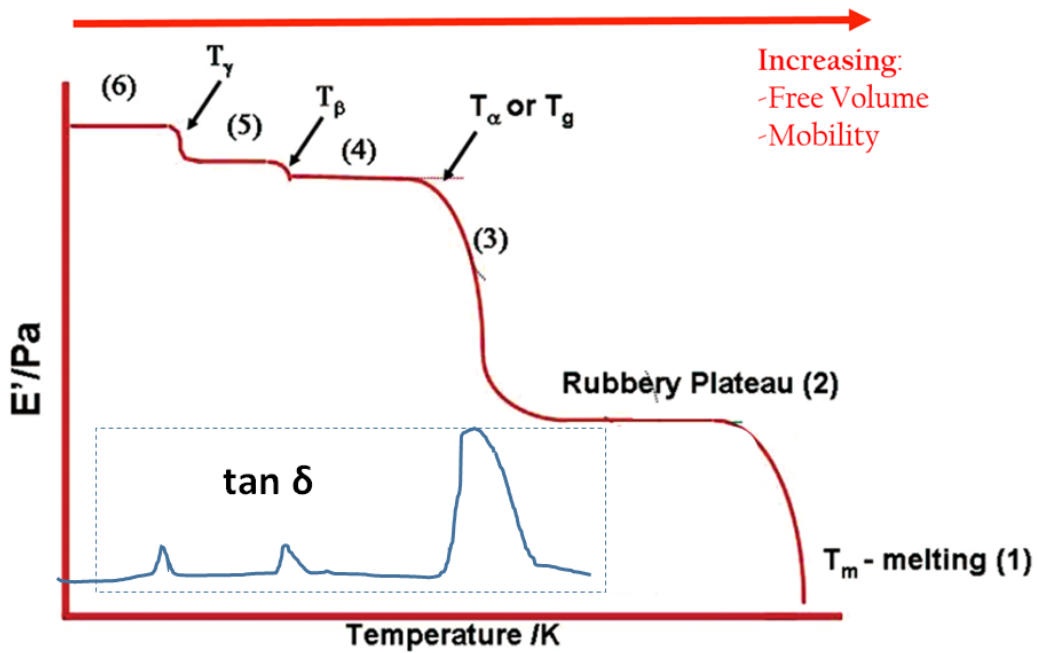


Figure 3.14: *Viscoelastic response of an idealised polymer from low to high temperature, representing a number of transitions depending on side chain and backbone motion. Adapted from [102].*

3.3 Molecular Property Testing

This representation is a model for what can be expected to be observed for a range of different polymers. However the behaviour of each polymer differs and variations of this behaviour are observed for our samples. At low temperatures, the molecule is compressed with polymer chains tightly packed, as temperature increases and free volume and mobility increase with it as the material experiences glassy transitions until eventually melting. The depiction of behaviour (6) - (1) in Figure 3.14 can be described:

6. Molecular mobility increases with temperature such that local motions can begin and T_γ **Transition** occurs, in cellulose; often associated with a molecules interaction with water [99].
5. Molecular mobility continues to increase, allowing for bend and stretch of local bond motion and T_β **Transition** occurs [103].
4. Side groups motion becomes available, imparting toughness and **Glass Transition, T_g** occurs.
3. Groups of 4-8 backbone atoms mobilise collectively [103].
2. As free volume continues to increase, reaching **The Rubbery Plateau** large scale chain movement of amorphous portion of chain occurs.
1. **Melting Temperature, T_m** where large scale chain slippage is observed.

Since the expected mobility response to temperature for a viscoelastic polymer has been outlined, we can align these expectations with observed results for the cellulose chains in tested films.

Testing Methods

Temperature ramps across a range of temperatures at a chosen frequency were the chosen testing method for these films. Using this testing method, a number of different procedures were developed that helped to understand the dynamic response of the cellulose films.

3.3 Molecular Property Testing

1. **Basic Temperature Ramp Procedure** (*-100 °C to + 260 °C at 2 °C/min at 1 Hz*): Performed on commercial films based off literature showing interesting dynamics for cellulose within this temperature region [104]. Upon removing films, it was clear that cellulose or softener degradation had onset during that temperature range due to a colour change to dark brown as well as extreme brittleness of films such that they couldn't be removed from clamps without breaking. Therefore, future tests for lab-made films the maximum temperature was reduced to avoid degradation but still include meaningful transitions up to 120 °C.
2. **Water Removal Procedure** (*-100 °C to + 120 °C at 2 °C/min at 1 Hz ($\times 2$)*): Performed on lab made films to assess the impact of water content on the dynamic properties of the films. Films were cooled to -100 °C and heated at 2 °C/min whilst undergoing an oscillation of 1 Hz up to 120 °C to ensure all free water was removed from the film over this temperature range. Furthermore, this will ensure no degradation of the cellulose chains which occurs ~ 200 °C as well as being lower than the boiling points of Glycerine ($T_B = 290$ °C), MPG ($T_B = 188$ °C) and Urea ($T_B = 332$ °C) to ensure that they are not removed with water. The DMTA chamber was kept sealed in order to prevent re-absorption of atmospheric water such that they remain in a nitrogen atmosphere whilst the film was cooled back to -100 °C and then heated back to 120 °C at 1 Hz. The difference between dynamic behaviour of these runs helped to identify and confirm the role of water in the molecular motion of the films.
3. **Multi-frequency Temperature Ramp Procedure** (*-100 °C to + 120 °C at 4 frequencies from 0.1, 1, 10 and Hz at 0.02 % strain*): Performed on the 8 % softener in bath glycerine lab based films in a step to understand how to link mechanical impact test with dynamic tests. Results were compared with the variation of mechanical properties observed in impact and slow puncture testing by converting operation speeds to strain rates that can compared to oscillation frequencies (see Section below). Furthermore, by observing the temperature shift of peaks at varying frequencies, Time-Temperature Superposition could be performed and an activation energy,

E_a calculated using equation 5.3

$$\ln(f) = \frac{E_a}{RT} \quad (3.15)$$

3.4 Strain rate conversions

In this thesis, four different testing techniques were used. each of which were operated at a different speed range: tensile testing (fixed speed), falling weight impact (fixed speed), slow puncture impact (range of speeds) and DMTA (range of speeds (frequencies)). In order to compare these testing methods, speeds and frequencies have been converted to strain rates such that mechanical and structural properties can be compared

3.4.1 Conversion of speed to strain rate (Impact, puncture and tensile testing)

Falling weight impact and slow puncture testing

For falling impact and slow puncture testing, the test speeds of 1 mm/min, 100 mm/min, 1000 mm/min and 120000 mm/min were converted to strain rates with units s^{-1} in order to draw comparisons with the frequencies of DMTA tests and constant speed of the tensile testing. These strain rates were calculated using the following derivation, using Figure 3.15(a-b) demonstrating dimensions of the calculations.

In order to calculate the strain rate for impact and slow puncture testing, the testing method is modelled as a centrally loaded circular plate with edges supported, shown in Figure 3.15(a). This derivation is taken from reference [105]. We first define the maximum stress, σ at the centre of the circular exposed area.

$$\sigma = \frac{6F}{4\pi t^2} (1 + \nu) \ln\left(\frac{r}{e}\right) \quad (3.16)$$

where F gives the applied force, t gives the thickness of the sample film, ν gives the Poisson's ratio, r gives the radius of the films ($r = 0.038$ mm) and e is related to the radius of the contact area and which for small values is given by $e = 0.325t$.

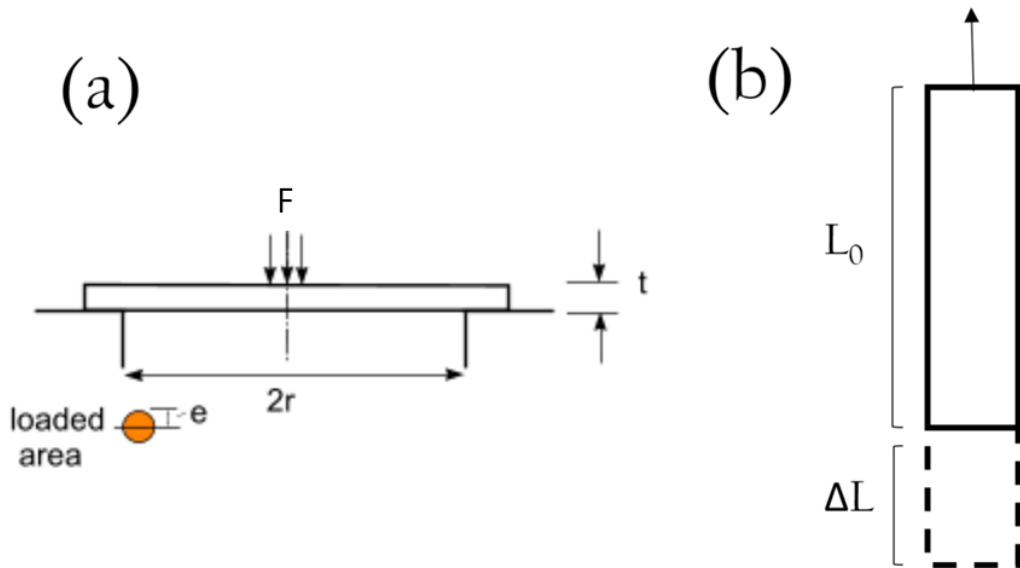


Figure 3.15: *Depiction of deformation used to calculate strain rates for (a) Impact and slow puncture testing (modelled as a centrally loaded circular plate with edges supported, adapted from [105]) and (b) Tensile Testing*

3.4 Strain rate conversions

Therefore, for an equibiaxial stress field, Hooke's law provides the strain:

$$\epsilon = \frac{6F}{4Y\pi t^2}(1 - \nu^2)\ln\frac{r}{e} \quad (3.17)$$

where Y gives the Young's Modulus

In order to eliminate Force, F, the maximum central deflection, x, is given by:

$$x = \frac{0.217Fr^2}{Yt^3} \quad (3.18)$$

Therefore, strain is calculated using:

$$\epsilon = \frac{3tx}{2\pi \times 0.217r^2}\ln\left(\frac{r}{0.325t}\right) \quad (3.19)$$

where we have assumed that $\nu = 0$ for small e

Therefore, strain rate is given by:

$$\dot{\epsilon} = \frac{3t \times \text{velocity}}{2\pi \times 0.217r^2}\ln\frac{r}{0.325t} \quad (3.20)$$

where velocity describes the velocity of impact.

This strain rate calculation must be ammended since impact and slow puncture tests concerned all directions of the films on impact, where as tensile testing and dynamic mechanical thermal analysis were performed in only one direction at a time. The strain rates from 3.20 should be doubled to give the same octahedral shear strain rates as for the uniaxial (Tensile and DMTA) tests, therefore:

$$\dot{\epsilon} = 2 \times \frac{3t \times \text{velocity}}{2\pi \times 0.217r^2}\ln\frac{r}{0.325t} \quad (3.21)$$

Equation 3.19 was used to convert the maximum extension of impact and slow puncture testing into a strain in order to normalise the extension. Equation 3.21 was used to calculate the strain rate of impact and slow puncture tests for speeds: 1 mm/min, 100, mm/min, 300 mm/min (commercial films only), 1000 mm/min and 120000 mm/min. In order to calculate these strain rates, the thicknesses of films was required, which are shown in Table 3.2. These strains and strain rates are represented on impact and slow puncture graphs in the results section of this

3.4 Strain rate conversions

thesis. As extension was different for each test, the strain rates varied for each sample film. Table 3.3 has been constructed to demonstrate the range of strain rates and comparison to speeds for each film.

Table 3.2: Table of average thickness of commercial and lab-based films.

Sample	Average thickness (mm)
Commercial Films	
Unsoftened	0.0294 ± 0.0006
3 Component Softener	0.0284 ± 0.0002
3 Component Softener (coated)	0.02986 ± 0.0001
3 Component Softener (TiO ₂)	0.0261 ± 0.0003
1 Component Softener	0.0306 ± 0.0001
Lab-based Films	
Unsoftened	0.0310 ± 0.0004
MPG 4 %	0.035 ± 0.002
MPG 8 %	0.041 ± 0.001
MPG 15 %	0.043 ± 0.003
Glycerine 4 %	0.031 ± 0.002
Glycerine 8 %	0.0420 ± 0.0003
Glycerine 15 %	0.046 ± 0.002
Urea 4 %	0.0393 ± 0.0003
Urea 8 %	0.051 ± 0.002
Urea 15 %	0.059 ± 0.001
3 Component Softener 4 %	0.0315 ± 0.0001
3 Component Softener 8 %	0.0357 ± 0.0002
3 Component Softener 15 %	0.0377 ± 0.0002
2 Component Softener 4 %	0.031 ± 0.003
2 Component Softener 8 %	0.041 ± 0.003
2 Component Softener 15 %	0.045 ± 0.002
Hemicellulose 4 %	0.0297 ± 0.0005
Hemicellulose 8 %	0.041 ± 0.002
Hemicellulose 15 %	0.0393 ± 0.0003

3.4 Strain rate conversions

Table 3.3: Table of falling weight and slow puncture impact speeds converted to strain rates.

Testing Speed (mm/min)	Strain rate range (1/s)
Slow Puncture	
1	0.00001 - 0.00002
100	0.001 - 0.002
300	0.003 - 0.007
1000	0.01 - 0.02
Falling weight	
120000	1 - 3

Tensile Testing

For consistency of results, the constant speed of tensile testing was also converted to a strain rate using the derivation shown below, with Figure 3.15(b) demonstrating the dimensions of calculations.

$$\dot{\epsilon} = \frac{\Delta\epsilon}{\Delta t} = \frac{\Delta L}{L_0 \Delta t} \text{ where speed} = \frac{\Delta L}{\Delta t} \quad (3.22)$$

$$\dot{\epsilon} = \frac{\text{speed}}{L_0} \quad (3.23)$$

*Equation 3.23 was used to calculate the strain rate of tensile tests. As speed (10 mm/min) and L_0 (3.8 cm) are constant throughout the tensile test procedure, the strain rate of tensile tests is always **0.00439 s⁻¹**. this value is represented on impact and puncture graphs throughout this thesis as a dotted line.*

3.4.2 Conversion frequency to strain rate (DMTA)

Dynamic Mechanical Thermal Analysis

In the DMTA multi-frequency testing procedure, frequencies of 0.1 Hz, 1 Hz, 10 Hz and 100 Hz were applied during temperature ramps of certain films. For each oscillation, the Time Period, $T = 1/f$. So, the peak of this oscillation is seen at $T/4$, as shown by Figure 3.16 Therefore, to find strain rate at this peak for a

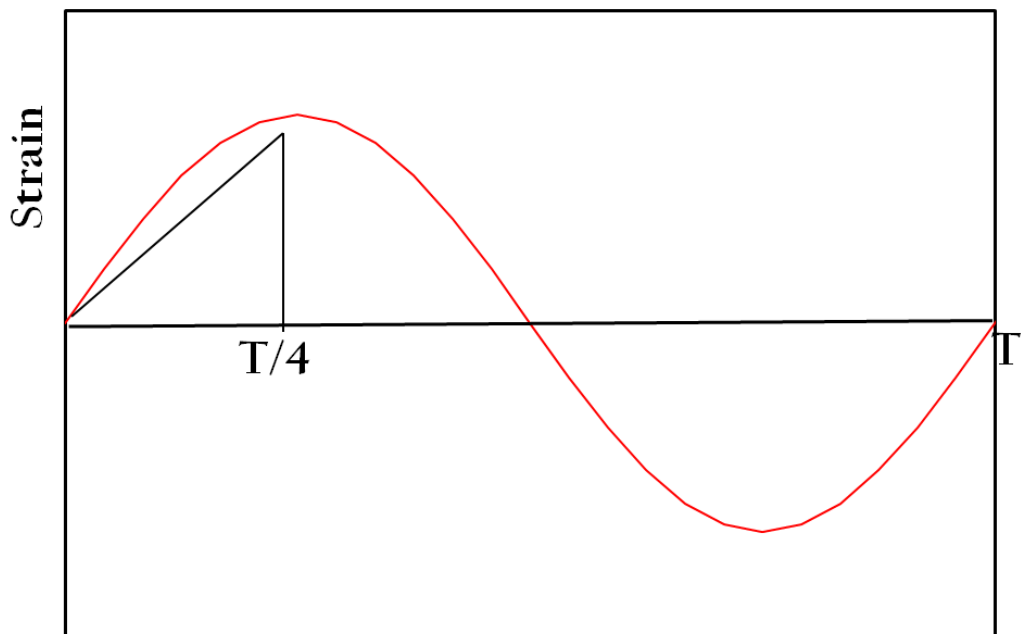


Figure 3.16: *Depiction of Time Period of oscillation*

3.4 Strain rate conversions

specific frequency:

$$\dot{\epsilon} = \frac{\Delta\epsilon}{t} = 4 \Delta\epsilon f \quad (3.24)$$

Where we say $\dot{\epsilon}$ is the maximum strain rate observed in room temperature impact graphs, for glycerine 20 % films, $\dot{\epsilon} = 0.01 \text{ s}^{-1}$. Furthermore, $\Delta\epsilon = 0.0002$ is the applied strain in dynamic testing.

Therefore, for dynamic frequencies of 0.1 Hz, 1 Hz, 10 Hz and 100 Hz, we obtain respective strain rates of 0.00008 s^{-1} , 0.0008 s^{-1} , 0.008 s^{-1} and 0.08 s^{-1} .

3.4.3 Summary of speeds and strain rates

In order to summarise the conversion of speeds and frequencies to one common and comparable property, strain rate; Table 3.4 has been produced to identify the range of speeds and strain rates used for each of the four testing methods used throughout this thesis: Tensile, falling weight impact, slow puncture and DMTA.

Table 3.4: *Summary of conversions of speeds and frequencies to strain rates for all testing methods*

Testing Speed (mm/min) / frequency (Hz)	Strain rate range (1/s)
Slow Puncture Impact	
1	0.00001 - 0.00002
100	0.001 - 0.002
300	0.003 - 0.007
1000	0.01 - 0.02
Falling weight Impact	
120000	1 - 3
Tensile Testing	
10	0.004
DMTA	
0.1	0.00008
1	0.0008
10	0.008
100	0.08

Chapter 4

Commercial Films, Results and Discussions

This Chapter contains the results and discussion of the experimental techniques applied to the set of commercial films containing an unsoftened sample, a 3 component softener sample (*This text has been removed by the author of this thesis for confidentiality reasons*) [REDACTED], with a coated and coloured version, as well as a 1 component softener sample (*This text has been removed by the author of this thesis for confidentiality reasons*) [REDACTED]. A summary of these films is included in Table 4. Each of these films were subject to tensile testing, impact and puncture testing and Dynamic Mechanical Thermal Analysis.

Table 4.1: *Summary of commercial films tested in this Chapter*

Film	Softener blend concentration	Softener in bath wt %
Commercial Unsoftened	No softener	0
3 component Softener	<i>(This text has been removed by the author of this thesis for confidentiality reasons)</i> [REDACTED]	~ 8
3 component Softener (coated)	<i>(This text has been removed by the author of this thesis for confidentiality reasons)</i> [REDACTED]	~ 8
3 component softener (TiO ₂)	<i>(This text has been removed by the author of this thesis for confidentiality reasons)</i> [REDACTED]	~ 8
1 Component Softener	<i>(This text has been removed by the author of this thesis for confidentiality reasons)</i> [REDACTED]	~ 8

4.1 Softener Content

The method employed to determine softener content in lab-made films outlined in Section 3.1.2 would not be effective for comparing softener content in commercial films due to the inclusion of coatings and additives that inhibit the removal of

softener molecules. As such, Futamura's estimations of softener content of films based off their production inputs are used. The softener in bath weight percentage of each of these softeners on plant is estimated to be *(This text has been removed by the author of this thesis for confidentiality reasons)* ██████████. Resulting in a softener in film content of *(This text has been removed by the author of this thesis for confidentiality reasons)* ██████████

4.2 Tensile Properties

In order to analyse tensile results, stress/strain curves were produced; from which values of Young's Modulus, Strength and strain at failure could be obtained. Typical stress strain curves for unsoftened and 3 component softened films in this films set are shown in Figure 4.1

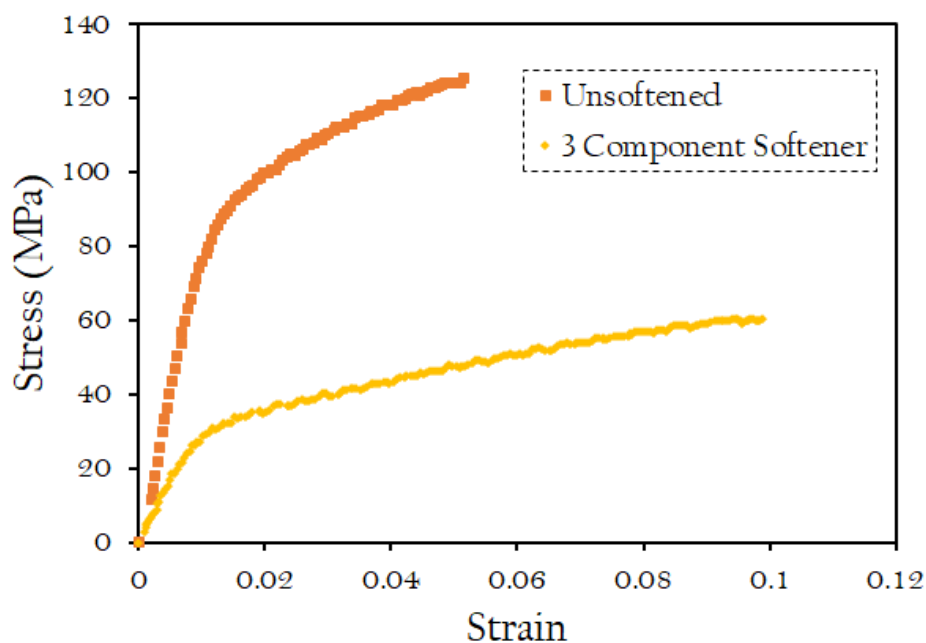


Figure 4.1: *Typical stress/strain curves for the unsoftened and 3 component softener commercial films*

4.2 Tensile Properties

These stress/strain curves demonstrate the effect of plasticisation on modulus and fracture point. The plasticised 3 Component Softener films exhibits a higher strain at failure and therefore higher ductility. However, in comparison to the unsoftened film, both modulus and strength are reduced. This trade-off between properties is an important consideration for Futamura. During testing, five repeats were performed for each material direction of each sample film to obtain stress/strain curves for each test from which Young's modulus, strength and strain at failure could be averaged. The data from these tests is presented in Table 4.2.

Table 4.2: *Tensile Test results of commercial films in machine and transverse directions for Young's Modulus, Strength and Strain at Failure*

	Modulus (GPa)	Strength (MPa)	Failure (%)
Transverse Direction			
Commercial Unsoftened	3.0 ± 0.3	50 ± 1	8 ± 1
3 component Softener	1.3 ± 0.1	30.5 ± 0.3	18.3 ± 0.6
3 component Softener (coated)	1.5 ± 0.1	35 ± 1	21.2 ± 0.8
3 component softener (TiO2)	2.1 ± 0.1	36 ± 1	14 ± 2
1 Component Softener	1.7 ± 0.1	36.4 ± 0.9	17 ± 1
Machine Direction			
Commercial Unsoftened	6.7 ± 0.2	122 ± 3	4.3 ± 0.2
3 component Softener	3.0 ± 0.3	60 ± 1	9.3 ± 0.8
3 component Softener (coated)	3.0 ± 0.4	66 ± 1	9.4 ± 0.9
3 component softener (TiO2)	3.7 ± 0.3	70 ± 2	7.8 ± 0.2
1 Component Softener	4.1 ± 0.2	74 ± 2	7.5 ± 0.8

These results show that the unsoftened film has the highest modulus and strength, with the lowest failure strain. Whilst the the 3 component softened films have lower modulus and strength but with higher strain at failure. In order to represent this data, the tensile properties of these commercial films have been represented by Ashby plots to compare mechanical properties, presented by Figures 4.2(a-c) of Young's Modulus, strength and strain at failure in both the machine and transverse directions plotted against each other. This initial set of commercial films have allowed for the determination of some basic material properties of the films. Including material property relationships, the difference in machine and transverse properties inherent and the effect of softeners on mechanical performance.

4.2 Tensile Properties

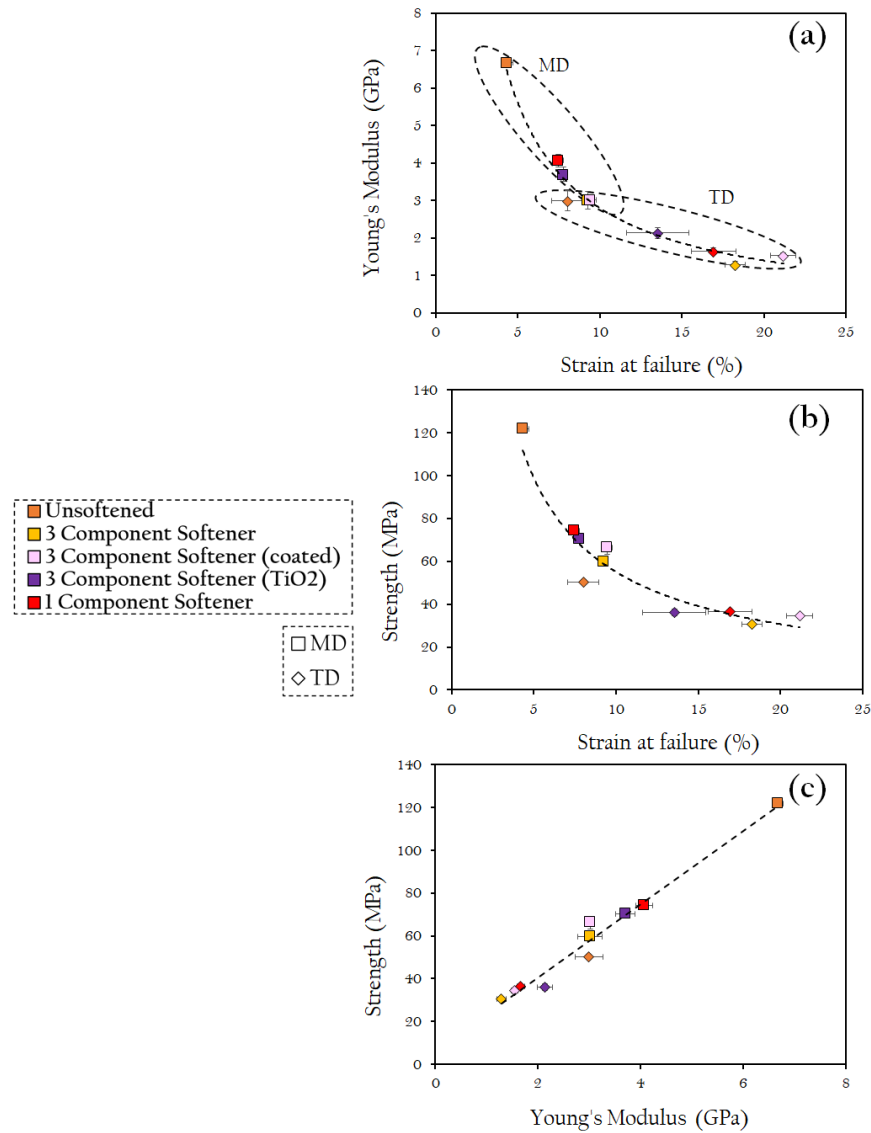


Figure 4.2: Ashby Plots depicting the variation of tensile properties for the commercial film set in their machine (square markers) and transverse (diamond markers) directions (a) Young's Modulus against strain at failure, (b) Strength against strain at failure and (c) Strength against Young's Modulus

4.2.1 Material property relationships

The trends between material properties: Modulus, strength and strain to failure are well accepted in polymeric materials and their trade off is confirmed by these films' 'Ashby Plots'. So-called, 'Ashby plots' compare mechanical properties and are often used as a material selection chart to evaluate the performance of a range of materials, making them a useful tool in this work [106].

For example, Figures 4.2(a-b) show a similar relationship between modulus and strength with strain at failure for all five films in both the machine and transverse directions. As strain at failure increases, Young's Modulus and strength decrease. This observation is due to an increase in internal molecular mobility, induced by the addition of plasticisers; therefore plasticisers can be said to decrease modulus and strength whilst increasing strain at failure. On the other hand, Figure 4.2(c) shows a positive linear relationship between strength and Young's Modulus for all five films, indicating these two properties' proportionality. Clearly, it would be desirable for films to be in the upper right hand corner region of this final figure, with high tensile strength and elastic modulus. However, as seen with the unsoftened film, these attributes come at the expense of strain to failure. That is to say that stiffer/stronger samples are more brittle.

Due to the expected compromise between stiffness/strength and ductility inherent in these samples, it is important to consider which of these properties is most desirable for the intended application. A high ductility is desirable to ensure that films do not fracture during the production process and a high stiffness and strength are essential in their application as film packaging. Since modulus and strength can be controlled and increased by increasing thickness of the sample, strain at failure is considered a more desirable material property. Managing these three properties is the main function of plasticisers in these materials.

4.2.2 Machine and transverse uniaxiality

Another important observation from Figures 4.2(a-c) is the variation between transverse (TD) and machine (MD) direction properties. The uniaxiality of these films arises from the extrusion casting technique as well as induced tension during rolling on the production line, depicted in Figure 4.3 and described in Section

2.2.2. The effect of these processes are evident in the variation of machine (square markers) and transverse (diamond markers) mechanical properties in the two perpendicular directions of the films, annotated on Figure 4.2(a) as dashed circles around machine and transverse regions of the Ashby plot.

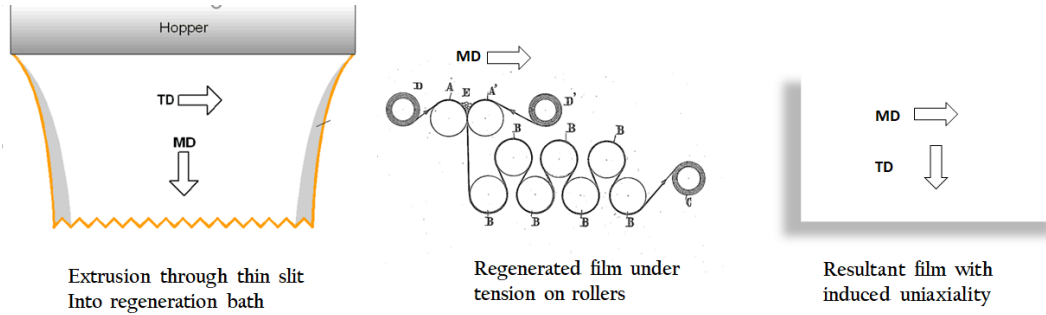


Figure 4.3: *Depiction of two processes that impart uniaxiality: extrusion and tension and resultant film with machine (MD) and transverse (TD) directions. Taken from [35][60]*

As seen on the plots in Figures 4.2(a-c); for every sample, modulus and strength are higher in the machine direction whilst strain to failure is higher in the transverse direction. This trend is evident for this commercial film set due to the induced machine direction caused by extrusion and rolling. The average ratio between the machine and transverse values of Young’s Modulus, strength and strain to failure are 2.1 ± 0.1 , 2.1 ± 0.1 and 2.0 ± 0.1 , respectively. Meaning that, on average, Young’s Modulus is 2.1 x greater in the machine direction, Strength is 2.1 x greater in the machine direction and strain to failure is 2.0 x greater in the transverse direction across this set of samples.

An increase in Young’s Modulus and strength in the machine direction can be attributed to the influence of the longitudinal cellulose fibre properties in the processing direction. During extrusion and rolling, films are stretched in the machine direction, causing the cellulose chains to align, resulting in increased stiffness and therefore an increased resistance to deformation, in comparison to the unaligned chains in the transverse direction. Conversely, values of strain to failure in the transverse direction are double those in the machine direction. This observation can also be attributed to the higher stiffness in the machine direction as the aligned chains have reduced mobility, resulting in a reduced resistance to

deformation. An increased phase of plastic deformation is indicative of increased toughness, characterised by the area under the stress strain curve, of a material as it can absorb more energy before breaking. This difference in orientation of the perpendicular directions of the films is due to stretching during the commercial process and is inducing a distinct effect on performance.

4.2.3 Variation of softener and additives

For each five of these films, the variation of softeners and additives results in a change of mechanical properties; giving insight into the performance of these additions, indicated in Table 4.2

It is immediately clear from Figure 4.2(c) that the unsoftened films has increased stiffness and strength across the machine and transverse directions of the film in comparison to the plasticised samples; with Young's Modulus = 6.7 ± 0.2 GPa, strength = 122 ± 3 MPa (MD) and Young's Modulus = 3.0 ± 0.3 GPa, strength = 50 ± 1 MPa (TD) compared ranges of Young's Modulus = 3.0 - 4.1 GPa, strength = 60 - 74 MPa (MD) and Young's Modulus = 1.3 - 2.1 GPa, strength = 30 - 36 MPa (TD) across the plasticised films. However, Figures 4.2(a-b) show a significant decrease in strain to failure for this unsoftened film of 4.3 ± 0.2 % (MD) and 8 ± 1 % (TD) when compared to plasticised films range of 7.4 % - 9.4 % (MD) and 13.5 % - 21.1 %. This coincides with the stress strain graphs, which had smaller regions of plastic deformation in the unsoftened sample. The increased failure strain of plasticised films can be attributed to the addition of softeners in order to reduce the brittleness of the samples. However, this reduced brittleness results in a decrease in modulus and strength.

After the unsoftened sample, the 3 component softener with TiO₂ particles and 1 component softened films have the next highest values for Young's Modulus across the film of 3.7 ± 0.1 GPa and 4.1 ± 0.2 GPa (MD). With this decrease in Modulus, an increase in strain to failure is observed of 7.8 ± 0.2 % and 7.5 ± 0.8 % (MD) for the TiO₂ and 1 component films, respectively. As this strain is less than that of the 3 component softener and its coated version, this result suggests that the addition of TiO₂ particles reduces the plasticisation effect of the 3 component softener. It is hypothesised that the interaction between TiO₂

4.3 Falling weight and slow puncture impact properties

particles and cellulose is ‘anti-plasticising’ by imparting stiffness and strength. Furthermore, these results show that although the one component softener has imparted a plasticisation effect, it is not as significant as that of the 3 component softener.

Finally, the 3 component softener and coated 3 component softener are shown to have similar values of both modulus and strength of Young’s Modulus = 3.0 ± 0.3 GPa and 3.0 ± 0.4 GPa and strength = 59 ± 1 MPa and 66 ± 1 MPa, respectively in the machine direction. Whilst, strain to failure is significantly increased to 9.2 ± 0.8 % and 9.4 ± 0.9 %, respectively in the machine direction. In fact strain to failure is even more notably increased in the transverse direction to values of 18.3 ± 0.6 % and 21.2 ± 0.8 %. These results demonstrate the effectiveness of the 3 component softener package and also suggest that the coating is imparting influence on the mechanical performance too, despite that not being its original function.

Experimenting with different concentrations of softeners and coatings is key to finding the optimum compromise of these three mechanical properties for any application. In order to do this, lab-scale films were produced and each softener added individually and as a blend in different percentages; as discussed in future Chapters 5 and 6.

4.3 Falling weight and slow puncture impact properties

The impact behaviour of films at certain strain rates measured through falling dart and slow puncture impact testing was analysed with force/extension graphs from which strain, normalised force and normalised energy could be extracted. From which normalised results were normalised with respect to thickness to account for any difference this may cause in material behaviour and energy was calculated by determining the area under the force/extension graph by way of integration. Figure 4.4 represents 2 typical force/extension graphs for both the unsoftened and the 3 component softened films in order to highlight some key diversities.

4.3 Falling weight and slow puncture impact properties

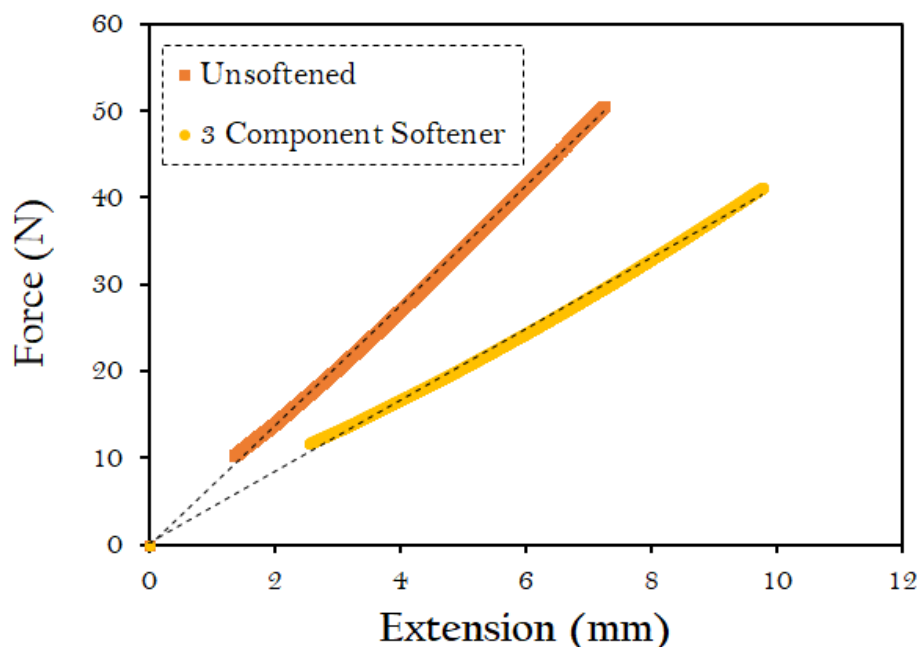


Figure 4.4: *Typical force/extension curves for the unsoftened and 3 component softener commercial films*

The disparity in impact behaviour between unsoftened and softened behaviour is immediately evident in Figure 4.4 with the unsoftened film exhibiting a higher force required for impact whilst the softened film exhibits a higher extension owing to increased ductility. Force/extension graphs like these were produced for each impact and puncture test; from which impact properties were obtained and averaged across 5 repeats.

The results of slow puncture and impact tests performed at speeds (1 mm/min, 100 mm/min, 300 mm/min, 1000 mm/min and 120000 mm/min) and converted to strain rates are shown in Figures 4.5(a-c) representing maximum strain, normalised maximum force and normalised energy (normalised with respect to the thickness of the sample to eliminate any enhanced material performance that thickness might impart). As the same circular geometry is used throughout, this tests all axis of the film's impact response simultaneously.

There are some key material findings produced from these figures that form

4.3 Falling weight and slow puncture impact properties

the basis of future impact analysis for lab made films. Firstly, the crack formation is outlined as a starburst fracture pattern, radiating cracks out in all directions from a single central point (not just breaking along the machine direction, as what might be expected based off tensile results). Secondly, there is a clear variation across material properties with applied strain rate indicating some timescale dependence on performance at room temperature. Lastly, the effect of plasticisers on impact behaviour can be analysed to determine their efficacy.

4.3 Falling weight and slow puncture impact properties

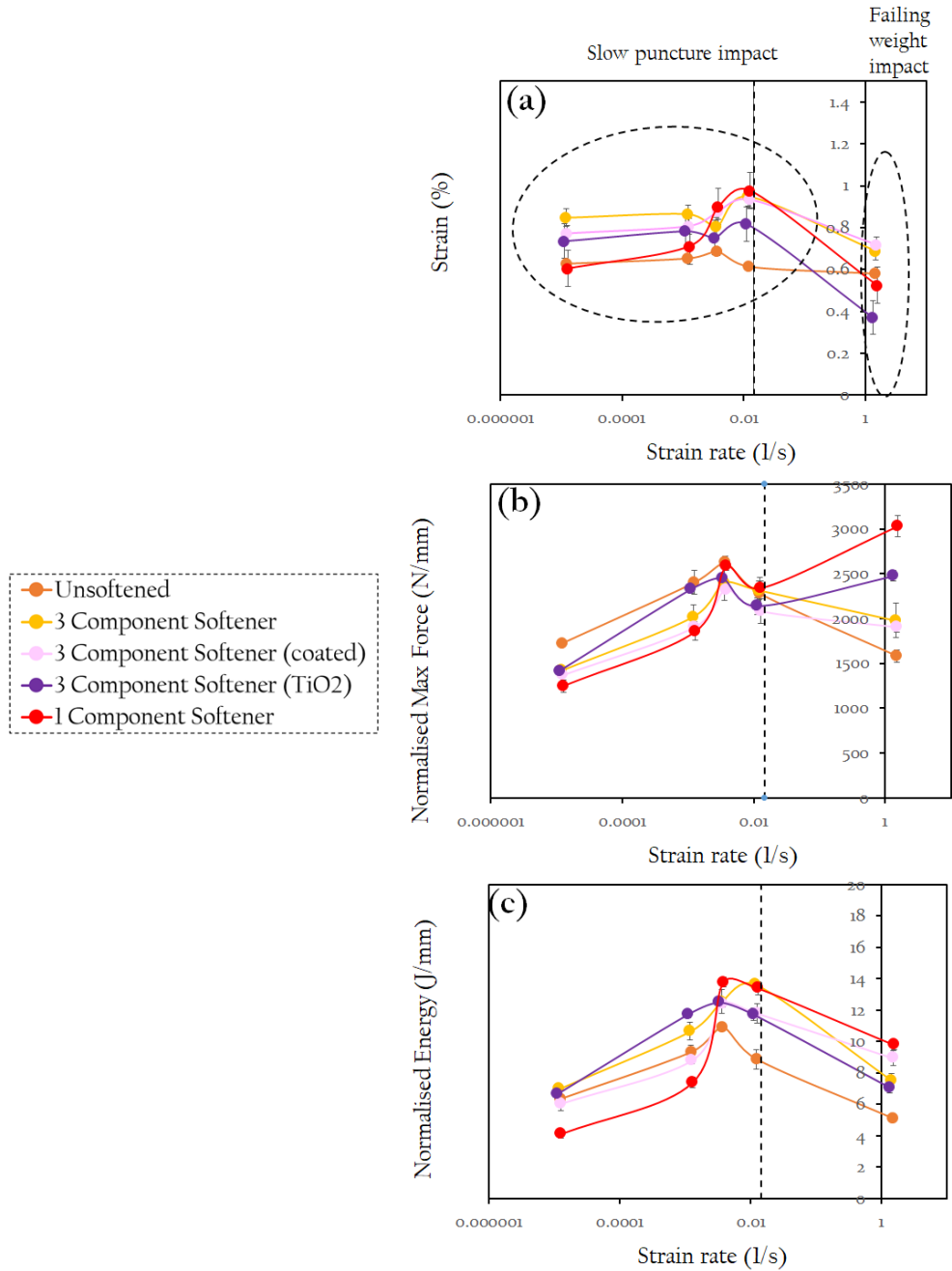


Figure 4.5: *Falling weight and slow puncture impact properties across a range of strain rates for the commercial film set where the black dotted line indicates the strain rate at which tensile testing was performed (a) Strain against strain rate, (b) Normalised Maximum Force against strain rate, (c) Normalised energy against strain rate*

4.3.1 Crack Formation

The first observation to note that was common for all five commercial films at all testing speeds was the starburst fracture pattern, whereby fracture lines occurred in all directions rather than in just one direction (i.e. transverse or machine direction), indicated by Figure 4.6.

Although no link between number of cracks, crack orientation or crack length with impact properties could be determined, this observation was important to show that films are subject to fracture in both the machine and transverse direction, meaning that uniaxiality is not a factor when it comes to impact mechanics. This is important in application as films are much more likely to experience impacts rather than tension and so their impact behaviour should be understood.

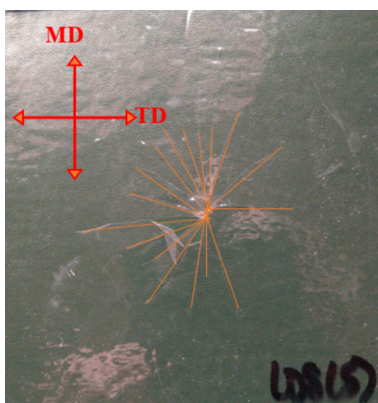


Figure 4.6: *Annotated image of crack formation of films from impact*

4.3.2 Strain rate dependency

Observing Figures 4.5(a-c), it is immediately clear that there is a variation of impact properties across the range of applied strain rates. For each of the five films; maximum strain, normalised maximum force and normalised energy experience a peak in performance around strain rates $\approx 0.003 - 0.01 \text{ s}^{-1}$. Where as, at higher impact speeds, the variation of proprieties is far more diverse; this is where the difference between materials and the results of softening becomes evident

These variations of impact speed are due to the fact that polymers experience different reaction times depending on the speed of external stimuli such as im-

4.3 Falling weight and slow puncture impact properties

pacts. Throughout this work, the quantification of this variation in macroscopic properties is attempted to align with microscopic dynamic properties through the use of DMTA. In later chapters, DMTA is used to identify the relaxation that explains this peak behaviour occurring at room temperature within this strain rate range.

4.3.3 Variation of softener and additives

At low 0.00001 s^{-1} and high 2 s^{-1} strain rates, the behaviour across all 5 films is more diverse than that of the middle three strain rates between $0.001 - 0.01 \text{ s}^{-1}$. For these results, maximum strain is an indicator of the ductility of the films since it defines how much the films are able to extend on impact. Normalised maximum force is an indicator of the strength since it demonstrates the maximum force the films can withstand. Normalised energy is combination of these two properties, being the energy required to fracture the films on impact; integrated from Force/extension curves shown in Figure 4.4 and normalised to sample thickness.

In Figure 4.5(a) the ductility of the 5 films is compared across minimum to maximum strain rates using the material property, maximum strain. Across this range, the 3 component softener appears to display superior behaviour, with a maximum peak strain of $0.948 \pm 0.3 \%$ at a strain rate of 0.01 s^{-1} . Each of the other softened samples exhibit similar peak behaviour with values ranging between 0.818% - 0.935% . On the other hand, the unsoftened sample exhibits generally lower ductility across the range of strain rates. In fact, at the position where other films exhibit a distinct peak, the unsoftened film displays only a small increase in maximum strain of $0.615 \pm 0.006 \%$. These results indicate that the plasticisers have successfully reduced the brittleness of films since their maximum strain is higher across a range of impacts.

In Figure 4.5(b), observing the variation in strength across the sample range, the behaviour is more complex and a switch in properties at the peak strain rate is observed. At low strain rates, the unsoftened film displays the highest maximum force of $1720 \pm 30 \text{ N/mm}$, where as the 1 component softener sample displays the lowest at $1250 \pm 70 \text{ N/mm}$. This is intuitively expected if this property

4.3 Falling weight and slow puncture impact properties

is aligned with strength from the tensile testing results, as higher strength and modulus were observed in the unsoftened sample. However, at the peak position for this property at a strain rate of 0.003 s^{-1} , the variation of maximum force between samples lessens with values ranging from $2100 \pm 100 \text{ N/mm}$ - $2340 \pm 80 \text{ N/mm}$. Then at higher speeds, the performance diversifies again but now, the 1 component softener displays the highest maximum force of $3000 \pm 100 \text{ N/mm}$ and the unsoftened sample displays the lowest maximum force at $1580 \pm 70 \text{ N/mm}$. The diversity in behaviour across these strain rates indicates the sensitivity of films performance to timescales. This is something that is hoped to be understood better through the use of dynamic testing and temperature variation such that this behaviour at room temperature can be understood at a range of temperatures and frequencies.

Finally, Figure 4.5(c) can be used to assess the variation of energy across the strain rates and film samples. This property shows similar behaviour to Maximum Force demonstrated in Figure 4.5(b), with a switch in performance superiority observed at the peak. At the lowest strain, the 1 component softener exhibits the lowest energy by a significant amount at $4.1 \pm 0.4 \text{ J/mm}$; whilst values for the other four films range between $6.0 \pm 0.6 \text{ J/mm}$ - $7.0 \pm 0.2 \text{ J/mm}$. At the peak, the 1 component softener gains the highest energy of $13.4 \pm 0.8 \text{ J/mm}$, whilst the lowest energy is exhibited by the unsoftened sample of $8 \pm 1 \text{ J/mm}$. Furthermore at the highest strain rate, diversity in performance is even more noticeable with the 1 component softener's energy being $9.8 \pm 0.8 \text{ J/mm}$ and the unsoftened sample being $5.1 \pm 0.4 \text{ J/mm}$. From these results, it can be concluded that the energy of the samples is more force dependent than strain dependent. It is hoped that understanding of this diversity in behaviour can be uncovered through the implementation of dynamic testing and experimental addition of plasticisers.

4.4 Dynamic Mechanical Thermal Analysis

Dynamic Mechanical Thermal Analysis was performed on commercial films in order to determine their molecular behaviour through changes in complex moduli: Storage modulus and loss modulus, as well as, $\tan\delta$ for the temperature range - 100 °C to + 260 °C at 1Hz. Results of this Basic Temperature Ramp Procedure are depicted in Figures 4.7(a-c). Understanding the peaks of DMTA figures and linking the transitions to the performance of softeners through macroscopic testing results will be a key focus of this work. Understanding the variation of the primary, α and secondary, β and γ , transitions observed in cellulose due to changes in dynamic behaviour will be vital to understanding this puzzle.

From these initial temperature ramps, some key dynamic properties have been determined that are analysed and understood more thoroughly in future chapters. Through these analysis, we tentatively identify the position of the glass transition temperature (T_g) of cellulose, along with other secondary transitions that have been identified in commercial films but not yet assigned. The effect of plasticisers on dynamic behaviour is immediately evident but is understood and quantified more thoroughly in future chapters by the individualising of softener packages.

4.4 Dynamic Mechanical Thermal Analysis

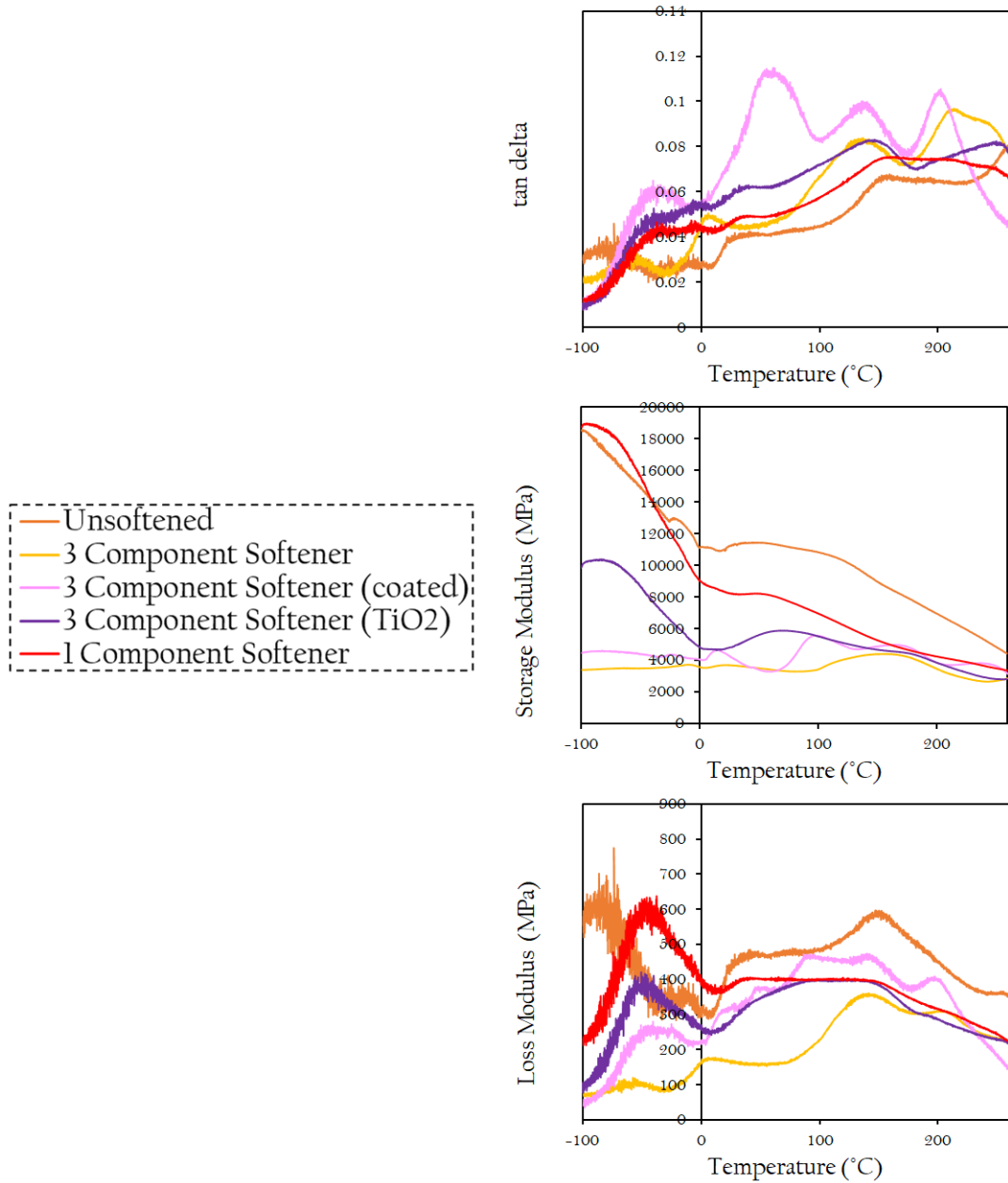


Figure 4.7: *Dynamic Mechanical Thermal Analysis of commercial film set from -100 °C to 260 °C at oscillating frequency of 1 Hz (a) tan δ against Temperature, (b) Storage Modulus against Temperature and (c) Loss Modulus against Temperature*

4.4 Dynamic Mechanical Thermal Analysis

Figure 4.7 shows the dynamic behaviour of these commercial cellulosic films to be extremely complex. Numerous peaks cannot be confidently assigned to specific transitions since the effect of softeners, additives and water in these systems results in an unclear pattern. This complexity justifies the separation of plasticiser blends to identify individual contributions of softeners and the relationship with mechanical properties in order to understand their mechanisms.

To attempt to analyse these complex curves, the first step is to try and identify some characteristic primary and secondary relaxations in cellulose and assign those to individual peaks. The first transition to be identified is that of the α relaxation at the glass transition temperature. Cellulose has a high T_g , with degradation temperature, T_d already being reached before T_g is achieved in un-plasticised cellulose. Typically T_g values range between 220 - 250 °C and the onset of T_d begins around 200 °C. This T_g value can be identified by a peak in $\tan\delta$ in the relaxation profile [107]. This small temperature window is broadened by the addition of plasticisers since they act to reduce T_g . For example, Erdmann et al reported a reduction of T_g of cellulose acetate powders from $T_g = 196.6$ °C to $T_g = 75.8$ °C through plasticisation with triethyl citrate [108]. Furthermore, the efficiency and contribution of softeners and effect on T can in fact be predicted using several theoretical models; the most elementary of those being the Fox Model [109]:

$$\frac{1}{T_g} = \frac{w(\text{cellulose})}{T_g(\text{cellulose})} + \frac{w(\text{plasticiser})}{T_g(\text{plasticiser})} \quad (4.1)$$

Where ω gives the mass fraction of the cellulose and plasticiser proportions and T_g of cellulose and plasticiser can be determined by literature to provide estimations for the plasticisation affect of softeners. Clearly, simple mathematics dictates that provided that the glass transition of the plasticisers are less than that of cellulose, then a plasticising effect is induced and T_g is reduced. Erdmann et al demonstrate the effectiveness of this theory at predicting plasticisation [108]. As well as this primary transition, the effects of plasticisation are also seen in secondary cellulose transitions.

The polymer dynamics of cellulose are a hotly debated topic, with complex contributions for each cellulose derivative. Each of their primary and secondary

4.4 Dynamic Mechanical Thermal Analysis

transitions are used to describe relaxations and molecular dynamics of the cellulose molecule. Generally, the relaxations are separated into the primary α transition, associated with the glass transition temperature, and at lower temperatures, several localised secondary transitions β , γ , δ , σ are observed as a result of local main chain dynamic movement, side group motion and rotational movement. For this work, α and β and γ relaxations are the focus since they are identified in future Chapters 5 and 6 and contributions to mechanical performance are documented.

- **alpha, α transition** is well defined as representing the glass transition of a polymer. The alpha transition shifts due to plasticisation effects that increase molecular motion [97]. Furthermore, plasticisation also has the effect of reducing the values of $\tan\delta$ and storage modulus at this alpha peak [108].
- **beta, β transition** typically occurs as a sub zero peak, typically between -50 °C to -20 °C. The cause of β peak has not been definitively defined but its impact on the mechanical properties of polymers is well accepted [110]. Theory says that β relaxations are a result of local main chain dynamic movement. For cellulose literature suggests that the motion of this peak is resultant of either cooperative motion of hydroxymethyl side groups with the backbone or motions of single monomer units [110][111]. Since plasticisers embed themselves into the polymer network, it is easy to understand how these might affect this motion and thus β relaxations.
- **gamma γ transition** typically occurs at very low temperatures and thus is not as well understood as other relaxations. It is associated with side group motion of polymers. For cellulose the origins of this motion manifests as methyl side group rotation, hydroxyl and methyl cooperative rotation or bounded water contribution, summarised by Einfeld et al [110]. It is this γ relaxation associated with water that will be investigated using water removal procedures in later chapters as we aim to highlight the importance and contributions of water in these systems.

4.4 Dynamic Mechanical Thermal Analysis

An example of the expected positions and variations of the α , β and γ transitions as a result of plasticisation is demonstrated by Figure 4.8. Wherein, Erdmann et al show the affect on transitions of the storage modulus and $\tan\delta$ profiles of cellulose acetate with increasing concentrations of glycerol triacetate (GTA) as a plasticiser [108]. This figure demonstrates the changes in relaxation dynamic peaks as a results of increasing plasticiser content. The identification and position of these peaks are well established for cellulose acetate, however for regenerated viscose cellulose, ranges for expected transitions could not be found in literature. As such, we might expect to observe these transitions at different positions for our systems.

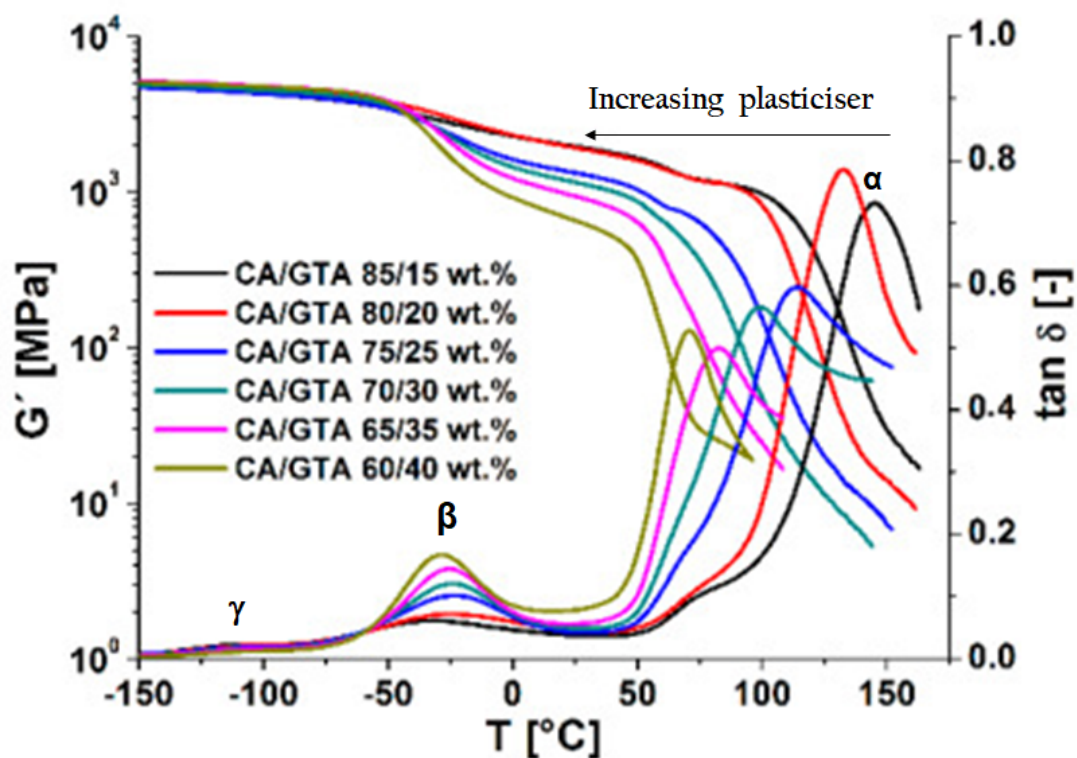


Figure 4.8: Storage modulus (G' in this example) and $\tan \delta$ profile of cellulose acetate plasticised by increasing concentrations (85/15 wt % - 60/40 wt %) GTA and the varying effect on primary (α) and secondary (β , γ) transitions. Adapted from [108]

In comparison to literature values, the commercial films behaviour demonstrated in Figures 4.7(a-c) shows that the addition of softeners and additives in the films has created a complex variation in the dynamic properties and observations of additional transitions, such that it is difficult to decipher individual relaxations. It is inherently challenging to assign one singular relaxation process to all the individual motions and orientations changing within the polymer, exacerbated by the inclusion of additional compounds. As such, Figures 4.9(a-b) have been created to focus on the expected temperature regions of the α (160 $^{\circ}\text{C}$ to 260 $^{\circ}\text{C}$) and a secondary transition (-100 $^{\circ}\text{C}$ to 0 $^{\circ}\text{C}$) of cellulose. $\tan \delta$ has been used to represent these peaks since it is a combination of loss and storage modulus properties.

4.4 Dynamic Mechanical Thermal Analysis

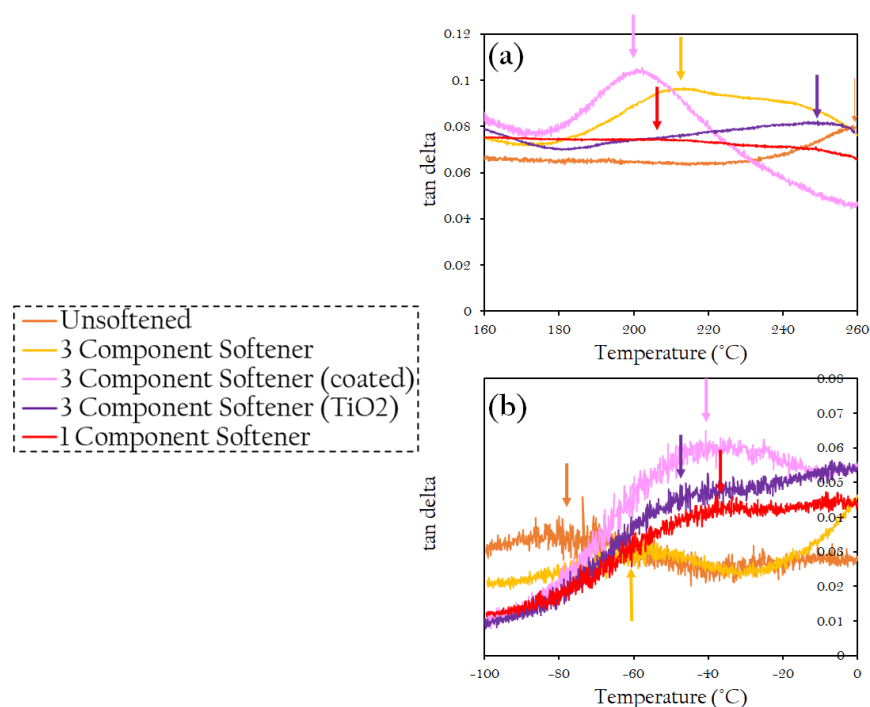


Figure 4.9: $\tan \delta$ transitions of commercial film set, with varying peak positions, zoomed in on (a) presumed α transition between 160 °C to 260 °C and (b) another secondary sub-zero relaxation between -100 °C to 0 °C

Figure 4.9(a) shows the variation in $\tan \delta$ associated with the α transition in cellulose. It is clear that plasticisation is resulting in reduction of T_g , as intended. In fact, the unsoftened sample, exhibits a T_g peak at ≈ 259 °C whilst for softened samples a reduction in T_g of up to 60 °C is observed, as the 3 component softener (coated) films displays a T_g of ≈ 202 °C. This was to be expected since a reduction of T_g is often associated with a plasticisation effect.

Figure 4.9(b) shows the variation of a secondary relaxation $\tan \delta$ peak of cellulose. Based off literature examples, in particular Figure 4.8 that shows the β relaxation of cellulose acetate to be in this sub zero region, we might be able to conclude that this is the β relaxation of cellulose. However, our results show that there are other secondary transitions that occur at higher temperatures than this sub zero peak, suggesting that it might in fact be the γ relaxation. This uncertainty is combated in future Chapters 5 and 6 where softeners are incorporated

into films individually such that β and γ transitions can be more confidently assigned. Nonetheless, the effect of plasticisation on this transition is evidenced by this Figure 4.9(b). The unsoftened film has the lowest sub-zero peak ≈ -70 °C, compared to the 3 component softener (coated) that exhibits this peak at a temperature of ≈ -43 °C. This is due to the interactions of plasticisation with molecular motions; whether these molecular motions are associated with β or γ contributions is discussed in future Chapters 5 and 6.

In addition to these processes, there are clearly other relaxations occurring and changing with plasticisation across this dynamic profile. Due to the complexity of softener blends and the undisclosed addition of coatings and colouring TiO_2 , the contributions of these relaxations are too complex to identify based off this data set. Therefore, future work focuses on the separation of softeners and control of concentration, as well as the zooming of this profile to concentrate specifically on secondary relaxations. The sub-zero relaxation was chosen to be the focus of plasticisation effects on the dynamic profile in future Chapters 5 and 6 since the effect of degradation on the cellulose chains is evident in their α relaxation due to their inherent high T_g , with T_d on setting before T_g is reached. Furthermore, this sub-zero peak is evident in all commercial films so is an excellent candidate for aligning the commercial and lab-based data sets.

4.5 Commercial films summary

To summarise this chapter: macroscopic (tensile and impact) and microscopic (DMTA) testing has been performed on commercial Cellophane films, produced and sold by The Futamura Group. Some key findings that will form the basis of analysis for future chapters are highlighted:

- **Tensile Testing** revealed (i) the uniaxiality of films due to processing method altering orientation of cellulose polymer chains and the resultant variation of properties across the machine and transverse directions (ii) the compromise of material properties and the need to prioritise either strength and modulus or strain to failure for application indicated by Ashby Plots and (iii) the effect of plasticisation on the mechanical properties of these

films resulting in increased strain to failure at the expense of modulus and strength.

- **Slow puncture and Impact Testing** revealed (i) crack formation properties of films, (ii) the timescale variation response of films that exhibit optimum impact properties dependent on the strain rate of impact and (iii) the result of plasticisation addition on the maximum strain, force and energy that the films may withstand during impact.
- **Dynamic Mechanical Thermal Analysis** has revealed a complex and varying relaxation profile for these films. The position of the a secondary sub zero and the α transition has been identified and the effect of plasticisation is clear. However, other constituents of the films such as coatings and colourings are resulting in additional transitions and shifting being observed, adding to the complexity of understanding these profiles. In particular, this technique is in need of a more fundamental study at this stage, prompting the next steps to look at each plasticisers contributions separately.

4.6 Next Steps


Ultimately, the goal of this work is to understand and predict plasticisation ability of various softeners on films. One way this can be achieved is to quantify the micro and macroscopic properties of films by linking mechanical performance and molecular dynamics. However at present, with this set of films, it is not possible to quantify this plasticisation effect due to the contribution of additional additives as well as the softeners, meaning that contribution and efficacy cannot be compared between compositions. Hence, separation of plasticisers is required.

To combat this challenge, the topic of the next chapter will be ‘lab-made films with varying softener content’, concentrating on unveiling the contributions of the commercial 3 component softener. It is expected that relaxation intensities and shifts depend on plasticiser efficacy and concentration [108]. As such, individual softeners: glycerine, MPG and urea (as well as a lab-recreated 3 component softener blend) have been incorporated into films and the same suite of tests:

tensile, falling weight and slow puncture impact as well as DMTA applied in order to quantify plasticisation affect and explain mechanical performance. Since degradation of the cellulose chain occurs before glass transition temperature is reached for the unsoftened sample of this film, it was decided that the effect on secondary transitions rather than α transition at T_g due to plasticisation should be assessed. Changes in the sub zero relaxation transition have been analysed and the efficacy of plasticisation quantified by comparison to mechanical performance.

Chapter 5

Plasticiser variation of lab-based films, Results and Discussion

In this chapter, results and discussions are presented for a series of films, where each softener in the commercial 3 component softener (glycerine, MPG and urea) is added individually to a swollen cellulose film, or 'wet gel' in a range of concentrations (4 %, 8 % and 15 %). The commercial 3 component blend containing *(This text has been removed by the author of this thesis for confidentiality reasons)*  is also recreated and incorporated into films using the same concentrations as the individual softeners. Tensile testing, falling weight and slow puncture impact, as well as dynamic mechanical thermal analysis have been performed to assess the contribution and efficacy of individual and blend softeners.

5.1 Softener Content

According to the process outlined in Section 3.1.2, cellulose wet-gel (post-casting film soaked in water) was plasticised with softeners: glycerine, MPG, Urea and a 3 component blend of the three using concentrations 4 %, 8 % and 15 % softener in water bath. Upon visual observations of the films, it was immediately clear that uptake of softeners was not uniform across the set of films. In fact, the migration of plasticisers from the internal film structure is a recognised phenomenon and it is known that maximum plasticiser content is reached at specific concentrations.

5.1 Softener Content

For glycerine films, this exceeded rate and resultant migration is associated with an oily cast on the surface of the films whilst urea exhibits migration as a white coated layer, as demonstrated by Figure 5.1 [112][113].

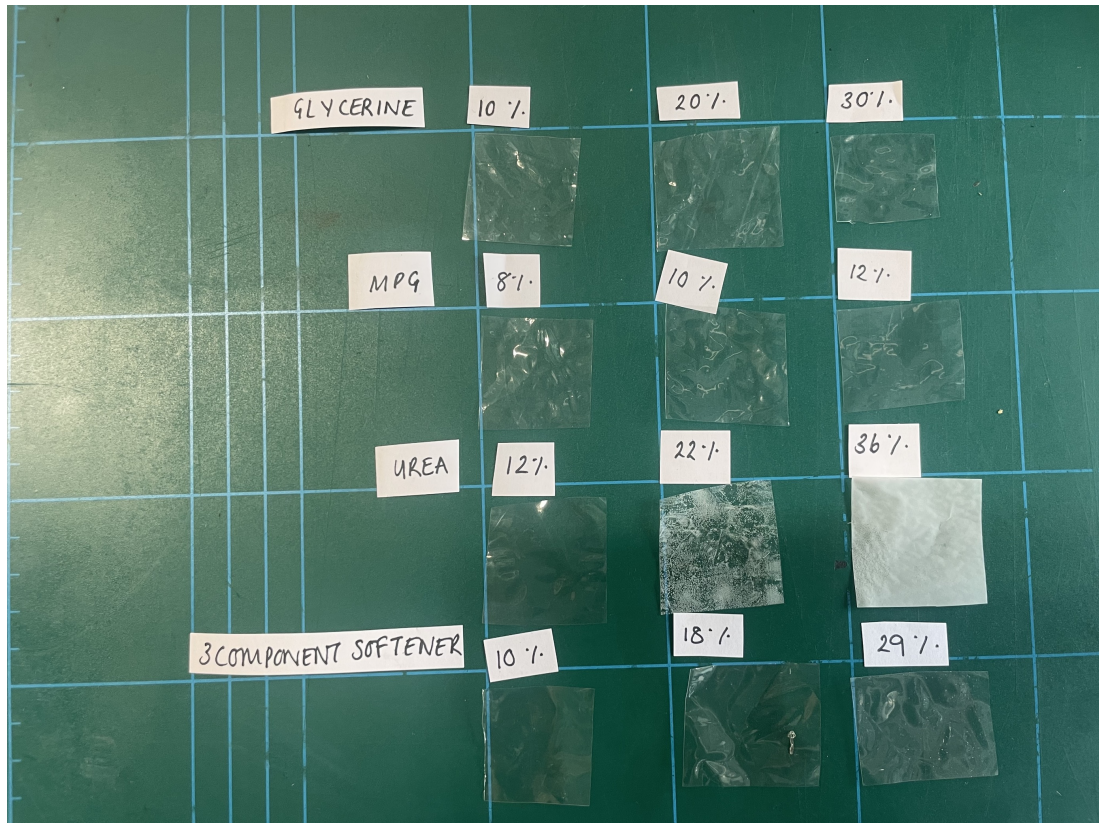


Figure 5.1: *Lab-softened films visual appearances. Migration effects clearly visible for Urea films*

5.1 Softener Content

Figure 5.1 shows a selection of lab softened films and their visual comparison to indicate the difference between films. For urea-softened films, the effects of migration are obvious due to their increasingly white coloring. In addition, for the 3 component softened film, the 29 % concentration film exhibits white spotting consistent with urea crystallisation. On the other hand for the MPG and Glycerine there is no evidence of migration. Due to these observations, the softener in film content was determined using the process outlined in Section 3.1.2 in order to determine softener uptake to assess plasticisation impact on performance more accurately, indicated in Table 5.1.

Table 5.1: *Table of lab-softened films and their softener in film content. Where 3 component softener: (This text has been removed by the author of this thesis for confidentiality reasons)*

Plasticised Film	Softener in Film (wt %)
MPG 4 %	8.0 ± 0.4
MPG 8 %	9.6 ± 0.2
MPG 15 %	11.8 ± 0.8
Glycerine 4 %	10.5 ± 0.7
Glycerine 8 %	20.0 ± 0.2
Glycerine 15 %	30.3 ± 0.5
Urea 4 %	11.6 ± 0.3
Urea 8 %	22 ± 1
Urea 15 %	36.4 ± 0.9
3 Component Softener 4 %	9.73 ± 0.08
3 Component Softener 8 %*	17.8 ± 0.3 *
3 Component Softener 15 %	28.5 ± 0.1

(This text has been removed by the author of this thesis for confidentiality reasons)

Table 5.1 indicates the variation of softener uptake across the three softeners and their 3 component blend. These results reveal that softener uptake was minimum for MPG softened films, with softener content ranging between 8.0 - 11.8 %. On the other hand, softener uptake was maximum for Urea, with softener in film values ranging between 11.6 % - 36.4 %. This softener in film uptake turns out to be important when considering the softening effect of these plasticisers, with softeners with higher uptake exhibiting superior plasticisation.

In fact, Urea, which Futamura have historically deemed a secondary softener and included in low concentrations in their 3 component softener blend, has been shown to potentially have a superior softening effect to that of glycerine, perhaps owing to its larger uptake in the films. To understand this variation in softener uptake, literature sources have been consulted to understand how each of the individual softeners interact with cellulose polymer chains to impart their softening effect.

The interactions between glycerine and cellulose have long been acknowledged and it is a traditional plasticiser of Cellophane. Early studies by Sweeting et al determined the interactions between cellulose polymer chains and glycerine molecules [114][115][116]. To understand the nature of softener uptake in cellulose wet gels and dried films, they measured the free volume in the cellulose film and determined whether softener uptake was proportional to this volume. In 1959 they reported the mechanisms behind the cellulose-glycerine interactions, along with the importance of the role of water in these interactions. They suggest that during softening, glycerine is diffused into films and replaces free water with glycerine solution due to glycerine's ability to form hydrogen bonds with cellulose. Upon wet gel drying, free water is removed and the effects of glycerine plasticisation are seen as the softener displaces water as it is removed in the drying process. Then, the cellulose chains contain mostly bound water and glycerine, that interact with cellulose OH groups. These interactions reduce hydrogen bonding between cellulose chains and thus incur plasticisation. As such, the affinity of softeners for cellulose hydroxyls is an important factor for plasticisation. This competitive exchange between water and softener is an important consideration in the uptake and plasticisation of films [115]. They conclude that the interactions between cellulose and water and cellulose and glycerine are extremely similar in terms of their interactions with cellulose hydroxyls and an optimum amount of displacement at certain relative humidity's is crucial to optimising properties. In fact, they report the enrichment factor (ratio of plasticiser content in film to plasticiser content in bath) between 0.96 - 1.03 for concentrations up to 95 % in wet gel, showing that softener solution vs water absorption is virtually identical as they occur in films in virtually the same ratio as that of the softener

bath, with no indication of preferential bonding [116]. As such, the softening effect of glycerine can be compared to swollen cellulose wet gel. Furthermore, this study also investigates the effect of ethylene carbonate, a hydrophobic molecule to determine its plasticising effect. They determined that this addition does not interact with cellulose chains or hydroxyls but in fact lies dormant between cellulose chains, allowing for cellulose-water and cellulose-cellulose interactions. In fact, at higher concentrations, the hydrophobicity actually acts to remove water from the internal structure of the polymer chains, resulting in an anti-plasticising effect and therefore films of high brittleness [115]. Furthermore, Paudel et al comment on glycerine in cellulose based films and its ability to maintain tensile strength whilst still imparting its well known softening effect. They suggest that the small hydrodynamic radii 0.31 nm allows for sufficient disruption to intermolecular forces between polymer chains to improve strain at failure, but still allow for interactions between cellulose chains such that modulus and strength are somewhat maintained [117][118].

Clearly, the interactions and affinities between cellulose, water and plasticisers are extremely important in the plasticiser uptake and ability of chosen softeners. In order to compare the softener uptake of glycerine with that of MPG, Urea and the lab-based 3 component softener Figure 5.2 has been created to compare the softener in bath and softener in film percentages, along with the enrichment factors (ratio of plasticiser content in film to plasticiser content in bath) of each film concentration, indicated in data labels. Enrichment factor is a useful quantity to measure softener uptake and has been calculated for this set of dried lab based films (it should be noted that enrichment factor will not be 1 for these films as it is in the example of reference [116], as that reference measured enrichment factor of wet films, whilst for our purposes, water has been removed in drying).

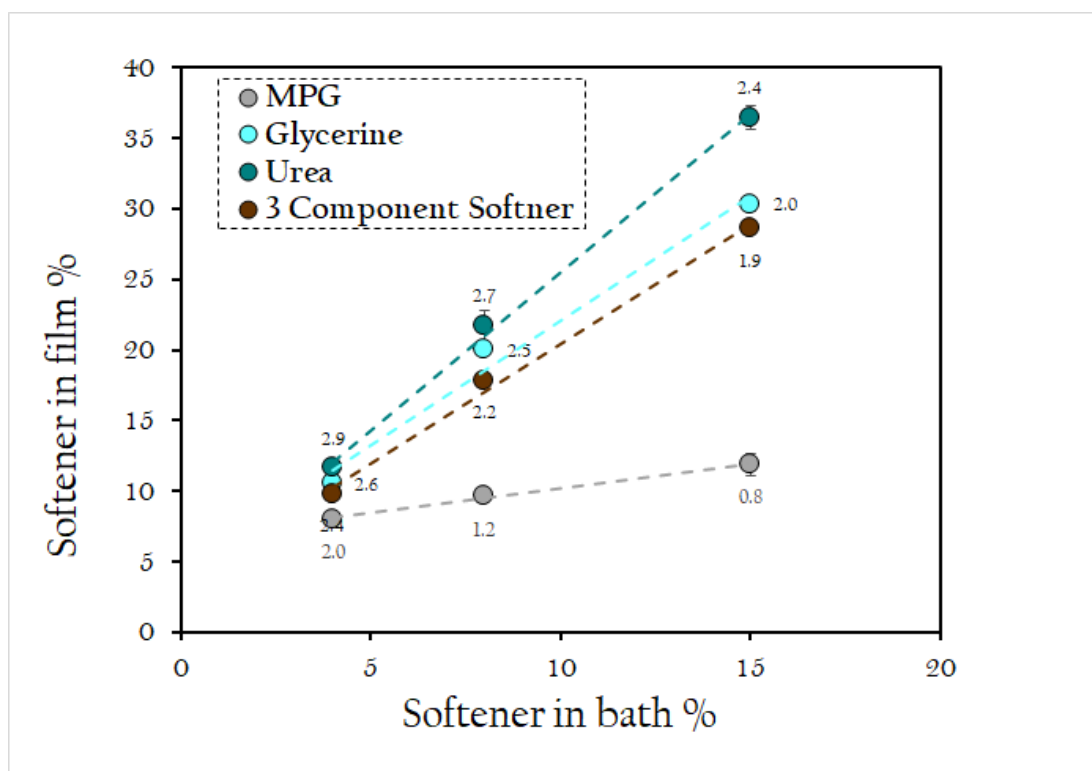


Figure 5.2: *Softener in film and softener in bath wt % comparison for individual and blend softeners of lab-plasticised films with enrichment factors indicated as data labels. Where the 3 component softener contains (This text has been removed by the author of this thesis for confidentiality reasons)*

This figure indicates the differences in uptake abilities of each softener. Urea demonstrates the highest uptake with enrichment factors 2.4 - 2.9 whilst MPG demonstrates the lowest uptake with enrichment factors as low as 0.8 - 2.0. The 3 component softener and glycerine exhibit similar uptake behaviour, as might be expected since the 3 component softener consists of (*This text has been removed by the author of this thesis for confidentiality reasons*) ██████████ and is therefore dominating properties. Based off glycerine's interactions with cellulose, the uptake of plasticisers in films depends on the ability to disrupt and replace water content in cellulose wet gel. This will depend on the individual softeners hydrogen bond forming abilities. This is impacted by the number of hydrogen bond forming sites on molecules. Referring to Figure 2.8 which shows the structure of these plasticiser molecules, glycerine (3 OH) and urea (2 amino, 1 carbonyl) both have 3 side groups with the ability to break and form hydrogen bonds with cellulose or water, whilst MPG (2 OH) contains only 2; giving a rise to a reasonable conclusion of there being less interactions between cellulose and water with softener, meaning that there is less disruption between polymer chains and thus reduced plasticisation.

Versino et al report the comparison of plasticisation of both glycerine and urea on starch films. They demonstrate that urea is the more effective softener of the two, probably due to the urea molecule being smaller and thus being able to embed between polymer chains more so than that of glycerine, highlighting molecular weight as another key indicator of plasticiser performance. They employed the use of ATR-FTIR to demonstrate the stronger bonding between starch OH groups to the NH and C=O groups on urea compared to those of the OH groups in glycerine. This results in an increased strain at failure as well as an observed reduction of T_g , measured by DSC for urea softened films [119]. These increased interactions help to explain the increased urea concentration observed in this work and resultant plasticising effect. However, as shown in Figure 5.1, migration properties of urea are evident in the 22 % and 36 % films, meaning that they have reached the maximum uptake at before the 22 % concentration.

Furthermore, Suyatma et al report the effect of MPG as a plasticiser [120]. On the contrary, despite MPG's lower molecular weight, it demonstrates an anti-plasticiser effect observed at low concentrations 5 - 15 %. This is associated with

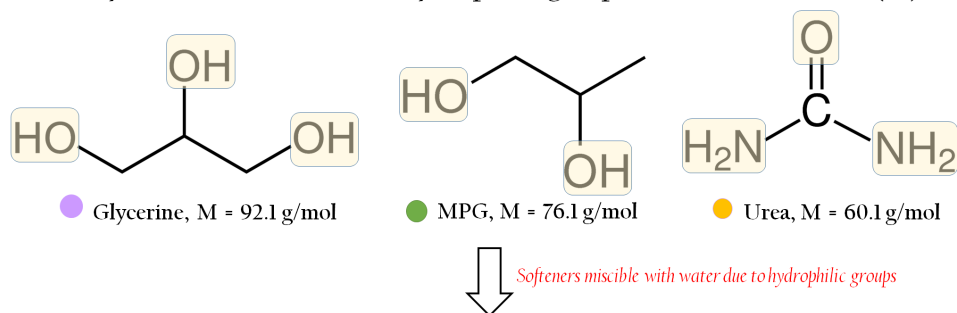
their lower hydrophilicity due to fewer OH groups, in comparison to urea and glycerine and thus reduced displacement of water in cellulose wet gel. Furthermore, it has been suggested that the high vapour pressure of MPG results in less uptake in the films, explaining their lower concentrations [121].

Versino et al also report the effect of a urea/glycerine 2 component softener on film performance [119]. They suggest that an observed decrease in mechanical properties is resultant of the preferential bonding between urea and glycerine hydrogen acceptors, leading to less displacement of water in wet gels. This could be the cause of reduced uptake of the 3 component softener in lab-based films in comparison to urea and glycerine individual uptakes.

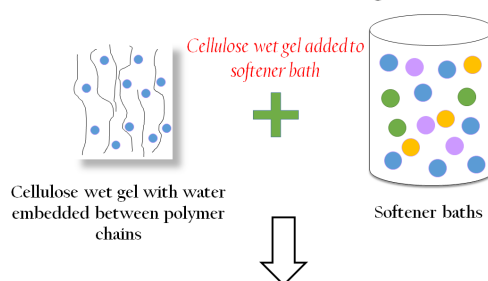
To summarise, size, shape, hydrophilicity and number of available hydrogen acceptors impacts on the ability of a chosen plasticiser to soften and impart ductility [122]. A lower molecular weight is associated with a greater ability to embed between polymer chains, increasing uptake. Whilst shape is also key in terms of the availability hydrogen bond acceptors to come into contact with polymer chain's OH groups, with chain plasticisers being associated with a greater ability to disrupt polymer chain interaction [122]. Furthermore, the number of available hydrogen acceptors, and associated hydrophilicity, is important for disrupting hydrogen bonding between polymer chains and displacing water to allow for the uptake of plasticisers, helping to explain why MPG has a low uptake into the films in comparison to urea and glycerine. Hydrophilicity allows for bonding with water in softener baths which then displaces water in films with softener solution. A schematic has been created to help visualise the actions of softeners and water with cellulose polymer chains, Figure 5.3.

5.1 Softener Content

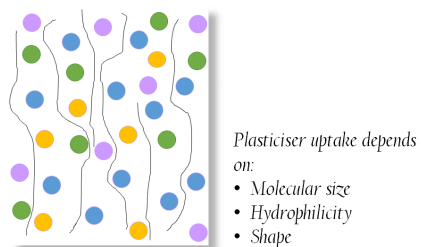
Softeners: Glycerine, MPG and Urea. Hydrophilic groups and molecular mass (M) indicated



Water ● baths containing softeners and water



Softener: water bath uptake in films



↓ *Films are dried, removing much of free water and leaving softener and bound water*

Dried cellulose film plasticised with molecules embedded between chains

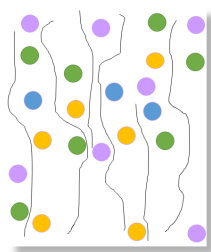


Figure 5.3: *Interactions of plasticisers (Glycerine, MPG and Urea) and water with cellulose polymer chains*

5.2 Tensile Properties

Similarly to the commercial set of films, samples were laser cut in to 10 dumbbells, 5 in the machine direction and 5 in the transverse direction, each of which were subject to tensile testing at a constant rate of 10 mm/min up to failure. Averaged results and their standard deviation error of these tensile tests can be seen in Table 5.2. These results were used to produce stress/strain graphs from which Young's Modulus, strength and strain at failure could be determined and averaged for each sample. The results of which are presented in Figures 5.4(a-c) that show Ashby Plots of this film set.

5.2 Tensile Properties

Table 5.2: *Tensile Test results of lab-based plasticised films in machine and transverse directions for Young's Modulus, Strength and Strain at Failure*

	Modulus (GPa)	Strength (MPa)	Failure (%)
	Transverse Direction		
Lab unsoftened	4.8 ± 0.1	62 ± 2	2.4 ± 0.4
MPG 8 %	3.7 ± 0.2	53 ± 1	1.9 ± 0.1
MPG 10 %	3.0 ± 0.1	37 ± 3	2.2 ± 0.3
MPG 12 %	2.8 ± 0.2	34 ± 2	1.8 ± 2
Glycerine 10 %	3.9 ± 0.2	40.5 ± 0.8	4.2 ± 0.3
Glycerine 20 %	3.6 ± 0.2	40 ± 1	4.2 ± 0.5
Glycerine 30 %	1.46 ± 0.03	19.3 ± 0.8	5.4 ± 0.6
Urea 12 %	4.1 ± 0.3	55 ± 2	3.8 ± 0.3
Urea 22 %	1.7 ± 0.1	28.5 ± 0.9	7.6 ± 0.3
Urea 36 %	1.8 ± 0.2	24 ± 2	7.7 ± 0.3
3 Component Softener 10 %	3.5 ± 0.2	51 ± 1	3.1 ± 0.3
3 Component Softener 18 %	3.6 ± 0.2	45 ± 2	5.1 ± 0.3
3 Component Softener 29 %	1.07 ± 0.05	22 ± 2	8.3 ± 0.9
	Machine Direction		
Lab unsoftened	6.6 ± 0.2	77 ± 1	2.0 ± 0.2
MPG 8 %	5.1 ± 0.2	60 ± 1	3.0 ± 0.4
MPG 10 %	3.8 ± 0.1	46 ± 4	3.1 ± 0.8
MPG 12 %	3.8 ± 0.1	44 ± 3	2.3 ± 0.4
Glycerine 10 %	3.9 ± 0.4	59 ± 3	3.9 ± 2
Glycerine 20 %	3.7 ± 0.4	54 ± 2	4.5 ± 0.4
Glycerine 30 %	1.8 ± 0.1	27 ± 1	6.0 ± 0.2
Urea 12 %	4.9 ± 0.3	72 ± 2	3.7 ± 0.2
Urea 22 %	2.4 ± 0.2	41 ± 3	5.7 ± 0.2
Urea 36 %	2.3 ± 0.3	27 ± 2	6.0 ± 0.4
3 Component Softener 10 %	4.8 ± 0.3	63 ± 1	3.4 ± 0.1
3 Component Softener 18 %	3.6 ± 0.5	58 ± 4	4.4 ± 0.4
3 Component Softener 29 %	2.2 ± 0.2	30 ± 3	6.4 ± 0.5

5.2 Tensile Properties

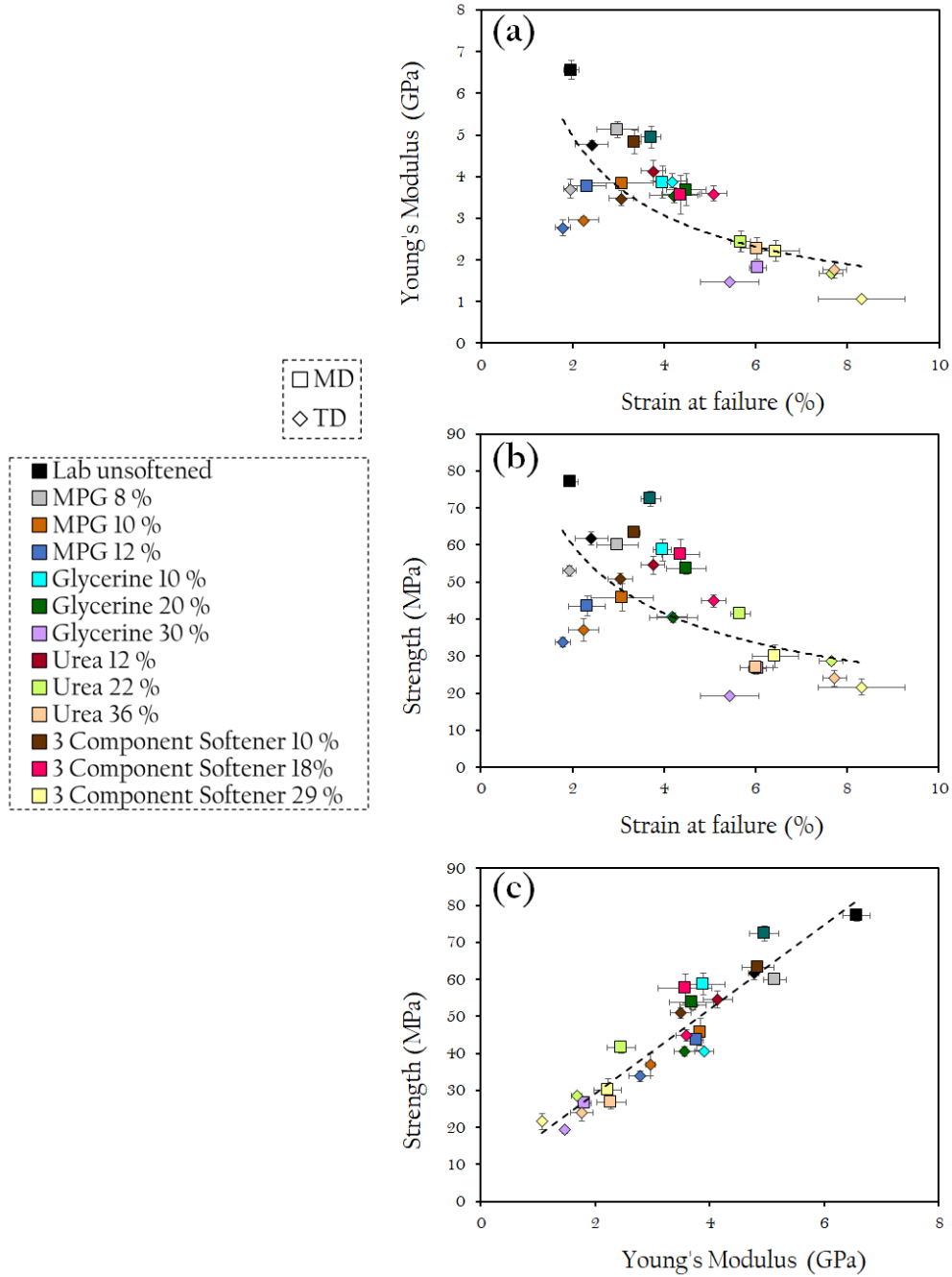


Figure 5.4: Ashby Plots depicting the variation of tensile properties for the lab-plasticised film set in their machine (square markers) and transverse (diamond markers) directions (a) Young's Modulus against strain at failure, (b) Strength against strain at failure and (c) Strength against Young's Modulus

5.2.1 Material property relationships

The first important observation for these films is the relationships between the three tensile properties: Modulus, strength and strain at failure. Figures 5.4(a-c) show that the same compromise between properties is observed with the lab-plasticised films as in the commercial films. Strength and Young's Modulus are proportional, whilst an increase in strain to failure associated with increasing plasticisation results in a reduction of these properties. Optimising plasticisation such that films can be tuned to the perfect position on this curve would be an ideal outcome of this project.

5.2.2 Machine and transverse uniaxiality

Furthermore, as with the commercial films, a variation between machine and transverse properties is observed for this lab-plasticised film set; however the difference between machine and transverse direction properties is less pronounced for these films. The average ratio between the machine and transverse values in commercial films of Young's Modulus, strength and strain to failure are 2.1 ± 0.1 , 2.1 ± 0.1 and 2.0 ± 0.1 , respectively. Whilst for this set of lab-plasticised films Young's Modulus is $1.3 \pm 0.1 \times$ greater in the machine direction, strength is $1.7 \pm 0.1 \times$ greater in the machine direction and strain at failure is $1.5 \pm 0.2 \times$ greater in the transverse direction.

This reduced variation window between machine and transverse properties arises due to the difference in production method for these lab-softened films compared to commercial films. As previously discussed, uniaxiality is imparted to the films during extrusion and rolling under tension during commercial processing. Since these films are only subject to extrusion before they are softened, the lack of rolling can be identified as the reason for the reduced alignment of chains the machine direction. Furthermore, during the lab-softened film production process, the films are clamped into frames and allowed to dry in an oven. During this drying process, films undergo shrinking due to water removal in all directions and owing to the dimensions of the frames, this is likely to impart some additional alignment to the films, but not as much as rolling under ten-

5.2 Tensile Properties

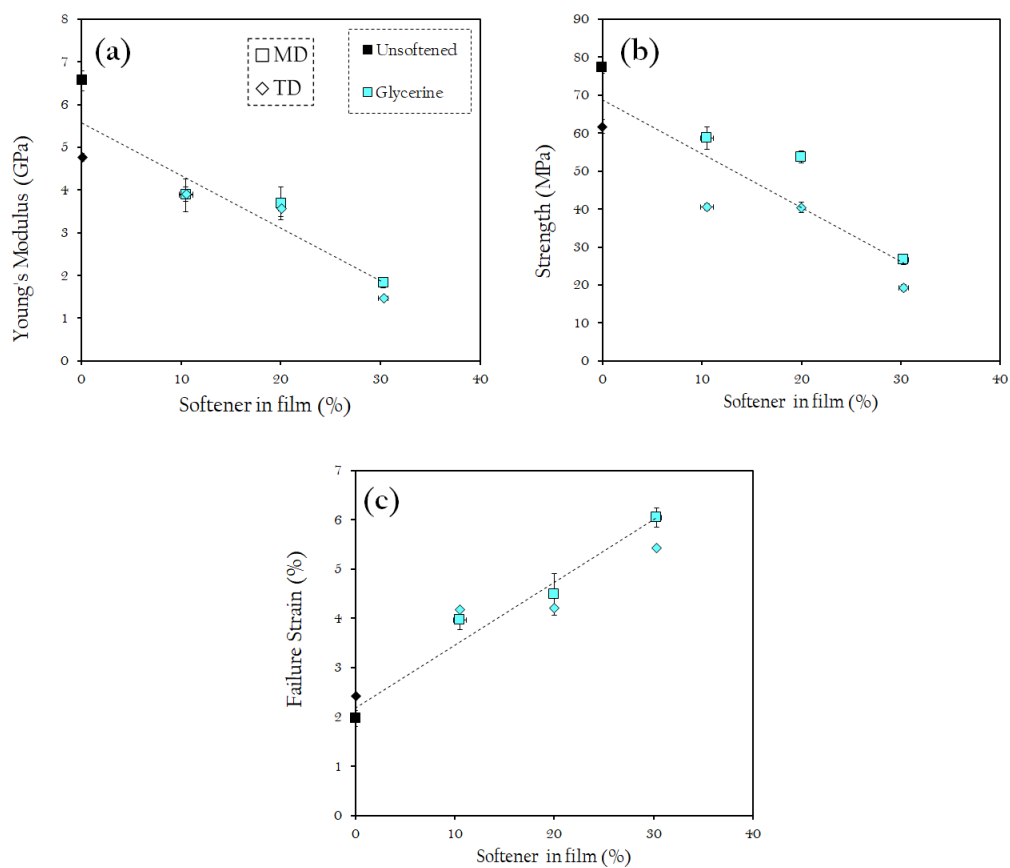


Figure 5.5: Variation of tensile properties with increasing Glycerine content (a) Young's Modulus (b) Strength and (c) Strain at failure

5.2 Tensile Properties

Figures 5.5(a-c) shows a distinct linear relationship between increasing glycerine content and modulus, strength and strain at failure. These results indicate the clear plasticising effect of glycerine; with the minimum values of Young's Modulus = 1.8 ± 0.1 GPa, Strength = 26 ± 1 MPa and maximum values of Strain at failure = 6.0 ± 0.2 % exhibited at the maximum softener content of 30 %. This is a clear indication of the softening effect of glycerine and its justification as a commercial softener. However, due to its effectiveness, the glycerine market capitalises on the necessity of this softener in a range of products. Costs of plasticiser are an important commercial factor for Futamura to consider, making the investigation of alternate plasticisers even more essential.

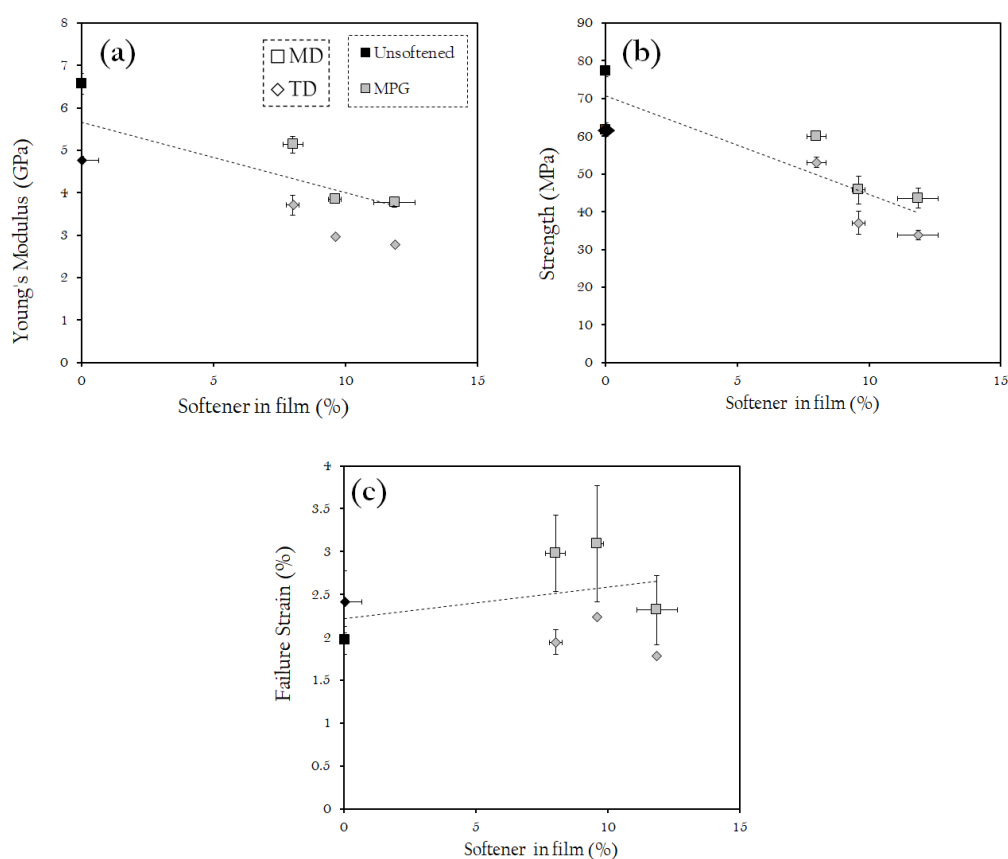


Figure 5.6: Variation of tensile properties with increasing MPG content (a) Young's Modulus (b) Strength and (c) Strain at failure

5.2 Tensile Properties

Figures 5.6(a-c) show a the relationship between increasing MPG content and modulus, strength and strain at failure. The first observation to note is that these films have the smallest uptake in softener content; with concentrations ranging between 8.0 % - 11.8 %; this is significantly less than that of the glycerine, urea or the 3 component softener. MPG's inability to remain embedded between polymer chains to impart ductility is evident in its impact on tensile properties. Investigating material properties with increasing MPG content, Young's Modulus reduces in the machine direction from 5.1 ± 0.2 GPa to 3.8 ± 0.1 GPa, along with strength from 60 ± 1 MPa to 44 ± 3 MPa. However, from Figure 5.6(c) it appears that MPG has little effect on the strain at failure with increasing concentration; with values in the machine direction reducing from 2.2 ± 0.3 % to 1.8 ± 0.2 %. This anti-plasticisation effect is also observed in MPG softened films by Suyatma et al [120]. Therefore, this plasticiser only acts to reduce modulus and strength whilst ductility remains low. As such, one recommendation from this thesis for Futamura is to reconsider the inclusion of this secondary plasticiser.

5.2 Tensile Properties

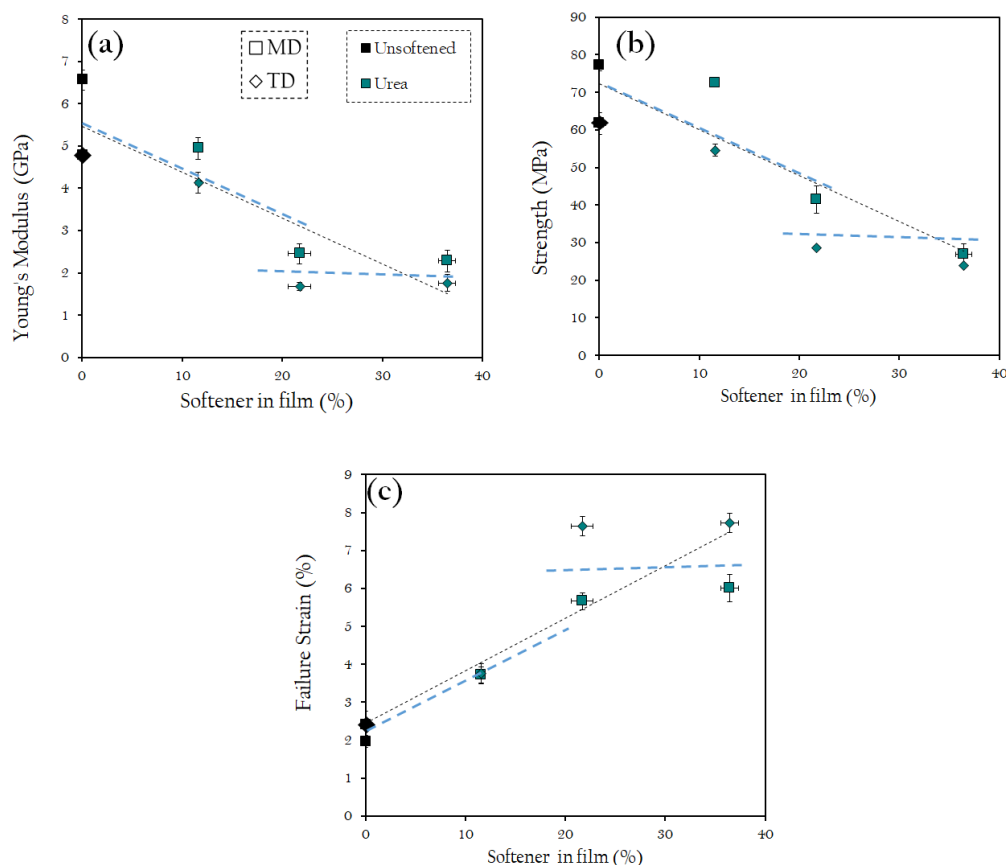


Figure 5.7: Variation of tensile properties with increasing Urea content, with blue dashed line indicating the plateau in properties experienced due to maximum uptake (a) Young's Modulus (b) Strength and (c) Strain at failure

Figures 5.7(a-c) show the relationship between increasing Urea content and modulus, strength and strain at failure. This plasticiser boasts the highest uptake of plasticiser in films, with softener content ranging from 11.6 % - 36 % due to its low molecular mass and three hydrophilic group's ability to displace water from cellulose wet gel. However, visual observations of these urea-based films in Figure 5.1 give evidence that urea has migrated out of the films for concentrations as low as 22 % and is deposited on the surface as a white coating. Therefore, urea reaches its maximum absorption between 12 % - 22 % concentration, meaning that it will be interesting to assess how this effects mechanical properties. Figures 5.7(a-c) prove urea's softener capabilities with increasing urea content resulting in a

5.2 Tensile Properties

decrease in strength and Young's Modulus and an increase strain at failure. However, the effects of higher plasticisation do appear to plateau, with values not varying much between 22 % and 36.4 % urea content. This minimal variation in mechanical properties, along with observed migration of urea suggests that the maximum urea content of films occurs between $\approx 12\%$ - 22 %. As such, another recommendation for Futamura from this project is to increase urea content of their softener blend but not surpassing a 22 wt %. With Futamura currently incorporating *(This text has been removed by the author of this thesis for confidentiality reasons)*

so, there is room for increase depending on costs of including urea in today's market.

In fact, due to its high uptake into the films urea's plasticiser abilities surpass those of glycerine with the same amount of softener in water bath. A reduction of Young's Modulus in the machine direction from 4.9 ± 0.3 GPa to 2.3 ± 0.3 GPa and strength from 72 ± 2 MPa to 27 ± 2 MPa are observed; whilst strain at failure exhibits an increase of $3.7 \pm 0.2\%$ to $6.0 \pm 0.4\%$ (with the middle concentration 22 % exhibiting a similarly high failure strain as the higher 36 % of $5.6 \pm 0.2\%$). Since urea has a drastic softening effect at the middle concentration, it is recommended that Futamura investigate the effect of increasing this softener content in their commercial films to replace the need for MPG. This work throws the role of urea as a 'secondary' plasticiser into question.

5.2 Tensile Properties

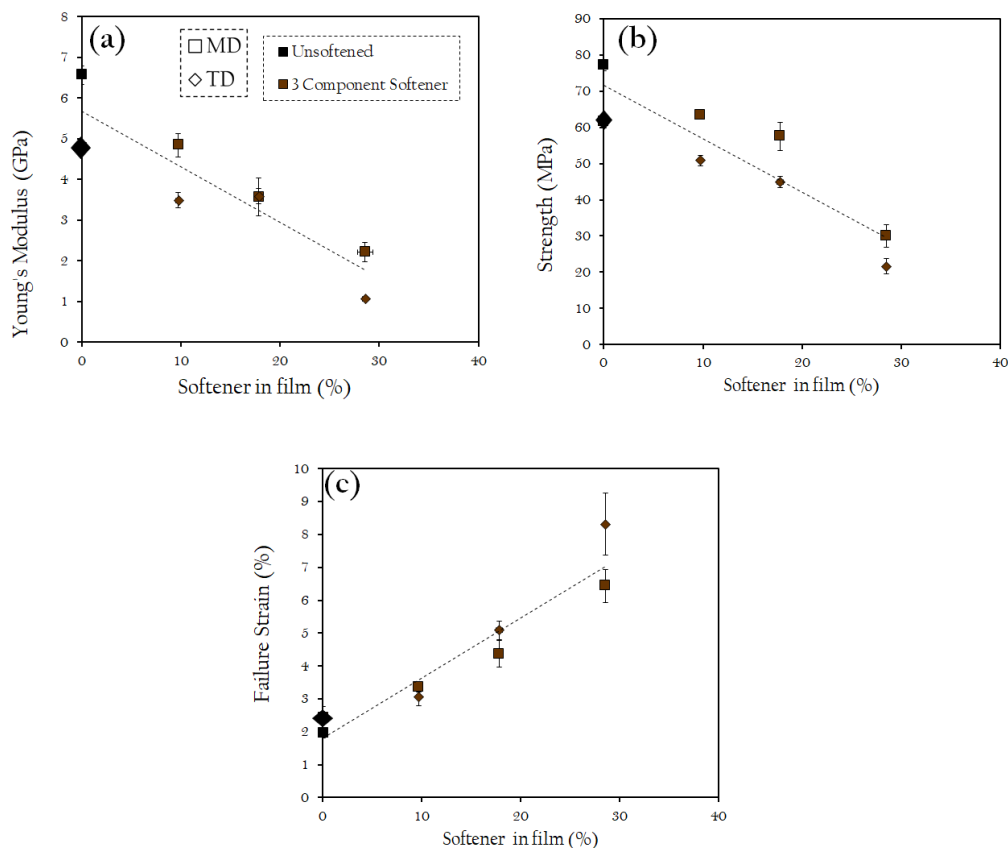


Figure 5.8: Variation of tensile properties with increasing 3 Component Softener content (a) Young's Modulus (b) Strength and (c) Strain at failure

Figures 5.8(a-c) show the relationship between increasing 3 Component Softener content and modulus, strength and strain at failure. These films exhibit the most significant softening effect, probably due to the cumulative softening abilities of the dominating (*This text has been removed by the author of this thesis for confidentiality reasons*) [REDACTED]. These results show a reduction of Young's Modulus in the machine direction with increasing 3 component softener content from 4.8 ± 0.3 GPa to 2.2 ± 0.2 GPa and strength from 63.3 ± 0.8 MPa to 30 ± 3 MPa, whilst strain at failure in the machine direction increases with 3 component softener content from 3.4 ± 0.1 % to 6.4 ± 0.5 %. These improved 3 component softener properties with increasing content are in contrast to the work of Versino et al, who report a 50:50 urea:glycerine

concentration results in a reduction of mechanical performance, hypothesised to be attributed to preferential hydrogen bonding between urea and glycerine rather than the polymer matrix [119].

The superiority of this 3 component softener package, shows the cumulative co-plasticisation ability of softeners to work together to impart plasticisation at these concentrations. However, with the individual contribution of glycerine, MPG and Urea having been investigated, this work throws the role of MPG into question. It is recommended that Futamura assess the pricing structure of these 3 components and consider altering the blend to obtain the best plasticisation economically.

5.2 Tensile Properties

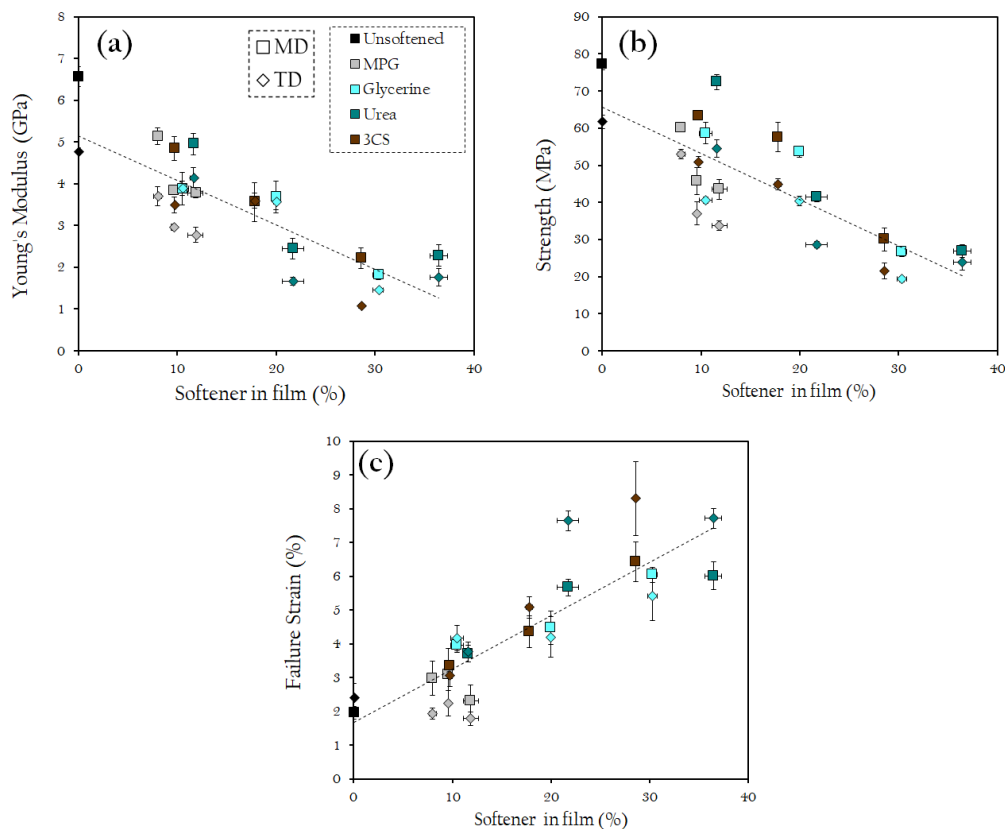


Figure 5.9: Variation of tensile properties with increasing Glycerine, MPG, Urea and 3 Component Softener content (a) Young's Modulus (b) Strength and (c) Strain at failure

Finally, Figures 5.9(a-c) have been created to represent the overall relationship between varying softener uptake for all individual and blend softeners and its effect on modulus, strength and strain at failure of those films. It is clear that glycerine and urea exhibit superior plasticising properties due to their increased uptake capability in comparison to MPG, since each film fits on the same trendline.

5.2.4 Comparison to commercial Films

In order to analyse the correlations between commercial and lab-softened films, there are two sets of films that are comparable: Both unsoftened films and the 3-component softener (*This text has been removed by the author of this thesis for confidentiality reasons*) films have been compared. Figures 5.10(a-c) have been produced to demonstrate the comparison between these film's behaviour.

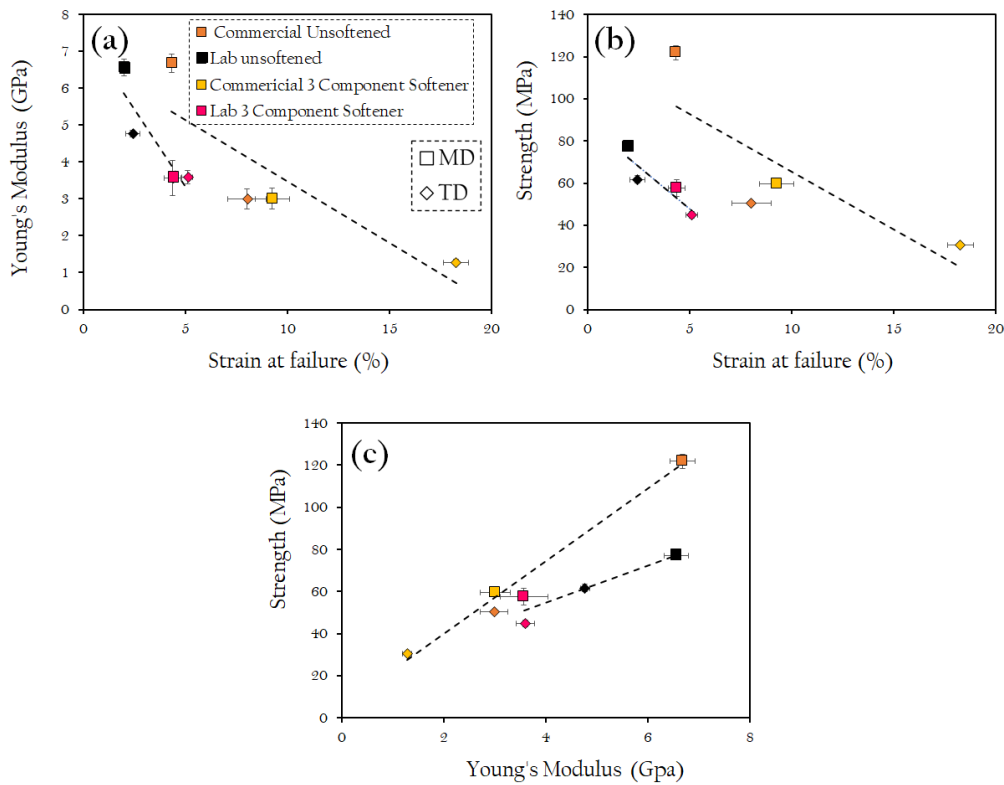


Figure 5.10: Ashby Plots depicting the variation of tensile properties for the commercial and lab-plasticised unsoftened and 3 component softener (*This text has been removed by the author of this thesis for confidentiality reasons*) films in their machine (square markers) and transverse (diamond markers) directions with dashed lines indicating the two different trendlines that result from production process causing a difference in orientation of polymeric chains (a) Young's Modulus against strain at failure, (b) Strength against strain at failure and (c) Strength against Young's Modulus

5.3 Falling weight and slow puncture impact properties

As seen in Ashby plots Figures 5.10(a-c), commercial and lab-based films follow the same trend in material property relationships but with two different trendlines. This difference in trendlines likely arises due to the difference in production processing in that commercial films are extruded and rolled under tension, whereas lab-based films are shrunk onto frames and don't undergo tension under rolling. This indicates that as well as the actual addition of plasticiser, the rolling process also acts to impart ductility and stiffness to films; as exhibited by the superior mechanical properties of the commercial films. This difference in production process causes an increased alignment in orientation of cellulose chains within the films. This is something that we have shown to impact mechanical performance, as shown by the diversity of machine and transverse directions in Ashby Plots. Since the relationships between commercial and lab based films show the same material dependence, conclusions when comparing lab and commercial films are justified.

5.3 Falling weight and slow puncture impact properties

The results of slow puncture and impact tests for lab based films performed at speeds (1 mm/min- 120000 mm/min) and converted to strain rates are shown in Figures 5.11(a-c) - 5.14(a-c) representing maximum strain, normalised maximum force and normalised energy. To produce these results, five repeats were performed for each sample at each speed, from which the average was calculated and error determined and plotted. This set of films exhibited the same starburst crack formation as commercial films, discussed in the previous chapter.

5.3.1 Variation of strain rate and softener

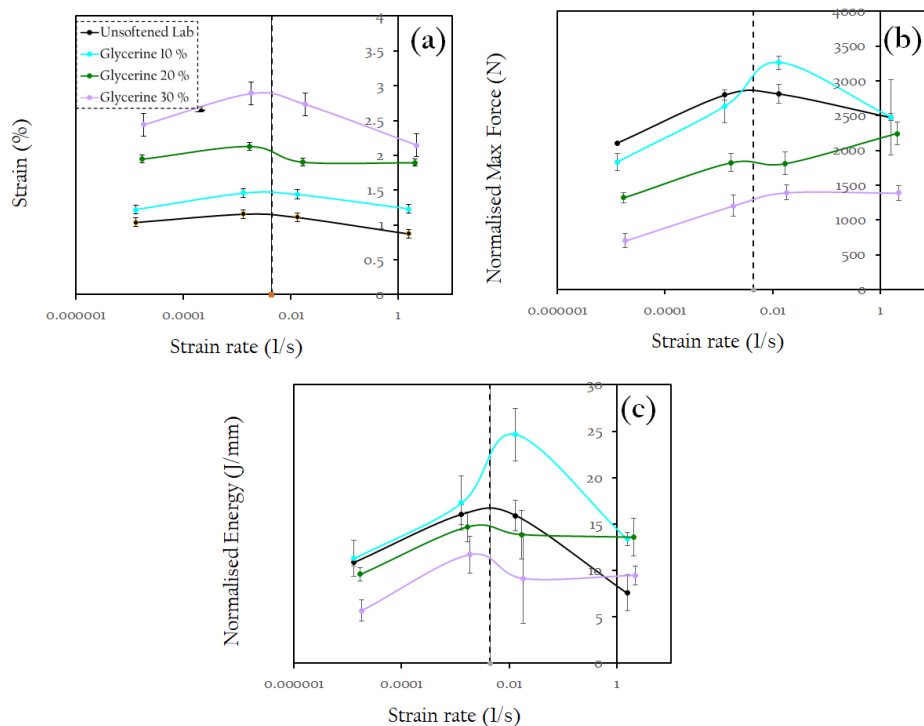


Figure 5.11: *Falling weight and slow puncture impact properties across a range of strain rates for glycerine lab-based film set where the black dotted line indicates the strain rate at which tensile testing was performed (a) Strain against strain rate, (b) Normalised Maximum Force against strain rate, (c) Normalised energy against strain rate*

Figures 5.11(a-c) show the variation of impact properties for glycerine plasticised films for a range of strain rates. Similarly to tensile results, these results indicate the effectiveness of this plasticiser; with increasing maximum strain but decreasing force and energy observed with increasing glycerine content. These lab based films exhibit a peak in impact properties between $\approx 0.001 - 0.01 \text{ s}^{-1}$. The films with maximum glycerine content, 30 %, exhibit the highest maximum strain of $2.89 \pm 0.02 \%$ at a strain rate of 0.001 s^{-1} . Whilst the minimum glycerine content films, 10 %, film exhibits a maximum strain of $1.46 \pm 0.02 \%$ at the same strain rate. This indicates the softening ability of glycerine to increase

5.3 Falling weight and slow puncture impact properties

the ductility of the films and prevent fracture on impact. On the other hand, maximum force and energy are observed for the 10 % glycerine film at a strain rate of 0.01 s^{-1} of $3260 \pm 90 \text{ N/mm}$ and $25 \pm 3 \text{ J/mm}$, respectively. On the other hand the minimum peak of force and energy is exhibited by the 30 % glycerine film at different strain rates. At 0.01 s^{-1} , maximum force = 1200 ± 200 whilst at 0.001 s^{-1} Energy = $9 \pm 4 \text{ J/mm}$. These results show the resultant reduction of force and energy associated with an increase in ductility as a result of glycerine addition. This reveals another necessary trade-off between properties for these materials with the maximum ductility seen at maximum softener content but with resulting minimum force and energy.

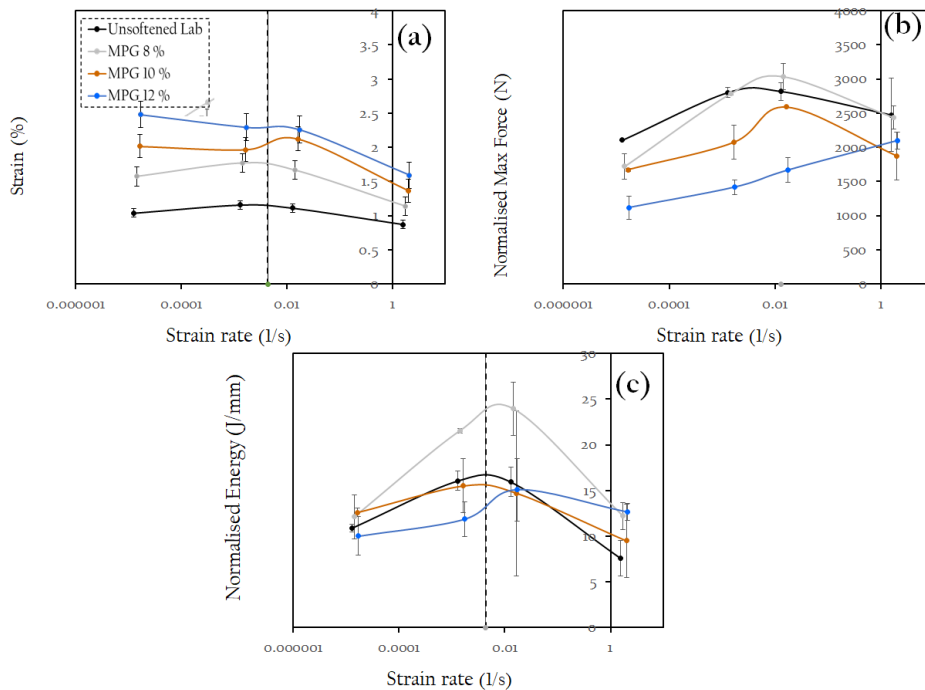


Figure 5.12: *Falling weight and slow puncture impact properties across a range of strain rates for MPG lab-based film set where the black dotted line indicates the strain rate at which tensile testing was performed (a) Strain against strain rate, (b) Normalised Maximum Force against strain rate, (c) Normalised energy against strain rate*

Figures 5.12(a-c) show the variation of impact properties for MPG plasticised films for a range of strain rates. Again, a variation of impact properties with

5.3 Falling weight and slow puncture impact properties

strain rate is observed. The maximum MPG content film, 12 %, demonstrates the maximum strain of this set of films. However, its plasticiser ability is not as significant as that of glycerine and at low strain rate 0.00001 s^{-1} , maximum strain of the 12 % films is $2.48 \pm 0.02 \%$ in comparison to that of the 8 % MPG film with a maximum strain of $1.77 \pm 0.02 \%$ at 0.001 s^{-1} . This small window of variation is indicative of the reduced uptake of MPG into the films in comparison with other softeners. Furthermore, a peak in maximum force and energy is observed at a strain rate of 0.01 s^{-1} for the minimum content MPG film, 8 %, of $3000 \pm 200 \text{ N/mm}$ and $24 \pm 3 \text{ J/mm}$, respectively. Conversely to maximum strain behaviour, there is a diverse range in performance observed for force and energy, despite the minimal increase in softener content. For example, at that same peak of strain rate 0.01 s^{-1} for force and energy, the 12 % softened film exhibits a lower Force and energy of $1700 \pm 200 \text{ N/mm}$ and 15 ± 3 , respectively. This indicates, that rather than imparting ductility through its plasticising effect, MPG only acts to reduce force or, in the case of tensile testing, strength. These impact properties reinforce this thesis' case to reconsider MPG's role in Futamura's 3 component commercial package.

5.3 Falling weight and slow puncture impact properties

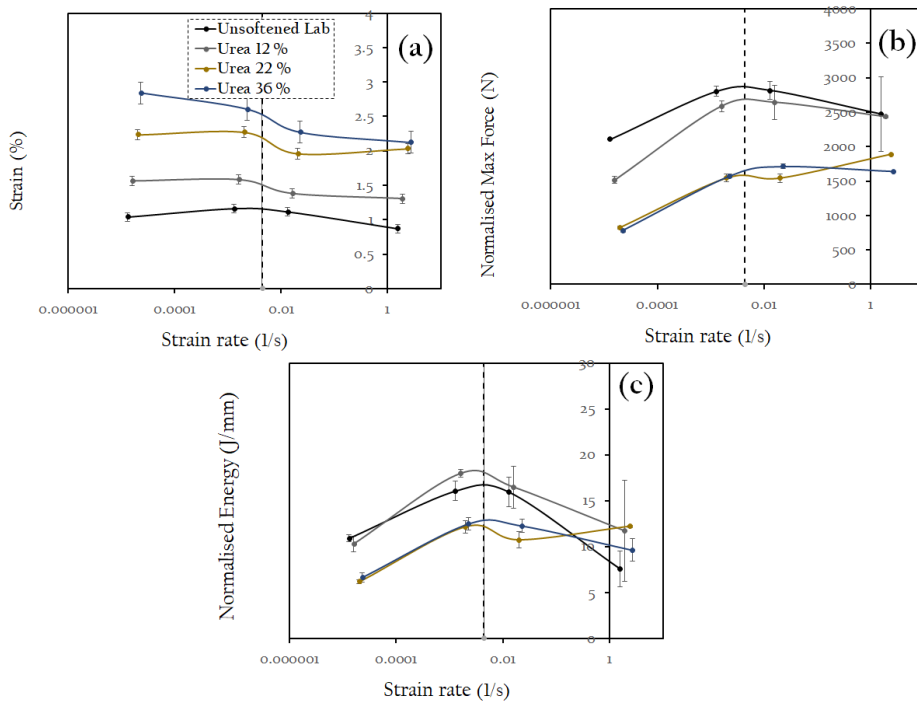


Figure 5.13: *Falling weight and slow puncture impact properties across a range of strain rates for urea lab-based film set where the black dotted line indicates the strain rate at which tensile testing was performed (a) Strain against strain rate, (b) Normalised Maximum Force against strain rate, (c) Normalised energy against strain rate*

5.3 Falling weight and slow puncture impact properties

Figures 5.13(a-c) show the variation of impact properties for urea plasticised films for a range of strain rates. Interestingly, for maximum strain, there is not a distinct peak in properties observed at a certain strain rate, and in fact the strain is fairly uniform for each film. Furthermore, the maximum values of strain are exhibited at the minimum strain rate tested at 0.00001 s^{-1} . For the films with the minimum urea content of 12 %, the maximum strain is $1.57 \pm 0.06 \%$ and for maximum urea content of 36 %, the maximum strain is $2.84 \pm 0.01 \%$. These results are in stark contrast to tensile results that demonstrate urea as the superior softener since their impact strain is lower than that of both glycerine and MPG softened films at their peak strain rate. However, this uniformity across strain rates can be considered an advantage in application since films are subject to a range of impact speeds, making this homogeneous performance desirable. Maximum force and energy exhibit similar strain rate dependency as other softened films with a peak between 0.001 s^{-1} - 0.01 s^{-1} . The 12 % urea film demonstrates the maximum force and energy of $2600 \pm 300 \text{ N/mm}$ and $18.0 \pm 0.4 \text{ J/mm}$. On the other hand, the 36 % urea film exhibits the lowest force and energy of $1570 \pm 20 \text{ N/mm}$ and $12.3 \pm 0.6 \text{ J/mm}$.

5.3 Falling weight and slow puncture impact properties

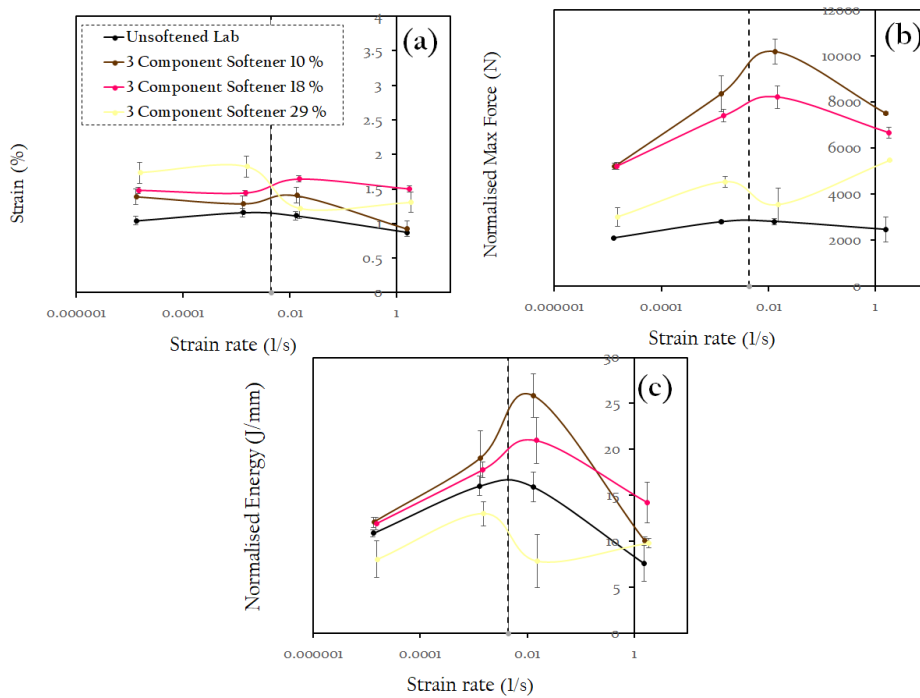


Figure 5.14: *Falling weight and slow puncture impact properties across a range of strain rates for 3 component softener lab-based film set where the black dotted line indicates the strain rate at which tensile testing was performed (a) Strain against strain rate, (b) Normalised Maximum Force against strain rate, (c) Normalised energy against strain rate*

5.3 Falling weight and slow puncture impact properties

Finally, Figures 5.14(a-c) show the variation of impact properties for 3 component plasticised films for a range of strain rates, exhibiting similar behaviour to glycerine-based films due to it making up *(This text has been removed by the author of this thesis for confidentiality reasons)* ██████████. The variation of maximum strain of these films is quite complex. Firstly, the maximum 3 component softener content film, 29 %, shows a dip in performance at just above tensile testing strain rate. This suggests that Futamura should not increase softener content as high as this as it would have a detrimental effect on impact behaviour at high strain rates. In fact, the *(This text has been removed by the author of this thesis for confidentiality reasons)* ██████████ film (comparable to Futamura's current commercial 3 component softened film) exhibits the most uniformly high strain properties at a maximum of 1.64 ± 0.01 % at a strain rate of 0.01 s^{-1} , in comparison to the minimum value of strain (similar to that of the unsoftened film) for the 29 % film of 1.22 ± 0.02 % at that same strain rate. Force and energy variation demonstrate a distinct peak at 0.01 s^{-1} for the 10 % and 18 % 3 component softener films, with 18 % exhibiting maximum values of $8200 \pm 500 \text{ N/mm}$ and $21 \pm 3 \text{ J/mm}$. Meanwhile at this same strain rate, the 29 % 3 component softener film demonstrates minimum values of both force and energy of $3500 \pm 700 \text{ N/mm}$ and $8 \pm 3 \text{ J/mm}$. This reduction of impact properties at higher softener concentrations for the 3 component softener could be indicative some preferential bonding between plasticiser molecules over that of cellulose chains and water, resulting in a lesser plasticising effect. Again, providing justification for the *(This text has been removed by the author of this thesis for confidentiality reasons)* ██████████ chosen by Futamura.

5.3.2 Comparison to commercial films

As with tensile test comparisons, unsoftened lab films could be compared to their commercial counterpart, as well as 3 component softened *(This text has been removed by the author of this thesis for confidentiality reasons)* ██████████ compared to the commercial 3 component softened film with no coatings or additives. Figures 5.15(a-c) demonstrate the variation in impact properties of these films across

5.3 Falling weight and slow puncture impact properties

a range of strain rates.

5.3 Falling weight and slow puncture impact properties

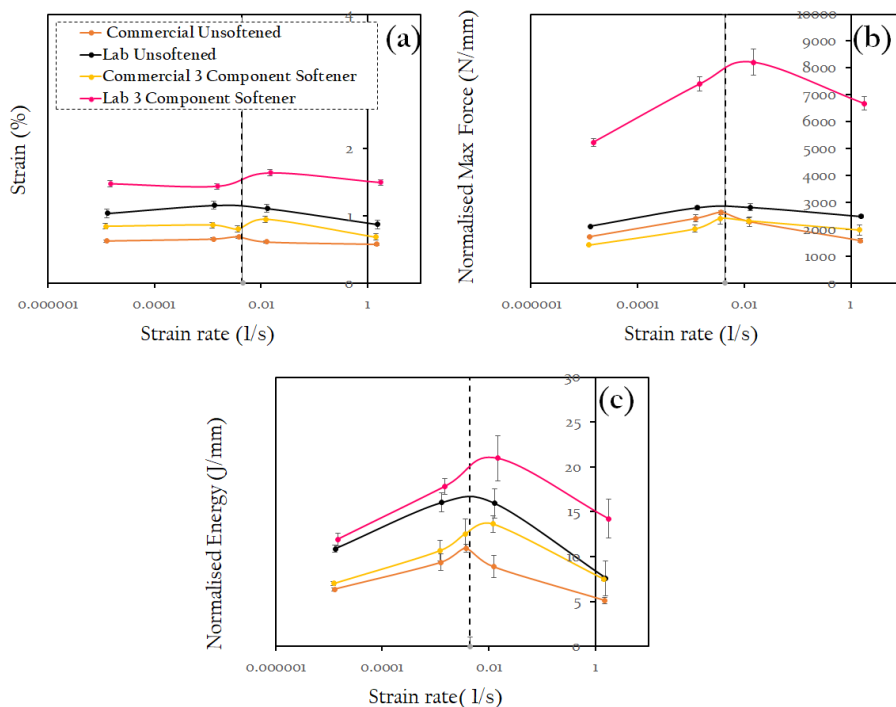


Figure 5.15: *Falling weight and slow puncture impact properties across a range of strain rates for the commercial and lab-plasticised unsoftened and 3 component softener (This text has been removed by the author of this thesis for confidentiality reasons) films where the black dotted line indicates the strain rate at which tensile testing was performed (a) Maximum strain against strain rate, (b) Normalised Maximum Force against strain rate, (c) Normalised energy against strain rate*

Unlike the results and comparisons between commercial and lab softened films in tensile testing, the lab softened films exhibit superior strain, force and energy in comparison to their commercial counterpart for both the unsoftened and 3 component softened films. This is likely due to the difference in production process that results in increased alignment of cellulose chain in commercial films and therefore increased variation of properties in their machine and transverse directions. This increased uniaxiality is seen to have a negative effect on impact properties of the films, presumably due to the non-uniformity of directional properties upon impact. This means that not only is there a compromise in property selection when optimising these films between ductility and strength; but also

the priority of either superior tensile or impact properties must be considered for application.

5.4 Dynamic Mechanical Thermal Analysis

Dynamic Mechanical Thermal Analysis was performed between $-100\text{ }^{\circ}\text{C}$ to $+120\text{ }^{\circ}\text{C}$ at a frequency of 1 Hz for each of the lab-softened films. This temperature range was chosen in order to investigate the variation of secondary transitions that can be associated with changes in plasticisation in a hope to investigate the complex dynamic behaviour seen in the commercial films set so that relaxations could be identified and to avoid degradation of the cellulose chain that onsets at $\approx 200\text{ }^{\circ}\text{C}$. Figures 5.16(a-d) have been produced to demonstrate the variation of $\tan\delta$ behaviour for each of the lab-softened films across this temperature range.

5.4 Dynamic Mechanical Thermal Analysis

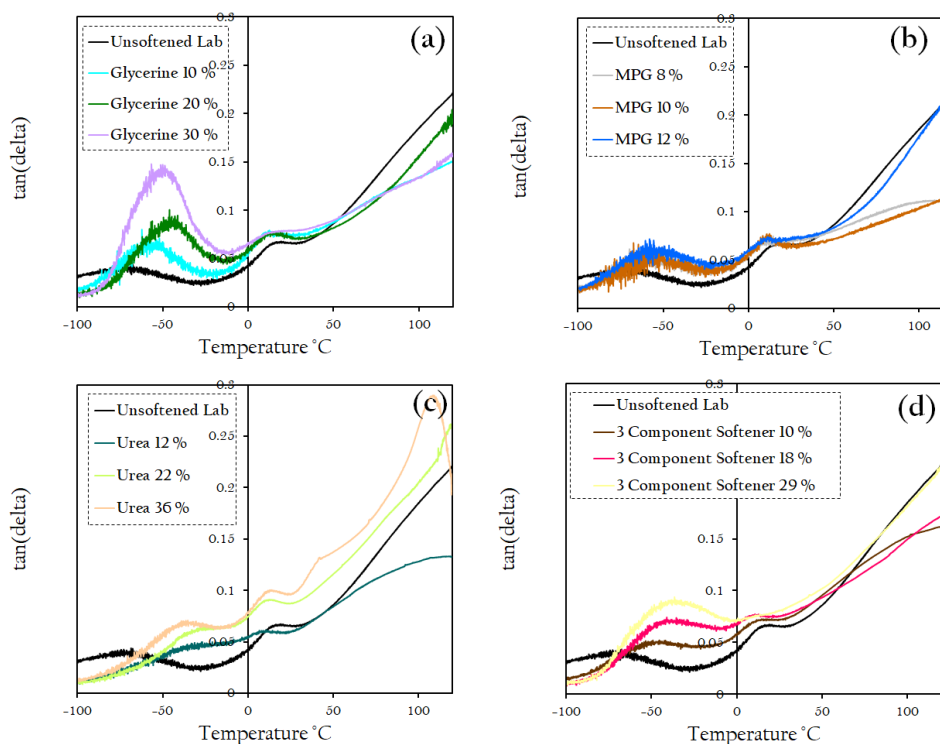


Figure 5.16: *Dynamic Mechanical Thermal Analysis, $\tan \delta$ profiles, of lab-plasticised film set from $-100\text{ }^{\circ}\text{C}$ to $120\text{ }^{\circ}\text{C}$ at oscillating frequency of 1 Hz (a) Glycerine (b) MPG (c) Urea and (d) 3 Component Softener, each compared to the lab-based unsoftened film*

These Figure 5.16(a-d) represent the changes to $\tan \delta$ across the chosen temperature change and the changes to two secondary peaks have been identified. The first peak, around room temperature, is assumed to be the β transition due to its behaviour with plasticisation aligning with that of literature in that the peak does not experience significant shifting but is amplified with increasing plasticiser content, impacting mechanical performance. However, discussion of this presumed β peak has been omitted from this thesis and the sub zero secondary transition has been the focus due to its prevalence in commercial dynamic profiles. Nonetheless, graphs examining this room temperature peak analysis are included in the Appendix, Figures A.1, A.2, A.3 and further investigations into the changes of this peak provide an excellent candidate for future work. However, for this work it is the sub zero peak that is focused on, that we will assign to be

the γ peak. This is because it is the most prevalent peak seen in commercial films and its association with water is documented in the literature. Since we have hypothesised the importance of a softener's ability to bring in water to films and the effect this has on performance, this γ peak is of particular interest. It should be noted that the positioning of these peaks is shifted to higher temperatures than those found in the literature of cellulose acetate [108]. This is advantageous for this work as it has allowed us to concentrate on the γ peak as it is occurring at higher temperatures, so is more easily measurable as its contributions are not well understood for cellulose [108].

5.4.1 Variation of softeners on γ transition

For each Figures 5.16(a-d), the amplitude and temperature shift of $\tan\delta$ for the presumed γ relaxation changes with increasing plasticisation content. To analyse this data and identify these peak positions and heights, an asymmetric double Sigmoidal function was plotted to data using python. An example of this fitting is demonstrated in Appendix Figure A.7. These changes are demonstrated by Figures 5.17(a-b). For example, the $\tan\delta$ amplitude of the unsoftened film is 0.0363, whilst softened films exhibit an increase in this peak with increasing plasticiser content. For example between minimum and maximum plasticiser contents; glycerine displays a peak increase from 0.064 ± 0.004 - 0.136 ± 0.001 , MPG from 0.051 ± 0.002 - 0.058 ± 0.002 , Urea from 0.040 ± 0.002 - 0.066 ± 0.005 and 3 Component Softener from 0.047 ± 0.006 - 0.082 ± 0.002 . On the other hand, the shifting of the γ transition with temperature is more complex with increasing plasticiser content. For example, the peak position of the γ transition in the unsoftened film is -58.8 °C. In comparison, the minimum through to maximum values of plasticisers range; for glycerine between -55.6 ± 0.9 °C down to -50.3 ± 0.8 °C and back up to 54.0 ± 0.1 °C, for MPG from -59.6 ± 0.7 °C to -57.6 ± 0.5 °C to 61 ± 2 °C, for Urea from -45 ± 1 °C to -36 ± 4 °C to -41 ± 3 °C and for the 3 component softener from -57 ± 2 °C to -48 ± 1 °C and to -47 ± 2 °C.

5.4 Dynamic Mechanical Thermal Analysis

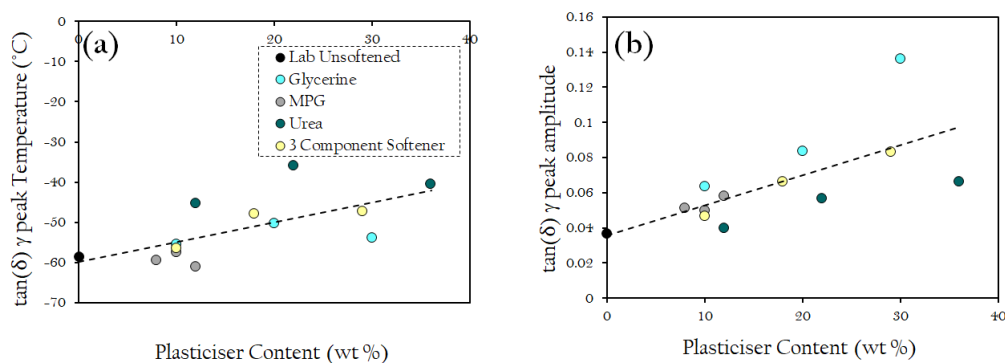


Figure 5.17: Variation of γ peak with plasticiser content of lab-plasticised films (a) temperature of γ transition (b) amplitude of γ transition

The γ transition typically occurs at very low temperatures and thus is not as well understood as other relaxations. It is often associated with side group motion of polymers or small scale local rearrangement of the main chain. For cellulose, the origins of this motion manifests as methyl side group rotation, hydroxyl and methyl cooperative rotation or bounded water contribution, summarised by Einfeld et al [110]. For our systems, we believe plasticiser content is disrupting and amplifying this molecular motion of polymer chains either on its own or cooperatively with water and as a result, this causes a change in both molecular and mechanical behaviours.

5.4.2 Comparison to tensile properties

To quantify this observed changed in dynamic behaviour with mechanical performance, the variation of the γ transition with plasticiser content was compared to the tensile properties of the films. As such Figures 5.18(a-c) - 5.19(a-c) have been produced to demonstrate the variation of $\tan \delta$ amplitude and temperature shift with Young's Modulus, strength and strain at failure.

5.4 Dynamic Mechanical Thermal Analysis

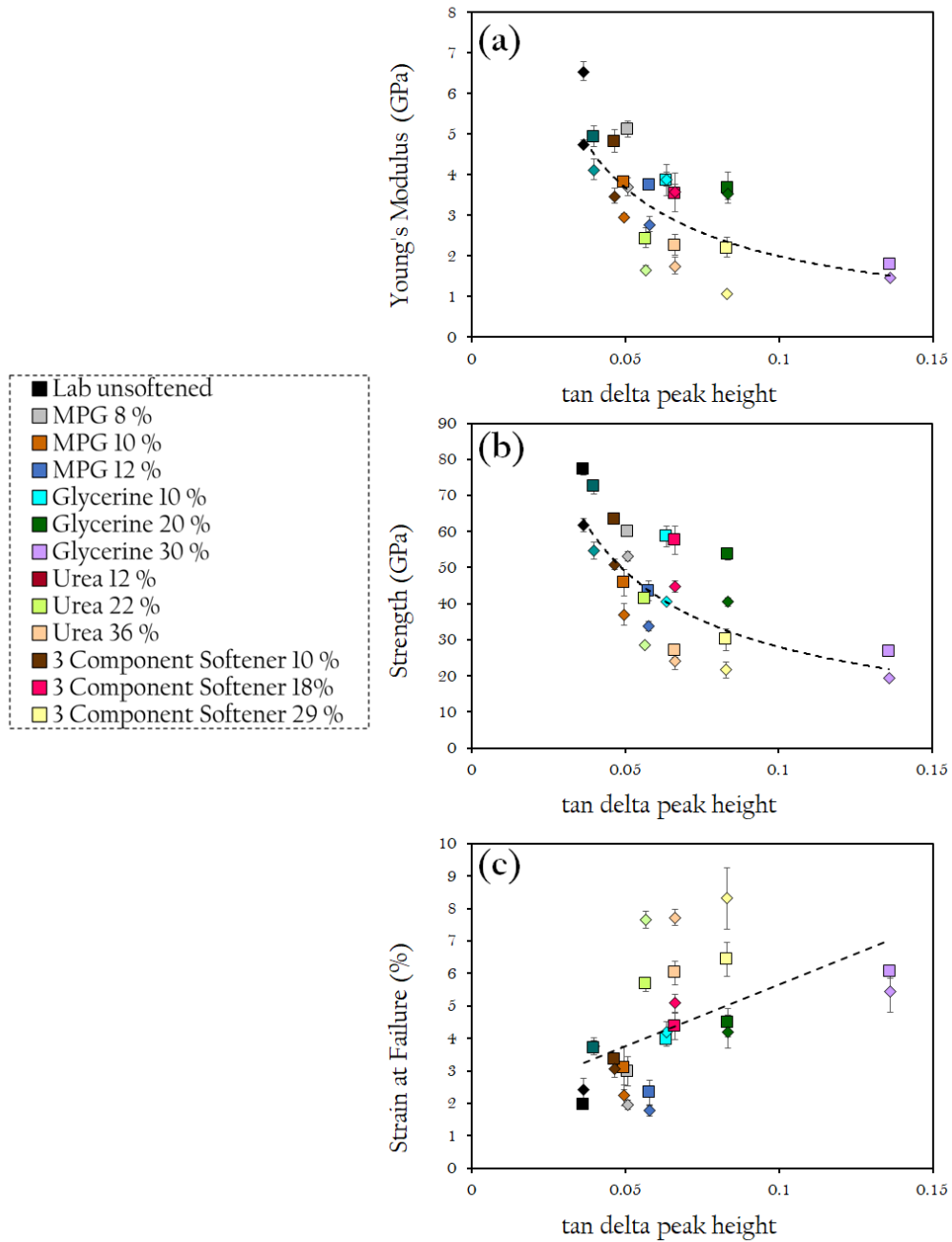


Figure 5.18: Variation of γ transition $\tan \delta$ peak amplitude with tensile properties for lab-plasticised film set (a) Young's Modulus (b) Strength and (c) Strain at Failure

5.4 Dynamic Mechanical Thermal Analysis

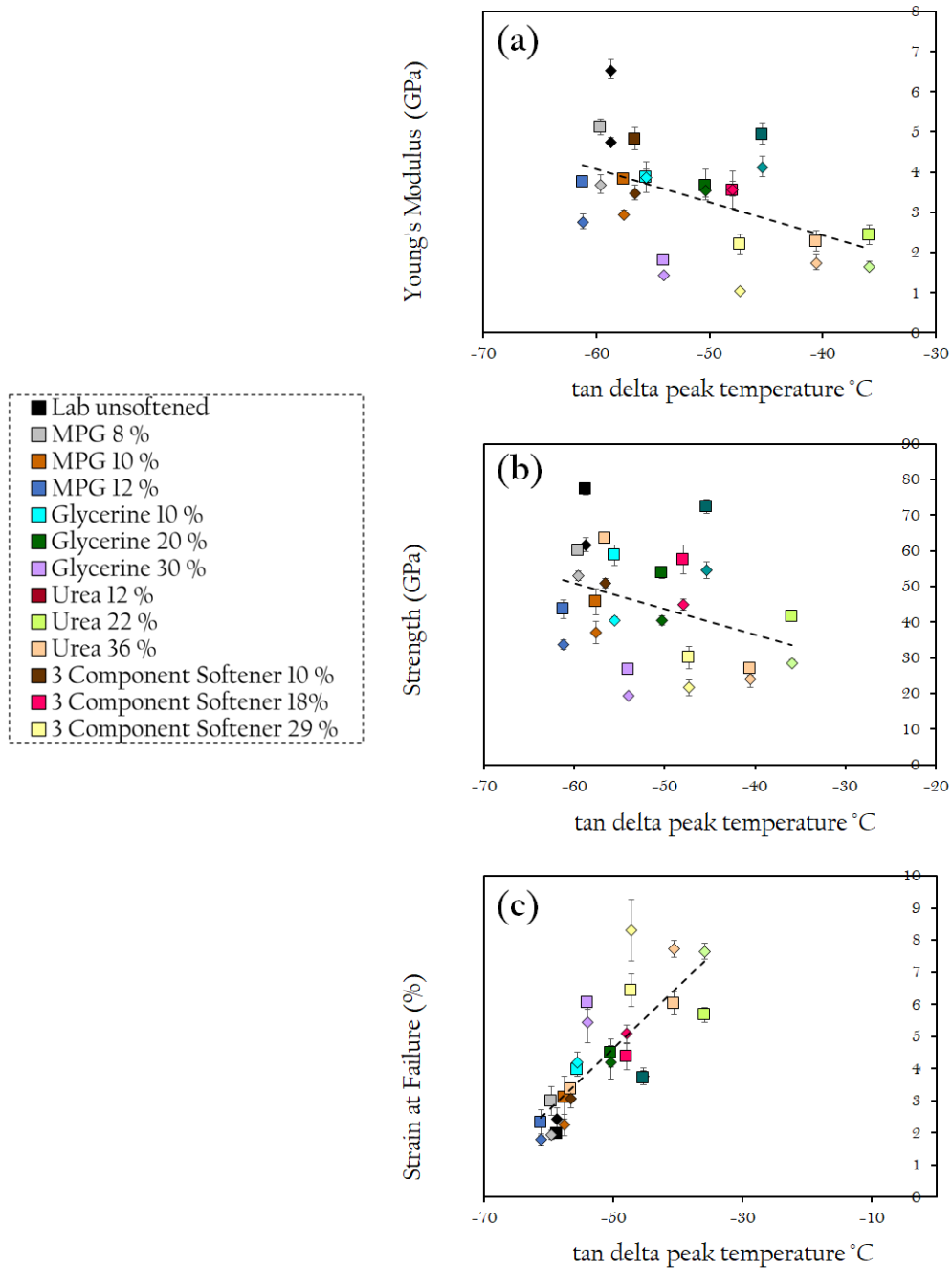


Figure 5.19: Variation of γ transition $\tan \delta$ peak temperature with tensile properties for lab-plasticised film set (a) Young's Modulus (b) Strength and (c) Strain at Failure

5.4 Dynamic Mechanical Thermal Analysis

Figures 5.18(a-c) demonstrate a clear relationship between tensile properties with γ peak amplitude. As Young's Modulus and Strength decrease, the $\tan \delta$ peak amplitude increases, associated with an increase in plasticisation. On the other hand, strain at failure exhibits a linear relationship between peak amplitude and thus plasticisation due to increased embedding of plasticisers between polymer chains, giving rise to heightened mobility. On the other hand, Figure 5.19(a-c) show a less distinct relationship between the γ transition temperature with Young's modulus and strength, whilst displaying a distinct linear relationship between temperature peak and strain at failure. These plots reveal that Young's Modulus and strength can be well predicted using $\tan \delta$ γ transition amplitude height, whilst strain at failure can also be well predicted using the peak temperature.

5.4.3 Water removal procedure

With the role of softeners being identified and the importance of their association with water being highlighted, another DMTA run procedure was performed in order to identify the role of water in plasticisation of the films by focusing on the assigned γ relaxation, whose association with water has been recognised in literature. Namely, a Water Removal Procedure was performed using the DMTA during which films were cooled to $-100\text{ }^{\circ}\text{C}$ and heated at $2\text{ }^{\circ}\text{C}/\text{min}$ whilst undergoing an oscillation of 1 Hz up to $120\text{ }^{\circ}\text{C}$ to ensure all free water was removed from the film over this temperature range. The DMTA chamber was kept sealed in order to prevent re-absorption of atmospheric water. Remaining in a nitrogen atmosphere, the film was cooled back to $-100\text{ }^{\circ}\text{C}$ and then heated back to $120\text{ }^{\circ}\text{C}$ at 1 Hz . The difference in peak positions and intensities between these runs helped to identify and confirm the role of water on the molecular motion of the films. The resultant $\tan \delta$ profiles are shown in Figures 5.20(a-c) - 5.23(a-c) for increasing plasticiser content for each of the softened films, with black lines denoting the second run where there should be no free water in films.

5.4 Dynamic Mechanical Thermal Analysis

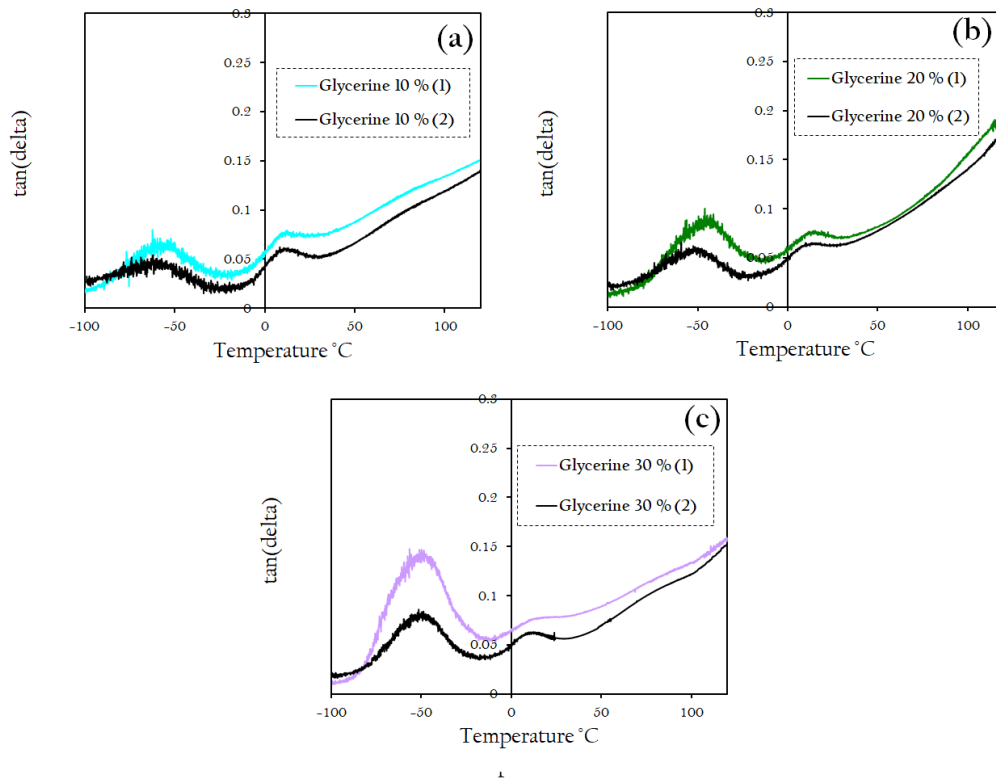


Figure 5.20: *Dynamic Mechanical Thermal Analysis (water removal procedure from $-100\text{ }^{\circ}\text{C}$ to $+120\text{ }^{\circ}\text{C}$) $\tan\delta$ profiles of glycerine lab-plasticised films (a) 10 % Glycerine film (b) 20 % Glycerine film (c) 30 % Glycerine film. Where run (1) represents the first run to remove free water from films and (2) represents the second run on the dried film.*

5.4 Dynamic Mechanical Thermal Analysis

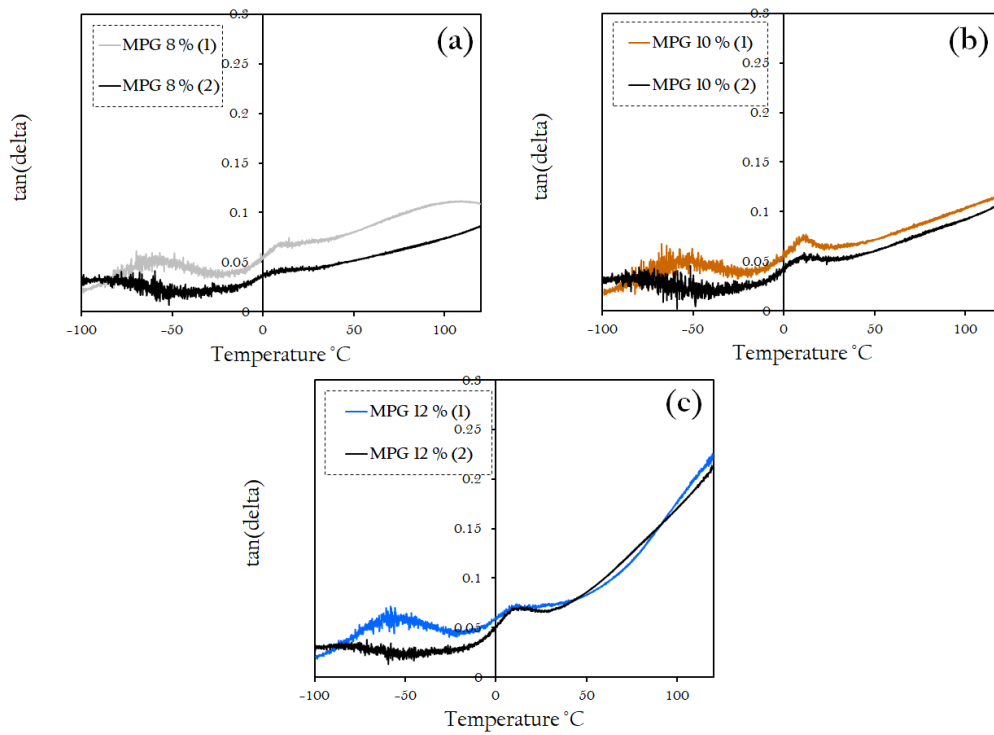


Figure 5.21: *Dynamic Mechanical Thermal Analysis (water removal procedure from -100 °C to + 120 °C) tan δ profiles of MPG lab-plasticised films (a) 10 % MPG film (b) 20 % MPG film (c) 30 % MPG film. Where run (1) represents the first run to remove free water from films and (2) represents the second run on the dried film.*

5.4 Dynamic Mechanical Thermal Analysis

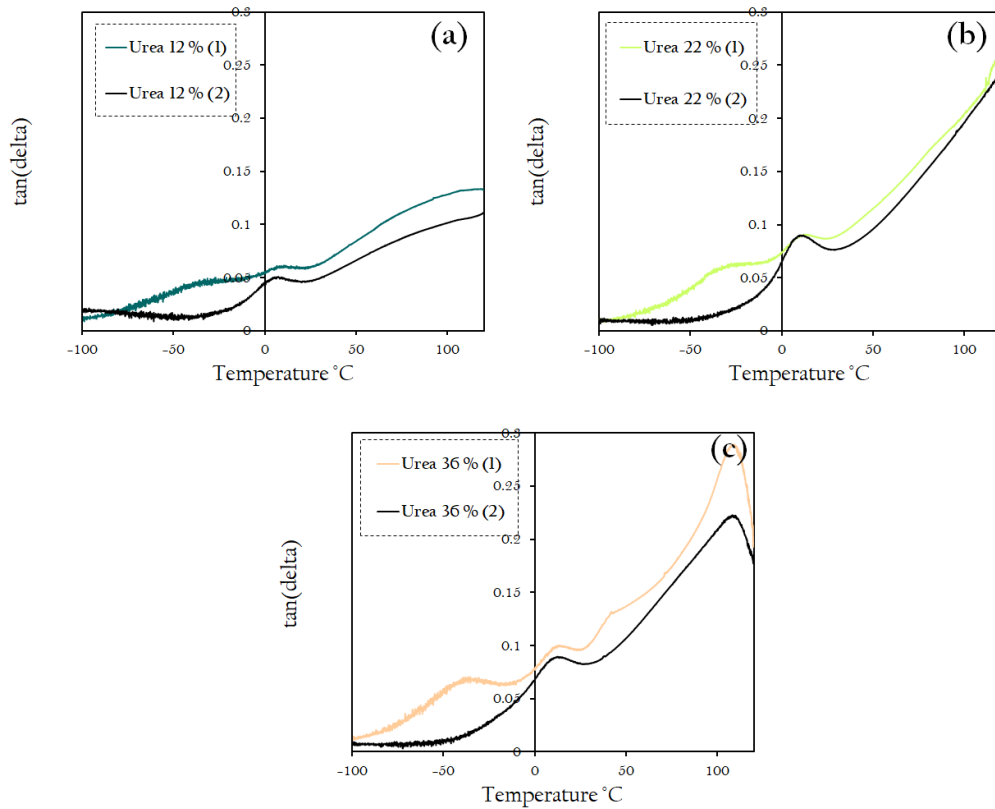


Figure 5.22: *Dynamic Mechanical Thermal Analysis (water removal procedure from $-100\text{ }^{\circ}\text{C}$ to $+120\text{ }^{\circ}\text{C}$) $\tan \delta$ profiles of urea lab-plasticised films (a) 10 % Urea film (b) 20 % Urea film (c) 30 % Urea film. Where run (1) represents the first run to remove free water from films and (2) represents the second run on the dried film.*

5.4 Dynamic Mechanical Thermal Analysis

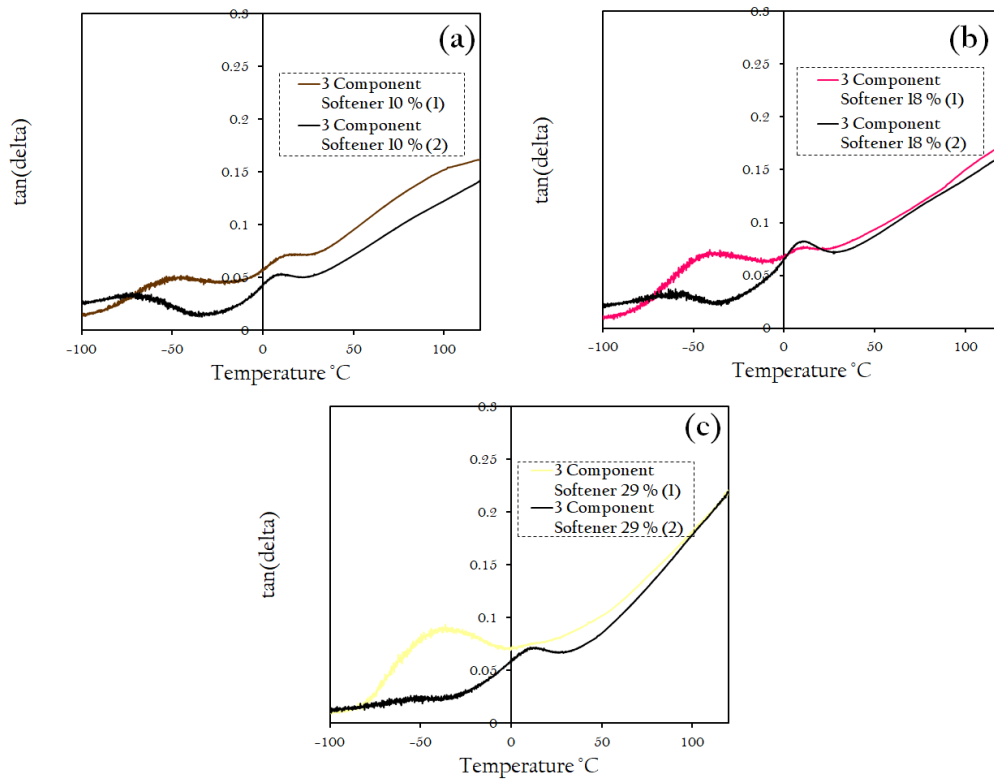


Figure 5.23: *Dynamic Mechanical Thermal Analysis (water removal procedure from $-100\text{ }^{\circ}\text{C}$ to $+120\text{ }^{\circ}\text{C}$) $\tan\delta$ profiles of 3 component softener lab-plasticised films (a) 10 % 3 Component Softener film (b) 20 % 3 Component Softener film (c) 30 % 3 Component Softener film. Where run (1) represents the first run to remove free water from films and (2) represents the second run on the dried film.*

5.4 Dynamic Mechanical Thermal Analysis

Figures 5.20(a-c) - 5.23(a-c) demonstrate the effect of water loss on the γ relaxation peak, which has been shown to be closely related to plasticising ability of films. With each second run for which free water is removed, the γ transition peak is shown to reduce in amplitude and shift to lower temperatures. These changes with the removal of water strengthens our hypothesis that this is the correct peak assignment for the γ relaxation, despite it occurring at higher temperatures than that of cellulose acetate seen in literature. Based on Figures 5.18(a-c) and 5.19(a-c), these changes to the γ transition can be associated with an increase in Young's Modulus and Strength and a decrease in strain to failure. This 'anti-plasticising' effect indicates the plasticising effect that water is inducing on films as without water they behave like an unsoftened film. Based on cellulose-plasticiser interactions with water, a hypothesis has been drawn to explain the behaviour of water in these films. Since the γ peak intensities are greater in films with higher softener concentrations, we can draw conclusions about how hydrogen bonding preferentially takes place inside these films. As increasingly plasticised films exhibit a greater drop in γ amplitude during this water removal process, we can sensibly conclude that higher plasticiser content results in higher water content of the films. This can be attributed to the fact that plasticisers themselves are hydrophilic. So, even-though the water content of baths is lower for higher plasticiser concentrations, water content of the films still increases because as well as interacting with polymer chains, plasticisers bond with water in both the wet gel and bath, which is retained in films in higher concentrations during drying.

This hypothesis highlights the importance of hydrophilicity of plasticisers. As such, further recommendations are suggested to improve Futamura's 3 Component Softener package. Since water clearly has a plasticising effect on films, it is suggested that Futamura investigate the employment of a hydrophilic plasticiser to bring water into films and induce plasticisation, as shown in the next chapter.

5.4.4 Multifrequency temperature ramps

Finally, a Multi-frequency Temperature Ramp Procedure was performed using the DMTA between -100 °C to + 120 °C at 4 frequencies from 0.1, 1, 10 and 100 Hz at 0.02 % strain on the 20 % softener in film glycerine films. These

5.4 Dynamic Mechanical Thermal Analysis

steps were performed to elucidate how frequency effects dynamic behaviour with temperature and therefore whether this can be aligned to the variation of impact properties. Furthermore, an activation energy was calculated using the theory of time temperature superposition and compared to literature values. Figure 5.24 demonstrates the difference in $\tan \delta$ profiles for this range of frequencies.

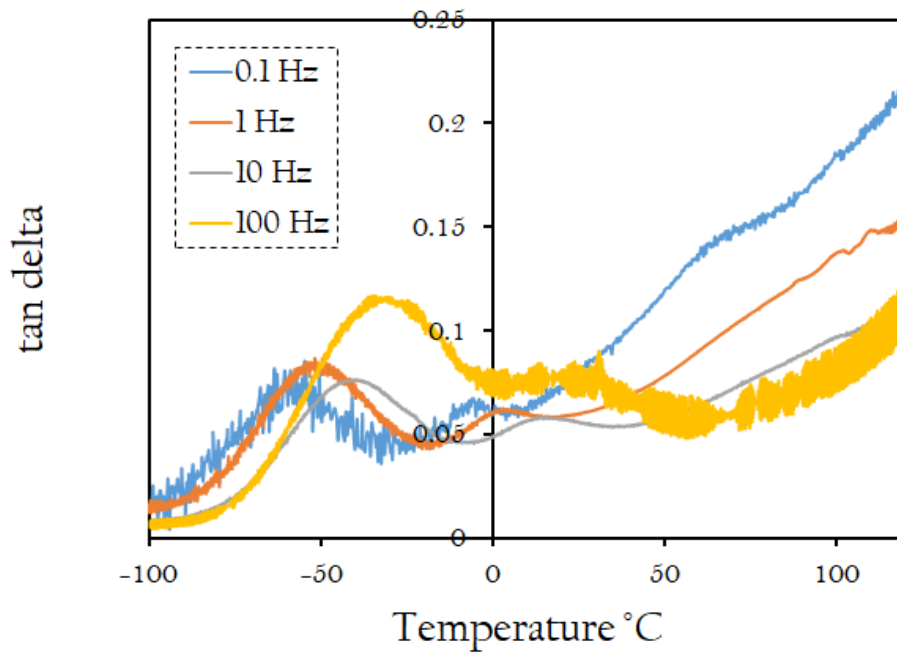


Figure 5.24: *Dynamic Mechanical Thermal Analysis (multifrequency scans at 0.1, 1, 10 and 100 Hz from -100 $^{\circ}\text{C}$ to + 120 $^{\circ}\text{C}$) $\tan \delta$ profile for 20 % glycerine films*

5.4 Dynamic Mechanical Thermal Analysis

Figure 5.24 demonstrates the shift in the relaxation profile with frequency. We can use and measure this shift to predict dynamic behaviour of the polymer at frequencies and temperatures inaccessible via measurement.

Comparison to Impact Behaviour

In order to compare dynamic behaviour to the strain rate at which films exhibit a peak in impact behaviour at room temperature, the strain rate of dynamic analysis was assessed. Impact strain rates were converted to DMTA frequencies in order to draw comparisons with impact tests behaviour with dynamic behaviour. With this conversion, the peak observed in impact behaviour at room temperature at a specific strain rate, could theoretically be aligned with a peak in dynamic properties across a range of temperatures and frequencies. Based off the strain rate conversions in Section 3.4.2, the time period of one dynamic oscillation is T and thus $T/4$ is the time taken for that sinusoidal peak to reach a maximum. Since $T=1/f$, the following equation was used to determine the strain rate:

$$\dot{\epsilon} = \frac{\Delta\epsilon}{t} = 4 \Delta\epsilon f \quad (5.1)$$

Rearranging for frequency:

$$f = \frac{\dot{\epsilon}}{4 \Delta\epsilon} \quad (5.2)$$

Where we say $\dot{\epsilon}$ is the maximum strain rate observed in room temperature impact graphs, for glycerine 20 % films, $\dot{\epsilon} = 0.01 \text{ s}^{-1}$. Furthermore, $\Delta\epsilon = 0.0002$ is the applied strain in dynamic testing. Therefore, we can identify peaks in impact behaviour at a certain strain rate and determine what frequency they occur at during an oscillation. These values give a frequency of $f = 12.5 \text{ Hz}$. Meaning that for the glycerine 20 % film, a peak in dynamic behaviour is expected at room temperature at a frequency of 12.5 Hz. If this is the case, this relaxation can be used to explain the peak in impact behaviour observed at that strain rate. For a somewhat back of the envelope calculation, this turns out to be remarkably accurate as for the 10 Hz frequency scan performed according to the above DMTA procedure, a peak is observed at 19.4 °C. This above zero peak, presumed to be the β transition, is observed in unsoftened and softened samples, with an increase

in peak amplitude observed with plasticisation, as show in Figures 5.16. Since changes in this peak are impacted by plasticisation content, we conclude that this must be some secondary side group motion of cellulose chains, impacted by the embedding of softeners between those chains. Urea exhibits the largest change in the room temperature peak with plasticisation, perhaps due to a combination of its alternative hydroxyl forming groups, shape and low molecular weight in comparison to the similarities between glycerine and MPG. This molecular motion has been used to explain a peak in macroscopic impact performance, the goal of this work. However, further work to characterise this β relaxation with frequency and plasticisation dependence would be advantageous to confirming this hypothesis.

Activation Energy of γ peak

Since polymer relaxations are frequency dependent, using Figure 5.24, the temperature shift of peaks at varying frequencies can measured using the theory of Time-Temperature Superposition (TTS) and an activation energy, E_a , can be calculated using Arrhenius equation 5.3.

Time temperature superposition principle is used throughout polymer physics to extend the measurable parameters of behaviour by shifting dependent behaviour. For example, in the case of Figure 5.24, the relaxation behaviour of transitions is frequency dependent. Using the fact that frequency has units s^{-1} , $\ln(f)$ can be plotted against the reciprocal temperature at which each respective peak is observed and the slope is related to the activation energy required for that peak relaxation [123]. The resultant graph from this analysis is seen in Figure 5.25

$$\ln(f) = \frac{E_a}{RT} \quad (5.3)$$

5.4 Dynamic Mechanical Thermal Analysis

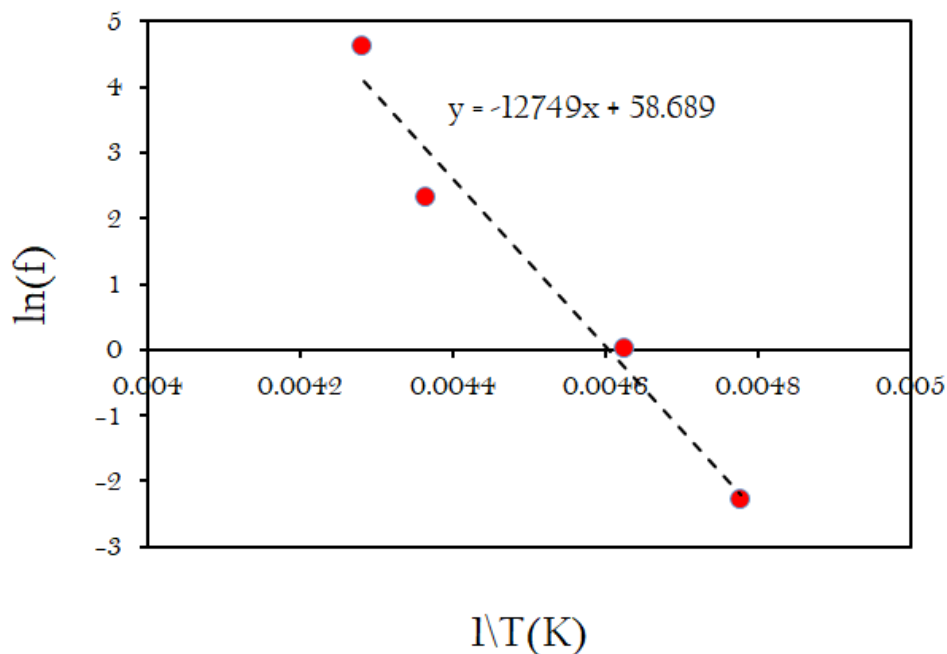


Figure 5.25: Arrhenius Plot of $\ln(f)$ against $1/T$ for glycerine 18 % films from $\tan\delta$ analysed across four frequencies 0.1, 1, 10, 100 Hz. Gradient = 13000 ± 2000

As indicated on Figure 5.25, the gradient of this plot is used to determine an activation energy, $E_a = 106 \pm 16$ kJ/mol for the γ relaxation. However, literature values suggest that this activation energy should be much lower with literature values ranging between 20 - 52 kJ/mol and being assigned to rotation of cellulose glucose ring around a single glycosidic linkage at the lower boundary or to local motion of the methyl and hydroxyl groups of one pyranose unit for the higher boundary [124][125]. We might explain that our higher value of activation energy is due to the shifted nature of our dynamic profile of these plasticised films in comparison with cellulose acetate. In addition, this disparity could be due to the fact that this transition is also governed by the removal of water, which we have shown it to be dependent on. Furthermore, Erdmann et al report an observed increase in this γ relaxation activation energy with plasticiser, explaining another potential origin of this higher value [108]. In future work, more multi-frequency scans could be performed and effect of plasticisation tracked to explain this γ

relaxation. These initial tests to investigate activation energy of films have shown some interesting initial findings, but we recognise more tests can be performed to help reveal the nature of this transition.

Elucidating the γ peak

Finally, this multifrequency scan can be used to explain the behaviour of the assigned γ transition. In Figures 5.19(a-c), the importance of temperature shifting of the γ transition on the mechanical performance of is observed. Where a strong linear relationship is seen between ductility and temperature at which this transition peak occurs. With these multifrequency scans, we also see a shift in temperature to higher temperatures with increasing frequency, demonstrated by Figure 5.26

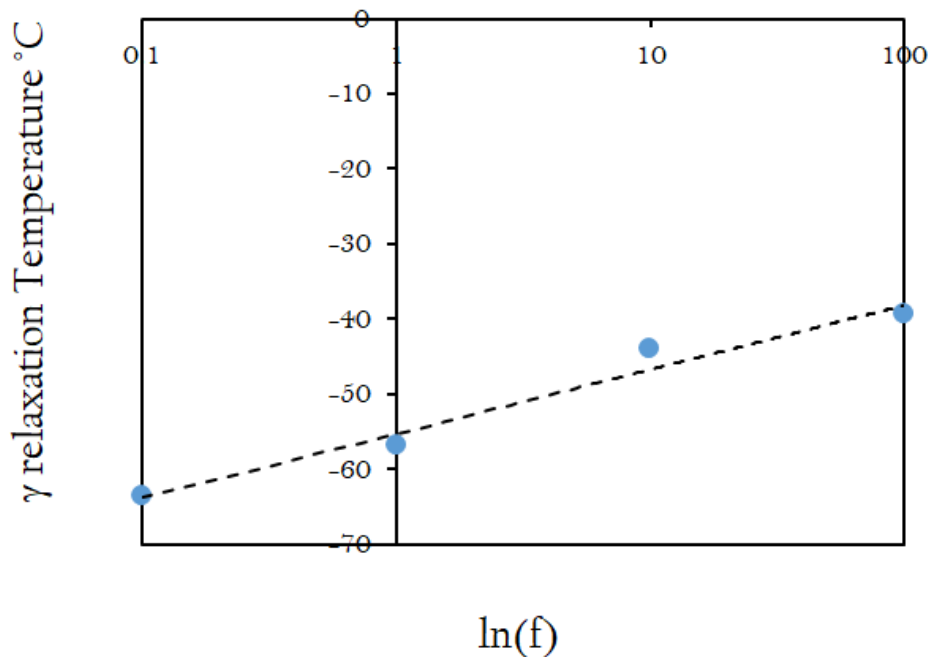


Figure 5.26: *Variation in temperature of γ peak with increasing frequency of temperature ramps*

This figure can help to identify the origin of molecular motion of the γ transition since in these results we see that temperature of that transition increases

5.5 Lab-based plasticiser variation summary

with frequency. Therefore, we suggest that this γ transition can be aligned to the molecular motion of side groups whose speed of molecular motion can be increased by plasticisers. Since this motion is affected by both frequency and plasticisers, further investigations might include the prediction of these two properties.

5.5 Lab-based plasticiser variation summary

In this chapter, with the individualised addition of plasticisers, recommendations have been made for how Futamura can experiment with the alteration of their plasticiser packages. This has been achieved using macroscopic and molecular testing to link the behaviour of films with increasing plasticiser content.

- Firstly, **Tensile Testing** has revealed the individual contributions of softeners and how they contribute in the 3 component softener blend. It has been determined that the softener uptake ability is important as increased softener content will lead to increased ductility. Furthermore, the type of softener is important when determining its uptake and effect on properties; softener size, shape and hydrophilic groups should be considered. Uptake depends on softener molecule structure, in particular the importance of a softeners affinity to water has been shown as extremely important for their ability to embedd between chains and plasticise. For individual softeners, the urea plasticiser has been identified as having the biggest effect on improving ductility with the least detriment to Modulus and strength, followed closely by the glycerine softener due to their similar hydrogen bond affinity and then by MPG with an anti-plasticising effect due to its lower number of hydroxyl groups. The 3 component softener displays the superior plasticising effect compared to individual softener, despite a lesser uptake in films. This reveals the cooperative effective of softeners and their cumulative efficacy.

- **Recommendations:** Futamura’s current 3 component softener package contains *(This text has been removed by the author of this thesis for confidentiality reasons)* [REDACTED]. With the presented rankings of these plasticisers with mechanical properties,

5.5 Lab-based plasticiser variation summary

it is recommended that Futamura investigate adjusting the concentrations of these softeners to incorporate more urea (up to 22 % to avoid migration) and less MPG (perhaps down to 0 % due to its anti-plasticising effect). This decision will depend on responses to current markets for each of these plasticisers and the concentrations will need to be carefully considered in order to optimise this blend.

- **Impact Testing** has revealed a variation in impact behaviour across a range of strain rates. Peak in behaviour is typically observed between 0.001 s^{-1} - 0.01 s^{-1} . Increasing softener content in films results in increased maximum strain, owing to increased ductility, whilst maximum force and energy are decreased with increasing plasticiser content.
 - **Recommendations:** As with tensile testing, MPG displays inferior softening abilities with maximum strain not increasing significantly with plasticisation but with a knock-on effect of reduced force and energy being observed. As such, supporting the case for reconsidering the incorporation of MPG in the 3 component softener blend. Furthermore, a recommendation on the total softener content of films can be made based on impact results. We see that for the maximum amount of softener in films, 29 %, a reduction in impact properties is observed at higher strain rates. In fact, the maximum impact properties are observed in the 18 % softener concentration. Thus we recommend that this concentration not be increased to the detriment of impact properties.
- **Dynamic Mechanical Thermal Analysis** has been able to assign the secondary relaxations: β and γ . In particular we have elucidated the behaviour of the γ relaxation with increased plasticisation and therefore increased water content. This has enabled a link between dynamic and mechanical properties, with a clear impact on secondary transitions quantified with increasing plasticiser content. Furthermore, the effect of water on plasticisation has been demonstrated through a water removal procedure. In addition, multi frequency scans have been performed in order to link

dynamic behaviour with strain rate dependent impact behaviour and to calculate an activation energy of the γ relaxation.

- **Recommendations:** This testing reinforces recommendations drawn from tensile and impact testing of individual and combination softeners. Furthermore, the effect of increasing water content on the plasticisation behaviour of films has been highlighted. As such, it is recommended that Futamura investigate the efficacy of alternate hydrophilic plasticisers. This could open up routes for greener, cheaper softeners and the potential removal of MPG from the softener package.

5.6 Next Steps

With the manufacturing of lab-softened films in this work, the behaviour of 3 component softener commercial films has started to be understood, with suggestions being proposed to Futamura about how the plasticisation of film is taking effect and what changes to the softener package might be experimented with.

Upon completion of this testing, there was a number of interesting directions to explore with various options for how the plasticisation of films could be investigated including changing concentrations of pre-existing softener packages and the inclusion of different hydrophilic softeners in that package. With Futamura's continued focus on sustainability, the choice was made to investigate alternative, plant-based softeners. Literature searches demonstrated the effect of residual hemicelluloses and their resultant plasticising effect. As a result, a hemicellulose blend, supplied by BioSep was incorporated into films using the same procedure as softeners in lab-plasticised films production. It was hoped that the addition of hemicelluloses in these films induces a plasticising effect on the films, with hemicelluloses being highly hydrophilic molecules with potential to act in the same way as traditional plasticisers in these films.

Chapter 6

Hemicellulose variation of lab-based films, Results and Discussion

In this chapter, results and discussions are presented for a series of films, where a hemicellulose hydrolysate blend and a 2 component softener blend containing *(This text has been removed by the author of this thesis for confidentiality reasons)* are added to a swollen cellulose film, or 'wet gel' in a range of concentrations (4 %, 8 % and 15 %). This has been done to further investigate the role of water which was highlighted as an extremely important factor in plasticisation in the previous chapter where traditional hydrophilic plasticisers were shown to bring water into films in order to induce softening. We do this with the aim of investigating 'green' softeners by utilising hemicellulose hydrolysate produced by Bio-Sep Limited; a technology company using ultrasonic processing of woody biomass to extract high-value, renewable biochemicals with a range of applications. Their '*Hemicellulose Hydrolysate*' is a hydrophilic combination of sugars extracted from spruce softwood using an ultrasonic process with mild organic acids. The syrup consists of *(This text has been removed by the author of this thesis for confidentiality reasons)*

Tensile testing, falling weight and slow puncture impact, as well as dynamic mechanical thermal analysis have been performed to assess the contributions of

6.1 Softener Content

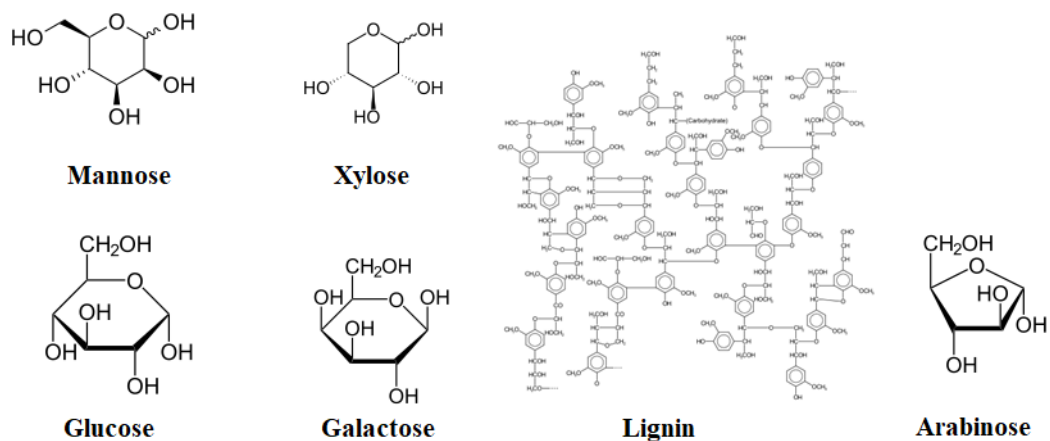


Figure 6.1: *Constituents of hemicellulose hydrolysate, depicted to indicate their hydrophilic nature due to number of hydrogen bond forming sites*

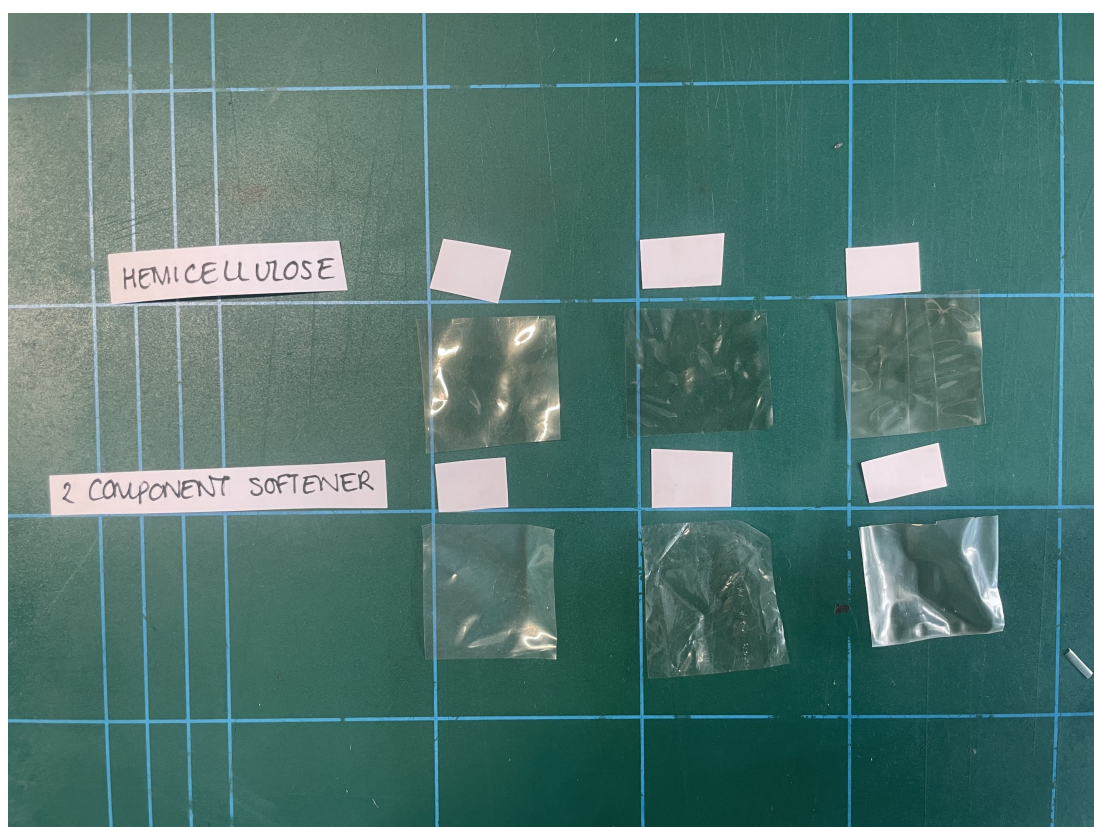


Figure 6.2: *Hemicellulose-incorporated films visual appearances. Migration effects visible as brown hue on films*

6.1 Softener Content

Due to these migration effects, it was clear that uptake of the hemicelluloses and 2 component softener was not uniform. As such, the wt % of hemicelluloses and the blend in films was calculated using the method outlines in Section 3.1, results of which are shown in Table 6.1

Table 6.1: *Table of lab-made films and their hemicellulose or 2 component softener (This text has been removed by the author of this thesis for confidentiality reasons)*

Plasticised Film	Softener in Film (wt %)
Hemicellulose 4 %	11.3 ± 0.3
Hemicellulose 8 %	18 ± 2
Hemicellulose 15 %	28 ± 2
2CS 4 %	8.4 ± 0.6
2CS 8 %	13.6 ± 0.2
2CS 15 %	31.9 ± 0.1

To quantify the uptake of these films, Figure 6.3 has been created to compare the hemicellulose in bath and hemicellulose in film percentages, along with the enrichment factors (ratio of plasticiser content in film to plasticiser content in bath) of each film concentration, indicated in data labels.

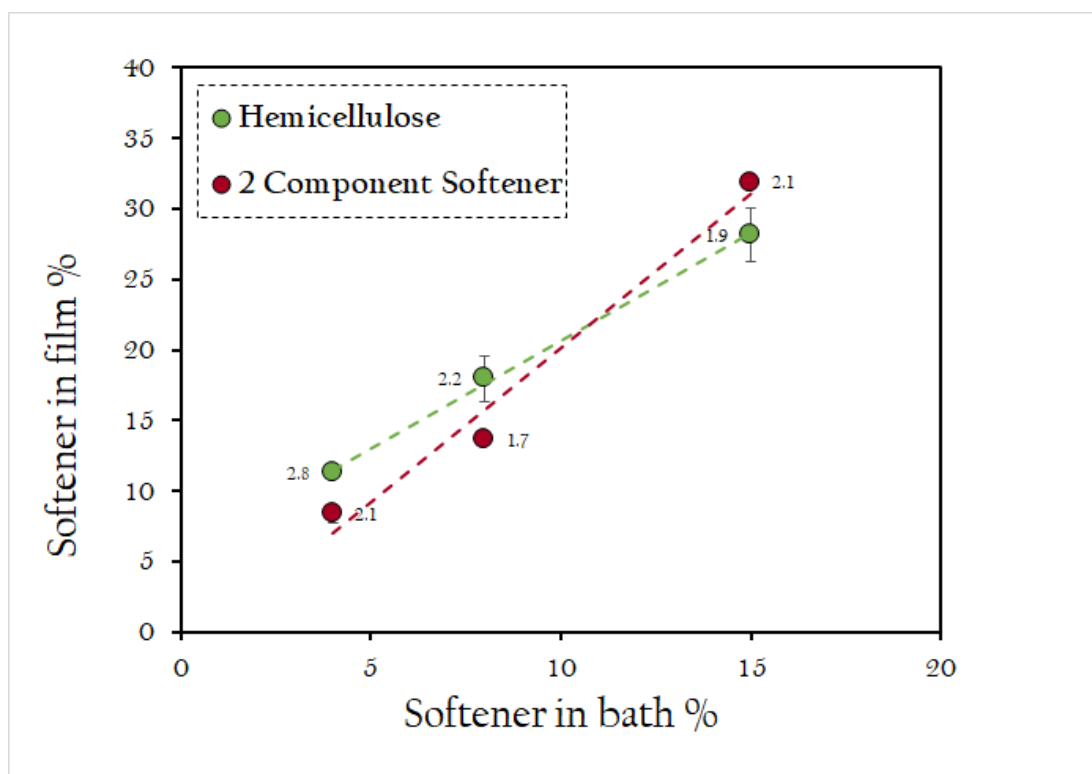


Figure 6.3: *Softener in film and softener in bath wt % comparison for hemicellulose-based films with enrichment factors indicated as data labels*

Figure 6.3 shows that for the hemicellulose films, softener in film content ranges from 11 % - 28 %, with enrichment factor decreasing from 2.8 - 1.9. For the 2 component softener, softener in film content ranges from 8 % - 32 % with enrichment factor decreasing from 2.1 to 1.7 and then increasing to 2.1. This variation in enrichment factor and uptake of hemicelluloses and glycerine into films reveals that there must be some changing competitive bonding and displacements occurring between polymer chains, hemicelluloses, glycerine and water. With macroscopic and molecular analysis of this set of films, we hope to uncover the behaviour of each of these components within films to explain this observation. Furthermore, the uptake of the 2 component softener and hemicellulose films was compared with the lab-softened glycerine film set to determine whether the hemicelluloses interfere with glycerine uptake, indicated in Figure 6.4.

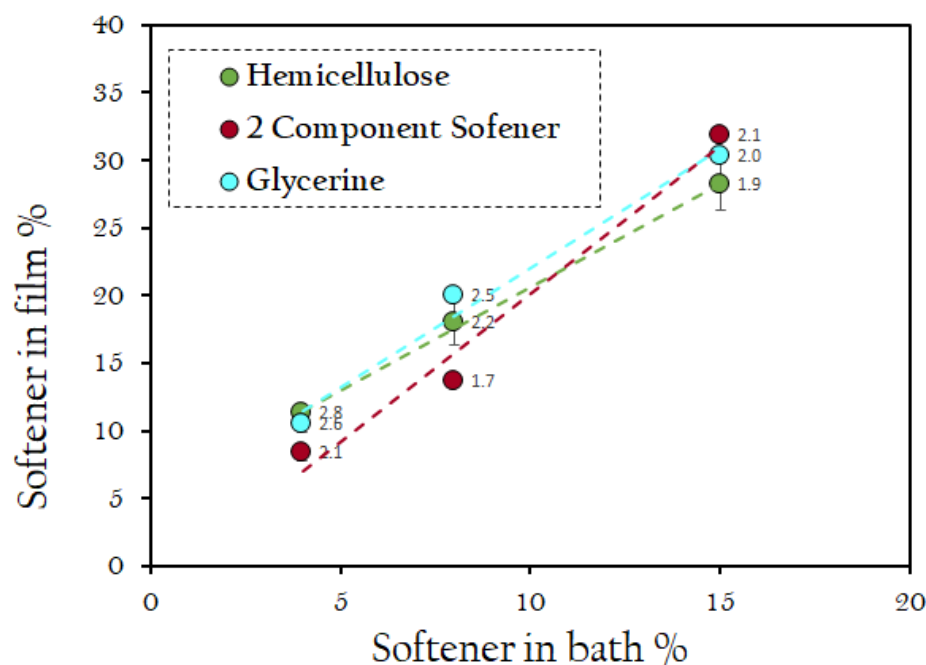


Figure 6.4: *Softener in film and softener in bath wt % comparison for hemicellulose-based films and lab softened glycerine film with enrichment factors indicated as data labels*

This figure demonstrates that the hemicelluloses do not seem to inhibit softener uptake in the 2 component softened film as its uptake is similar, potentially higher, than that of glycerine. This supports the conclusion that hemicellulose are unable to embed between polymer chains, allowing the glycerine component of the 2 component softener full dominion over the polymer.

6.2 Tensile Properties

Similarly to both commercial and lab-softened films, hemicellulose-based samples were laser cut in to 10 dumbbells, 5 in the machine direction and 5 in the transverse direction; each of which were subject to tensile testing at a constant rate of 10 mm/min up to failure. These results were used to produce stress/strain graphs from which Young's Modulus, Strength and Strain at failure could be determined

6.2 Tensile Properties

and averaged for each sample, the results of which can be seen in Table 6.2.

Table 6.2: *Tensile Test results of lab-hemicellulose films in machine and transverse directions for Young's Modulus, Strength and Strain at Failure*

	Modulus (GPa)	Strength (MPa)	Failure (%)
	Transverse Direction		
Hemicellulose 11 %	8.6 ± 0.3	108 ± 1	1.46 ± 0.07
Hemicellulose 18 %	6.7 ± 0.4	74 ± 6	1.2 ± 0.1
Hemicellulose 28 %	9.4 ± 0.8	78 ± 7	0.90 ± 0.09
2 Component Softener 8 %	4.5 ± 0.2	68 ± 3	1.7 ± 0.1
2 Component Softener 14 %	2.5 ± 0.2	53.6 ± 0.2	2.27 ± 0.06
2 Component Softener 32 %	2.7 ± 0.3	40.7 ± 0.6	3.9 ± 0.2
	Machine Direction		
Hemicellulose 11 %	11.3 ± 0.8	120 ± 11	1.23 ± 0.07
Hemicellulose 18 %	8.5 ± 0.6	98 ± 8	1.26 ± 0.04
Hemicellulose 28 %	10.0 ± 0.6	105 ± 7	1.3 ± 0.1
2 Component Softener 8 %	7.6 ± 0.3	82 ± 5	1.7 ± 0.2
2 Component Softener 14 %	3.0 ± 0.3	56 ± 6	2.0 ± 0.2
2 Component Softener 32 %	4.1 ± 0.2	53 ± 1	5.1 ± 0.2

6.2 Tensile Properties

This data is presented in Figures 6.5(a-c) that show Ashby Plots of this hemicellulose film set.

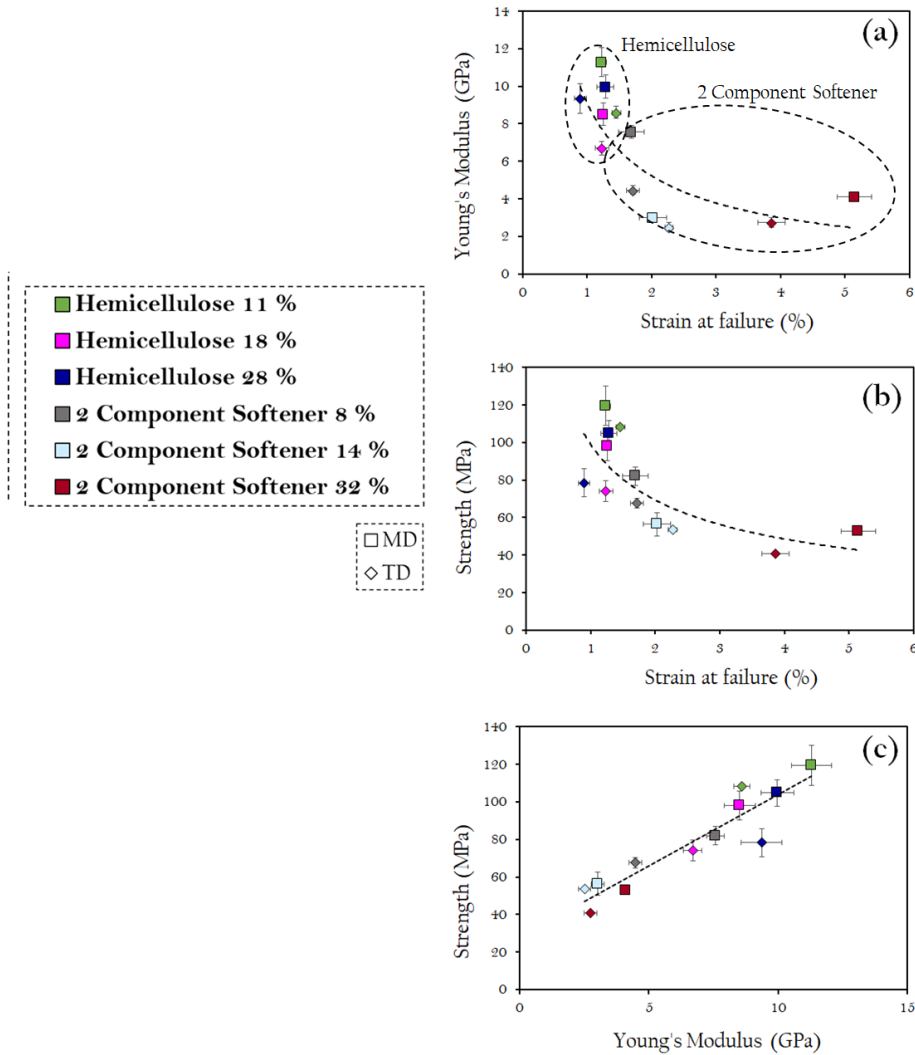


Figure 6.5: *Ashby Plots depicting the variation of tensile properties for the hemicellulose-based film set in their machine (square markers) and transverse (diamond markers) directions (a) Young's Modulus against strain at failure, (b) Strength against strain at failure and (c) Strength against Young's Modulus*

6.2.1 Material property relationships

Similarly to other sets of films, the first important observation is the relationships between the three tensile properties: Modulus, strength and strain at failure. Figures 6.5(a-c) show that the same compromise between properties is observed as in the lab-plasticised films and commercial films. Strength and Young's Modulus are proportional, whilst an increase in strain to failure, associated with increasing plasticisation, results in a reduction of these properties.

6.2.2 Machine and transverse uniaxiality

Furthermore, as with the lab-plasticised and commercial films, a variation between machine and transverse properties is observed for this hemicellulose film set. For comparison, the average ratio between the machine and transverse values in commercial films of Young's Modulus, strength and strain to failure are 2.1 ± 0.1 , 2.1 ± 0.1 and 2.0 ± 0.1 , respectively. Whilst for lab-plasticised films, average ratios are 1.3 ± 0.1 , 1.7 ± 0.1 and 1.5 ± 0.2 , respectively. For this set of hemicellulose films Young's Modulus is $1.3 \pm 0.1 \times$ greater in the machine direction, strength is $1.3 \pm 0.05 \times$ greater in the machine direction and strain at failure is $1.1 \pm 0.1 \times$ greater in the transverse direction.

The similarity of these ratios with lab-plasticised films supports the hypothesis drawn in the previous chapter to explain the reduced ratios of machine and transverse properties due to the orientation of cellulose polymer chains. We propose that uniaxiality is imparted to the films during extrusion and rolling under tension during commercial processing. Since these films are only subject to extrusion before they are softened, the lack of rolling as well as shrinking on to frames during drying can be identified as the reason for the reduced alignment of chains the machine direction.

6.2.3 Variation of hemicelluloses

Hemicellulose-based films were produced in order to investigate the plasticising effect of a potential novel softener blend in order to determine their possible inclusion in Futamura's products. As such, Figures 6.6(a-c)-6.7(a-c) have been

6.2 Tensile Properties

produced to indicate the variation of Young's Modulus, strength and strain at failure with increasing hemicellulose and 2 component softener content of films.

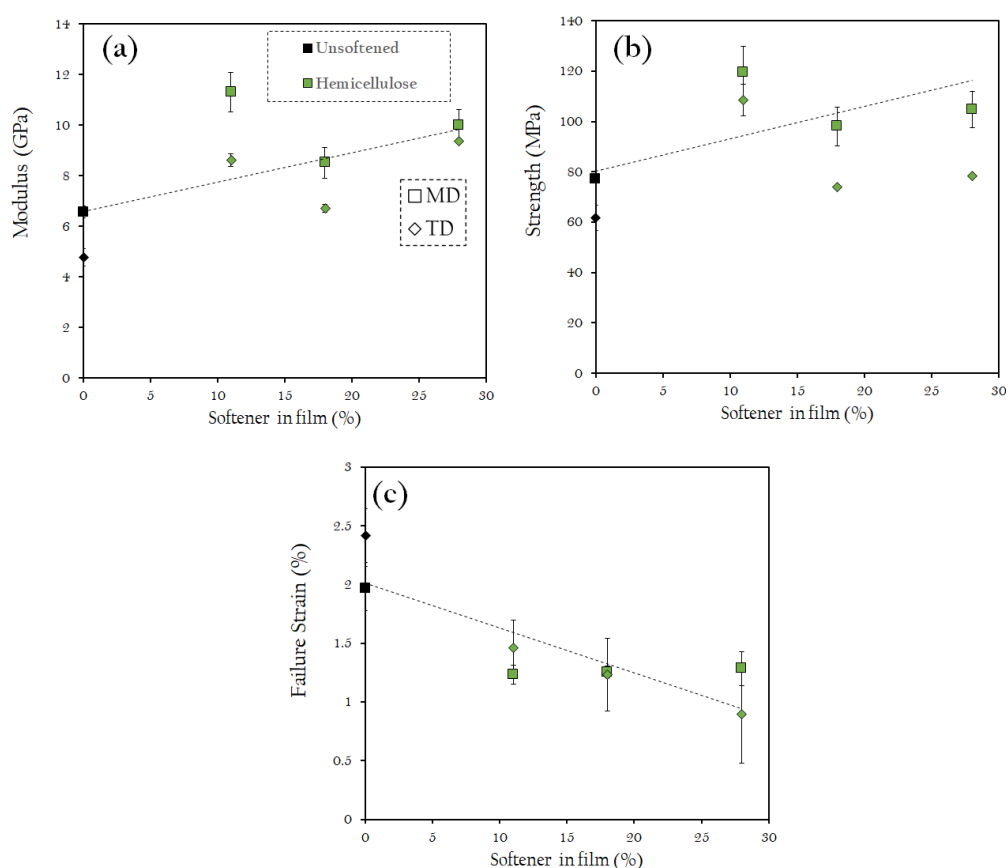


Figure 6.6: Variation of tensile properties with increasing hemicellulose content (a) Young's Modulus (b) Strength and (c) Strain at failure

Figures 6.6(a-c) show a distinct relationship between increasing hemicellulose content and modulus, strength and strain at failure. However, instead of the desired softening effect, these hemicelluloses have induced an anti-plasticising effect with Young's Modulus and strength increasing and strain at failure decreasing with sugar content. For example, hemicellulose films exhibit a maximum in both Young's Modulus and strength at the lowest concentration, 11 %, of 11.3 ± 0.8 GPa and 120 ± 11 MPa, respectively. This initial increase in properties is followed by a decrease and subsequent plateau with increasing hemicellulose content

6.2 Tensile Properties

with values of Young's Modulus and strength at maximum, 28 %, content being 10.0 ± 0.6 GPa and 105 ± 0.7 MPa, respectively. Furthermore, strain at failure for hemicellulose films experience an initial drop to 1.23 ± 0.07 % and subsequently plateau, with 28 % hemicellulose content strain at failure being 1.3 ± 0.1 %. This indicates that maximum absorption of hemicellulose is reached at the 10 % concentration and that the increased hemicellulose addition only leads to more depositing as a coating on the surface of the films, rather than embedding between polymers. This is supported by the increasing darkness of higher concentration films seen in Figure 6.2. This result could be due to the fact that hemicellulose molecules are larger than that of low molecular weight traditional plasticisers and therefore less able to embed themselves between polymer chains. Furthermore, this could be due to different preferential interactions occurring within the films. It could be that due to hemicellulose's multiple hydrogen bond acceptors, water preferentially bonds with these sugars rather than polymer chains, removing water content from internal polymer structure since the hemicelluloses that they are bonded to are too large to embed between polymer chains. This would explain their inferior mechanical performance in comparison to the unsoftened film since any residual water content in films is removed by bonding with the hemicelluloses. In essence, the hemicellulose monosaccharides are described as 'too' large and hydrophilic and therefore detrimental to performance.

6.2 Tensile Properties

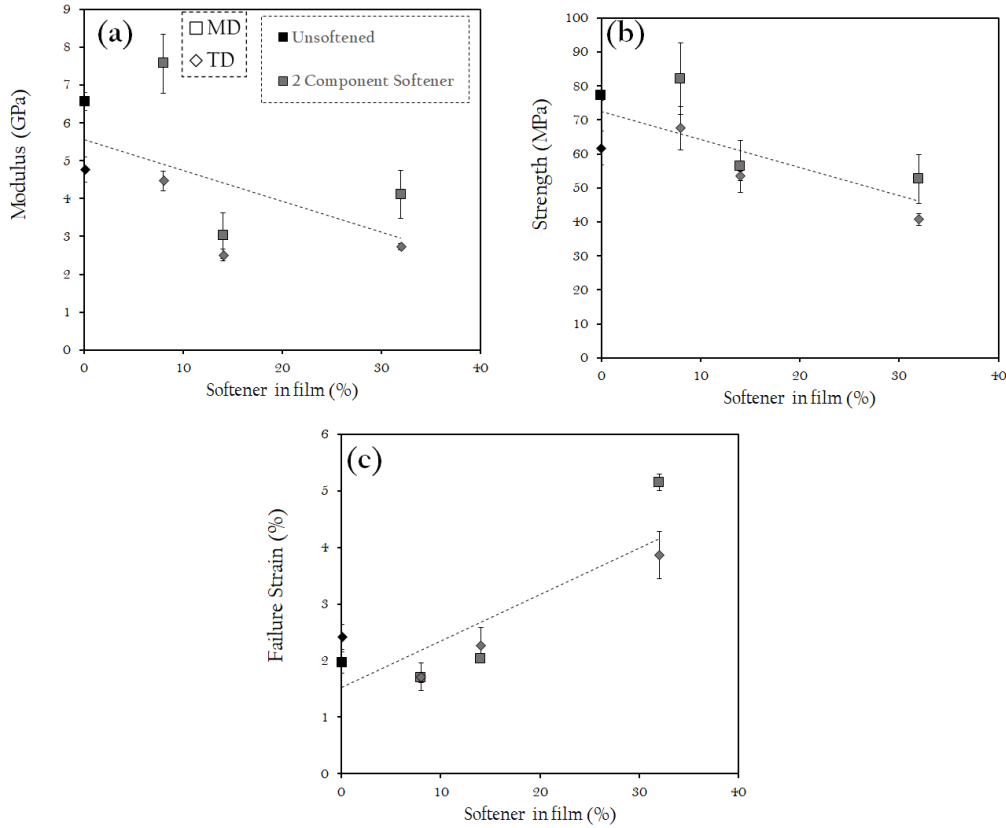


Figure 6.7: Variation of tensile properties with increasing 2 component softener content (a) Young's Modulus (b) Strength and (c) Strain at failure

Figures 6.7(a-c) show a complex relationship between increasing 2 component softener content and modulus, strength and strain at failure. With addition of this proposed plasticiser blend, an initial anti-plasticising effect followed by a plasticising effect is observed. For example; for minimum, 8 %, content, Young's Modulus and strength increase and strain at failure decreases compared to unsoftened films to 7.6 ± 0.3 GPa , 82 ± 5 MPa and 1.7 ± 0.2 % in the machine direction, respectively. In contrast, at higher concentrations of 2 component softener, a plasticising effect is seen, with Young's modulus and strength decreasing and strain at failure increasing to 4.2 ± 0.2 GPa, 53 ± 1 MPa and 5.1 ± 0.2 % in the machine direction, respectively. This effect can be attributed to the ongoing competition of hydrogen bonding between polymer chains, glycerine, hemicellu-

lose and water with varying concentrations. In the hemicellulose only film, we hypothesised that the water in cellulose wet gel preferentially bonds with the hemicelluloses and since they are too large to embed between chains, an anti-plasticising effect is seen due to the removal of water as a plasticiser. This effect is seen at low concentrations for this 2 component softener as demonstrated by the anti-plasticisation at 8 % content. However at higher concentrations, the increased percentage of glycerine included in the 2 component softener is able to penetrate the cellulose polymer chains and bring in water from the softener bath whilst hemicelluloses are displaced from the films due to their size. This gives rise to a softening effect despite the inclusion of hemicelluloses.

Figures 6.6(a-c)-6.7(a-c) show the relationship between increasing hemicellulose and 2 component softener content with modulus, strength and strain at failure to give an overall picture of the attempted incorporation of these potential plasticisers. On the contrary, we demonstrate that these monosaccharides actually have an anti-plasticising effect. We hypothesise that this anti-plasticising effect is due to the inability of hemicelluloses to embed between polymers since they are larger than traditional plasticisers. Furthermore, due to their extremely hydrophilic nature, water in films preferentially bonds with hemicelluloses rather than between polymer chains, thus resulting in a reduced water content of final films are therefore reduced ductility. As such, the recommendation for Futamura to consider hydrophilic softeners should be amended to: Softeners with similar hydrophilicity as glycerine and urea as well as small enough molecular weight to embed between cellulose chains.

6.2.4 Comparison to commercial and lab-plasticised films

In order to analyse the correlations of tensile behaviour between commercial, lab-plasticised and hemicellulose-based films we can compare the 3 component softener (*This text has been removed by the author of this thesis for confidentiality reasons*) [REDACTED] commercial film, the 18 % 3 component softener lab-plasticised film and the 14 % 2 component softener (*This text has been removed by the author of this thesis for confidentiality reasons*)

6.2 Tensile Properties

████████████████████ films. Figures 6.8(a-c) have been produced to demonstrate the comparison between these film's tensile behaviour.

6.2 Tensile Properties

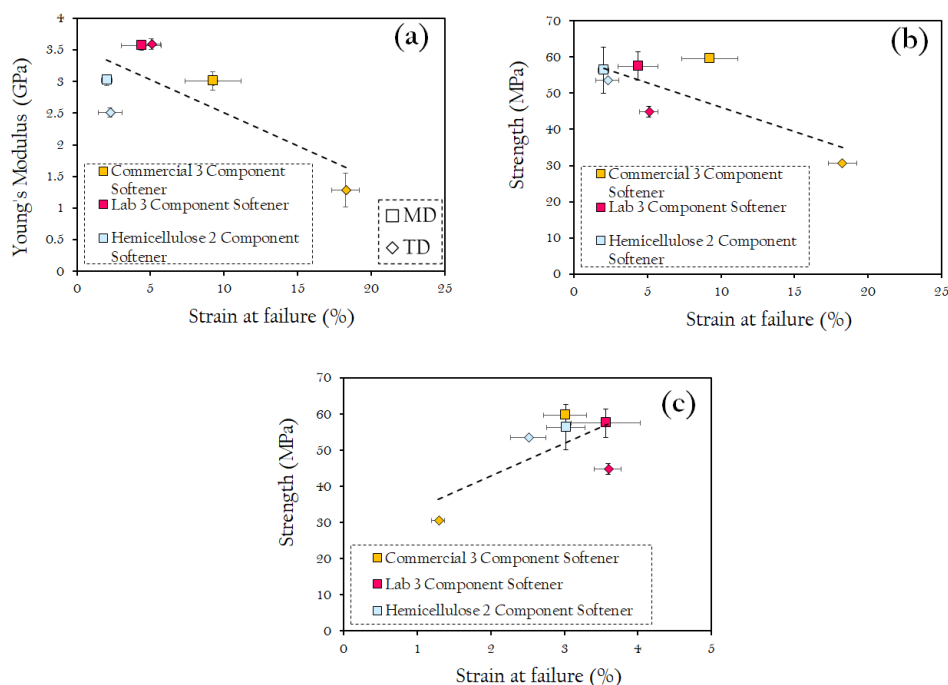


Figure 6.8: *Ashby Plots depicting the variation of tensile properties for the commercial, lab-plasticised and hemicellulose based films that contain (This text has been removed by the author of this thesis for confidentiality reasons) ██████████ in their machine (square markers) and transverse (diamond markers) directions (a) Young's Modulus against strain at failure, (b) Strength against strain at failure and (c) Strength against Young's Modulus*

Figures 6.8(a-c) demonstrate the performance and variation between these three comparable films that all contain (This text has been removed by the author of this thesis for confidentiality reasons) ██████████. In the lab-plasticised and hemicellulose based films, there is a much smaller difference between machine and transverse properties, arising from the difference in production process from the commercial films in that they are not rolled under tension during softening but are shrunk onto frames, inducing less orientation. Furthermore, the values of ductility are higher in the commercial film owing to this increased orientation of cellulose chains. On the other hand, the Young's modulus and strength don't see much variation across the 3 films machine directions, showing that orientation is essential for increasing ductility since Young's modulus and strength can be increased by other means.

6.3 Falling weight and slow puncture impact properties

The results of slow puncture and impact tests for hemicellulose-based films performed at speeds (1 mm/min- 1000 mm/min) and converted to strain rates are shown in Figures 6.9(a-c) - 6.10(a-c) representing maximum strain, normalised maximum force and normalised energy. Unfortunately, due to the poor mechanical performance of these anti-plasticised films, there was not a sufficient number of test-able films to perform tests at high impact speeds of 120000 mm/min, thus this speed was omitted from this data set. Nonetheless, the variation of impact behaviour was measured at slower puncture speeds. To produce these results, five repeats were performed for each sample at each speed, from which the average was calculated and error determined and plotted. This set of films exhibited the same starburst crack formation as commercial and lab-plasticised films.

6.3.1 Variation of hemicelluloses

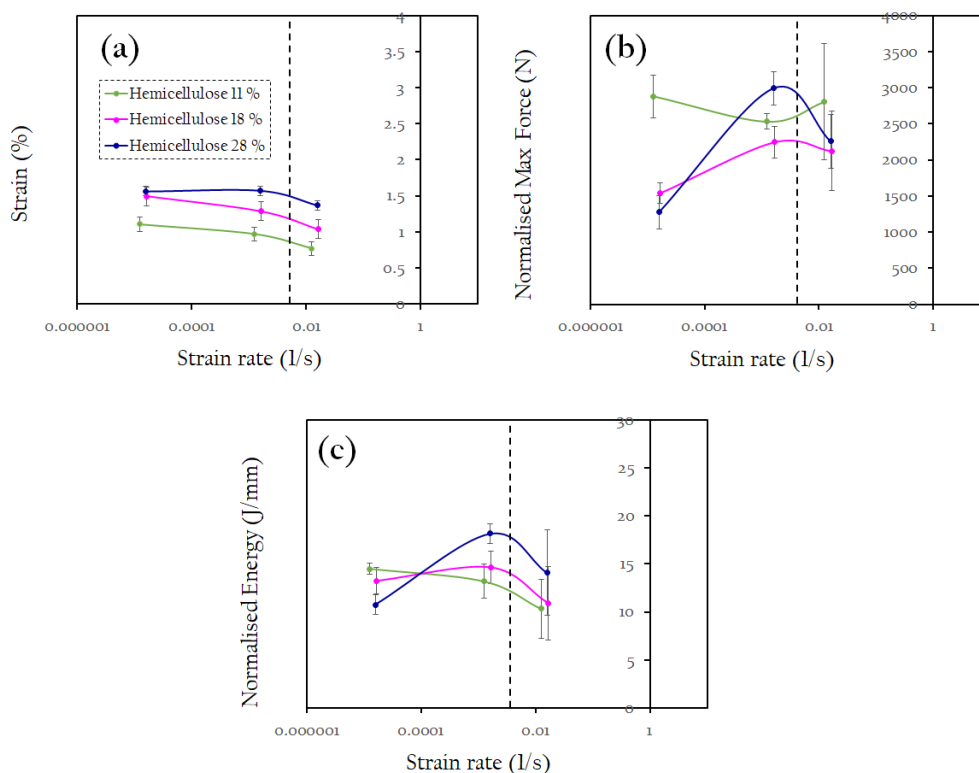


Figure 6.9: *Falling weight and slow puncture impact properties across a range of strain rates for hemicellulose lab-based film set where the black dotted line indicates the strain rate at which tensile testing was performed (a) Strain against strain rate, (b) Normalised Maximum Force against strain rate, (c) Normalised energy against strain rate*

Figure 6.9(a-c) show the variation of impact properties for hemicellulose-based films for a range of strain rates. For maximum strain behaviour, each of the sugar films exhibits a maximum at lower strain rates around 0.00001 s^{-1} with strain decreasing up to 0.01 s^{-1} . The strain at the maximum hemicellulose content at 28 % shows the highest values. For example at the 0.00001 s^{-1} strain rate, 11 % and 18 % hemicellulose content films show strains of $1.11 \pm 0.02 \%$ and $1.49 \pm 0.04 \%$, respectively whilst at 28 % hemicellulose content, the strain at this strain rate is $1.56 \pm 0.08 \%$. At higher strain rates the difference between films concentrations becomes clearer; at 0.01 s^{-1} the strain rate of 11 % films is 0.77

6.3 Falling weight and slow puncture impact properties

± 0.04 % whilst for the 28 % films strain is 1.57 ± 0.01 %, showing a greater variation of performance due to hemicellulose content. This increased strain in higher concentrations in films is in contrast to the results of tensile testing that reveal a decrease in ductility with concentration. Again this highlights the contest between the preference of superior impact or tensile behaviour.

Furthermore, the maximum force and energy of these hemicellulose films is quite complex. For maximum force, the order of films ranking changes for each strain rate. At the middle strain rate 0.001 s^{-1} , 11 % hemicellulose content film exhibits a dip in properties whilst 18 % and 28 % films exhibit a peak in force. For the 11 % film, this is a drop from $2900 \pm 300 \text{ N/mm}$ to $2500 \pm 100 \text{ N/mm}$. Where as for the 18 % film an increase from $1500 \pm 100 \text{ N/mm}$ to $2200 \pm 200 \text{ N/mm}$ and for the 28 % a significant increase from $1300 \pm 200 \text{ N/mm}$ to $3000 \pm 200 \text{ N/mm}$. Similarly, energy behaviour exhibits a clear peak at 0.001 s^{-1} and a variation between impact behaviour at different strain rates and re-ordering of films superiority. For example between 0.00001 s^{-1} and 0.01 s^{-1} the 11 % film exhibits a drop in energy from $14.5 \pm 0.6 \text{ J/mm}$ to $10 \pm 3 \text{ J/mm}$ whilst the 28 % film exhibits an peak and subsequent decrease in values from $11 \pm 1 \text{ J/mm}$ to $18 \pm 1 \text{ J/mm}$ and down to $14 \pm 4 \text{ J/mm}$. This energy behaviour mirrors the force behaviour, again showing that energy is more force dependent than strain dependent.

6.3 Falling weight and slow puncture impact properties

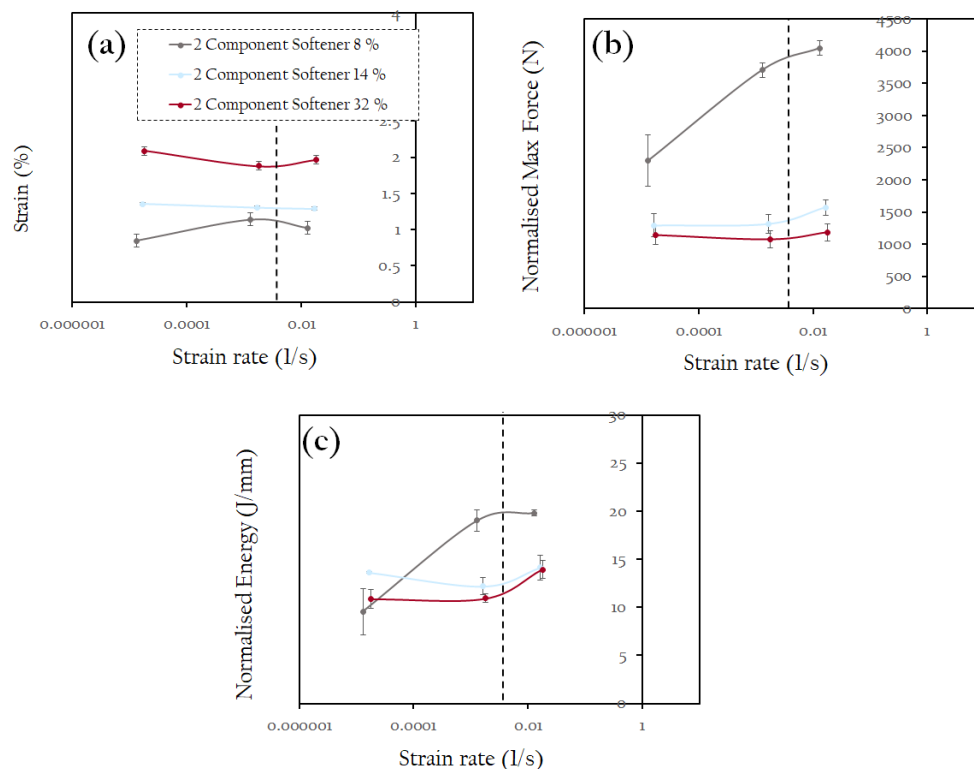


Figure 6.10: *Falling weight and slow puncture impact properties across a range of strain rates for 2 component softener lab film set where the black dotted line indicates the strain rate at which tensile testing was performed (a) Strain against strain rate, (b) Normalised Maximum Force against strain rate, (c) Normalised energy against strain rate*

For tensile behaviour of the 2 component softener films, we observed an initial anti-plasticising effect, followed by a plasticising effect with increasing plasticisation; revealing some cooperative action of glycerine and hemicelluloses. In impact behaviour shown in Figures 6.10(a-c), a similarly complex performance is revealed. For maximum strain with increasing plasticisation across the 3 tested strain rates, values are fairly constant. The lowest 2 component softener content, 8 % exhibits a small peak at 0.001 s^{-1} of $1.14 \pm 0.02 \%$. On the other hand, the maximally softened film, 32 %, exhibits the highest maximum strain overall, supporting tensile results that give evidence for the effect of glycerine component inducing ductility despite the effect of hemicelluloses. At 0.00001 s^{-1} a strain of

6.3 Falling weight and slow puncture impact properties

2.09 ± 0.06 % is observed whilst at 0.001 s^{-1} , a decrease is observed at the same strain rate the the 8 % experiences a peak of 1.88 ± 0.01 %.

Maximum force and energy exhibit similar behaviours across strain rates. The minimum content, 8 %, 2 component softened film exhibits the highest values with an observed peak at the highest strain rate of 0.01 s^{-1} , with values of force and energy of $4000 \pm 100 \text{ N/mm}$ and $19.8 \pm 0.3 \text{ J/mm}$, respectively. On the other hand, the higher softener content films, 14 % and 32 %, which in tensile tests exhibit a softening effect, demonstrate significantly lower values of force and energy across strain rates. For example the maximum value of the 32 % films for force and energy is $1200 \pm 100 \text{ N/mm}$ and $14 \pm 1 \text{ J/mm}$. This drastic drop supports the initial anti-plasticising effect, followed by a plasticising effect due to the contributions of glycerine between polymer chains counteracting and displacing hemicellulose effects.

6.3.2 Comparison to commercial and lab-plasticised films

In order to analyse the correlations between impact behaviour of commercial, lab-plasticised and hemicellulose-based films we can compare the 3 component softener (*This text has been removed by the author of this thesis for confidentiality reasons*) [REDACTED] commercial film, the 18 % 3 component softener lab-plasticised film and the 14 % 2 component softener (*This text has been removed by the author of this thesis for confidentiality reasons*) [REDACTED] films. Figures 6.11(a-c) have been produced to demonstrate the comparison between these film's tensile behaviour.

6.3 Falling weight and slow puncture impact properties

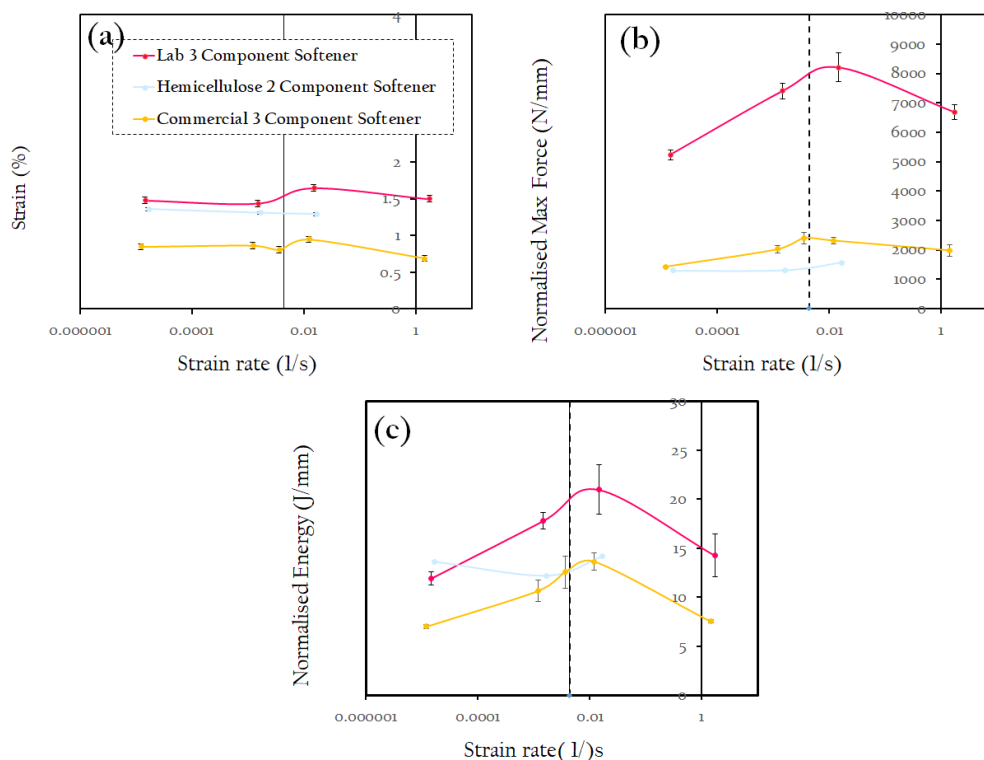


Figure 6.11: *Falling weight and slow puncture impact properties across a range of strain rates for the commercial, lab-plasticised and hemicellulose films that contain (This text has been removed by the author of this thesis for confidentiality reasons) ██████████, where the black dotted line indicates the strain rate at which tensile testing was performed (a) Strain against strain rate, (b) Normalised Maximum Force against strain rate, (c) Normalised energy against strain rate*

Unlike the results and comparisons between commercial, lab-softened and hemicellulose based films in tensile testing, the lab made films exhibit superior strain and energy in comparison to their commercial and hemicellulose counterparts. This is likely due to the difference in production process that results in increased alignment of cellulose chain in commercial films and therefore increased variation of properties in their machine and transverse directions, as discussed in the previous section. The hemicellulose-based film has very similar behaviour to the commercial film, despite having the supposed advantage of less orientation due to the same production method being utilised as in the lab-softened films. This suggests that any advantage of this lab production method is counteracted

by the anti-plasticising effect that the hemicelluloses have on the 2 component softener.

6.4 Dynamic Mechanical Thermal Analysis

Dynamic Mechanical Thermal Analysis was performed between $-100\text{ }^{\circ}\text{C}$ to $+120\text{ }^{\circ}\text{C}$ at a frequency of 1 Hz for each of the hemicellulose-based films. In accordance with lab-plasticised films from the previous chapter, this temperature range was chosen in order to investigate the variation of the γ peak that is associated with changes in plasticisation as well as water content and to avoid degradation of the cellulose chain that onsets at $\approx 200\text{ }^{\circ}\text{C}$. Figures 6.12(a-b) have been produced to demonstrate the variation of $\tan\delta$ transition behaviour for each of the hemicellulose-based films across this temperature range.

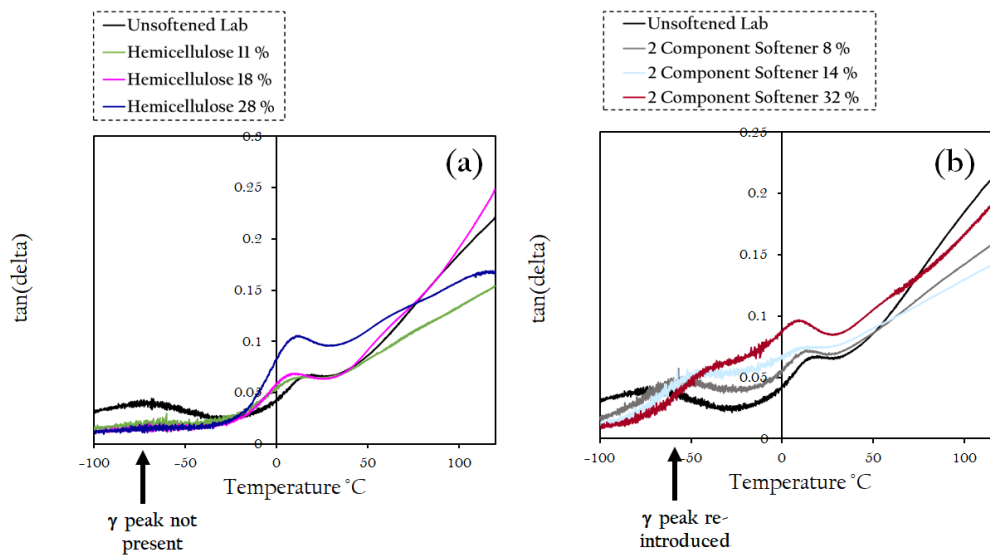


Figure 6.12: *Dynamic Mechanical Thermal Analysis, $\tan \delta$ profiles, of hemicellulose-based film set from $-100\text{ }^{\circ}\text{C}$ to $120\text{ }^{\circ}\text{C}$ at oscillating frequency of 1 Hz (a) Hemicellulose films (b) 2 Component Softener films, each compared to the lab-based unsoftened film. Position of expected γ transition annotated on graphs.*

These figures represent the changes to $\tan\delta$ across the chosen temperature range. Annotated on the figures is the observation that for 100 % hemicellulose-based films, the γ peak appears to have disappeared; whilst for the 2 component softener, the γ peak is reintroduced due to the addition of glycerine. For hemicellulose-based films, the disappearance of the γ peak has been analysed and the cause hypothesised. Furthermore, the reintroduction of the γ peak in the 2 component softened films as a result of glycerine incorporation has been analysed. In addition, the presence of a room temperature peak, presumed to be the β relaxation is observed, even with the hemicellulose-based films that exhibit no γ transition. As shown in previous chapter results and Figure 6.12(a-b), this room temperature peak is effected by increasing plasticisation content. It appears that amplitude of this peak increases with concentration whilst temperature of this transition doesn't experience shifting as a result of plasticisation. Future work to identify the cause of this peak transition would help characterise the effect of plasticisation. On the other hand, the γ relaxation has been attributed to the contribution of water on these systems which can be altered by the inclusion of certain plasticisers. Graphs detailing the trends of this presumed β transition with plasticisation and tensile properties are included in the Appendix A.4 A.5 A.6.

6.4.1 Variation of hemicelluloses on γ transition

For Figures 6.12(a-b), the amplitude and temperature shift of the $\tan\delta$ γ relaxation is an important indication of the performance of hemicelluloses and plasticisers and their ability to incorporate water within films, as shown in the previous chapter.

Figure 6.12(a) shows a drastic difference between the γ relaxation between unsoftened and hemicellulose films. In fact, for the hemicellulose films, the expected γ relaxation is not present, only the room temperature peak. Since the role of water in films and the effect of moisture content on the γ relaxation was highlighted in the previous chapter, we can make conclusions about the bonding occurring between polymers, water and hemicelluloses based off this lack of γ relaxation. The room temperature peaks are left for future investigations and

6.4 Dynamic Mechanical Thermal Analysis

graphs of room temperature peak and plasticiser content are included in the Appendix A.4, although it is hypothesised that this peak is resultant of a polymer chain movement that exists with and without the inclusion of plasticisers but is still affected by their presence. We propose that the lack of γ peak for hemicellulose-based films reveals a very low water content. We suggest that this is due to preferential bonding between hydrogen groups that is unfavourable in terms of performance. Since hemicelluloses are extremely hydrophilic, they remove free and bound water from films via hydrogen bonding but as they are too large to embed between cellulose polymers, are deposited instead on the surface as a coating. Then, upon drying, this water is removed, leaving a film that has been anti-plasticised due to the removal of all water that would usually be free and bound between polymer chains, acting as a plasticiser. This reduced water content observed in DMTA results is in support of conclusions made about the tensile performance of films.

On the other hand, with the incorporation of glycerine with hemicelluloses into the 2 component softener, the reintroduction of water into films is immediately evident. As the softener:hemicellulose blend content increases, as does amplitude of the γ relaxation and temperature position. These changes are demonstrated by Figures 6.13(a-b) to compare amplitude and temperature of the γ transition with increasing plasticiser content.

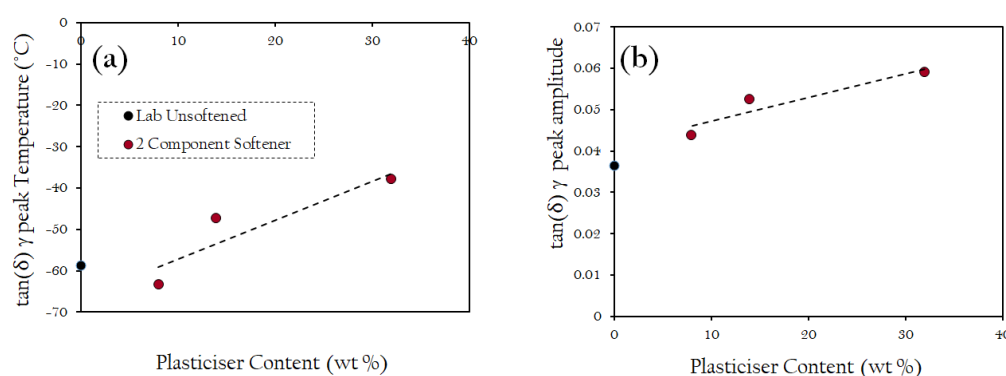


Figure 6.13: Variation of γ peak with 2 component softener content (a) temperature of γ transition (b) amplitude of γ transition

As shown by Figures 6.13(a-b), the 2 component softener content impacts

amplitude and temperature at which the γ relaxation occurs, with both demonstrating a linear relationship. For the values with the lowest, 8 %, 2 component softener content γ transition temperature and amplitude are both below the line of best fit, with values of -64 ± 1 °C and 0.044 ± 0.005 , respectively. This is indicative of a reduced plasticising effect and resultant anti-plasticising, as evidenced by the tensile results of this section. On the other hand, at the maximum 2 component softener content, 32 %, the $\tan\delta$ temperature and amplitude increase to -38 ± 2 and 0.059 ± 0.003 , respectively. This linear relationship again highlights the importance of plasticisation on the γ relaxation of cellulose, hypothesised to be a result of the plasticiser's, in this case glycerine's, ability to maintain water content of films.

6.4.2 Comparison to tensile properties

Furthermore, in order to align mechanical and microscopic properties, the characteristics of the γ peaks have been compared to tensile properties, shown in Figures 6.14(a-c) - 6.15(a-c).

6.4 Dynamic Mechanical Thermal Analysis

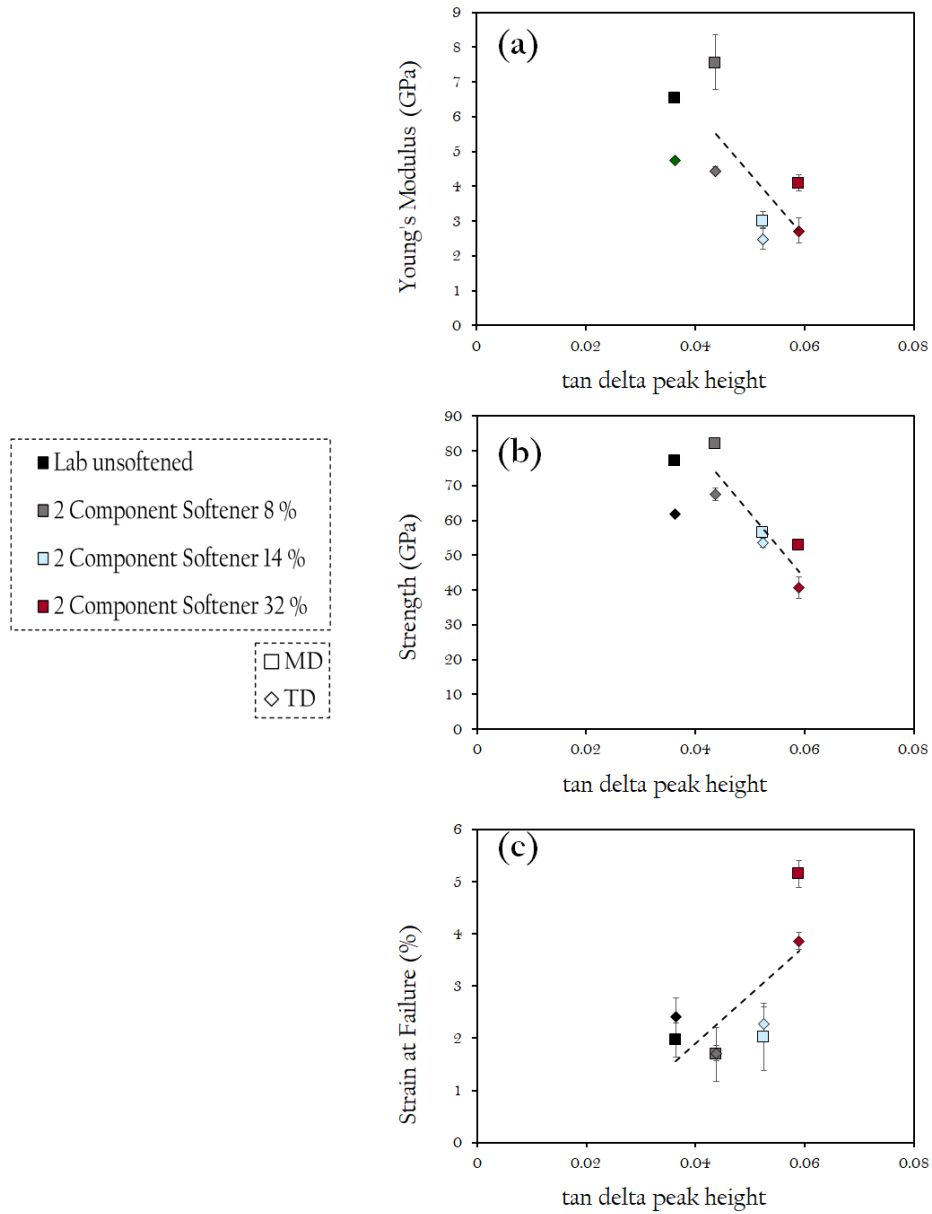


Figure 6.14: Variation of γ transition $\tan \delta$ peak amplitude with tensile properties for 2 component softener films (a) Young's Modulus (b) Strength and (c) Strain at Failure

6.4 Dynamic Mechanical Thermal Analysis

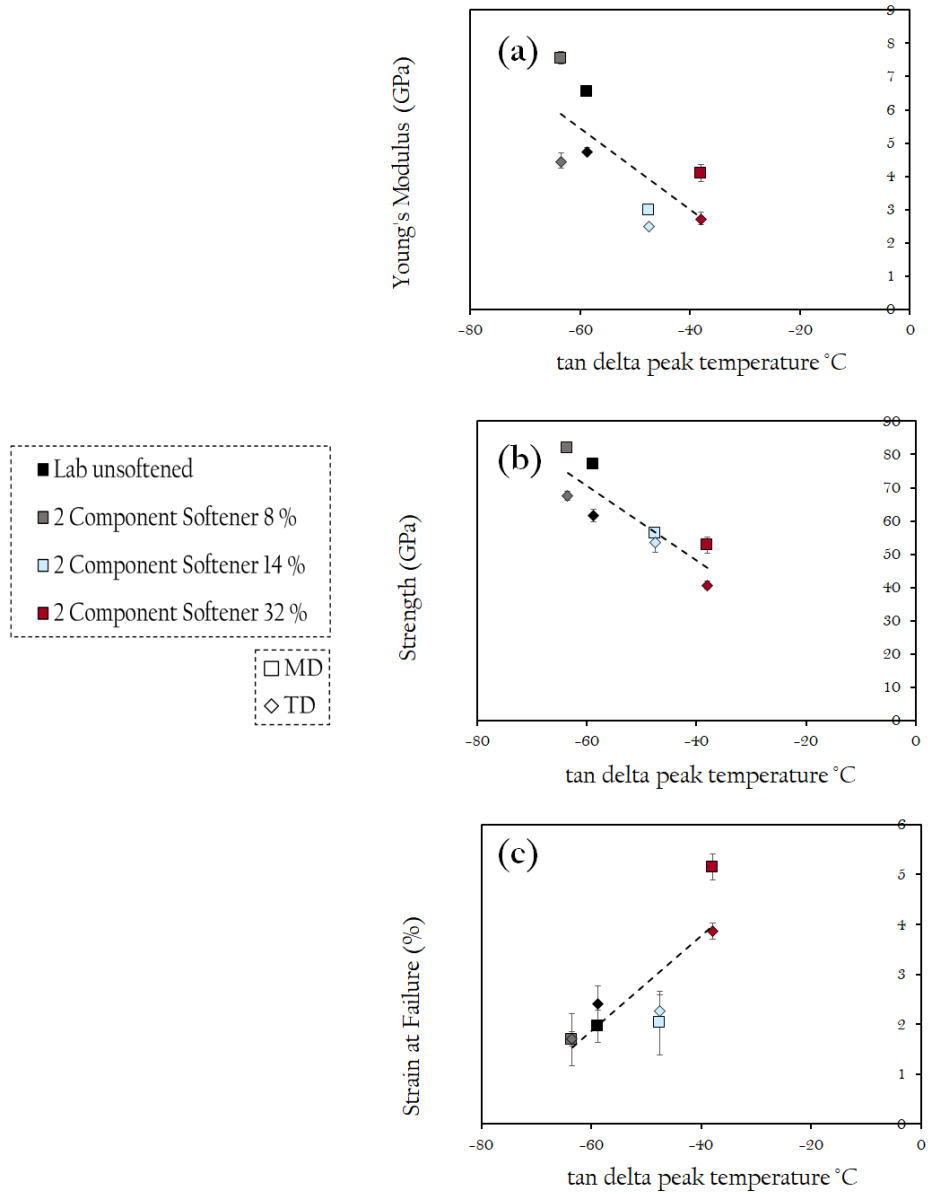


Figure 6.15: Variation of γ transition $\tan \delta$ peak temperature with tensile properties for 2 component softener films (a) Young's Modulus (b) Strength and (c) Strain at Failure

As seen in Figures 6.14(a-c) - 6.15(a-c), there is a clear dependence of tensile properties with the γ relaxation due to the way that plasticisers and water affect the intermolecular forces and mobility of polymer chains, thus impacting their mechanical performance. For example in Figures(a-b), Young's Modulus and strength decrease as $\tan \delta$ peak amplitude and temperature increase, both of which are identified as indicators of plasticisation due to the effects of water in films. Furthermore, in Figures(c), strain at failure increases with peak amplitude and temperature, showing that this γ relaxation is responsible for the increasing ductility of materials.

6.4.3 Comparison to lab-plasticised films

The variation in both amplitude and temperature at which the γ relaxation occurs with tensile performance has been compared for the 3 Component softened (*This text has been removed by the author of this thesis for confidentiality reasons*) ██████████ and the 2 component softened (*This text has been removed by the author of this thesis for confidentiality reasons*) ██████████ lab-softened films , as shown in Figures 6.16(a-c) - 6.17(a-c).

6.4 Dynamic Mechanical Thermal Analysis

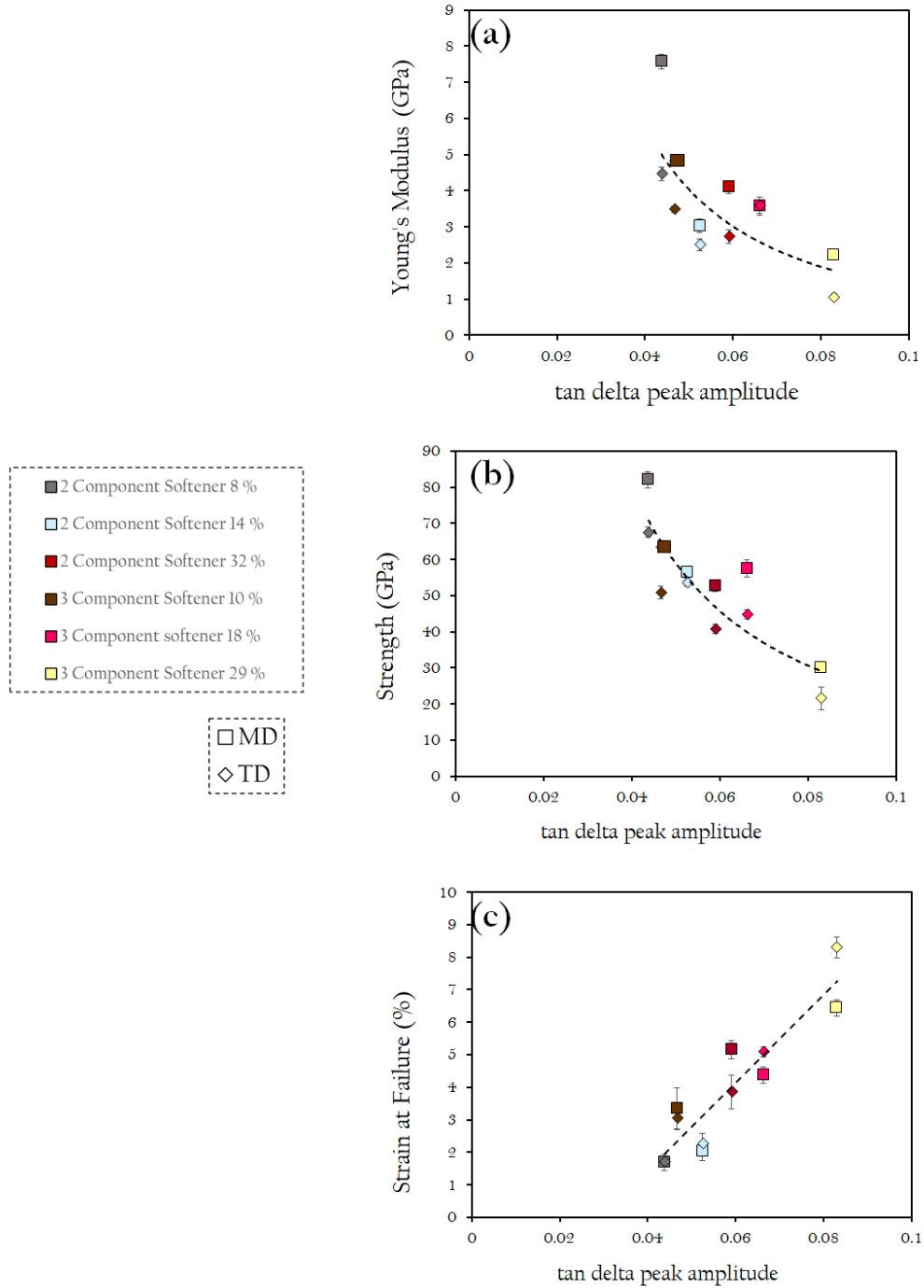


Figure 6.16: Comparison of variation of γ transition $\tan\delta$ peak amplitude with tensile properties for 3 component and 2 component softener films (a) Young's Modulus (b) Strength and (c) Strain at Failure

6.4 Dynamic Mechanical Thermal Analysis

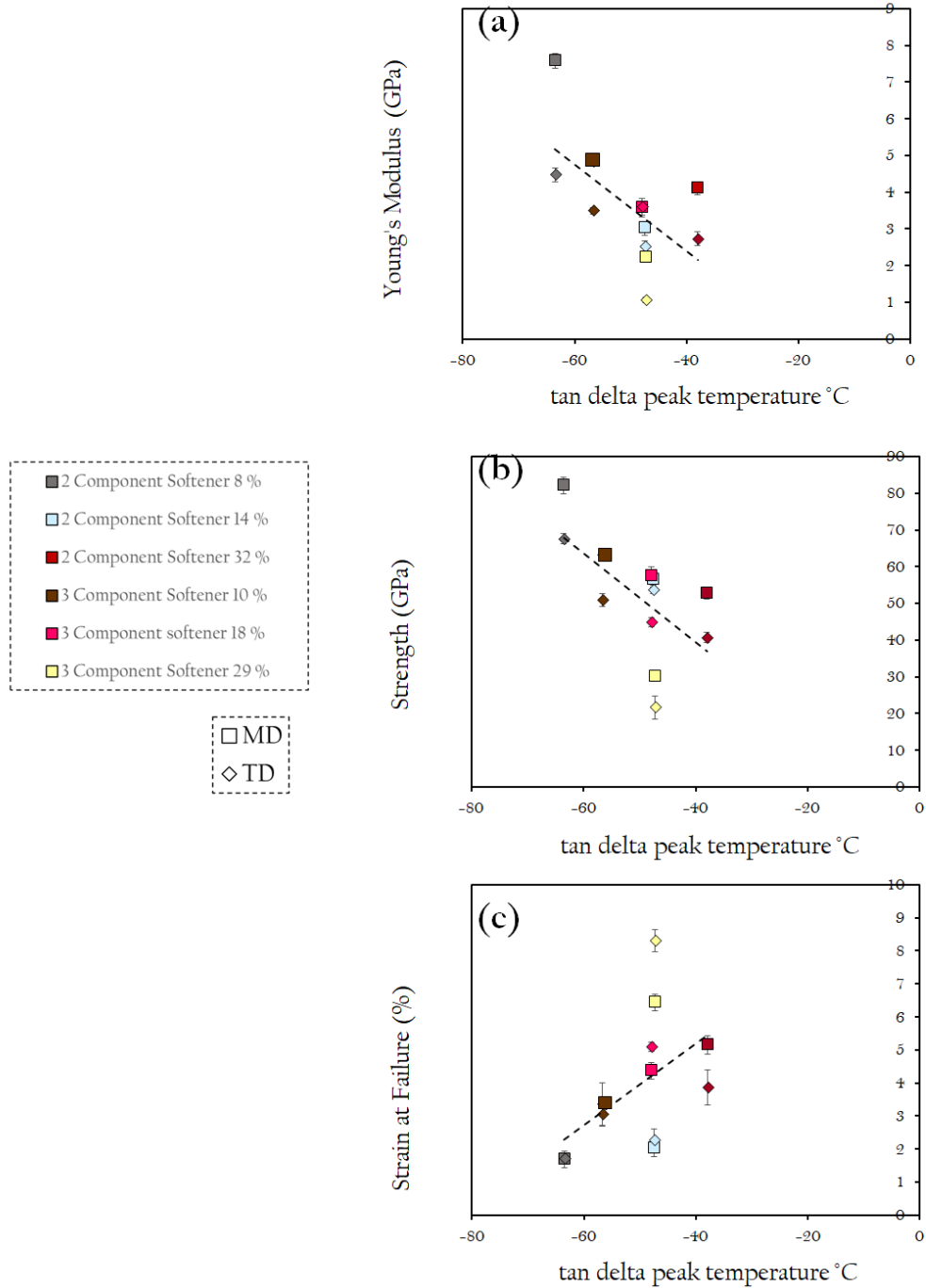


Figure 6.17: Comparison of variation of γ transition and δ peak temperature with tensile properties for 3 component and 2 component softener films (a) Young's Modulus (b) Strength and (c) Strain at Failure

The relationship between the properties of the γ relaxation and the mechanical properties of both films sets fit on the same trendlines. This asserts the relationship between this gamma relaxation and plasticisation. With an increase in both amplitude and temperature resulting in increased ductility but decreased stiffness and strength across these two comparable films. The fact that the 2 component softener still exhibits a softening effect to both the γ relaxation and tensile properties even at low concentrations and mixed with the anti-plasticising hemicelluloses, speaks for its softening ability.

6.4.4 Water removal procedure

For completeness and to verify the effect of water seen in Chapter 5, the Water Removal Procedure was applied to hemicellulose and 2 component softener films. For this process, films were cooled to $-100\text{ }^{\circ}\text{C}$ and subsequently heated to $120\text{ }^{\circ}\text{C}$ whilst oscillating at a frequency of 1 Hz. Once films had reached this temperature it is concluded that all free water has been removed. Remaining under the nitrogen atmosphere, films are cooled back down to $-100\text{ }^{\circ}\text{C}$ and subsequently heated to $120\text{ }^{\circ}\text{C}$ again. The results from these tests can be seen in $\tan\delta$ profiles in Figures 6.18(a-c) - 6.19(a-c), with the black line representing the second temperature ramp where films should have no free water.

6.4 Dynamic Mechanical Thermal Analysis

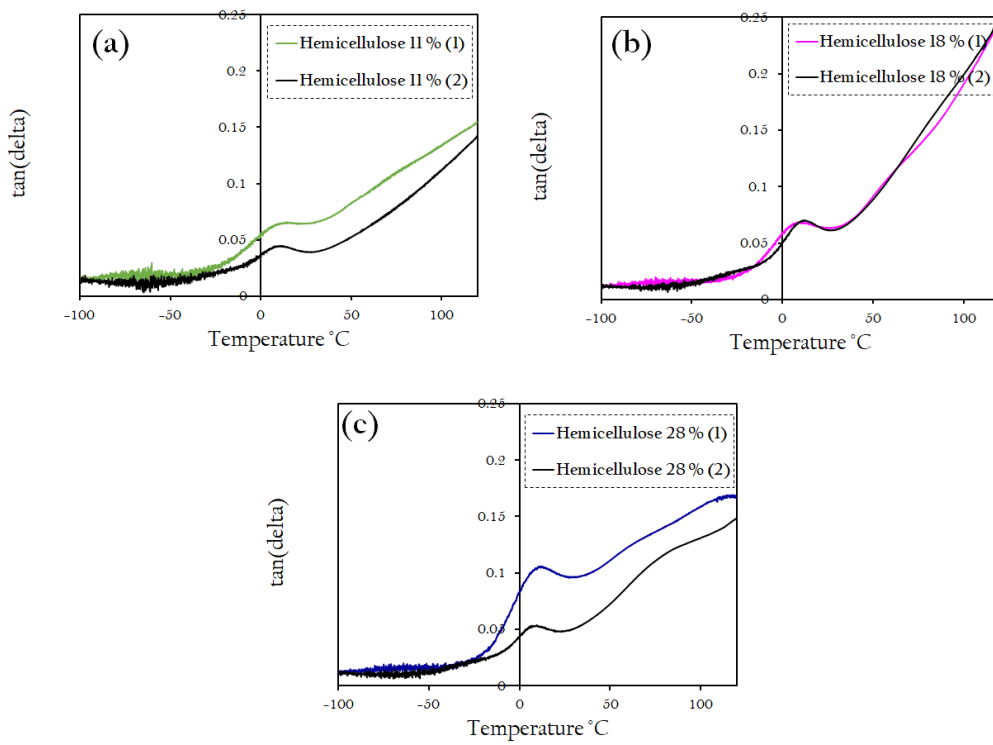


Figure 6.18: *Dynamic Mechanical Thermal Analysis (water removal procedure from -100 $^{\circ}\text{C}$ to + 120 $^{\circ}\text{C}$) $\tan \delta$ profiles of hemicellulose-based films (a) 11 % hemicellulose film (b) 18 % hemicellulose film (c) 28 % hemicellulose film. Where run (1) represents the first run to remove free water from films and (2) represents the second run on the dried film.*

6.4 Dynamic Mechanical Thermal Analysis

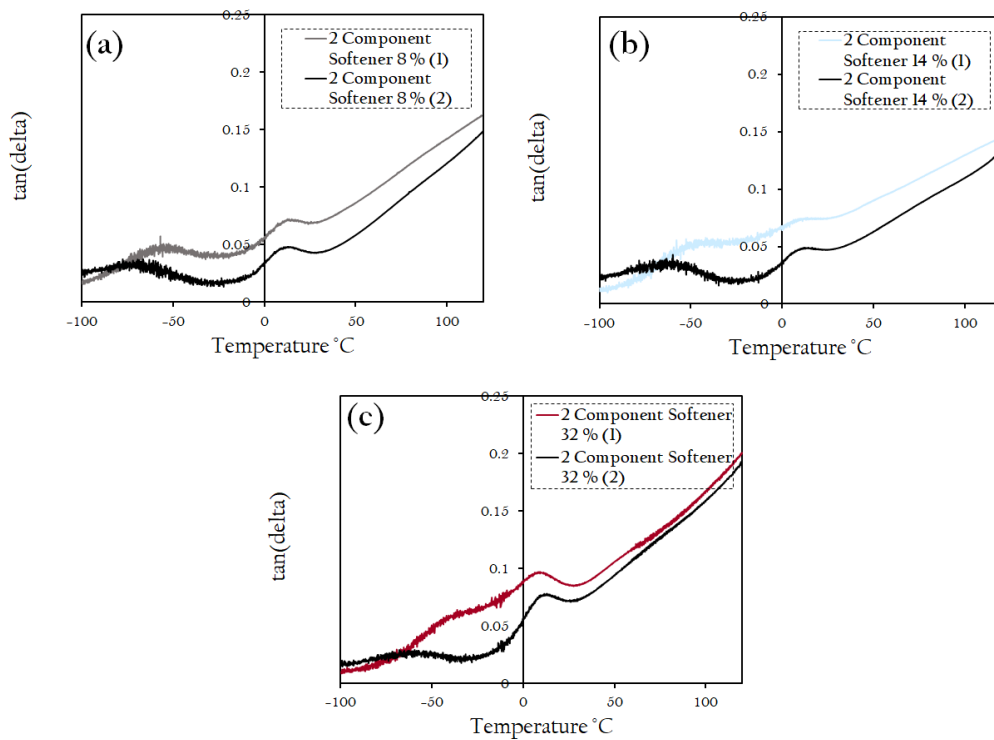


Figure 6.19: *Dynamic Mechanical Thermal Analysis (water removal procedure from -100°C to $+120^{\circ}\text{C}$) $\tan \delta$ profiles of 2 component softener lab-based films (a) 8 % 2 Component Softener film (b) 14 % 2 Component Softener film (c) 32 % 2 Component Softener film. Where run (1) represents the first run to remove free water from films and (2) represents the second run on the dried film.*

6.4 Dynamic Mechanical Thermal Analysis

As previously seen and annotated in Figure 6.12(a), the position where a γ transition might be expected in hemicellulose-based films is flat. To investigate this further, the water removal procedure was performed, as shown in Figures 6.18(a-c). Upon the second heating procedure, a dip is observed in the expected γ position. This suggests that the extremely low water content of hemicellulose-based films is totally removed during this water removal process, evidenced by the dip at the position of an expected γ transition. Thus this process has resulted in a completely dry films with no free or bound water between chains. Despite this observation, in previous ‘water removal’ procedures carried out on plasticised films (Figures 5.20(a-c) - 5.23(a-c)), a γ relaxation peak is still observed on the second run, just at a reduced amplitude and shifted to lower temperatures for glycerine, MPG and 3 component softened films whilst the peak is flat in urea-based films. As a result of these different observations between plasticised and hemicellulose films, we can draw hypothesis about how this procedure is effecting water content in films.

Water exists in-between cellulose polymer chains as either ‘free’ or ‘bound’. The former is unbound by polymer chains and thus easily removed during drying procedures. On the other hand, bound water is restricted by hydroxyl groups of either polymer chains or plasticisers and thus exhibits different properties to pure water. Both of these types of water induce a softening effect on films as when free water is removed during the water removal procedure, a γ relaxation that we have shown to be linked to plasticisation is still observed. In glycerine, MPG, 3 component softened and 2 component softened films, we suggest that both bound and free water contribute to the softening effect of films since they still exhibit a γ relaxation upon free water removal. This is why, for the previous set of plasticised films, when free water is removed during this water removal procedure, a peak in the γ transition is still observed as a result of this water bound between polymer chains or plasticisers. On the other hand, we suggest that in urea-based films, the water exists between polymer chains as only free water so still exhibits a strong softening effect but is removed completely on heating, as evidenced by the lack of γ relaxation on the second run. Finally, in the hemicellulose films, the water that would normally be free or bound between polymer chains or plasticisers, is extracted by hemicelluloses that are unable to embedd between polymer chains

6.5 Lab-based hemicellulose variation summary

and deposited on the surface, where it is removed during the drying process of film production. Therefore the water removal process results in no free or bound water remaining in the hemicellulose films, as evidenced by the dip in the expected position of a γ relaxation peak. The classification of these water types constitute excellent candidates for future work to confirm these hypothesis. Examples on the analysis of bound water have been demonstrated in literature employing the use of Differential Scanning Calorimetry [126].

On the other hand, for the 2 component softener films, Figures 6.19(a-c), show a reduction of amplitude and decrease in temperature of the γ relaxation, associated with a reduction in plasticising due to the hypothesised removal of free water between polymer chains through this removal process, leaving behind only bound water. Unlike the hemicellulose films, this peak does not become either completely flat or dipped, suggesting that the residual bound water is still inducing some ductility of films. Whether this water is bound to polymer chains or plasticisers is yet to be elucidated, although we propose it is probably a mixture of both as this behaviour is also observed in unsoftened and softened films when this water removal procedure was performed, suggesting that the water is probably bound to both polymer chains and plasticisers. Since there is a shifting of the γ peak during this procedure that is consistent with a reduction in plasticisation observed across all film sets, this suggests that it is the ‘free’ water in the system is that is responsible for imparting ductility above that of the unsoftened film. Thus we suggest again that plasticisers should not be ‘too’ hydrophilic as they will likely bind to water and this is not the form of water that imparts additional ductility. As such, despite the hemicellulose set of films being an unexpected anti-plasticiser, we were able to draw another conclusion through the identification of water types from this work to help elucidate the actions of polymers through the linking of dynamic and mechanical behaviour.

6.5 Lab-based hemicellulose variation summary

In this chapter, the addition of a hemicellulose blend and a 2 component softener containing *(This text has been removed by the author of this thesis for confidentiality reasons)* ██████████ to compare to

6.5 Lab-based hemicellulose variation summary

Futamura's 3 component softener has been investigated in an attempt to recognise alternative plasticisers suitable for cellulosic films. The selection of these potential plasticisers was based off the results of Chapter 5 that suggested that hydrophilicity is a desirable property in a plasticiser due to the important effect that water has on ductility. Despite this theory, the hemicellulose contribution resulted in an anti-plasticising effect and the 2 component softener has a lesser softening effect in comparison to commercial plasticiser. The reasons for this have been hypothesised to be reliant on the hemicellulose's superior ability to bond with water whilst being too large to embed between polymer chains and thus result in an anti-plasticising effect in comparison to the unsoftened films which still contain some water content. As such, recommendations have been made for how Futamura can approach investigating future potential plasticisers. This has been achieved using a combination of macroscopic and molecular testing to link the behaviour of films with increasing hemicellulose and 2 component softener content.

- Firstly **Tensile Testing** has revealed the contributions of the hemicellulose blend and the 2 component softener with increasing concentrations. The hemicellulose blend exhibits a clear anti-plasticising effect with increasing content as Young's Modulus and strength increase whilst strain at failure decreases. On the other hand, the 2 component softener shows an initial anti-plasticising effect at low concentrations, but at higher concentrations displays a increase in ductility; suggesting the glycerine content is able to plasticise despite the inclusion of hemicelluloses.
 - **Recommendations:** It appears that the inclusion of hemicelluloses as plasticisers when added post casting is not effective at improving mechanical performance. This is somewhat disappointing since literature has shown that the inclusion of residual hemicelluloses in films has a plasticising effect, presumably due to the fact that rather than embedding between chains they must be incorporated into the cellulose chains via some other method that still allows for the incorporation, rather than removal of, water [3]. As such, one route could be to consider altering early stages of the viscose process such that some

6.5 Lab-based hemicellulose variation summary

residual hemicelluloses remain in films to provide a wholly green plasticising effect. Furthermore, other alternative plasticisers should be investigated with the findings of this thesis in mind i.e hydrophilicity and ability to embed between polymer chains are extremely important factors to determining plasticisation due to the ability to retain free water in films.

- **Impact Testing** at a range of strain rates has again revealed a variation in impact behaviour. Peak behaviour for hemicellulose-based films supports an anti-plasticising effect and for the 2 component softener the plasticising effect both support results seen in tensile testing. Again, impact behaviour is extremely important with regards to the functionality of films in application. Despite the coating of hemicelluloses that were unable to embed in to films observed on the surface of the films, this unfortunately did not impart any additional resistance to impact in films.
- Finally, **Dynamic Mechanical Thermal Analysis** has been used to identify and analyse the patterns of the γ relaxation with regards to anti-plasticisation and plasticisation. There is an observed lack of the γ peak in hemicellulose-based films and re-appearance of this peak in 2 component softened films. Furthermore, the water removal procedure results support the hypothesis that the water embedded between polymer chains is largely responsible for the plasticisation effects in films. The nature of this water and discussion of the contribution of free and bound water has been identified. As such, we suggest that these extremely hydrophilic hemicelluloses are not suitable as plasticisers if they cannot embed between chains themselves since they only act to remove water to the surface that is evaporated during the drying process.
 - **Recommendations:** The dip in the position of an expected γ relaxation observed in the hemicellulose films has suggested a theory that it is free water in the films that is inducing the plasticising effects above that of the base softening induced by bound water that is evident even in unsoftened films. As such plasticisers act to increase the amount

6.5 Lab-based hemicellulose variation summary

of free and bound water in films. Again it is clear that there is an optimum hydrophilicity of plasticisers such that there is sufficient free water able to exist between cellulose chains rather than bonding with the plasticisers in films. As such, future alternative plasticisers should be selected with this in mind.

Chapter 7

Conclusions

7.1 Summary of outcomes

The aim of this thesis was to understand and reveal the links between molecular relaxation behaviour and macroscopic mechanical properties of Futamura's commercial cellulose films using structural molecular and macroscopic testing techniques in order to make recommendations about their production process with the ultimate goal of improving both sustainability and costs. With this motivation, the use of plasticisers in films was examined, including the separation and incorporation of Futamura's 3 component blend in increasing concentrations in lab-softened films both individually and as a blend that recreated Futamura's commercial package. Moreover, the inclusion of alternate potential green plasticisers in the form of a hemicellulose hydrolysate was explored in another set of lab-softened films.

With these goals in mind; tensile testing, impact testing at varying strain rates and dynamic mechanical thermal analysis were performed on the commercial, lab-softened and hemicellulose-based films in order to uncover their performance drivers. Investigation of the commercial 3 component softener proved to be complicated, so the decision was made to separate its constituents and incorporate them into films individually at different percentages. Analysis has allowed for each of these testing methods to be linked, characterising relationships between molecular and mechanical properties. Key findings along with a 'master

plot', Figures 7.1(a-c) - 7.4(a-c) displaying the data across all 3 film sets for each techniques are described:

- **Tensile Testing** has elucidated the uniaxiality of films and resultant variation of machine and transverse properties, with heightened alignment of polymer chains observed in commercial films due to rolling under tension during drying and softening processes. In addition to this, material property relationships have been shown using Ashby Plots and the compromise between stiffness, strength and strain at failure highlighted. The effect of the impact of traditional plasticisers and hemicellulose-based anti-plasticisers has been quantified and the contribution of individual components determined, such that recommendations have been made regarding Futamura's continued development of their softener packages. All three properties fall on a similar trendline and we can use Ashby plots to express the mutually exclusive nature of Young's Modulus and strength with strain at failure that arise as a result of both orientation of cellulose polymer chains and softener content.

7.1 Summary of outcomes

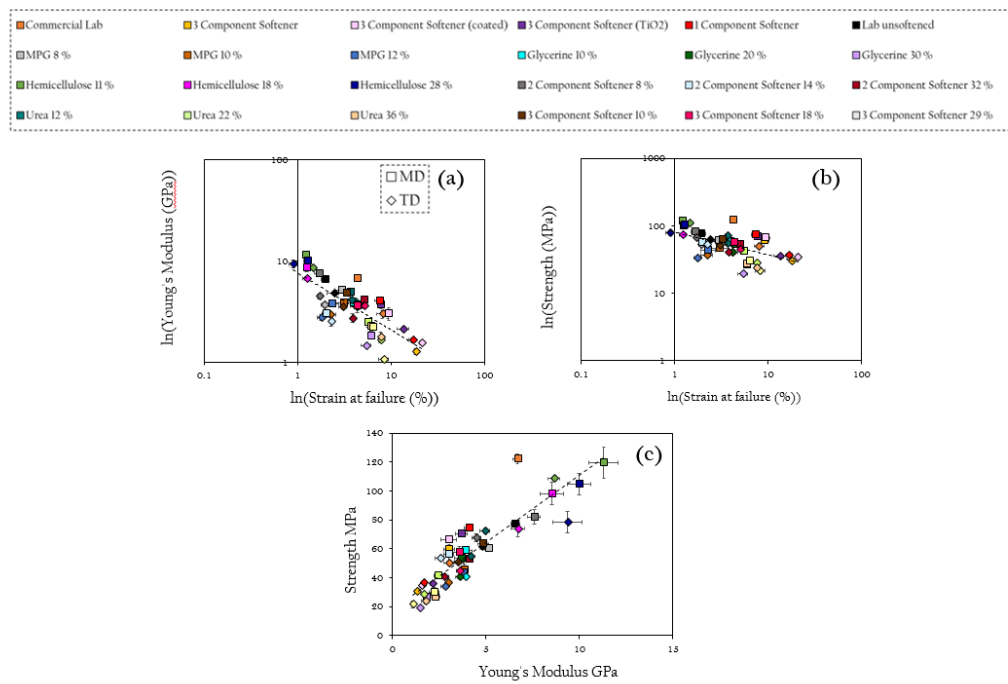


Figure 7.1: *Master Ashby Plots providing comparisons between tensile properties for commercial and lab-made films where the axis of (a) and (b) have been presented on a logarithmic scale to display the relationship between Young's modulus and strength with strain at failure*

- **Dynamic Mechanical Thermal Analysis** has been used to analyse the molecular relaxations of cellulose polymer chains across a range of frequencies and temperatures. With this technique, relaxation profiles of $\tan\delta$, storage modulus and loss modulus have been compared with ranging plasticiser/anti-plasticiser content. This has led to the identification of the α relaxation associated with T_g at temperatures above 200 °C, an around room temperature transition that has been tentatively linked to the β transition as well as the peak in impact behaviour seen at certain strain rates at room temperature and finally, a γ relaxation in the sub-zero region that has been associated with plasticiser performance, the role of water and mechanical properties of films. This final γ relaxation has been the focus of this technique and has been used to explain the competitive bonding between polymer chains, plasticisers, anti-plasticisers and water and the resultant effect this has on softener uptake and therefore performance. This relaxation has been quantitatively linked to tensile performance and the water removal procedure of films has allowed for the hypothesis that it is unbound, free water that is responsible for the additional plasticisation above the unsoftened films through the ability of plasticisers to bring additional water in between the polymer network. A master plot of $\tan\delta$ in the temperature region of the γ relaxation has been included for all films as well as a graph depicting the variation of the amplitude of this relaxation compared to tensile properties. In particular, we present a strong correlation between height of the gamma relaxation with increasing plasticiser and water content with Young's Modulus, strength and strain at failure.

7.1 Summary of outcomes

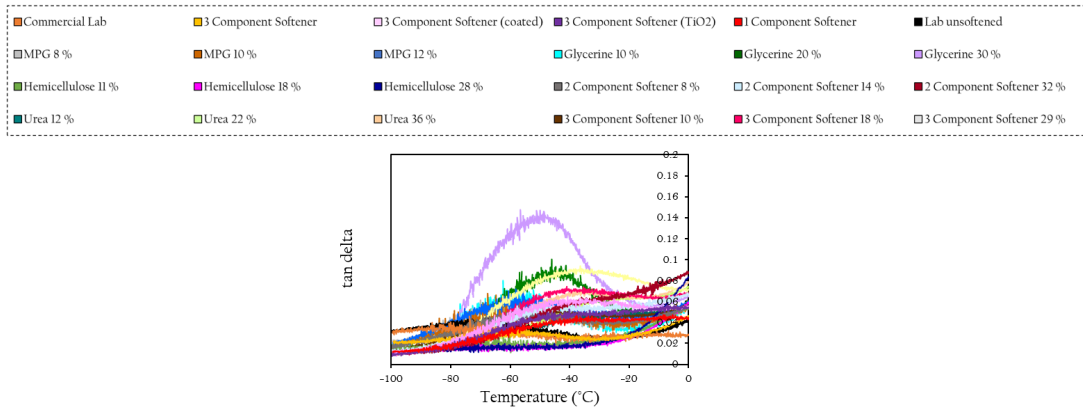


Figure 7.2: Master DMTA temperature ramp $\tan\delta$ profiles providing comparisons between dynamic transitions for commercial and lab-made films

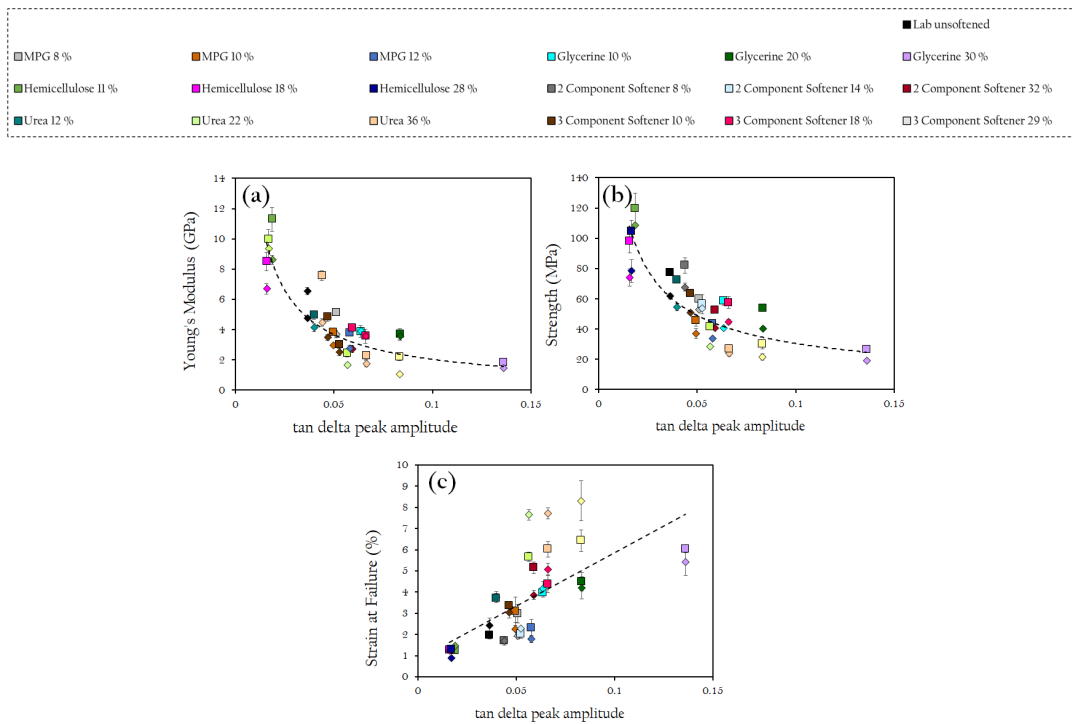


Figure 7.3: Master plot of the variation of γ transition $\tan\delta$ peak amplitude with tensile properties

7.1 Summary of outcomes

- Impact Testing** at a range of speeds has determined that impact behaviour of these films is rate dependent, an important discovery considering the range of impacts they might experience in their application as packaging materials. A peak in impact behaviour is typically observed between 0.001 s^{-1} - 0.01 s^{-1} . The behaviour of maximum strain, force and energy have been quantified and the effect of plasticisers and anti-plasticisers on this variable performance established, leading to further suggestions to Futamura's plasticising process.

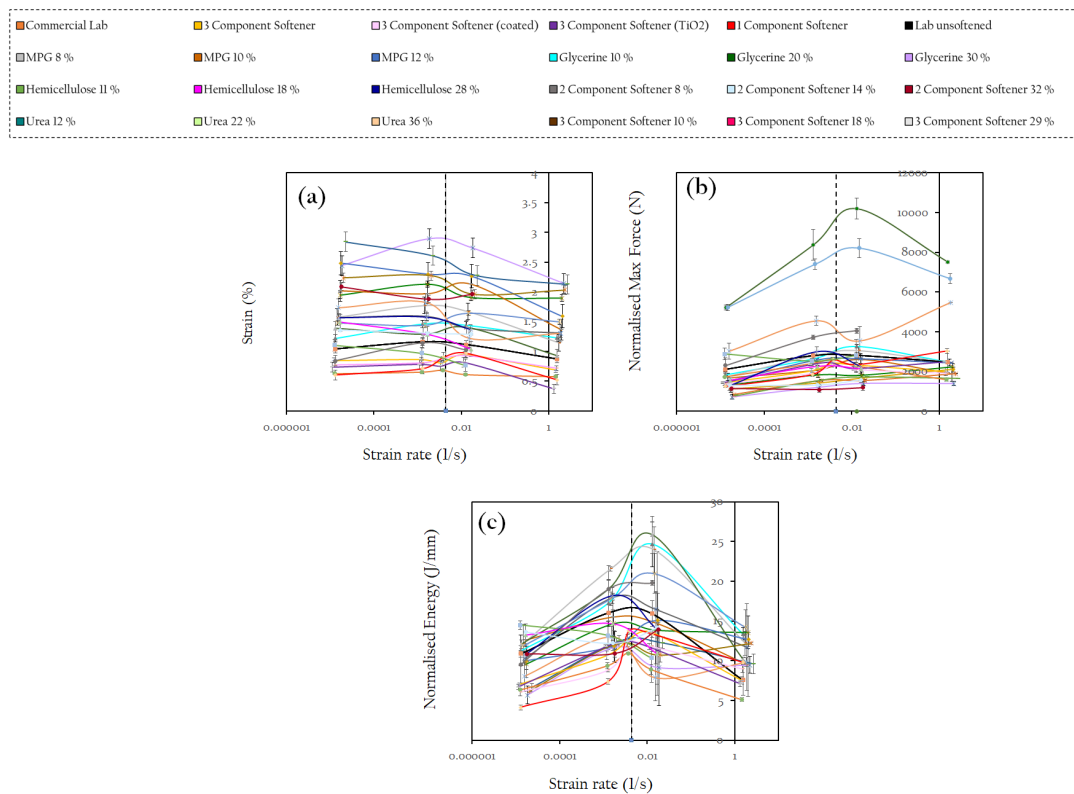


Figure 7.4: Master falling weight and slow puncture impact graphs providing comparisons of impact properties across a range of strain rates for commercial and lab-made films

As a result of these techniques, we can draw hypothesis about the internal actions inside the films to explain performance with regards to the effectiveness of a plasticiser. There are two important properties of effective cellulose plasticisers highlighted in this work.

1. **Size.** A plasticiser should be of sufficiently small molecular weight such that it is able to embed between cellulose polymer chains and displace water from cellulose wet gel with softener in solution.
2. **Hydrophilicity.** A plasticiser should have sufficient hydrophilic groups such that there is preferential bonding for an optimum ratio of water is incorporated into films. This should ensure that there is enough free and bound water in films that have both been seen to induce plasticisation effects in comparison to hemicellulose-based films with very little free or bound water content.

It is for these reasons that low molecular weight plasticisers such as glycerine and urea with 3 hydrophilic groups are shown to have excellent uptake and softening abilities in films due to their ability to embed between polymer chains and incorporate increased moisture content within films. On the other hand, it was shown that large hemicellulose monosaccharides with many hydrophilic groups have an anti-plasticising effect on films due to their inability to embed between polymer chains and removal of water due to preferential bonding and subsequent migration to the surface of the film.

With these analysis and hypothesis, the following suggestions are proposed to Futamura for how they can alter their plasticisers packages to improve performance.

1. **Urea content:** Urea has been found to be an effective plasticiser with effects greater than that of glycerine seen at lower concentrations (22 %) of glycerine's maximum properties at higher concentrations. In fact with migration effects seen at this 22 % concentration of urea, it could be that a superior plasticising effect is demonstrated at even lower content. With Futamura currently incorporating (*This text has been removed by the author of this thesis for confidentiality reasons*) ██████████ in their 3 component

softener package at (*This text has been removed by the author of this thesis for confidentiality reasons*) █████ softener in film content; this equates to only (*This text has been removed by the author of this thesis for confidentiality reasons*) █████ in films. Since this plasticiser has been ruled out as a secondary plasticiser, considering cost implications, Futamura might consider increasing this percentage of urea. It is suggested that with an increase of urea content in a softener package, this would reduce the overall softener content of films due to the demonstration of cooperative effects of softeners in the 3 component blend in this work; therefore a reduction of plasticiser costs might be seen.

- 2. MPG content:** MPG has been found to be the least effective softener in Futamura's current commercial package. In fact, it was found to have extremely low uptake in films as well as an anti-plasticising effect, making its inclusion as a secondary softener in the commercial package counterproductive. As such, we suggest that Futamura consider the omission of this component in their 3 component softener and experiment with the optimising of a dual softener of glycerine and urea depending on cost considerations. It is hoped that this will reduce costs further since glycerine and urea boast superior plasticising abilities at lower concentrations, eliminating the need for MPG and reducing overall softener content.
- 3. Alternative Plasticisers:** Despite the hopes of the inclusion of a potential hemicellulose blend inducing a softening effect based on their extremely hydrophilic nature, this trial did not have the desired outcomes. In fact, an anti-plasticising effect was observed with the inclusion of this sugar blend. Despite this, the importance of free and bound water content of films has been highlighted through this work and thus the inclusion of alternate hydrophilic plasticisers that result in an optimum balance of free and bound water in films could be investigated further. This is provided that they meet the criteria outlined above regarding their size and optimal number of hydrophilic groups. With identification of a low cost, suitable alternative softener; Futamura might open another avenue for the plasticisation of these films.

4. **Plasticiser content:** This has been shown to be extremely important to the performance of films. Softener content depends on uptake of that particular molecule into the polymer chains of films and for some plasticisers this reaches a maximum and migration effects are observed. This can result in a plateau or even reduction of mechanical properties. For whatever changes that are made to the softener blend, plasticiser content should be incrementally increased and uptake and performance measured to ensure optimum content has been achieved.

To summarise, we analysed the mechanical and molecular properties of commercial and lab-softened films in order to elucidate the performance of softeners. From this work, hypothesis have been provided and recommendations for how Futamura should adjust their current commercial 3 component softener to enhance performance.

7.2 Future Work

In addition to the suggested changes to softener processing, some proposals of future work towards the characterisation and improvement of these films are provided.

Future work can be separated into two branches of goals (1) Future testing and (2) making changes to the films. For the former, this should be done to better understand and evidence the hypothesis provided in this thesis, as well as provide more information about films properties that are useful to their applications. Whist the latter is to improve Futamura's process and production to improve both costs and sustainability of their products to enable their continued success in the bio-packaging market. Details on such recommendations to improve plasticisation are included in the previous section.

In order to prove hypothesis of this thesis with regards to the role of plasticisers and water intake, an important next step would be to analyse the water content of the films. Quantifying the proportions of bound and free water within these systems would support theories about the actions of plasticisers and preferential bonding between each of these components. Free water content can be

easily determined using techniques such as Thermogravimetric analysis (TGA) to determine weight loss and therefore water content when heated above the boiling temperature of water. Bound water, on the other hand, requires more specialist techniques such as Differential Scanning Calorimetry, where the quantity of bound water can be determined through the analysis of a broad peak between 230 - 250 K [126]. This understanding of the presence of types of water in this cellulose system would allow for the confirmation of concluding hypothesis.

Furthermore, another avenue to explore to provide theoretical models of these polymer:plasticiser:hemicellulose:water systems might be through the use of molecular simulations. This field has been gaining traction in the field of cellulosic materials and has been used to identify how the presence of water impacts ring opening of dialcohol cellulose (ring-opened cellulose) and thus provides molecular mobility, affecting material properties and inducing plasticisation [127]. For initial molecular simulation tests we propose a modelled cellulose molecule consisting of just 6 sugar monomers to keep simulation times short for some initial testing. We would incorporate this cellulose molecule with water and selected plasticisers in the concentrations: cellulose (70 %), softener (20 %) and water (10 %). From such simulations, hydrogen bond interaction energy can be determined and compared to identify interactions between each of these components.

In addition to finalising and confirming hypothesis made through testing in this thesis, another important property of films to assess is their water and gas barrier properties. With 40 % of all food produced in the United States going to waste, it is imperative that food packaging selection acts to prevent moisture and oxygen transfer to inhibit decay and prolong shelf life [128]. The dominant method determining oxygen barrier properties is a common oxygen permeability analyser based on ASTM international standards. A stream of oxygen gas is flowed across one side of the film whilst a stream of nitrogen gas on the opposite side transfers the desorpted oxygen gas to an analyser to determine the oxygen content [129]. These results can then be used to characterise the transmission rate, permeance and permeability of the film. On the other hand, moisture permeability is an inherently difficult property to measure due to cellulose's hydrophilic nature. Isothermal thermal gravimetric analysis (TGA) is most often

implemented, whereby the mass of a cellulose film changes over time due to water absorption or desorption when subjected to a controlled temperature program [130]. Typically, cellulose films fall into the poor moisture barrier category; However, numerous successful approaches have been made to improve these moisture barrier properties including esterification with more carbon numbers of hexanoyl and dodecanoyl chloride and using cellulose materials with a higher lignin content due to increased hydrophobicity [131][132]. Futamura alter the moisture and gas barrier of their films using coatings; investigations into the function of these coatings would be an essential step to optimising these films for their intended application as packaging.

With this work, we have embarked on the beginning steps of a large scale commercial sustainability project that will see the revolution of these plant-based films. This work, along with future directions, will instigate the alleviation of relying on costly plasticisers, making cellulosic films *the* sustainable packaging of the future.

Appendix A

Additional Figures

A.1 Room temperature peak analysis

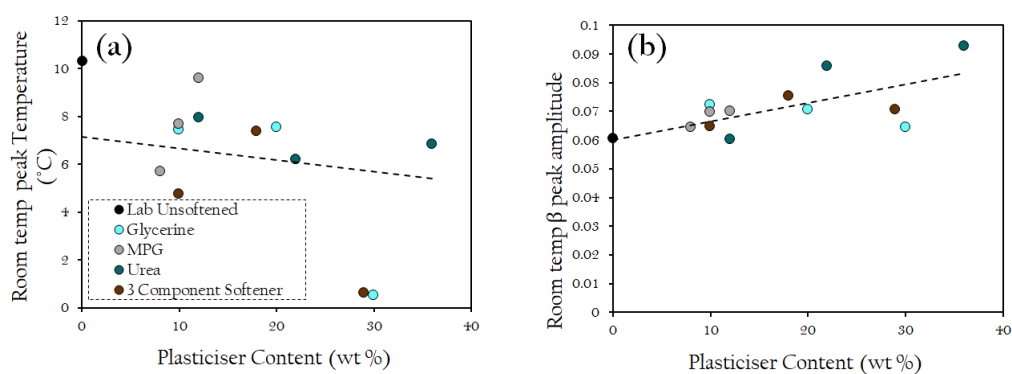


Figure A.1: Room Temperature presumed β peak variation with plasticiser content
(a) Shift in temperature (b) Increase in peak intensity

A.1 Room temperature peak analysis

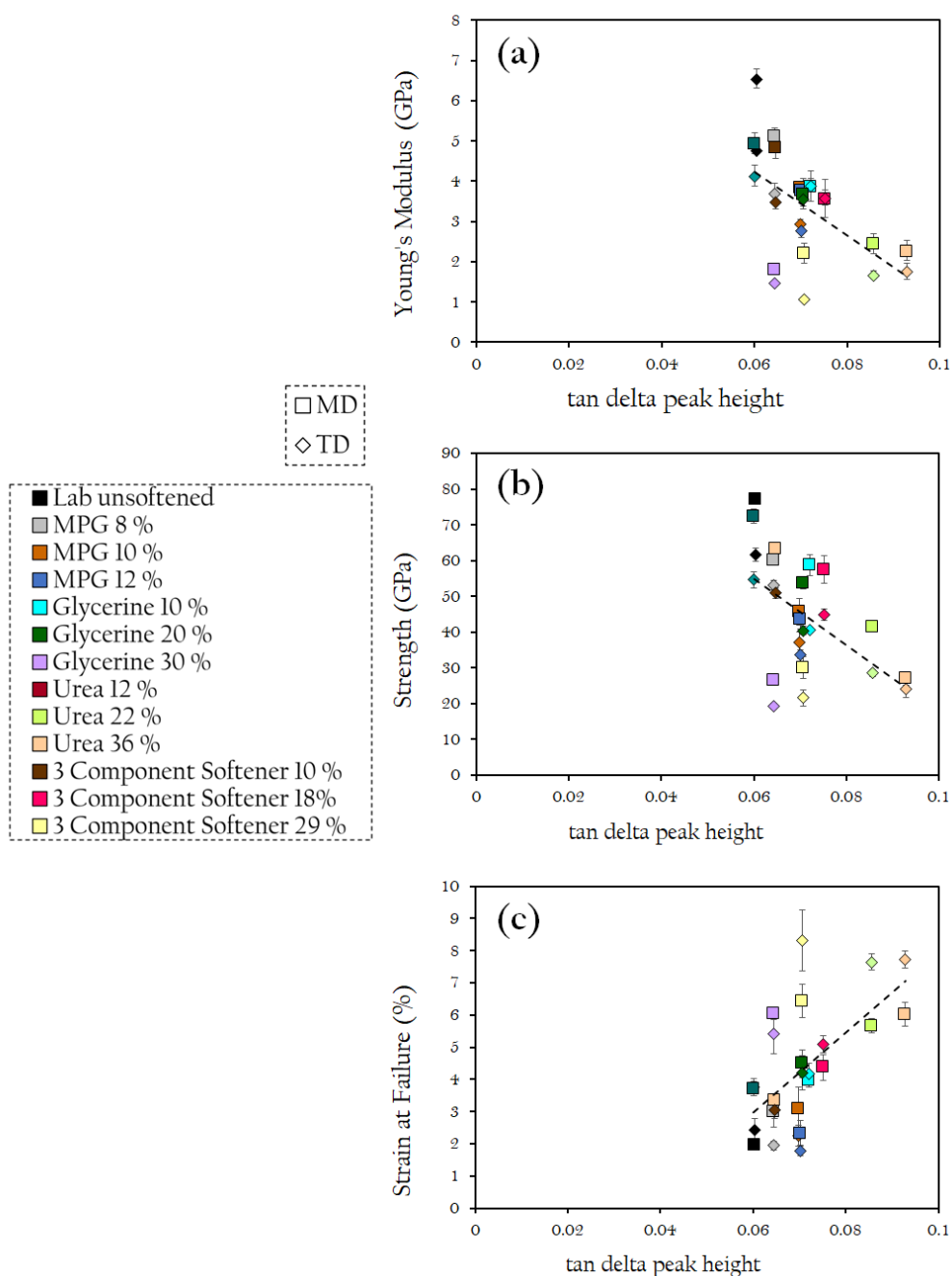


Figure A.2: Variation of mechanical performance of plasticised films with $\tan \delta$ presumed β peak height

A.1 Room temperature peak analysis

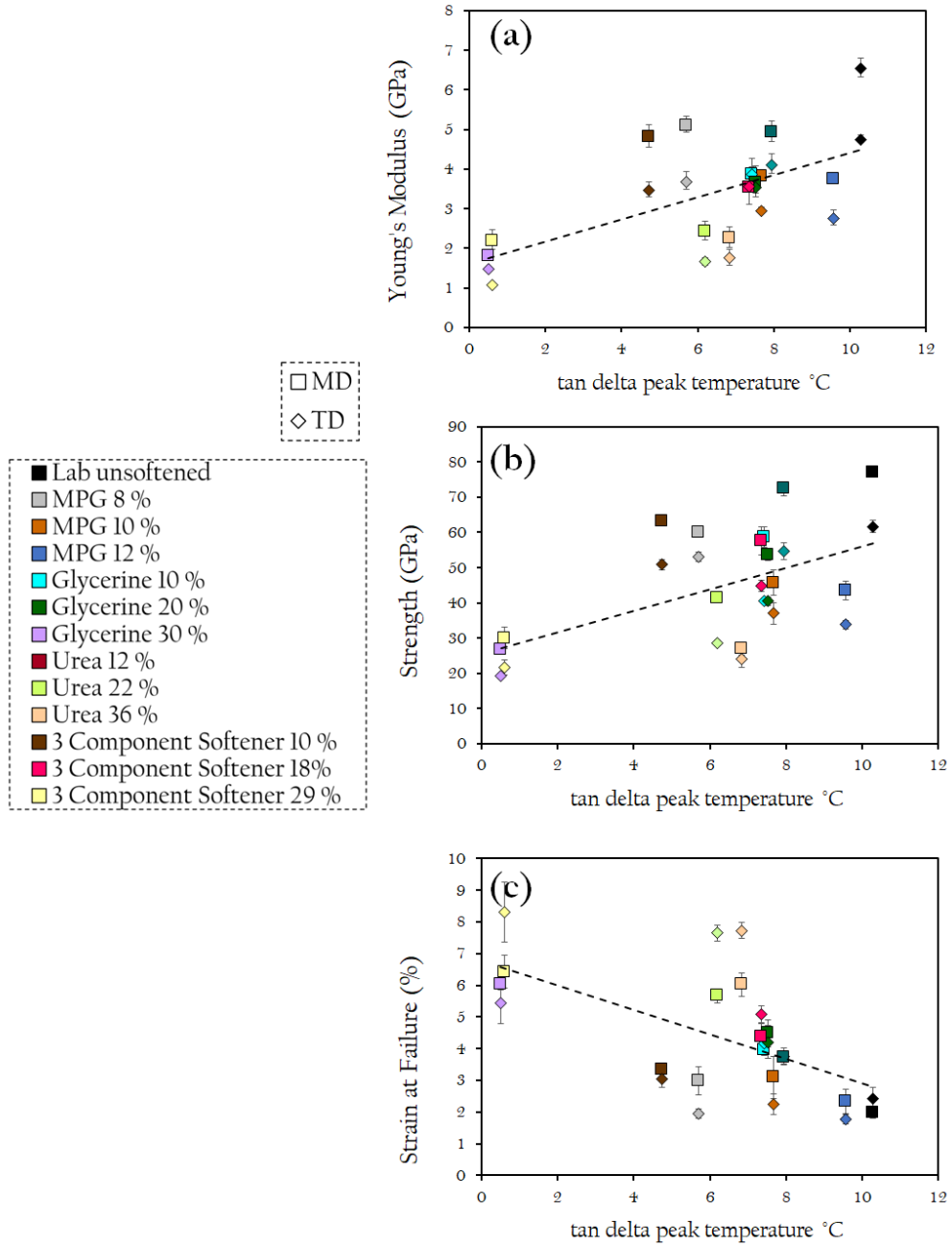


Figure A.3: Variation of mechanical performance of plasticised films with $\tan\delta$ presumed β peak temperature

A.1 Room temperature peak analysis

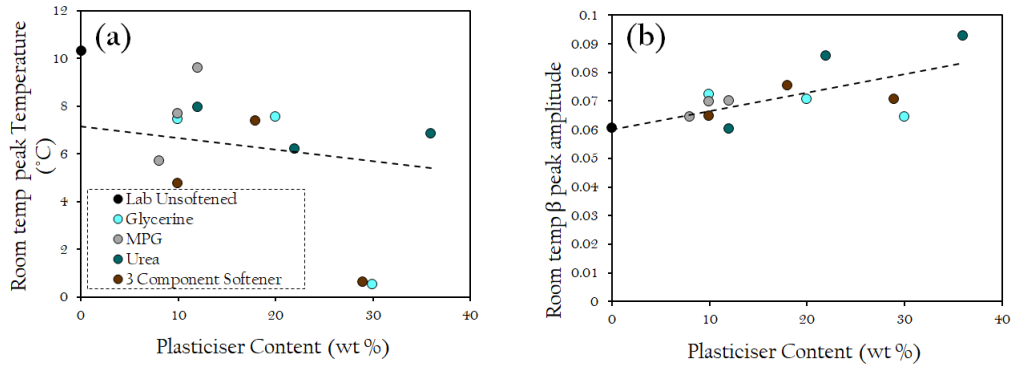


Figure A.4: Room Temperature presumed β peak variation with hemicellulose and 2 component softener content (a) Shift in temperature (b) Increase in peak intensity

A.1 Room temperature peak analysis

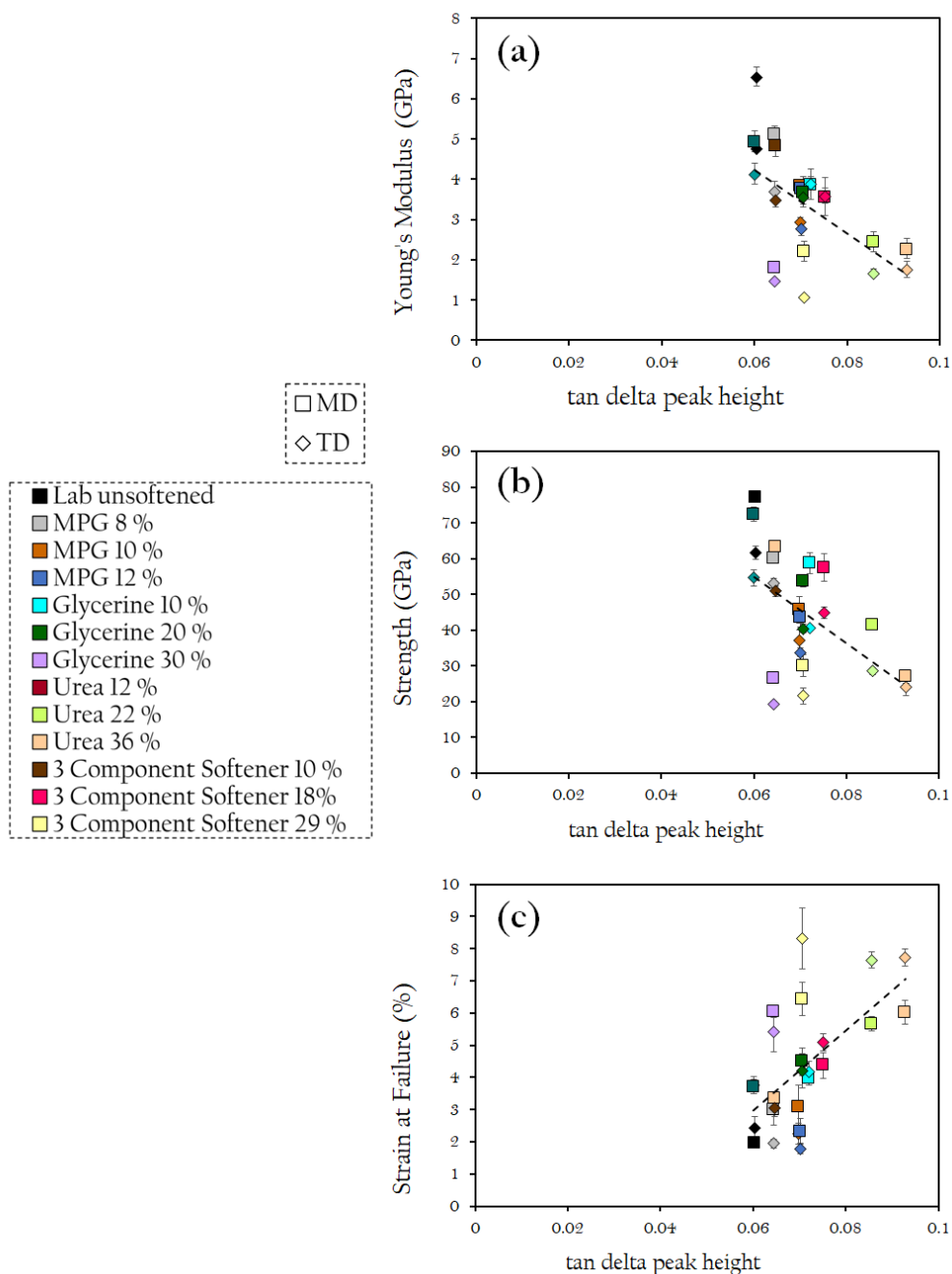
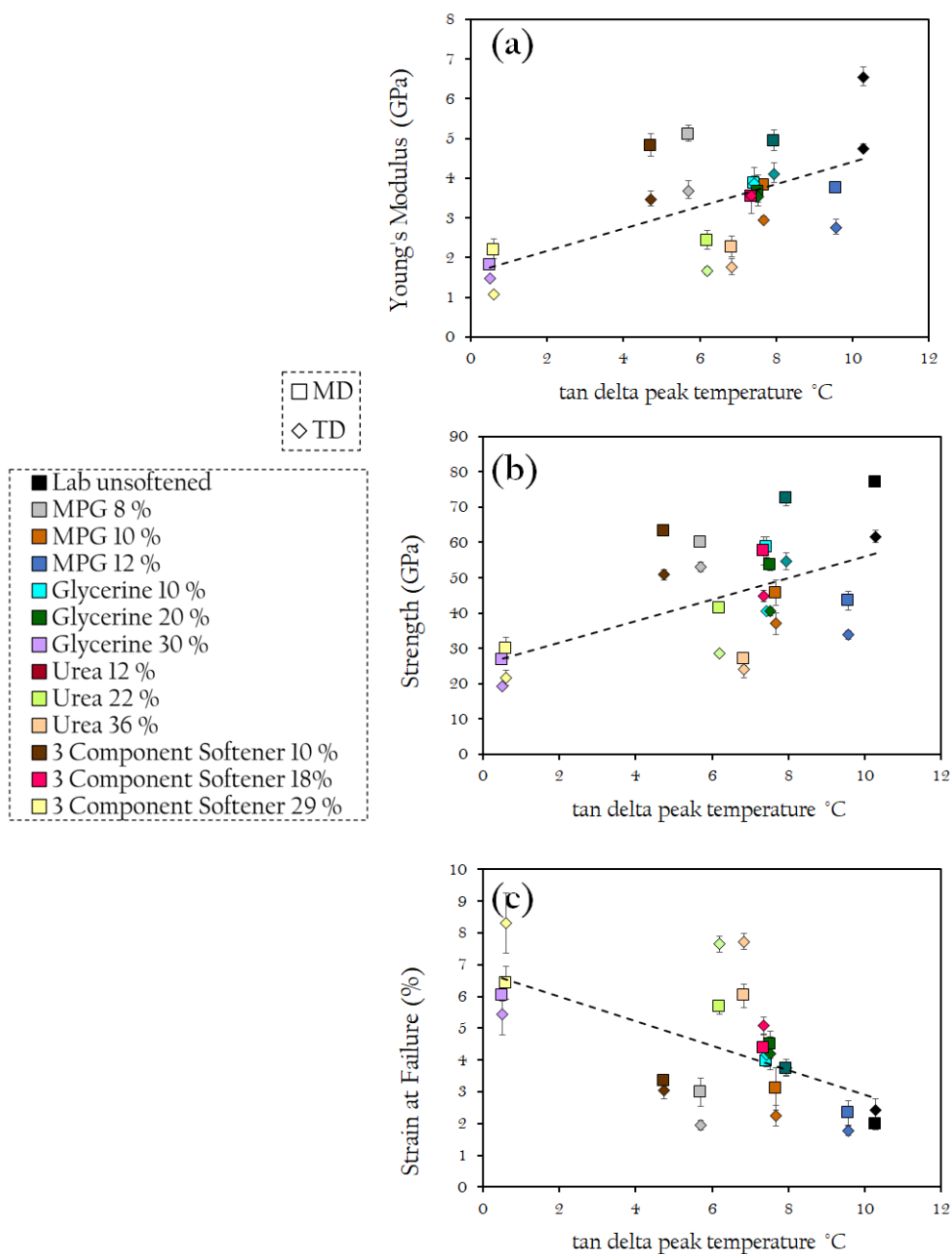


Figure A.5: Variation of mechanical performance of hemicellulose films with $\tan\delta$ presumed β peak height

A.1 Room temperature peak analysis



A.2 Dynamic relaxations fittings

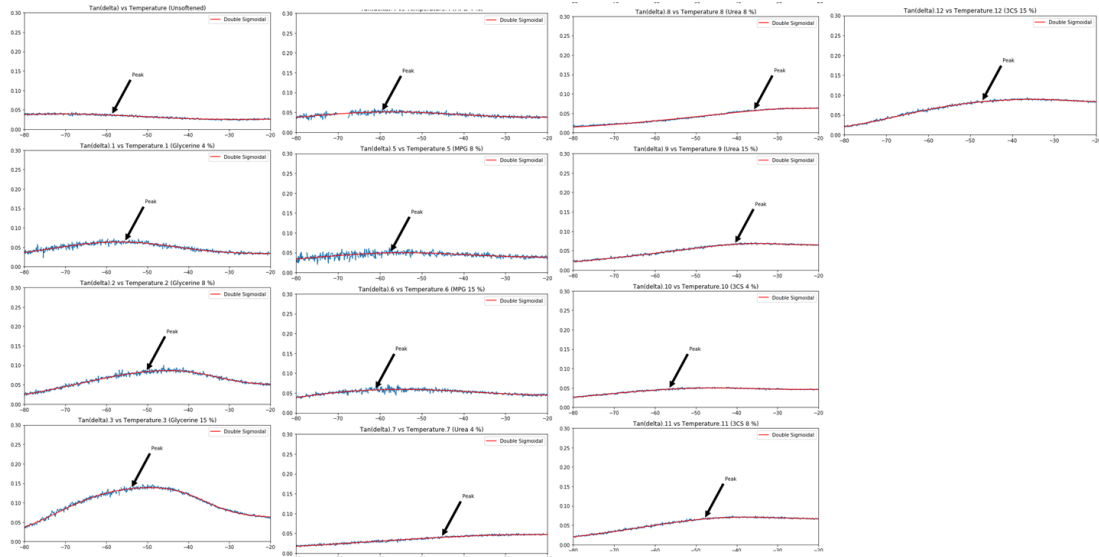


Figure A.7: *Asymmetric double Sigmoidal function fitting applied by python to determine peak positions of $\tan\delta$ γ transition*

References

- [1] United nations environment programme: From pollution to solution: A global assessment of marine litter and plastic pollution. <https://www.unep.org/interactives/pollution-to-solution/>. Accessed: 2023-06-28. [iv](#), [38](#)
- [2] The Futamura Group: About us. <https://www.futamuragroup.com/en/>. Accessed: 2023-06-28. [2](#), [4](#), [13](#), [19](#), [29](#)
- [3] Hamid M. Shaikh, Kiran V. Pandare, Greeshma Nair, and Anjani J. Varma. Utilization of sugarcane bagasse cellulose for producing cellulose acetates: Novel use of residual hemicellulose as plasticizer. *Carbohydrate Polymers*, 76(1):23–29, 2009. [4](#), [33](#), [37](#), [46](#), [186](#)
- [4] A Payen. Mémoire sur la composition du tissu propre des plantes et du ligneux. *Comptes Rendus Hebdomadaires des Séances de l'Académie des Sciences*, 7(7), 1838. [7](#)
- [5] A Brogniart, AB Pelonze, and R Dumas. Report on a memoir of m. payen, on the composition of the woody nature. *Comptes Rendus*, 8:51–53, 1839. [7](#)
- [6] Shiro Kobayashi, Keita Kashiwa, Junji Shimada, Tatsuya Kawasaki, and Shin-ichiro Shoda. Enzymatic polymerization: The first in vitro synthesis of cellulose via nonbiosynthetic path catalyzed by cellulase. *Makromolekulare Chemie. Macromolecular Symposia*, 54-55(1):509–518, 1992. [7](#), [19](#)
- [7] A.D. French. Glucose, not cellobiose, is the repeating unit of cellulose and why that is important. *Cellulose*, 24:4605–4609, 2017. [8](#), [19](#)

REFERENCES

- [8] Dieter Klemm, Brigitte Heublein, Hans-Peter Fink, and Andreas Bohn. Cellulose: Fascinating biopolymer and sustainable raw material. *Angewandte Chemie International Edition*, 44(22):3358–3393, 2005. [8](#), [9](#), [13](#), [23](#)
- [9] Atalla R.H. Blackwell J. et al. Glasser, W.G. About the structure of cellulose: debating the lindman hypothesis. *Cellulose*, 19:589–598, 2012. [8](#), [19](#)
- [10] Jim Pfaendtner Christoph Krumm and Paul J. Dauenhauer. Millisecond pulsed films unify the mechanisms of cellulose fragmentation. *Chemistry of Materials*, 28(9):3108–3114, 2016. [8](#), [19](#)
- [11] H. Staudinger. Über polymerisation. *Berichte der deutschen chemischen Gesellschaft (A and B Series)*, 53(6):1073–1085, 1920. [9](#), [19](#)
- [12] Darvill A. Roberts K. Sederoff R. Staehelin A. Albersheim, P. *Plant Cell Walls (1st ed.)*. Garland Science, 2010. [10](#)
- [13] Nelson BJ Grossniklaus U Vogler H, Felekis D. Measuring the mechanical properties of plant cell walls. *Plants (Basel)*, 4(2):167–182, 2015. [10](#)
- [14] Yuan Liu Gui Cheng Yang Han Min Zeng Min Zhi Rong, Ming Qiu Zhang. The effect of fiber treatment on the mechanical properties of unidirectional sisal-reinforced epoxy composites. *Composites Science and Technology*, 61(10):1437–1447, 2001. [11](#)
- [15] Gibson Lorna J. The hierarchical structure and mechanics of plant materials. *Journal of the Royal Society Interface*, 9(10):2749–2766, 2012. [11](#)
- [16] Lina Zhang Sen Wang, Ang Lu. Recent advances in regenerated cellulose materials. *Progress in Polymer Science*, 53:169–206, 2016. [12](#), [38](#)
- [17] Nick bywater: The global viscose fibre industry in the 21 st century the first 10 years. <https://api.semanticscholar.org/CorpusID:28521667>. Accessed: 2023-08-30. [12](#)
- [18] William L. Hyden. Manufacture and properties of regenerated cellulose films. *Industrial Engineering Chemistry*, 21(5):405–410, 1929. [13](#)

REFERENCES

- [19] R. .Granacher, C.; Sallmann, 1939. US Patent 2179181. [13](#), [19](#)
- [20] Herbert Sixta Paul Kosma Thomas Rosenau, Antje Potthast. The chemistry of side reactions and byproduct formation in the system NMMO/cellulose (lyocell process). *Progress in Polymer Science*, 26(9):1763–1837, 2001. [13](#), [14](#)
- [21] H.J Purz J Ganster H.-P Fink, P Weigel. Structure formation of regenerated cellulose materials from NMMO-solutions. *Progress in Polymer Science*, 26(9):1473–1524, 2001. [14](#)
- [22] Aakash Sharma, Shailesh Nagarkar, Shirish Thakre, and Guruswamy Kumaraswamy. Structure–property relations in regenerated cellulose fibers: comparison of fibers manufactured using viscose and lyocell processes. *Cellulose*, 26, 2019. [14](#)
- [23] Robin D. Rogers Kenneth R. Seddon. Ionic liquids–solvents of the future? *Science*, 302:792–793, 2003. [14](#)
- [24] Frank Hermanutz, Marc Philip Vocht, Nicole Panzier, and Michael R. Buchmeiser. Processing of cellulose using ionic liquids. *Macromolecular Materials and Engineering*, 304(2), 2019. [14](#), [15](#)
- [25] Richard P. Swatloski, Scott K. Spear, John D. Holbrey, and Robin D. Rogers. Dissolution of cellose with ionic liquids. *Journal of the American Chemical Society*, 124(18):4974–4975, 2002. [14](#), [19](#)
- [26] André Pinkert, Kenneth N. Marsh, Shusheng Pang, and Mark P. Staiger. Ionic liquids and their interaction with cellulose. *Chemical Reviews*, 109(12):6712–6728, 2009. [15](#)
- [27] G. Gurau H. Wang and R. D. Rogers. Ionic liquid processing of cellulose. *Chemical Society Reviews journal*, 41:1519–1537, 2012. [15](#)
- [28] Keith E. Gutowski, Grant A. Broker, Heather D. Willauer, Jonathan G. Huddleston, Richard P. Swatloski, John D. Holbrey, and Robin D. Rogers.

REFERENCES

- Controlling the aqueous miscibility of ionic liquids: aqueous biphasic systems of water-miscible ionic liquids and water-structuring salts for recycle, metathesis, and separations. *Journal of the American Chemical Society*, 125(22):6632–6633, 2003. [15](#)
- [29] Shengdong Zhu, Yuanxin Wu, Qiming Chen, Ziniu Yu, Cunwen Wang, Shiwei Jin, Yigang Ding, and Gang Wu. Dissolution of cellulose with ionic liquids and its application: a mini-review. *Green Chemistry*, 8:325–327, 2006. [15](#)
- [30] Kenji Kamida, Kunihiko Okajima, Toshihiko Matsui, and Keisuke Kowsaka. Study on the solubility of cellulose in aqueous alkali solution by deuteration IR and ^{13}C NMR. *Polymer Journal*, 16(12):857–866, 1984. [16](#)
- [31] Jie Cai and Lina Zhang. Rapid dissolution of cellulose in LiOH/urea and NaOH/urea aqueous solutions. *Macromolecular bioscience*, 5(6):539–548, 2005. [16](#)
- [32] Thomas Heinze, René Dicke, Andreas Koschella, Arne Henning Kull, Erik-Andreas Klohr, and Wolfgang Koch. Effective preparation of cellulose derivatives in a new simple cellulose solvent. *Macromolecular Chemistry and Physics*, 201(6):627–631, 2000. [16](#)
- [33] Thomas Heinze and Andreas Koschella. Solvents applied in the field of cellulose chemistry: a mini review. *Polímeros*, 15:84–90, 2005. [16](#)
- [34] D.N.S. Hon. Cellulose: a random walk along its historical path. *Cellulose*, 1:1–25, 1994. [16](#), [17](#), [19](#)
- [35] J.E.Brandenburger, 1918. US Patent 1266766. [17](#), [19](#), [20](#), [79](#)
- [36] Ai. Hisano. Cellophane, the new visuality, and the creation of self-service food retailing. *Harvard Business School Working Paper*, 17-106, 1917. [17](#), [20](#), [21](#)

REFERENCES

- [37] Li Shen and Martin K. Patel. Life cycle assessment of man-made cellulose fibres. *Lenzinger Berichte*, 88:1–59, 2010. [17](#)
- [38] Frank A. Müller, Lenka Müller, Ingo Hofmann, Peter Greil, Magdalene M. Wenzel, and Rainer Staudenmaier. Cellulose-based scaffold materials for cartilage tissue engineering. *Biomaterials*, 27(21):3955–3963, 2006. [17](#)
- [39] Haque B Bhuiyan M.A.R Ali A Islam M.N. Kabir S.M.F, Sikdar P.P. Cellulose-based hydrogel materials: chemistry, properties and their prospective applications. *Prog Biomater.*, 7(3):153–174, 2018. [17](#)
- [40] Rajen Kundu, Pushpa Mahada, Bhawna Chhirang, and Bappaditya Das. Cellulose hydrogels: Green and sustainable soft biomaterials. *Current Research in Green and Sustainable Chemistry*, 5, 2022. [17](#)
- [41] Christian Aulin, Julia Netrval, Lars Wågberg, and Tom Lindström. Aerogels from nanofibrillated cellulose with tunable oleophobicity. *Soft Matter*, 6, 2010. [17](#)
- [42] Wang YZ. Long LY, Weng YX. Cellulose aerogels: Synthesis, applications, and prospects. *Polymers (Basel)*, 10(6):623, 2018. [17](#)
- [43] Martin Gericke, Jani Trygg, and Pedro Fardim. Functional cellulose beads: Preparation, characterization, and applications. *Chemical Reviews*, 113(7):4812–4836, 2013. [18](#)
- [44] Jr. Reichardt E. P O’Neill, J. J., 1951. US Patent 2,543,928. [18](#)
- [45] Helen sharp: Preserving papyrus: caring for 4000-year-old documents. <https://www.britishmuseum.org/blog/preserving-papyrus-caring-4000-year-old-documents>. Accessed: 2023-08-02. [19](#)
- [46] E. F. Armstrong. Charles frederick cross. 1855-1935. *Obituary Notices of Fellows of the Royal Society*, 1(4):459–464, 1935. [19](#)
- [47] S. Nishikawa and S. Ono. ’transmission of x-rays through fibrous, lamellar and granular substances. *Proceedings of the Royal Society of London. Series A, Mathematical and Physical Sciences*, 7:131, 1913. [19](#)

REFERENCES

- [48] Futamura: Natureflex. <https://www.natureflex.com/uk/>. Accessed: 2023-08-02. [19](#), [29](#)
- [49] George W. Stocking and Willard F. Mueller. The cellophane case and the new competition. *The American Economic Review*, 45(1):29–63, 1955. [20](#)
- [50] J.K. Winkler. *The DuPont Dynasty*. Literary Licensing, 2013. [21](#)
- [51] D.A. Hounshell, J.K. Smith, and J.K. Smith. *Science and Corporate Strategy: Du Pont R and D, 1902-1980*. Studies in Economic History and Policy: USA in the Twentieth Century. Cambridge University Press, 1988. [21](#)
- [52] DuPont. Cellophane: Modern merchandising aid. *Published Collections Department*, 1928. [21](#)
- [53] Manuscripts DuPont Advertising Department records (Accession 1803), Hagley Museum Archives Department, and Wilmington Library. Advertisement for dupont cellophane. *Saturday Evening Post*, 1945. [22](#)
- [54] Hagley Museum and Wilmington Library. Advertisement for dupont cellophane, 1947. [22](#)
- [55] Manuscripts, Hagley Museum Archives Department, and Delaware Library, Wilmington. Advertisement for dupont cellophane. *The Saturday Evening Post*, 1950. [22](#)
- [56] J.P. Harrington and W.A. Jenkins. *Packaging Foods with Plastics*. Taylor & Francis, 1991. [22](#)
- [57] United States Environmental Protection Agency. *AP 42, Fifth Edition, Volume I*. United States Environmental Protection Agency, 1990. [23](#)
- [58] Qingxian Miao, Lihui Chen, Liulian Huang, Chao Tian, Linqiang Zheng, and Yonghao Ni. A process for enhancing the accessibility and reactivity of hardwood kraft-based dissolving pulp for viscose rayon production by cellulase treatment. *Bioresource Technology*, 154:109–113, 2014. [23](#)

REFERENCES

- [59] The Futamura Group. Viscose technology, 2020. Futamura Documents on Viscose Technology. 24
- [60] Kris Malfait Colin Daffern. The principles and practice of casting regenerated cellulose film, 2001. Futamura Documents. 24, 79
- [61] W. L. Hyden. Manufacture and properties of regenerated cellulose films. *Industrial Engineering Chemistry*, 21:405–410, 1929. 25, 26
- [62] Gordon C. Inskip and Prescott Van Horn. Cellophane. *Industrial & Engineering Chemistry*, 44(11):2511–2524, 1952. 25, 26
- [63] S.L. Rosen. *Fundamental Principles of Polymeric Materials*. A Wiley - Interscience publication. Wiley, 1982. 29
- [64] Mustafizur Rahman and Christopher S. Brazel. The plasticizer market: an assessment of traditional plasticizers and research trends to meet new challenges. *Progress in Polymer Science*, 29(12):1223–1248, 2004. 29, 30, 31
- [65] Chemical economics handbook report on plasticizers. <https://www.spglobal.com/commodityinsights/en/ci/products/plasticizers-chemical-economics-handbook.html>. Accessed: 2023-08-07. 30
- [66] Joel frados. plastics engineering handbook of the society of the plastics industry, inc. 1976. <https://api.semanticscholar.org/CorpusID:137250766>. Accessed: 2023-09-01. 30
- [67] D. Feldman. Plastics technology handbook. *Journal of Polymer Science Part C: Polymer Letters*, 26(6):275–275, 1988. 30
- [68] J. Sweeney I. M. Ward. *Mechanical Properties of Solid Polymers: Third Edition*, chapter 10, pages 261–284. John Wiley Sons, Ltd, 2012. 30, 61
- [69] Melissa Gurgel Adeodato Vieira, Mariana Altenhofen da Silva, Lucielen Oliveira dos Santos, and Marisa Masumi Beppu. Natural-based plasticizers and biopolymer films: A review. *European Polymer Journal*, 47(3):254–263, 2011. 31, 33

REFERENCES

- [70] I. Greener Donhowe and Fennema. The effects of plasticizers on crystallinity, permeability, and mechanical properties of methylcellulose films. *Journal of Food Processing and Preservation*, 17(4):247–257, 1993. [31](#)
- [71] A.S. Wilson and Institute of Materials. *Plasticisers: Principles and Practice*. Institute of Materials, 1995. [31](#)
- [72] P. Fedorko, David Djurado, M. Trznadel, B. Dufour, Patrice Rannou, and J. Travers. Insulator-metal transition in polyaniline induced by plasticizers. *Synthetic Metals*, 135:327–328, 2003. [31](#)
- [73] Maëva Bocqué, Coline Voirin, Vincent Lapinte, Sylvain Caillol, and Jean-Jacques Robin. Petro-based and bio-based plasticizers: Chemical structures to plasticizing properties. *Journal of Polymer Science Part A: Polymer Chemistry*, 54(1):11–33, 2016. [32](#)
- [74] Paul H. Daniels. A brief overview of theories of pvc plasticization and methods used to evaluate pvc-plasticizer interaction. *Journal of Vinyl and Additive Technology*, 15(4):219–223, 2009. [32](#)
- [75] G. Wypych. *Handbook of Plasticizers*. Elsevier Science, 2023. [32](#)
- [76] Mridula Chandola and Sujata Marathe. A QSPR for the plasticization efficiency of polyvinylchloride plasticizers. *Journal of Molecular Graphics and Modelling*, 26(5):824–828, 2008. [32](#)
- [77] Yachuan Zhang and J. H. Han. Mechanical and thermal characteristics of pea starch films plasticized with monosaccharides and polyols. *Journal of Food Science*, 71(2):109–118, 2006. [33](#)
- [78] Thomas Karbowiak, Hubert Hervet, Liliane Léger, Dominique Champion, Frédéric Debeaufort, and Andrée Voilley. Effect of plasticizers (water and glycerol) on the diffusion of a small molecule in iota-carrageenan biopolymer films for edible coating application. *Biomacromolecules*, 7(6):2011–2019, 2006. [33](#)

- [79] Sandeep Paudel, Sumi Regmi, and Srinivas Janaswamy. Effect of glycerol and sorbitol on cellulose-based biodegradable films. *Food Packaging and Shelf Life*, 37, 2023. [35](#)
- [80] Orin C. Hansen Jr., Leon Marker, and Orville J. Sweeting. The effect of softeners on the elastic modulus of regenerated cellulose sheet. *Journal of Applied Polymer Science*, 5(18):655–662, 1961. [35](#)
- [81] A. Jangchud and M.S. Chinnan. Properties of peanut protein film: Sorption isotherm and plasticizer effect. *Food Science and Technology*, 32(2):89–94, 1999. [35](#)
- [82] Olivier Orliac, Antoine Rouilly, Françoise Silvestre, and Luc Rigal. Effects of various plasticizers on the mechanical properties, water resistance and aging of thermo-moulded films made from sunflower proteins. *Industrial Crops and Products*, 18(2):91–100, 2003. [35](#), [36](#)
- [83] M.C. Galdeano, M.V.E. Grossmann, S. Mali, L.A. Bello-Perez, M.A. Garcia, and P.B. Zamudio-Flores. Effects of production process and plasticizers on stability of films and sheets of oat starch. *Materials Science and Engineering: C*, 29(2):492–498, 2009. [36](#)
- [84] Xiaofei Ma and Jiugao Yu. The plasticizers containing amide groups for thermoplastic starch. *Carbohydrate Polymers*, 57(2):197–203, 2004. [36](#)
- [85] Nugraha E Suyatma, Lan Tighzert, Alain Copinet, and Véronique Coma. Effects of hydrophilic plasticizers on mechanical, thermal, and surface properties of chitosan films. *Journal of Agricultural and Food Chemistry*, 53(10):3950–3957, 2005. [36](#)
- [86] Munehiko Tanaka, Kiyomi Iwata, Romanee Sanguandeeikul, Akihiro Handa, and Shoichiro Ishizaki. Influence of plasticizers on the properties of edible films prepared from fish water-soluble proteins. *Fisheries science*, 67(2):346–351, 2001. [36](#)

REFERENCES

- [87] Camille Decroix, Yvan Chalamet, Guillaume Sudre, and Vergelati Carroll. Thermo-mechanical properties and blend behaviour of cellulose acetate/lactates and acid systems: Natural-based plasticizers. *Carbohydrate Polymers*, 237:1160–1172, 2020. [37](#)
- [88] Samiris Côcco Teixeira, Rafael Resende Assis Silva, Taíla Veloso de Oliveira, Paulo César Stringheta, Marcos Roberto Moacir Ribeiro Pinto, and Nilda de Fátima Ferreira Soares. Glycerol and triethyl citrate plasticizer effects on molecular, thermal, mechanical, and barrier properties of cellulose acetate films. *Food Bioscience*, 42, 2021. [37](#)
- [89] Rafael C. Rebelo, Diana C. M. Ribeiro, Patricia Pereira, Francesco De Bon, Jorge F. J. Coelho, and Armenio C. Serra. Cellulose-based films with internal plasticization with epoxidized soybean oil. *Cellulose*, 30(3):1823–1840, 2023. [37](#)
- [90] Roland Geyer, Jenna R. Jambeck, and Kara Lavender Law. Production, use, and fate of all plastics ever made. *Science Advances*, 3(7), 2017. [38](#)
- [91] Manjusri Misra Mohanty, Amar Kumar and L. T. Drzal. Sustainable biocomposites from renewable resources: opportunities and challenges in the green materials world. *Journal of Polymers and the Environment*, 10:19–26, 2002. [38](#)
- [92] Mingyue Zhang, Gill M. Biesold, Woosung Choi, Jiwoo Yu, Yulin Deng, Clara Silvestre, and Zhiqun Lin. Recent advances in polymers and polymer composites for food packaging. *Materials Today*, 53:134–161, 2022. [38](#)
- [93] J. H. Poynting. The Wave Motion of a Revolving Shaft, and a Suggestion as to the Angular Momentum in a Beam of Circularly Polarised Light. *Proceedings of the Royal Society of London Series A*, 82(557):560–567, July 1909. [57](#)
- [94] Noah R. Menard Kevin P. Menard. *Dynamic Mechanical Analysis: Third Edition*. CRC Press, 2020. [57](#), [59](#), [61](#)

REFERENCES

- [95] Sam F. Edwards. Relaxation phenomena in polymers. *Polymer International*, 32:435–435, 1993. 57
- [96] Roger D Corneliussen Brostow Witold. *Failure of Plastics*. Munich New York: Hanser Publishers, 1986. 57
- [97] J. Ferry. *Viscoelastic properties of polymers*. New York: Wiley, 1980. 61, 91
- [98] Ta instruments: Discovery dma: Dynamic mechanical analyser. Brochure: "https://www.tainstruments.com/wp-content/uploads/Discovery-DMA-Brochure.pdf". Accessed: 2023-08-20. 62
- [99] B. E. Read N. G. McCrum and G. Williams. *Anelastic and dielectric effects in polymeric solids*. New York: Wiley, 1967. 63, 65
- [100] Haynes: What is a crankshaft and what does it do? <https://haynes.com/en-gb/tips-tutorials/what-is-car-crankshaft>. Accessed: 2023-07-17. 63
- [101] Senthil Kumar Kaliappan. Characterization of physical properties of polymers using AFM force-distance curves. Master's thesis, University of Siegen, 2007. 63
- [102] Perkin elmer: Dynamic mechanical analysis: A beginners guide. Brochure: <https://resources.perkinelmer.com/corporate/cmsresources/images/44-74546gde;ntroductiontodma.pdf>. Accessed : 2023 – 08 – 20. 64
- [103] R. F. Boyer. Dependence of mechanical properties on molecular motion in polymers. *Polymer Engineering & Science*, 8(3):161–185, 1968. 65
- [104] S. A. Bradley and S. H. Carr. Mechanical loss processes in polysaccharides. *Journal of Polymer Science: Polymer Physics Edition*, 14(1):111–124, 1976. 66
- [105] Roy Mech: Loaded Flate Plates. https://www.roymech.co.uk/Useful_Tables/Mechanics/Plates.htm. 2023 – 10 – 13. 67, 68
- [106] M. Ashby. *Materials selection in mechanical design (3rd ed.)*. Butterworth-Heinemann, Burlington, Massachusetts, 1999. 78

REFERENCES

- [107] M. Scandola and G. Ceccorulli. Viscoelastic properties of cellulose derivatives: Effect of diethylphthalate on the dynamic mechanical relaxations of cellulose acetate. *Polymer*, 26(13):1958–1962, 1985. [90](#)
- [108] Heim HP Erdmann R, Kabasci S. Thermal properties of plasticized cellulose acetate and its -relaxation phenomenon. *Polymers (Basel)*, 13(9):13–56, 2021. [90](#), [91](#), [92](#), [93](#), [96](#), [133](#), [146](#)
- [109] Thomas G Fox Jr and Paul J Flory. Second-order transition temperatures and related properties of polystyrene. i. influence of molecular weight. *Journal of Applied Physics*, 21(6):581–591, 1950. [90](#)
- [110] J. Einfeldt, D. Meißner, and A. Kwasniewski. Polymerdynamics of cellulose and other polysaccharides in solid state-secondary dielectric relaxation processes. *Progress in Polymer Science*, 26(9):1419–1472, 2001. [91](#), [134](#)
- [111] G.P. Mikhailov, A.I. Artyukhov, and V.A. Shevelev. Dielectric and NMR study of the molecular mobility of cellulose and of its derivatives. *Polymer Science U.S.S.R.*, 11(3):628–640, 1969. [91](#)
- [112] L’opez O. V. Lencina M.M. S. Garc’ia M. A. Andreucetti N. A. Ciolino A. E. Ninago, M. D. and M.A. Villar. Enhancement of thermoplastic starch final properties by blending with poli(ϵ -caprolactone). *Carbohydrate Polymers*, 74(4):573–581, 2015. [99](#)
- [113] Rungsinee Sothornvit, David S. Reid, and John M. Krochta. Plasticizer effect on the glass transition temperature of beta-lactoglobulin films. *Transactions of the American Society of Agricultural and Biological Engineers*, 45:1479–1484, 2002. [99](#)
- [114] Orville J. Sweeting, Roman Mykolajewycz, Eric Wellisch, and Richard N. Lewis. Softener absorption by regenerated cellulose. uptake from 10% aqueous glycerol. *Journal of Applied Polymer Science*, 1(3):356–360, 1959. [101](#)
- [115] Eric Wellisch, Lamont Hagan, Leon Marker, and Orville J. Sweeting. Interaction of cellulose with small molecules. glycerol and ethylene carbonate. *Journal of Applied Polymer Science*, 3(9):331–337, 1960. [101](#), [102](#)

REFERENCES

- [116] Roman Mykolaiewycz, Eric Wellisch, Richard N. Lewis, and Orville J. Sweeting. Softener absorption by regenerated cellulose. *Journal of Applied Polymer Science*, 2(5):236–240, 1959. [101](#), [102](#)
- [117] Sandeep Paudel, Sumi Regmi, and Srinivas Janaswamy. Effect of glycerol and sorbitol on cellulose-based biodegradable films. *Food Packaging and Shelf Life*, 37, 2023. [102](#)
- [118] Stanley G. Schultz and A. K. Solomon. Determination of the Effective Hydrodynamic Radii of Small Molecules by Viscometry . *Journal of General Physiology*, 44(6):1189–1199, 1961. [102](#)
- [119] R Florencia Versino, María Alejandra García. Starch films for agronomic applications: comparative study of urea and glycerol as plasticizers. *International Journal of Environment Agriculture and Biotechnology*, 3, 2018. [104](#), [105](#), [118](#)
- [120] Nugraha E. Suyatma, Lan Tighzert, Alain Copinet, and Véronique Coma. Effects of hydrophilic plasticizers on mechanical, thermal, and surface properties of chitosan films. *Journal of Agricultural and Food Chemistry*, 53(10):3950–3957, 2005. [104](#), [114](#)
- [121] A. E. Sloan. *Properties and effects of humectants in intermediate moisture foods*. PhD thesis, University of Minnesota, 1976. [105](#)
- [122] Rungsinee Sothornvit and John M Krochta. Plasticizer effect on mechanical properties of β -lactoglobulin films. *Journal of Food Engineering*, 50(3):149–155, 2001. [105](#)
- [123] Perkin elmer: Relaxation of pmma and calculation of the activation energy. Brochure: <https://resources.perkinelmer.com/lab-solutions/resources/docs.pdf>. Accessed: 2023-08-23. [145](#)
- [124] H Montes, JY Cavallé, and K Mazeau. Secondary relaxations in amorphous cellulose. *Journal of non-crystalline solids*, 172:990–995, 1994. [146](#)
- [125] Golnaz Jafarpour, Eric Dantras, Alain-Michel Boudet, and Colette Lacabanne. Study of dielectric relaxations in cellulose by combined dds and tsc. *Journal of Non-Crystalline Solids*, 353(44 - 46), 2007. [146](#)

REFERENCES

- [126] Kunio Nakamura, Tatsuko Hatakeyama, and Hyoe Hatakeyama. Studies on bound water of cellulose by differential scanning calorimetry. *Textile Research Journal*, 51(9):607–613, 1981. [185](#), [198](#)
- [127] Patric Elf, Hüsamettin Deniz Özeren, Per A. Larsson, Anette Larsson, Lars Wågberg, Robin Nilsson, Poppy Thanaporn Chaiyupatham, Mikael S. Hedenqvist, and Fritjof Nilsson. Molecular dynamics simulations of cellulose and dialcohol cellulose under dry and moist conditions. *Biomacromolecules*, 24(6):2706–2720, 2023. [198](#)
- [128] Jinwu Wang, Douglas J. Gardner, Nicole M. Stark, Douglas W. Bousfield, Mehdi Tajvidi, and Zhiyong Cai. Moisture and oxygen barrier properties of cellulose nanomaterial-based films. *ACS Sustainable Chemistry*, 6(1):49–70, 2017. [198](#)
- [129] Erol Ayranci and Sibel Tunc. A method for the measurement of the oxygen permeability and the development of edible films to reduce the rate of oxidative reactions in fresh foods. *Food Chemistry*, 80:423–431, 2003. [198](#)
- [130] Perkin Elmer. Thermogravimetric analysis (tga): a beginner’s guide. Brochure: [https://resources.perkinelmer.com/lab-solutions/resources/docs/faq_beginners – guide – to – thermogravimetric – analysis_09380c01.pdf](https://resources.perkinelmer.com/lab-solutions/resources/docs/faq_beginners_guide_to_thermogravimetric_analysis_09380c01.pdf), 2010. [199](#)
- [131] Liliana C. Tomé, Carla M.B. Gonçalves, Marta Boaventura, Lúcia Brandão, Adélio M. Mendes, Armando J.D. Silvestre, Carlos Pascoal Neto, Alessandro Gandini, Carmen S.R. Freire, and Isabel M. Marrucho. Preparation and evaluation of the barrier properties of cellophane membranes modified with fatty acids. *Carbohydrate Polymers*, 83(2):836–842, 2011. [199](#)
- [132] K.L. Spence, R.A. Venditti, O.J. Rojas, Y. Habibi, and J.J. Pawlak. The effect of chemical composition on microfibrillar cellulose films from wood pulps: water interactions and physical properties for packaging applications. *Cellulose*, 17(4):835–848, 2010. [199](#)